



UNIVERSITAT DE
BARCELONA

Role of PI3K in pericytes during angiogenesis

Ana Raquel Martins Figueiredo



Aquesta tesi doctoral està subjecta a la llicència **Reconeixement- NoComercial – SenseObraDerivada 3.0. Espanya de Creative Commons.**

Esta tesis doctoral está sujeta a la licencia **Reconocimiento - NoComercial – SinObraDerivada 3.0. España de Creative Commons.**

This doctoral thesis is licensed under the **Creative Commons Attribution-NonCommercial-NoDerivs 3.0. Spain License.**

A fluorescence microscopy image showing a dense network of blood vessels. The vessels are stained with blue and red dyes. Small green and yellow spots are scattered throughout the network, representing pericytes and PI3K staining, respectively. The central part of the image shows a more complex, interconnected network of vessels.

Role of PI3K in pericytes during the angiogenesis

ANA RAQUEL MARTINS FIGUEIREDO
PHD THESIS, BARCELONA, JUNE 2017



UNIVERSITAT DE
BARCELONA



FACULTAT DE FARMÀCIA I CIÈNCIES DE L'ALIMENTACIÓ

UNIVERSITAT DE BARCELONA

Programa de Doctorat en Biomedicina

Role of PI3K in pericytes during angiogenesis

Memòria presentada per

Ana Raquel Martins Figueiredo

per optar al títol de doctora per la Universitat de Barcelona.

Aquesta tesi ha estat realitzada sota la direcció de

Mariona Graupera i Garcia-Milà

en el Laboratori de Senyalització Vasculat ubicat en l'Institut d'Investigació Biomèdica de Bellvitge (IDIBELL).

Directora de tesi

**Dra. Mariona Graupera
i Garcia-Milà**

Tutor

**Dr. Francesc Viñals
Canals**

Doctoranda

**Ana Raquel
Martins Figueiredo**

Ana Raquel Martins Figueiredo, Barcelona, Juny 2017

This thesis work titled “Role of PI3K in pericytes during angiogenesis” has been developed in the Vascular Signalling Laboratory at IDIBELL (L’Hospitalet de Llobregat, Barcelona).

Financial Support:

- Gobierno de España - Ministerio de Ciencia e Innovación (MICINN). SAF2010-15661 and SAF2013-46542-P
- People Programme (Marie Curie Actions) of the European Union’s Seventh Framework Programme FP7/2013-2016/ under REA grant agreement 317250. VESSEL-317250. Title of the project: “Vascular Endothelial Interactions and Specialization”
- Instituto de Salud Carlos III (ISCIII). PIE13/00022 (ONCOPROFILE, 2014-2016)
- Generalitat de Catalunya - Agència de Gestió d’Ajust Universitaris i de Recerca (AGAUR) - 2014-SGR-725

During the present work Ana Raquel Martins Figueiredo performed two secondments: one in Dr. Ralf Adams laboratory, under the supervision of Dr. Rodrigo Dieguez-Hurtado belting at the Max Planck Institute, Münster (Germany); and other in Christer Betsholtz laboratory, under the supervision of Marco Castro belting at Uppsala University Hospital, Uppsala (Sweden) thanks to the financial support from Marie Curie Actions - VESSEL-317250



Aos meus avós,

*por tornarem tudo possível
e por me ensinarem a persistir e não desistir*

Ao Manel,

*que mudou a minha vida de muitas formas
e que me fez perceber que o mais importante é sermos felizes*

Acknowledgement

First of all, I would like to say thanks to all of you that went with me during these four years of PhD! These years have changed me in many aspects and were one of the most enriching of my life, both professionally and personally. I am extraneously grateful to all of you =).

A ti **Mariona Graupera**, MUCHAS GRACIAS por la oportunidad de juntarme a tu grupo, por el entusiasmo con que llevas la ciencia, por la alegría y perseverancia que tienes y que transmites todos los días y por la humildad y generosidad con que lo haces. Eres una grande científica, llena de nuevas ideas, que nunca desiste y ácima de todo que Ama lo que hace.

Many thanks to **Julie Guillermet**, to **Rodrigo Hurtado** and to **Àngels Fabra** for being willing to read my work and be part of my thesis committee. Gracias también al **Álvaro** y **José Carlos** por aceptaren con tanto entusiasmo ser suplentes de mi tribunal. Muchas gracias.

I also want to thank all the members of the VESSEL team. It was a unique opportunity to be part of this incredible group. All the meeting and discussions were very important for this work and for my development as a scientist.

Abstract

Pericytes (PCs) are important regulators of the vascular development promoting vessel growth and stabilization. They have recently emerged as a therapeutic target to promote or inhibit angiogenesis. Therefore, advancing our basic understanding on PCs biology and its molecular regulators during physiological angiogenesis is essential to develop PC-related therapies. One of the major pathways leading to cellular proliferation, migration, and survival is relayed by PI3K. Data from our laboratory and others have demonstrated isoform selectivity stimulating PI3K signalling in the regulation of both, the ECs and vSMCs. Interestingly, in these two cell populations' p110 α seems to be the major isoform.

By using pharmacological and genetic tools together with cultured PCs and retinal systems we have found that PCs pass through different states during vessel development, and that PI3K signalling regulates these cells in an isoform-specific manner. We have seen that immature and active PCs promote vessel growth while, mature and quiescent PCs result in vascular stabilization and remodelling. Moreover and unexpectedly, our results have identified p110 β as the key regulator of PCs proliferation and growth. Inactivation of p110 β in PCs, but not p110 α , results in PC proliferation arrest and in several morphological changes, which resemble a more mature PC. Lack of p110 β in PCs also leads to a more mature vascular plexus. We observed reduced vessel density, EC proliferation arrest and increased deposition of collagen IV. Furthermore, PTEN seems to be the regulator of PI3K in PCs, opposing the p110 β effects and, leading to a more mature and stable PC and subsequently also more mature vasculature.

Since p110 β -PI3K controls PC growth and proliferation, it suggests that target therapy directed to p110 β in cancer could affect PCs. Using a pancreatic neuroendocrine tumour mouse model (RIP1-Tag2) we have seen that pharmacological inhibition of p110 β impacts on tumour progression and in PCs growth. However, it also results in a slight reduction in the overall survival of the animal, without affecting their metastatic potential. Therefore, other studies are needed to further investigate p110 β as a possible PC-specific target therapy.

Contents

Acknowledgements.....	7
Abstract.....	9
List of figures.....	19
List of tables.....	25
List of abbreviations.....	27
1. Introduction.....	35
1.1. Blood vessels and their origin	35
1.1.1. Intussusceptive angiogenesis	36
1.1.2. Sprouting angiogenesis	37
1.1.2.1. Activation of a quiescent vessel and basement membrane degradation	38
1.1.2.2. Tip and stalk cell selection.....	39
1.1.2.3. Sprout anastomosis	41
1.1.2.4. Lumen Formation	42
1.1.2.5. Vascular maturation and stabilization	43
1.1.2.6. Vessel regression	45
1.1.2.7. Vessel quiescence.....	46
1.2. PC cells	47
1.2.1. Ontogeny	47
1.2.2. Distribution and morphology	49
1.2.3. Identification.....	51
1.2.4. Functions	53
1.2.4.1. Regulation of blood flow	53
1.2.4.2. Immune function	54

1.2.4.3.	Blood hemostasis	54
1.2.4.4.	Regulation of vascular development.....	55
1.3.	Signalling pathways implicated in PCs and in their paracrine regulation with the endothelium during sprouting angiogenesis.....	56
1.3.1.	PDGF-B/PDGFR β	56
1.3.2.	Sphingosine-1-phosphate	57
1.3.3.	Angiopoetin-1 and 2.....	59
1.3.4.	Transforming growth factor- β	59
1.3.5.	Other regulators	61
1.4.	PCs in cancer therapy	62
1.5.	Mouse models for studying vascular development in physiology and pathology	64
1.5.1.	Retinal model.....	64
1.5.2.	The RIP1-Tag2 transgenic mouse model	66
1.6.	PI3K signalling pathway	68
1.6.1.	Class I PI3K.....	71
1.6.1.1.	Signalling inputs and isoform specificity	73
1.6.1.2.	Signalling outputs and downstream effectors	76
1.6.1.3.	Regulation by PTEN.....	80
1.7.	PI3K and angiogenesis	82
1.7.1.	Class I PI3K and regulation of ECs biology	82
1.7.2.	Class I PI3K and regulation of PCs biology	86
1.7.3.	PTEN regulation during angiogenesis.....	88
1.8.	PI3K and cancer	90
1.8.1.	PI3K in tumour vasculature.....	92
2.	Objectives	97

3. Materials and Methods	99
3.1. Mouse experiments	99
3.1.1. Mouse care	99
3.1.2. Genetically modified mice and inducible genetic experiments	99
3.1.3. RIP1-Tag2 mice	103
3.1.4. Induction of Cre mediated gene deletion	104
3.1.5. Mouse genotyping.....	104
3.1.5.1. Tissue digestion.....	104
3.1.5.2. PCR.....	104
3.1.6. Postnatal mouse retina isolation and staining.....	107
3.1.6.1. Eyes extraction and retina isolation	107
3.1.6.2. Staining of whole-mount retinas	108
3.1.6.2.1. Immunofluorescence staining with primary antibodies	116
3.1.6.2.2. <i>In vivo</i> proliferation assay by EdU detection	110
3.1.7. Confocal imaging	111
3.1.8. Methods used for quantifying vessel features.....	111
3.1.8.1. Radial expansion.....	111
3.1.8.2. Vascular branching.....	112
3.1.8.3. Number of sprouts	113
3.1.8.4. Filopodia quantification.....	113
3.1.8.5. PC coverage.....	113
3.1.8.6. Quantification of proliferative PCs	114
3.1.8.7. Quantification of proliferative ECs	115

3.1.8.8.	Quantification of collagen IV staining intensity in the retinal vasculature	116
3.1.9.	Pharmacological inactivation of p110 β <i>in vivo</i> using the RIP1-Tag2 model	116
3.1.9.1.	Evaluation of the animal status and determination of endpoint survival	117
3.1.9.2.	Determination of pancreatic tumour number and burden of RIP1-Tag2.....	118
3.1.9.3.	Determination of the hemorrhagic phenotype of the tumours	119
3.1.9.4.	Determination of macro-metastasis in liver and mesentery	119
3.1.9.5.	Immunodetection of proteins	120
3.1.9.5.1.	Immunohistochemistry	120
3.1.9.5.2.	Immunofluorescence	120
3.1.9.6.	Immunohistochemistry and immunofluorescent analysis	121
3.1.9.6.1.	Vascular analysis.....	122
3.1.9.6.2.	Micro-metastasis analysis	122
3.2.	Cell culture.....	123
3.2.1.	Culturing of mouse brain PC cells	123
3.2.2.	Culturing of mouse lung EC (mLECs)	124
3.2.2.1.	EC isolation from mouse lungs.....	124
3.2.2.2.	Tissue digestion.....	124
3.2.2.3.	First selection	125
3.2.2.4.	Second selection	125
3.2.3.	Co-cultures of PCs and mLECs	126
3.2.3.1.	Migration Assay	126

3.2.3.2.	Proliferation Assay.....	127
3.2.4.	Pharmacological treatments in PCs	128
3.2.4.1.	PCs migration assay upon PI3K specific inhibition (wound healing assay)	128
3.2.4.2.	PCs proliferation assay upon PI3K specific inhibition	129
3.2.4.3.	PCs viability assay using MTS assay upon PI3K specific inhibition	130
3.2.4.4.	PCs treatment to Western immunoblotting	130
3.2.4.5.	Immunofluorescence of cultured PCs and mLECs	130
3.2.5.	Protein extraction and Western immunoblotting	131
3.2.5.1.	Protein lyses and sample processing	131
3.2.5.2.	Protein electrophoresis and membrane transference	132
4.	Results.....	135
	Part I- PI3K in PCs during physiological angiogenesis.....	135
4.1.	PCs during vascular development.....	135
4.1.1.	PCs differentiation during vessel maturation.....	135
4.1.2.	Collagen IV and vascular deposition.....	137
4.1.3.	PCs promote EC proliferation and migration	142
4.2.	PI3K regulation of PCs- <i>in vivo</i> and <i>in vitro</i> studies	146
4.2.1.	PI3K activity during angiogenesis.....	146
4.2.2.	PCs express all class IA isoforms	148
4.2.3.	p110 α -PI3K regulates AKT phosphorylation	150
4.2.4.	PI3K regulates PCs cells in an isoform dependent manner	152
4.2.5.	PI3K controls PC biology in a isoform dependent manner during sprouting angiogenesis – The model selection	152

4.2.6.	The efficiency of PDGFR β (BAC)-CreERT2	153
4.2.7.	p110 α -PI3K isoform does not regulates PCs biology during sprouting angiogenesis	155
4.2.8.	p110 β -PI3K isoform is the key regulator of PCs biology during sprouting angiogenesis	163
4.3.	Paracrine regulation of EC by PI3K signalling in PCs	170
4.3.1.	p110 α inactivation in PCs leads to defects in EC motility ...	170
4.3.2.	p110 β inactivation in PCs leads to severe vascular defects	175
4.4.	PTEN regulates PI3K function in PCs during the sprouting angiogenesis (ongoing experiments).....	183
Part II-PI3K in PCs during pathological angiogenesis.....		189
4.5.	Investigating the role of PI3K in PCs during tumoral angiogenesis	189
4.5.1.	p110 β impacts on tumour PCs and impairs tumour progression	189
4.5.2.	p110 β inhibition does not affect with the metastatic potential	190
5.	Discussion	195
5.1.	PCs differentiate during the retinal development.....	195
5.2.	PCs control EC migration and proliferation <i>in vitro</i>	198
5.3.	Class IA-PI3K selectively regulates PCs biology <i>in vitro</i>	199
5.4.	Class IA-PI3K selectively regulates PCs biology during sprouting angiogenesis.....	202
5.5.	Inactivation of PI3K in PCs leads to severe vascular defects	205
5.6.	PTEN opposes PI3K signalling in PCs during sprouting angiogenesis	209

5.7. p110 β impacts on tumour PCs and impairs tumour progression	212
5.8. Concluding remarks.....	213
6. Conclusions	215
7. References	217
Appendix.....	245

List of Figures

Figure 1.1. Blood vessel formation.....	37
Figure 1.2. The different cellular events occurring during sprouting angiogenesis.....	38
Figure 1.3. Activation of quiescent vessel.....	40
Figure 1.4. Vascular anastomosis and lumen formation.....	42
Figure 1.5. PCs recruitment.....	43
Figure 1.6. Vessel maturation and stabilization.....	45
Figure 1.7. Developmental Origin of Mural Cells.....	48
Figure 1.8. PCs Anatomy.....	50
Figure 1.9. PCs identification.....	55
Figure 1.10. Signalling pathways regulating PC and EC cross-talk during sprouting angiogenesis.....	58
Figure 1.11. Growth of retinal blood vessels.....	65
Figure 1.12. The tumour progression of RIP1-TAG2 mice model.....	67
Figure 1.13. PI3Ks family.....	69
Figure 1.14. Classes of mammalian PI3Ks.....	71
Figure 1.15. Downstream class I-PI3K signalling.....	77
Figure 1.16. Isoform-specific roles of class I PI3Ks.....	91
Figure 1.17. Vascular targeting strategies in cancer with PI3K inhibitors.....	94
Figure 3.1 Tamoxifen injection, eye isolation and retina dissection.....	108
Figure 3.2. Radial Expansion.....	112
Figure 3.3. Branching Points.....	112
Figure 3.4. Number of Sprouts and Filopodia.....	113
Figure 3.5. PC coverage in the vessel area.....	114

Figure 3.6. PC proliferation.....	115
Figure 3.7. Number of proliferative EC.	116
Figure 3.8. Collagen IV integrate density.	117
Figure 3.9. RIP1-Tag2 tumoural model.....	118
Figure 3.10. Formula to determine the tumour volume (Va).....	119
Figure 3.11. Immunocytochemistry image with T-antigen staining.....	122
Figure 3.12. Migration assay for EC-PC co-cultures.....	127
Figure 3.13. Proliferation assay for EC-PC co-cultures.....	128
Figure 4.1. Vessel maturation during the sprouting angiogenesis.....	136
Figure 4.2. PC coverage of vessels increases during maturation.....	138
Figure 4.3. PCs change their morphology during the maturation.....	139
Figure 4.4. PC and EC proliferation decreases during maturation.....	140
Figure 4.5. Deposition of collagen IV increases during maturation.....	141
Figure 4.6. Characterization of WT PCs and ECs cells.....	142
Figure 4.7. EC in co-culture with PCs increased the BrdU incorporation.....	144
Figure 4.8. EC in co-culture with PCs increased migration.....	145
Figure 4.9. PI3K activity is upregulated during the sprouting angiogenesis....	147
Figure 4.10. PCs cells express all class IA-PI3k isoforms.....	148
Figure 4.11. Only p110 α -PI3K inactivation in PCs reduced the levels of pAKT.....	149
Figure 4.12. The p110 α -PI3K regulates PC viability and migration.....	151
Figure 4.13. The p110 β -PI3K isoform regulates PC proliferation.....	152
Figure 4.14. Efficient induction and specificity of Pdgfr β -CreERT2.....	154
Figure 4.15. Efficient induction and specificity of Pdgfr β -CreERT2.....	155
Figure 4.16. p110 α inactivation did not affect PC coverage using NG2 marker in the sprouting front of the retina.	157

Figure 4.17. p110 α inactivation did not affect PC coverage using the NG2 marker in the remodelling plexus of the retina.	158
Figure 4.18. p110 α inactivation did not affect PC coverage using desmin marker.....	159
Figure 4.19. p110 α inactivation did not affect morphology.....	160
Figure 4.20. p110 α inactivation did not affect PC proliferation in the angiogenic front.....	161
Figure 4.21. p110 α isoform inactivation did not affect PC proliferation in the remodelling plexus.....	162
Figure 4.22. p110 β inactivation impacts on PC coverage using NG2 marker in the sprouting front of the retina.....	164
Figure 4.23. p110 β inactivation slight reduced PC coverage in the remodelling plexus of the retina when used the NG2 marker.....	165
Figure 4.24. p110 β inactivation did not affect PC coverage using desmin marker.	166
Figure 4.25. PCs morphology changes after p110 β inactivation.....	167
Figure 4.26. p110 β inactivation leads to PC proliferation arrest in the angiogenic front.....	168
Figure 4.27. p110 β inactivation leads to PC proliferation arrest in remodelling plexus.....	169
Figure 4.28. p110 α inactivation in PCs results in radial expansion arrest in P6 retinas.....	171
Figure 4.29. p110 α inactivation in PCs did not result in radial expansion defects in P9 retinas.	172
Figure 4.30. p110 α inactivation do not affect the vascular density, sprouts or filopodia in the vascular front of the retina.....	173
Figure 4.31. p110 α inactivation do not affect the vascular density in the remodelling plexus.....	174

Figure 4.32. p110 α inactivation do not affect the EC proliferation in the sprouting front.....	174
Figure 4.33. p110 α inactivation do not affect PC proliferation in the remodelling plexus.....	175
Figure 4.34. p110 β inactivation in PCs results in reduced radial expansion in P6 retinas.....	176
Figure 4.35. p110 β inactivation in PCs do not affect radial expansion in P9 retinas.....	177
Figure 4.36. p110 β inactivation leads to reduced vascular density but not impacts in the sprouts or filopodia in the vascular front of the retina.....	177
Figure 4.37. p110 β inactivation in PCs results in reduced vascular density in the remodelling plexus.....	178
Figure 4.38. p110 β inactivation in PCs resulted in EC proliferation arrest in the sprouting front.....	179
Figure 4.39. p110 β inactivation in PCs resulted in EC proliferation arrest in the remodelling plexus.....	180
Figure 4.40. p110 β inactivation in PCs did not affect cell death in the vasculature.....	181
Figure 4.41. p110 β inactivation leads to increased deposition of collagen IV in angiogenic front.....	182
Figure 4.42. PTEN inactivation results in increased PC coverage in the angiogenic front and slight reduced PC coverage in the remodelling plexus of the P6 retina.....	184
Figure 4.43. PTEN inactivation results in increased PC coverage in the angiogenic front and no changes in the remodelling plexus of the P9 retina...	185
Figure 4.44. PCs morphology changes after PTEN inactivation.....	186
Figure 4.45. PTEN inactivation in PCs results in reduced expansion of the plexus in P9 retinas.....	187
Figure 4.46. PTEN inactivation results in higher vascular density in the angiogenic front area.....	187

Figure 4.47. PTEN inactivation do not changed the vascular density in the remodelling plexus area.....	188
Figure 4.48. Pharmacological inhibition of p110 β -Class I PI3K in RIP1-Tag2 leads to a slight reduction of overall survival but impairs tumour progression.	191
Figure 4.49. Pharmacological inhibition of p110 β -Class I PI3K in RIP1-Tag2 leads to PC depletion.....	192
Figure 4.50. Pharmacological inhibition of p110 β -Class I PI3K in RIP1-Tag2 do not affect metastasis.....	193
Figure 5.1. Schematic model of PI3K and PTEN regulation of PCs during sprouting angiogenesis.....	211

List of Tables

Table 1.1. Murine PC Markers.....	52
Table 3.1. Mouse lines.....	102
Table 3.2. PCR conditions and primers.....	105
Table 3.3. List of primary antibodies used for immunofluorescence in mouse.....	109
Table 3.4. List of secondary antibodies used for immunofluorescence in mouse.....	110
Table 3.5. List of primary antibodies used in RIP1-Tag2 studies.....	121
Table 3.6. PI3K inhibitors used <i>in vitro</i>	137
Table 3.7. Reducing agents, phosphatase and protease inhibitors used for the different lyses buffers.....	133
Table 3.8. Primary antibodies used for immunoblotting.....	133
Table 3.9. Secondary antibodies used for immunoblotting.....	134
Table 3.10. ECL protocol.....	134
Table 4.1. PI3K inhibitors.....	149

List of abbreviations

(HIF)-1 α hypoxia-inducible factor

4E-BP1 4E-binding protein 1

AJ Adheren junction

AKT Protein kinase B

ALK Activin receptor-like kinase

AMIS Apical membrane initiation site

ANG Angiopogetin

APC/C Anaphase-promoting complex or cyclosome

ARF ADP-ribosylation factor

Axl Axl receptor tyrosine kinase

BAD Bcl-2 associated death promoter

BCRs B cell receptors

BM Basement membrane

BTK Bruton's tyrosine kinase

CD13 alanyl (membrane) aminopeptidase

CDC42 Cell division control protein 42 homolog

CDC6 Cell division control protein 42 homolog

CDH1 Cadherin-1 presursor

CDKI cyclin-dependent kinase inhibitor

CREB Cyclic-AMP response element-binding protein

DAPI 4',6-diamidino-2-phenylindole

DAPT N-[N-(3,5-Difluorophenacetyl)-L-alanyl]-S-phenylglycine t-butyl ester

DII4 Delta-like 4

DMSO Dimethyl sulfoxide

DNA Deoxyribonucleic acid

DTT Dithiothreitol

EC Endothelial cell

ECM Extracellular matrix

EdU 5-ethynyl-2-deoxyuridine

eNOS Endothelial nitric oxide synthase

ERG ETS-related gene

ETS2 Euro Truck Simulator 2

FAK Focal adhesion kinase

FBS fetal bovine serum

FGF Fibroblast growth factor

FKHR Forkhead

Flt-1 Fms-like tyrosine kinase 1 (VEGFR-1)

Flt-4 Fms related tyrosin kinase 4 (VEGFR-3)

FoxC1 Forkhead box protein C1

FoxC2 Forkhead box protein C2

FoxM1 Forkhead box protein M1

FoxO Forkhead box O transcription factors

GAB GRB2-associated-binding protein

GAP GTPase-activating protein

GEFs Guanine nucleotide exchange factors

GFP Green fluorescent protein

GPCR G-protein-coupled-receptor

GSK3 Glycogen synthase kinase 3

GSK-3A Glycogen synthase kinase-3 alpha

GSK-3B Glycogen synthase kinase-3 beta

HER2 Human Epidermal Growth Factor Receptor 2

Hes Hairy enhancer of split

Hey Hairy and enhancer-of-split related with YRPW motif protein

HHT Hereditary hemorrhagic telangiectasia

HIF Hypoxia inducible factor

HIF-1 α hypoxia inducible factor α

Hsp90 Heat shock protein 90

HSPGs Heparin sulfate proteoglycans

IF Immunofluorescence

IKK I κ B kinase

iSH2 Inter-SH2 domain

JNK c-Jun N-terminal kinases

MAPK mitogen-activated protein kinase

MC Mural cell

MDM2 Mouse double minute 2 homolog

miRs MicroRNAs

mLECs Mouse lung EC

MMPs Matrix metalloproteinases

MT1-MMP Membrane type 1-matrix metalloproteinase 1

mTORC1 Mammalian target of rapamycin complex 1

mTORC2 Mammalian target of rapamycin complex 2

MVD Microvascular density

NaCN Sodium cyanide

N-cadherin Neural cadherin

NCID Notch intracellular domain

NDST N-deacetylase/N-sulfotransferase

NEDD4 Neural precursor cell expressed developmentally down-regulated protein 4

Nek2A

NFAT Nuclear factor of activated T cells

NF- κ B Factor nuclear kappa B

NG2 Neural-glia 2

NICD NOTCH intracellular domain

NLS Nuclear localization signal or sequence

NMII Non-muscle myosin II

NO Nitric oxide

Nrarp NOTCH-Regulated Ankyrin Repeat Protein

NRP Neuropilin, also NP

ON Overnight

p110 α Protein encoded by the PIK3CA gene

p16INK4A Cyclin-dependent kinase 4 inhibitor A

p21Cip1/Waf1 Cyclin-dependent kinase inhibitor

p53 Tumour protein 53

PAGE Polyacrylamide gel electrophoresis

PAK Serine/threonine-protein kinase

PAR3 Partitioning defective 3 homolog

PAR6 Partitioning defective 6 homolog

PBS Phosphate-buffered saline

PBST Phosphate-buffered saline-Tween 20

PBSTX Phosphate-buffered saline-Tween 20- Triton-X 100

PC PC

PCR Polymerase chain reaction

PDGF-B Platelet-derived growth factor-B

PDGFR β Platelet-derived-growth factor receptor beta

PDK-1 Phosphoinositide-dependent kinase 1

Pdxl2 Podocalyxin 2

PFA Paraformaldehyde

PFBC Primary familial brain calcification

PH Pleckstrin homology

PHS Primary head sinus

PI Phosphatidylinositide; see also PtdIns

PI3K Phosphoinositide 3-kinase

PIGF Placenta growth factor

PIK3CA Phosphatidylinositol-4,5-Bisphosphate 3-Kinase Catalytic Subunit Alpha; p110 α

PIKfyve Phosphatidylinositol-3-Phosphate/Phosphatidylinositol 5-Kinase, Type III

PIP Phosphatidylinositol 3-phosphate; see also PtdIns(3)P

PIP2 PtdIns 4,5-bisphosphate; see also PtdIns(4,5)P2

PIP3 PtdIns 3,4,5-trisphosphate; see also PtdIns(3,4,5)P3

PLK1 Polo Like Kinase 1

PRAS40 Proline-rich AKT substrate

pS6 Phospho-s6 ribosomal protein

PtdIns Phosphatidylinositide; see also PI

PtdIns(3)P Phosphatidylinositol 3-phosphate; see also PIP

PtdIns(3,4)P2 PtdIns 3,4-bisphosphate

PtdIns(3,4,5)P3 PtdIns 3,4,5-trisphosphate; see also PIP3

PtdIns(4,5)P2 phosphatidylinositol 4,5-bisphosphate; see also PIP2

PtdIns4P PtdIns-4-phosphate

PTEN Phosphatase and tensin homolog

PX Phox homology

Pyk2 Proline-rich tyrosine kinase 2

PyMT Polyoma middle T

RAC Ras-related C3 botulinum toxin

RAC1 Ras-related C3 botulinum toxin substrate 1

RBD RAS binding domain

RGS5 G protein signalling 5

RHEB Ras homologue enriched in brain

ROCK Rho-associated protein kinase

RT Room temperature

RTKs Tyrosine kinase receptors

S1P Sphingosine-1-phosphate

S1P1-5 G-protein coupled receptor

S6K p70 ribosomal protein S6 kinase

SDF Stromal cell-derived factor

SDF-1a Stromal cell-derived factor 1

SDF-1 α stromal cell-derived factor

SEM Standard error of the mean

Sema3 Semaphorin3

SGO1 Shugoshin 1

SH2 Src-homology 2

siRNA Small interference RNA

SKP2 F-box protein

Src Proto-oncogene tyrosine-protein kinase

TBS Tris-buffered saline

TBST Tris-buffered saline with tween

TCL Total cell lysate

TCRs T cell receptors

TGF β Transforming growth factor beta

TJs Tight junctions

TNF α Tumor necrosis factor alfa

TSC2 Tuberous sclerosis 2

VCAM-1 Vascular cell adhesion molecule 1

VE-cadherin Vascular endothelial cadherin

VEGF Vascular endothelial growth factor

VEGFR Vascular endothelial growth factor receptor

VM Venous malformations

vSMC Vascular smooth muscle cell

ZO1 Zonula occuldens-1 protein

α -SMA Alpha-smooth muscle actin

ERT2 Human estrogen receptor

BrdU 5-bromo-2'-deoxyuridine

EdU 5-ethynyl-2'-deoxyuridine

Tag T-antigen

PanNETs Pancreatic neuroendocrine tumours

1. Introduction

1.1. Blood vessels and their origin

The cardiovascular system is formed by the heart, blood and a large network of blood vessels, comprised of arteries and veins (large vessels), arterioles, venules and capillaries (smaller vessels). It supplies the body with oxygen and nutrients and removes the waste products of metabolism. This system starts to develop early during embryonic development. In fact, this network constitutes the first organ system that is developed in the embryo and after birth, blood vessel formation continues to facilitate growth and repair. Problems in the formation of blood vessels during early stages of development are often lethal (Adams and Alitalo, 2007; Carmeliet, 2005).

Blood vessels are formed by several layers that differ between different vessel types, depending on their size and function. Thus, large vessels (arteries and veins) are formed by three layers: 1) the *tunica intima*, formed by endothelial cells (ECs), the basement membrane (BM) and an elastic layer; 2) the *tunica media*, formed by multiple layers of a type of mural cells (MCs) called vascular smooth muscle cells (vSMC) and elastin and 3) the *tunica adventitia* formed by connective tissue. Smaller vessels, like capillaries, are formed by ECs, the MCs from the microvessels called pericytes (PCs) and the BM. During development, blood vessels can be mainly formed by two sequential processes: **vasculogenesis** and **angiogenesis** (Figure 1.1) (Adair and Montani, 2010; Carmeliet, 2005).

Vasculogenesis is the formation of blood vessels from mesoderm-derived EC precursors called angioblasts. Mesodermal stem cells differentiate into hemangioblasts that give rise to hematopoietic stem cells and angioblasts. Angioblasts, in turn, have the capacity to differentiate into ECs, they start to migrate and aggregate forming blood islands, finally lining up to form a network of tubes formed by differentiated ECs. This process involves cell to cell and cell to extracellular matrix (ECM) interactions that are regulated spatially and

temporally by different kinds of molecular factors. Vasculogenesis takes place mainly during early development, however, it can also occur in certain pathologies like tumours, ischemia and endometriosis (Adair and Montani, 2010; Potente et al., 2011).

Angiogenesis, on the other hand, is the formation of the vessels from pre-existing ones. It takes place after early embryogenesis and proceeds throughout life, in both health and disease. Angiogenesis starts with the sprouting of new vessels followed by the formation of vascular loops by the connection with other vessels (anastomosis) and the stabilization of the vascular network by vessel pruning (Adair and Montani, 2010; Betz et al., 2016; Potente et al., 2011). This process is complex and tightly regulated by multiple molecular pathways that control not only ECs but also perivascular cells. There are different types of angiogenesis: the **intussusceptive angiogenesis** and **sprouting angiogenesis**:

1.1.1. Intussusceptive angiogenesis

This type of angiogenesis involves the formation of blood vessels through a splitting process, where the vessel wall extends into the lumen causing a single cell to split into two (Adair and Montani, 2010; De Spiegelaere et al., 2012). PCs actively participate in this type of angiogenesis, where they are responsible for the secretion of ECM components and for the maturation and stabilization of the newly formed vessels (Díaz-Flores et al., 2009). Blood vessels are remodelled with minimal ECs proliferation and migration, and without proteolysis of ECM components. Therefore, this type of angiogenesis is faster and more efficient when compared to the sprouting angiogenesis as it only requires reorganization of ECs and does not rely on cell proliferation or migration. Intussusceptive angiogenesis plays a major role in the vascular development of embryos, where growth is fast and the nutrients and gases are limited (Adair and Montani, 2010; De Spiegelaere et al., 2012).

1. Introduction

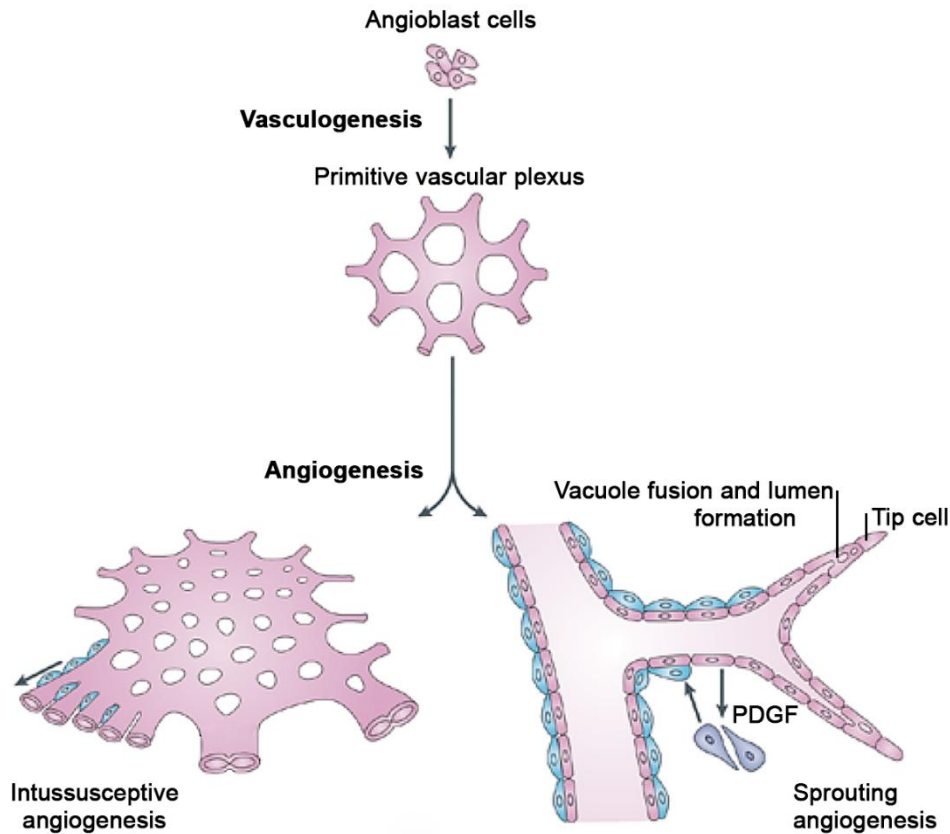


Figure 1.1. Blood vessel formation. Blood vessels can be formed mainly by two types of processes: the vasculogenesis and the angiogenesis. In the vasculogenesis EC differentiate from precursor angioblasts cells to form a primitive plexus of capillaries, which remodel and expand by angiogenesis. Angiogenesis can occur by intussusceptive or sprouting angiogenesis. Intussusceptive angiogenesis (on the left) involves the splitting, by the formation of translumen pillars (arrow), and growing of vessels in a metabolically efficient manner. In sprouting angiogenesis (on the right), EC proliferate behind the tip cell of a growing branch in response to different types of cytokines such as vascular endothelial growth factor (VEGF). Both forms of angiogenesis require the recruitment of MCs that, among others, can be regulated by platelet-derived growth factor subunit B (PDFB) secreted by the ECs (Adapted from (ten Dijke and Arthur, 2007).

1.1.2. Sprouting Angiogenesis

Sprouting angiogenesis is the most common process by which vessels expand during the vascular development. In hypoxic or nutrient-deficient conditions, different types of growth factors and chemokines start to be secreted from tissues, stimulating ECs from the vessel wall to form a new sprout and, thus, supply the tissues with nutrients (Adair and Montani, 2010; De Spiegelaere et al., 2012). Therefore, during this process several signalling

pathways are involved promoting the correct vascular development. Briefly, upon the release of pro-angiogenic factors, ECs and PCs become active in promoting (by matrix metalloproteinases (MMPs)-dependent mechanisms) remodelling processes in the cell-cell junctions (vascular endothelial (VE)-cadherin, ZO-1, and others) and the enzymatic degradation of the BM. PCs start to detach from the vessel and migrate, allowing tip cells' migration in response to guidance signals. Subsequently, the sprout elongates by proliferation of stalk cells, which ends up with the formation of a lumen. Tip cells from the neighbouring sprouts encounter and anastomose to form a perfused branch. Upon perfusion, ECs become quiescent phalanx cells, deposit BM, establish a barrier and are covered by mature PCs (Díaz-Flores et al., 2009; Welte et al., 2013) (Figure 1.2).

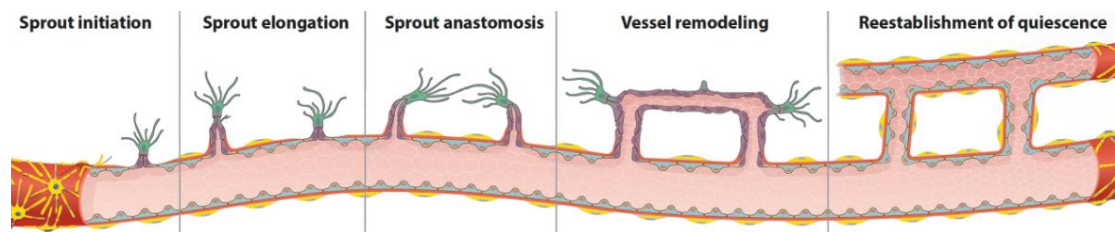


Figure 1.2. The different cellular events occurring during sprouting angiogenesis. The sprout initiation and elongation, sprout anastomosis, vessel remodelling, and the reestablishment of vessel quiescence (Adapted from (Potente and Carmeliet, 2016)).

1.1.2.1. Activation of a quiescent vessel and basement membrane degradation

ECs and PCs share the BM which is formed by proteins that create a sleeve around the endothelial tubules (Eble and Niland, 2009). In fact, the BM and the coat of PCs prevent ECs from leaving their positions and therefore allowing vessel stabilization.

During the initial phase of vascular sprouting, quiescent vessels must be activated and ECs liberated in a process that requires proteolytic breakdown of the BM and detachment of PCs. Different pro-angiogenic factors, such as the vascular endothelial growth factor A (VEGF-A) and proteases of the class of

1. Introduction

matrix metalloproteinases (MMPs) can promote this process (Potente et al., 2011).

VEGF-A promotes changes in endothelial polarity, junctions and in the degradation of the BM (Glaser et al., 2010; Potente et al., 2011). Additionally both, ECs and PCs when activated can degrade the BM via secretion of MMPs. In fact, PCs, can produce MMPs such as MMP2, MMP3 and MMP9 promoting EC migration in the surrounding ECM (Caporali et al., 2016)

Moreover, activated PCs start to swell in order to shorten their metabolic processes and to increase their somatic volume, adopting an “angiogenic phenotype” (Díaz-Flores et al., 2009). The PCs detachment is stimulated by angiopoietin-2 (Ang-2), an angiogenic growth factor stored by ECs for rapid release (Augustin et al., 2009). In this stage, PCs start to migrate, their number in the parent vessels decreases and PC/endothelium surface contacts become markedly lower (Figure 1.3.) (Díaz-Flores et al., 1991, 2009).

1.1.2.2. Tip and stalk cell selection

Sprouting blood vessels are formed by two different types of ECs populations: the **tip cells**, which guide the sprouts allowing attractive and repulsive directional signals through present dynamic filopodia; (Phng and Gerhardt, 2009) and the **stalk cells**, which constitute the base of the sprout and maintain the connection to the parental vessel (Phng and Gerhardt, 2009; Siekmann et al., 2013).

VEGF stimulates the VEGF receptor 2 (VEGFR2) that when internalized, triggers the activation of ERK1/2 signalling pathway promoting tip cell migration towards the gradient of VEGF-A (Walti et al., 2013). The filopodia facilitate the migration towards the ECM area, secreting large amounts of proteolytic enzymes and they act as a sensor of VEGF-VEGFR, pulling the tip along the VEGF-A stimulus (Adair and Montani, 2010; Walti et al., 2013). It is also known that PCs can determine the sprout formation and guidance of the new vessel formed, migrating ahead of ECs and expressing VEGF (Bergers and Song, 2005; Díaz-Flores et al., 2009; Morikawa et al., 2002; Ozerdem et al., 2005).

The neighbouring ECs in the vessel wall then follow the tip cell to form stalk cells, that elongate the newly formed vascular sprout through cell proliferation (Caporali et al., 2016) and are responsible for the formation of a vascular lumen and the establishment of adherent and tight junctions to maintain the integrity of the new sprout (Dejana et al., 2009; Gerhardt et al., 2003).

Additionally, Notch pathway controls the tip and stalk EC specification upon VEGFR activation (Eilken and Adams, 2010; Phng and Gerhardt, 2009). Therefore, VEGFR2 activation in ECs leads to an increased expression of the Notch ligand Delta-like 4 (Dll4), which binds to Notch receptors in the neighbouring ECs. The signalling triggers the release of the Notch intracellular domain (NICD) that acts as a transcriptional factor, down-regulating Dll4 expression and up-regulating canonical target genes such as Hes, Hey and Nrap, leading to the inhibition of tip cell phenotype, and thus, promoting the differentiation into stalk cell (a process named lateral inhibition). Moreover, the activation of Dll4 leads to a reduction of VEGFR2 expression in stalk cells and increase of the levels of VEGFR1, making those cells less sensitive to VEGF (Welti et al., 2013).

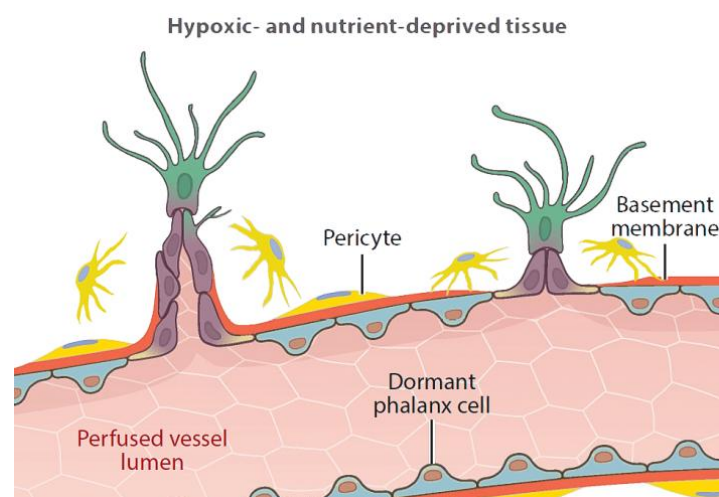


Figure 1.3. Activation of quiescent vessel. Upon secretion of different pro-angiogenic factors quiescent vessels are activated. PCs started too detached from the vessel allowing EC migration and growth. In the leading edge of the vasculature sprouting blood vessels are formed by two types of EC populations: the tip cell that guide the sprout and the stalk cell, which maintain the connection to the parental vessel (*Adapted from (Potente and Carmeliet, 2016)*).

1.1.2.3. Sprout anastomosis

Vascular anastomosis is the process that generates connections between angiogenic sprouts and blood vessels, being fundamental for vascular network formation. This process can happen between two sprouts, involving two tip cells ('head-to-head' anastomosis), or between sprouts and a functional blood vessel, involving only one tip cell ('head-to-side' anastomosis) (Figure 1.4) (Betz et al., 2016).

Anastomosis starts from the formation of filopodia contacts between sprouts that stabilize in one location and that are reinforced by the deposition of adherent junction (AJ) proteins, such as Cdh5/VE-cadherin, at the contact site (Lenard et al., 2013; Phng et al., 2013). An apical membrane initiation site (AMIS) is formed at this contact site and an apical membrane is added. After the formation of such contacts and EC polarization, an interconnected luminal space and multicellular perfused tubes start to develop by two different cellular mechanism: anastomosis type I (for lumenized sprouts) and anastomosis type II (non-lumenized sprouts) (Betz et al., 2016).

In type I anastomosis, apical membrane starts to form invaginations through blood pressure and fuse at the contact sites, generating a unicellular tube containing cells with a transcellular lumen. The transition from a unicellular to a multicellular tube in type I anastomosis involves cell rearrangements and cell splitting (Gebala et al., 2016; Lenard et al., 2013). The type II anastomosis occurs in the absence of blood. The occurrence of this mechanism is different between the vascular beds and depends on the degree of blood pressure and the presence or absence of a lumen in the participating tip cells (Helker et al., 2013).

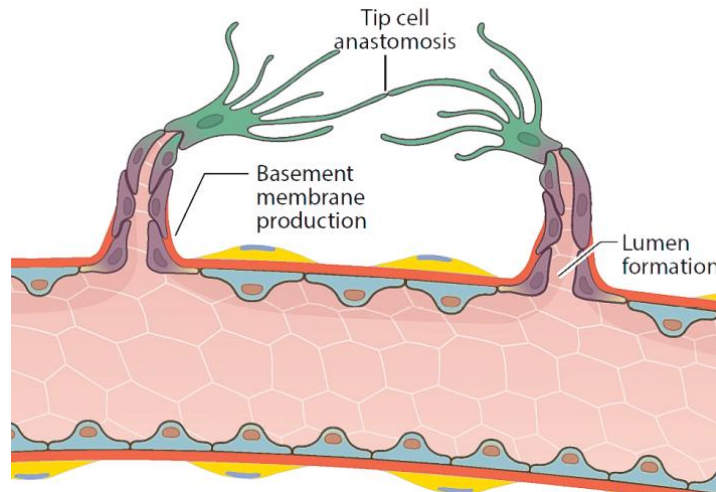


Figure 1.4. Vascular anastomosis and lumen formation. Sprout anastomosis can be initiated by the formation of filopodia contacts between two sprouts involving two tip cells (‘head-to-head’ anastomosis), which eventually stabilize in one location. To give rise a functional vessel a proper lumen have to be formed and expanded (Adapted from (Potente and Carmeliet, 2016)).

1.1.2.4. Lumen formation

Vessels need lumen for a proper function (Figure 1.4). Lumen formation can occur by means of different types of mechanisms in the vasculature, such as cord hollowing, cell hollowing, transcellular lumen formation and lumen ensheathment. In angiogenic sprouts, the formation of lumen is still a matter of discussion as different blood vessels may use different mechanisms for lumen formation. It was shown that the main mechanisms are the cell hollowing, during which the lumen is generated by intracellular (pinocytic) vacuoles that interconnect with vacuoles from neighbouring ECs; and the cord hollowing, where ECs go through shape changes and rearrange their junctions to create a central lumen (Herwig et al., 2011; Lenard et al., 2013). However, Gebala *et al.* recently have proposed the formation of “inverse blebs” that protrude into the surrounding EC and start to recruit actomyosin to respond to the local deformation, allowing the progression of lumen formation (Gebala et al., 2016). Also, Helker *et al.* suggest that ECs migrate collectively as a sheet over the blood stream and eventually at the lateral edge start to migrate downwards and engulf the lumen, in a process called lumen ensheathment (Helker et al., 2013).

1. Introduction

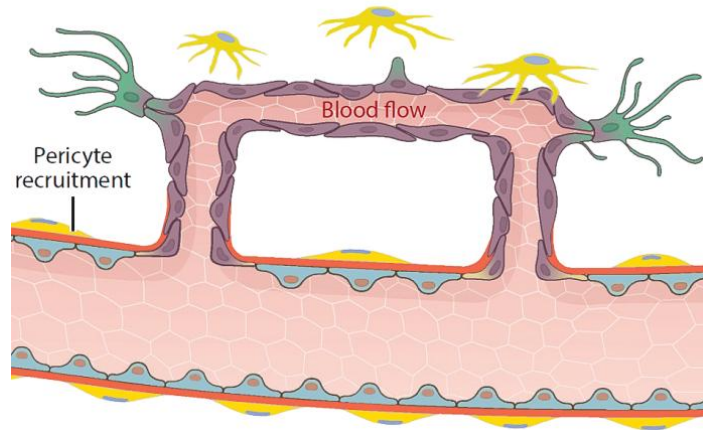


Figure 1.5. PCs recruitment. The recruitment of PCs is essential to vascular stabilization and maturation. (Adapted from (Potente and Carmeliet, 2016)).

1.1.2.5. Vascular maturation and stabilization

In order to become functional, vessels must mature and stabilize. At the network level, maturation involves remodelling into a hierarchically branched network and adaptation of vascular patterning to local tissue needs (Potente et al., 2011). Blood flow is a determinant factor that is decisive for vessel fate: vessels with a high flow expand and vessels with a low flow regress (le Noble et al., 2004). Arteries form a high-pressure system that allows the blood transportation into capillaries, whereas veins face low-pressure gradients (Potente et al., 2011).

Different cellular and non-cellular components in the blood vessels are coordinately involved in the regulation of vessel stability, which includes three major steps: the formation of tight junctions between ECs and the vessels, the formation of an ECM and the recruitment of PCs (Patel-Hett and D'Amore, 2011; Stratman and Davis, 2012; Xu and Cleaver, 2011).

EC-EC junctions play a key role in maintaining vessel integrity and vessel permeability, being considered as essential for vascular maturation. In the endothelium, junctional complexes include AJs, tight junctions (TJs) and Gap junctions (Bazzoni and Dejana, 2004). AJs are responsible for the initiation of cell-to-cell contacts and are formed by members of the cadherin family, where

the transmembrane adhesive protein - VE-cadherin - is one of the most important ones (Bazzoni and Dejana, 2004; Dejana et al., 2009; Vestweber, 2007). TJs, such as claudin family (principally Claudin-5), also mediate adhesion and communication between neighbouring cells, and are specifically involved in the regulation of paracellular permeability and cell polarity (Bazzoni and Dejana, 2004). Finally, the formation of Gap junctions structures allows the passage of small molecular weight solutes between neighbouring cells.

The other important aspect of the vascular stabilization is the deposition of the ECM into the BM. The ECM provides necessary contacts between ECs and the surrounding tissues, preventing the vessels from collapsing. In quiescent vessels, ECs and PCs share the same BM that is formed by collagen IV, laminin, elastin and other components (Carmeliet, 2003). The newly formed vessels then start to recruit PCs to ensure stabilization and maturation of the vasculature (Figure 1.5 and 1.6). ECs release chemokines, such as platelet-derived-growth factor B (PDGFB) that bind to its receptor platelet-derived-growth factor receptor beta (PDGFR β) on PCs, leading to their recruitment (Caporali et al., 2016). This PCs coverage first contributes to the stability of new vessels by creating the BM in cooperation with ECs and then promotes endothelial maturation and endothelial barrier formation by the release of paracrine factors like transforming growth factor beta (TGF β) and Ang-1. Additionally, TGF β secreted by ECs triggers the activation of TGF β receptor 2 on PCs, which in turn promotes the inhibition of PCs proliferation and stimulate the production of contractile and ECM proteins, leading to PCs attachment by upregulation of N-cadherin through Notch signalling (Caporali et al., 2016).

1. Introduction

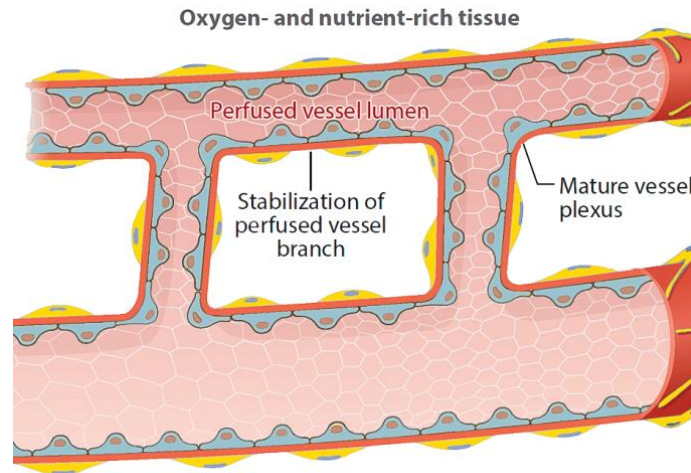


Figure 1.6. Vessel maturation and stabilization. Sprouting angiogenesis results in new formed and stable vessels. (*Adapted from (Potente and Carmeliet, 2016)*).

1.1.2.6. Vessel regression

The other process of sprouting angiogenesis is a vessel regression (or pruning) that occurs during vessel network remodelling and maturation. Vessel regression is a mechanism of vasculature reorganization that allows the vascular system to adapt to changes in hemodynamical and metabolic effects. Thereby, pruning helps in the acquisition of a mature hierarchical and more efficient angioarchitecture (Ferrara and Kerbel, 2005).

Although, few studies have addressed the specific mechanisms it has been established that vascular regression happens as a coordination of two different phases: cessation of blood flow to the formed vessels and a gradual removal of vessel wall components (Baluk et al., 2004). Therefore, for regression to occur, vessels have to lose their integrity and stability as a result of degradation of the vascular BM, detachment of PCs from the vessels and/or unstable EC junctions (Benjamin et al., 1999).

The soluble proteases MMP-1 and MMP-10 increase tube regression by degradation of collagen type I (Davis and Senger, 2005; Saunders et al., 2005). MMP-10 cleaves collagen IV, laminin and perlecan, which are responsible for the establishment of vessel BM and the maintenance of vascular tube networks.

Moreover, overexpression of Ang2 results in impairment in the association of tumoural PCs and ECs leading to tumour vessel regression (Cao et al., 2007). Ang2 antagonizes Ang1-mediated Tie2 signalling and causes detachment or loss of PCs leading to vessel destabilization (Hammes et al., 2004).

VE-cadherin plays an important role in the maintenance of ECs junctions. However, VE-cadherin cleavage by proteases such as the disintegrin and metalloprotease ADAM10, diminishes the tight adhesion between cells. (Schulz et al., 2008).

ECs apoptosis induced mainly by Wnt signalling pathway and also ECs contractility mediated by Rho-kinase signalling result in retraction of vessel sprouting (Lobov et al., 2005; Mavria et al., 2006). Vessel regression may also be a consequence of loss or decrease in signals that promote EC survival and vessel stability such as PI3K/AKT and the ERK1/2-MAPK pathways (Im and Kazlauskas, 2007; Mavria et al., 2006).

1.1.2.7. Vessel quiescence

Once tissues are supplied with sufficient oxygen and nutrients, vessels start becoming quiescent. Therefore, VEGF expression is hampered and the endothelial oxygen sensors are inactivated, finally leading to a shift in the endothelial behaviour towards a quiescent phenotype (Potente et al., 2011). These ECs reduce their proliferation and blood vessels mature, however they still need to maintain their integrity. In this way VEGF released from ECs can act as a survival factor due to activation of pro-survival pathways such as the PI3K signalling cascade (Warren and Iruela-Arispe, 2010). Thereby, VEGF expression in blood vessels prevents ECs from becoming apoptotic and disrupting vessel integrity. Moreover, fibroblast growth factors (FGFs) and the Ang-1 / Tie-2 signalling pathways can also help to maintain vessel quiescence and survival by stabilizing EC-EC junctions and by suppressing mediators of the apoptotic pathway, respectively (Augustin et al., 2009; Beenken and Mohammadi, 2009).

1.2. PC Cells

All blood vessels are formed by an inner wall of ECs that is surrounded by the supportive cells called MCs. MCs, depending on their localization, are commonly subdivided into vSMC and PCs. vSMC are associated with vessels of a big calibre (arteries and veins), whereas PCs are present in the smallest ones (arterioles, venules and capillaries) (van Dijk et al., 2015).

PCs were described for the first time in the 1870s by Eberth (Eberth, C.J., 1871) and Rouget (Rouget, C., 1873) and called as “Rouget Cells”. Later on, Zimmermann (Zimmermann, K.W, 1923) renamed them as “PCs” referring to their localization in close proximity with ECs. The currently definition of a mature PC states that it is a cell embedded within the vascular BM of small blood vessels, being formed by a huge nucleus oriented to the abluminal side of the microvessel and with extended structures used to directly interact with the adjacent ECs (Allt and Lawrenson, 2001). Among other functions, PCs are key regulators of vascular development, being considered as the important angioregulators participating in vessel formation, remodelling and stabilization (Armulik, 2005; Kelly-Goss et al., 2014).

1.2.1. Ontogeny

The different cell types that form the vasculature do not arise from a single embryonic source, and cells from several sources can acquire the same fate (Bautch, 2011). PCs can be generated during embryonic and postnatal development (Armulik et al., 2011; Winkler et al., 2011) and, like vSMC, they can have different development origins (Majesky, 2007; Majesky et al., 2011).

During the embryonic development, MCs from the head and thymus come, in the majority, from the neural crest, whereas in the gut, lung, liver and heart a mesothelium origin has been suggested. Mesothelial cells undergo epithelial-to-mesenchymal transition (EMT), migrating into the organs where they can differentiate into fibroblasts, vSMCs and PCs. In the aorta, at least four

developmental origins were found (secondary heart field, neural crest, somities, and splanchnic mesoderm) (Armulik et al., 2011) (Figure 1.7). Bone marrow cells can also differentiate into cells that morphologically resemble PCs (Ozerdem et al., 2005). In addition, transdifferentiation from ECs has been suggested, although this is not a major route of PC formation during normal development (DeRuiter et al., 1997).

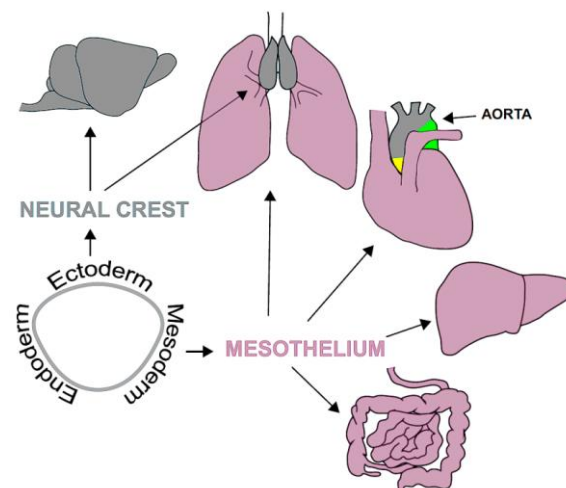


Figure 1. 7. Developmental Origin of Mural Cells. Ectoderm-derived neural crest gives rise to vSMCs and PCs in the (Central Nervous System) CNS and thymus (Gray). Mural cells in coelomic organs are all mesoderm- and mesothelium-derived (pink). Epicardial mesothelium gives rise to mural cells in heart, lung mesothelium to PCs in the lung, etc. The vSMC around aorta has a multiple developmental origins, indicated by different colours (yellow-secondary heart field; grey-neural crest; green-somite) (Adapted from (Armulik et al., 2011))

Less is known about how PCs grow and extend along growing vessels during postnatal development. PCs may be considered as progenitors and/or descendent cells (Díaz-Flores et al., 2009). It is not clear whether they can develop by the cell division of pre-existing ones, through the recruitment of pre-existing vSMCs and/or by differentiation from immature mesenchymal cells, or both. For example, in the CNS there is a lack of immature mesenchymal cells, which could suggest that the new PCs develop mainly by division of pre-existing ones (Armulik et al., 2011)

1.2.2. Distribution and morphology

PCs and vSMCs are thought to derive from the same lineage sharing different kinds of features such as the perivascular position in blood vessels (van Dijk et al., 2015). Despite the similarities, PCs and vSMC have different characteristics: vSMC are found in large vessels that are exposed to high levels of hemodynamic stress (arteries and veins), while PCs are mainly localized in the microvasculature (pre-capillary arterioles, capillaries and collecting venules) in a single layer of cells (Armulik et al., 2011; van Dijk et al., 2015). Even so, there is a gradual transition (a continuum of phenotypes) between PCs and vSMC in both terminal arterioles and venules (Valladares F. et al., 1991a). It was classically established by Zimmermann three types of PCs according to their localization: precapillary, capillary and postcapillary (Zimmermann, K.W., 1923). Also, vSMC are placed in a perpendicular way along the whole length of the vessel, encircling the entire endothelial surface. In contrast, PCs are attached to the longitudinal axis of the capillaries. Moreover, vSMCs normally maintain an elongated and flattened nucleus, while PCs are formed by a prominent nucleus, with a small amount of perinuclear cytoplasm that extends processes along the abluminal surface of blood microvessels (**Figure 1.8 A**) (Armulik et al., 2011; van Dijk et al., 2015).

PCs and ECs share the same BM, which covers the majority of PC-EC interface (Gerhardt and Betsholtz, 2003). It is known that PCs and ECs regulate BM assembly and that PCs probably contribute to BM products. Mature PCs are embedded within the BM, however it was also described as incomplete or even absent BM coverage in the immature vasculature or in pathological conditions where the BM is still synthesized or shows a high turnover (Figure 1.8 B) (Armulik et al., 2011; van Dijk et al., 2015). Distinct places where the BM is interrupted allow the direct contact between both cell types. Different types of connections are created between PCs and ECs and the number and size of these contacts may vary between the tissues. Peg-socket, close or occluding contacts, adhesion plaques, GAP and TJs are different types of connections between PCs and ECs: (1) in the peg-socket structures, PCs form cytoplasmic elongations (pegs) that are inserted in the invaginations of the

endothelial membrane (sockets) - these contacts are enriched in Connexin 43 mediated gap and (N-cadherin-based) adherence junctions; (2) the occluding contacts happens when the two membranes come very close together, and are located at the edge of the PCs processes playing an anchor role; (3) the adhesion plaques anchor PCs to the ECs via a matrix of fibronectin microfilament bundles that is connected to the cell's actin cytoskeleton via integrins; (4) Gap and TJs-like structures have also been reported. These junctional complexes facilitate the transmission of biological and mechanical signals between PCs and ECs (Armulik et al., 2011; van Dijk et al., 2015).

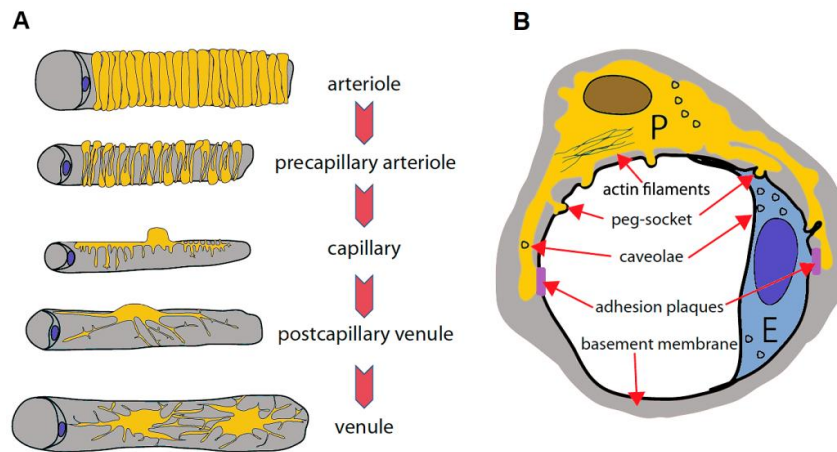


Figure 1. 8. PCs Anatomy. (A) Localization of PCs in the different types of vessel (from arteriole to venule). The arterioles and precapillary arterioles are formed by a single vSMC layer that encircles the entire abluminal side of the endothelium. vSMCs around arterioles have a flattened shape with few cytoplasmic process, whereas around precapillary arterioles the cell bodies are distinctly protruding and there are more cytoplasmic processes. The capillaries are surrounded by PCs formed by rounded cell body and present primary and secondary cytoplasmic processes. On postcapillary venules the vSMC body are flatted and present several branching processes, whereas vSMCs covering venules have a relatively big cell body with many branching processes, which, unlike arteriolar vSMCs, do not wrap circularly around the endothelium. (B) Ultrastructural characteristics of PCs and PC-EC interactions. The mature capillary PC (marked with P) has a discoid nucleus that is surrounded by a small amount of cytoplasm containing protein-producing organelles and mitochondria. Despite being separated by the shared BM, PCs and ECs (marked with E) make numerous direct contacts of different type: schematically depicted are peg-socket contacts and adhesion plaques (Adapted from (Armulik et al., 2011)).

1. Introduction

PCs are not present in all organs in the same proportion. PCs-ECs ratios can vary between 1:1 and 10:1, also PC coverage in the endothelial abluminal surface can range between 70% and 10% (Sims, 1986). These differences are: (1) organ specific, being positively correlated with endothelial barrier properties, for example the CNS is thought to be the organ with highest PCs coverage around microvessels; (2) are dependent of EC turnover, where more coverage of PCs is associated with less EC turnover; (3) and also linked with blood pressure, where we see large coverage in lower body parts (reviewed by (Armulik et al., 2011)). Lymphatic capillaries lack PCs, by a *Foxc2* and *VEGFR3* dependent mechanism that blocks its recruitment, whereas collecting lymphatic vessels show an vSMC layer with a absent BM (Petrova et al., 2004).

1.2.3. Identification

Although, morphologic, structural and spatial characteristics are used to identify PCs, the inherent complexity of these cells make difficult their identification since there are different types of perivascular cells in the microvasculature (Sims, 2000) and several types of PCs may co-exist in the same vascular bed (Kurz et al., 2008). Thus, the usage of several markers is important for the identification of PCs (Armulik et al., 2011), nevertheless none of them is specific or a general pan-PC marker (none recognizes all PCs) (Díaz-Flores et al., 2009).

There is a great number and variety of macromolecules that PCs may express, including growth factors, receptors, cytokines, enzymes and adhesion molecules (Table 1).

Table1.1. Murine PC Markers

PC marker	Other cell types expressing the marker	Comments	References
PDGFRβ (Platelet-derived growth factor receptor – beta)	Interstitial mesenchymal cells during development; Smooth muscle; In the CNS certain neurons and neuronal progenitors; Myofibroblasts; Mesenchymal stem cells	Receptor tyrosine kinase; Functionally involved in PC recruitment during angiogenesis; Useful markers for brain PCs	Lindahl et al., 1997; Winkler et al., 2010;
NG2 (chondroitin sulfate proteoglycan 4)	Developing cartilage, bone, muscle; Early postnatal skin; Adult skin stem cells; Adipocytes; vSMC; Neuronal progenitors; Oligodendrocyte progenitors	Integral membrane chondroitin sulfate proteoglycan; Involved in PC recruitment to tumour vasculature; Useful marker for retinal PCs	Ozerdem et al., 2001; Ruiter et al., 1993; Huang et al., 2010
CD13 (alanyl (membrane) aminopeptidase)	vSMC, inflamed and tumour endothelium; Myeloid cells; Epithelial cells in the kidney and gut	Type II membrane zinc-dependent metalloprotease; Useful marker for brain PCs	Demietzel and Krause, 1991; Kunz et al., 1994
αSMA (alpha-smooth muscle actin)	Smooth muscle; Myofibroblasts; Myoepithelium	Structural protein; Quiescent PC do not express α SMA; Expression in PCs is commonly upregulated in tumours and inflammation; Not expressed in retinal PC	Nehls and Drenckhahn, 1993
Desmin	Skeletal; Cardiac; Smooth muscle	Structural protein; Useful PC marker outside skeletal muscle and heart	Nehls et al., 1992
RGS5 (regulator of G protein signalling 5)	Cardiomyocytes?; vSMC	Regulate heterotrimeric G protein by activating GTPase activity; Angiogenic PC marker	Bondjers et al., 2003; Cho et al., 2003

1. Introduction

The most common are the **membrane markers**, which include the PDGFR β , CD146, aminopeptidase A and N (CD13), endoglin, and neural-glial 2 (NG2); and **cytosolic markers** such as α SMA, non-muscle myosin, desmin, vimentin, nestin and G protein signalling 5 (RGS5). However, all these markers showed a dynamic expression, being dependent on several factors: a) species-specificity (α SMA is expressed in PCs from chicken embryo brain, but not in PCs of mouse embryo and human brain do not express α SMA (Gerhardt et al., 2000); b) vessel type; c) quiescent or angiogenic stages of the blood vessels; d) tissue-specificity, and e) pathological conditions (Buschard et al., 1996; Dvorak and Feng, 2001; Schlingemann et al., 1996; Sundberg et al., 1993). Therefore, in order to identify the PC populations, a set of markers is used (Díaz-Flores et al., 2009). For instance, the PCs from capillaries of mouse retina are NG2⁺/ α -SMA⁻, whereas the PCs from arterioles and venules are respectively NG2⁺/ α -SMA⁺ and NG2⁻/ α -SMA⁻, but they all equally express CD146 and PDGFR β (**Figure 1.9**) (Crisan et al., 2012).

1.2.4. Functions

Over the last decades, several functions have been assigned to PCs such as: regulation of blood flow, immune functions, blood hemostasis and, the regulation of vascular development.

1.2.4.1. Regulation of blood flow

Several studies claim that PCs have the capacity to contract and to relax leading to the maintenance of local and tissue homeostasis, by the regulation of microvascular blood flow and modification of vessel calibre (Díaz-Flores et al., 1991; Sims, 2000). Therefore, there is much evidence that confirms these contractile proprieties: (1) PCs extend multiple processes that envelop and compress ECs, presenting several cytoskeletal elements that form a contractile apparatus; (2) they produce several contractile proteins, like actin, myosin,

tropomyosin and cyclic GMP-dependent protein kinase, whose expression is dependent on the tissue and the blood flow requirements; and also (3) express different kind of receptors that regulate contractility, such as endothelin receptor (endothelin-a vasoconstrictor produced by ECs), cholinergic and adrenergic receptors; (4) PCs respond to vasoactive substances like angiotensin II and nitric oxid, that are produced by ECs (Díaz-Flores et al., 2009).

1.2.4.2. Immune function

PCs were shown to display characteristics that resemble macrophage cells, such as the presence of lysosomes and an efficient capacity to uptake soluble small molecules (pinocytosis) and macromolecules (phagocytosis) (Díaz-Flores et al., 2009; Thomas, 1999). They also express the major histocompatibility complex (MHC) class II proteins, acting as antigen-presenting cells for T-lymphocytes, and are known to up-regulate their activity in response to tissue injury, specific diseases and bacterial infection. PCs that behave as macrophages (pericytal macrophages) may originate from bone marrow mesenchymal progenitors, named fibrocytes, and along with lymphocytes they can contribute to an immune response (Díaz-Flores et al., 2009).

1.2.4.3. Blood hemostasis

PCs can participate in the coagulation process after microvascular injury or rupture by the regulation and expression of several molecules. They interfere with the activation of the tissue factor, which is fundamental for the initiation of the extrinsic pathway of blood coagulation, coactivating factor IX and X, but also providing a membrane surface for the prothrombinase complex (Díaz-Flores et al., 2009; Kim et al., 2006).

1. Introduction

1.2.4.4. Regulation of vascular development

PCs play an active role in new blood vessel formation and stabilization. The process of angiogenesis is complex and is regulated by multiple molecular pathways in which PCs are key regulators, controlling the recruitment, ECM modulation, paracrine signalling and direct interactions with ECs, which will be further discussed below (Armulik et al., 2011; Caporali et al., 2016; Díaz-Flores et al., 2009).

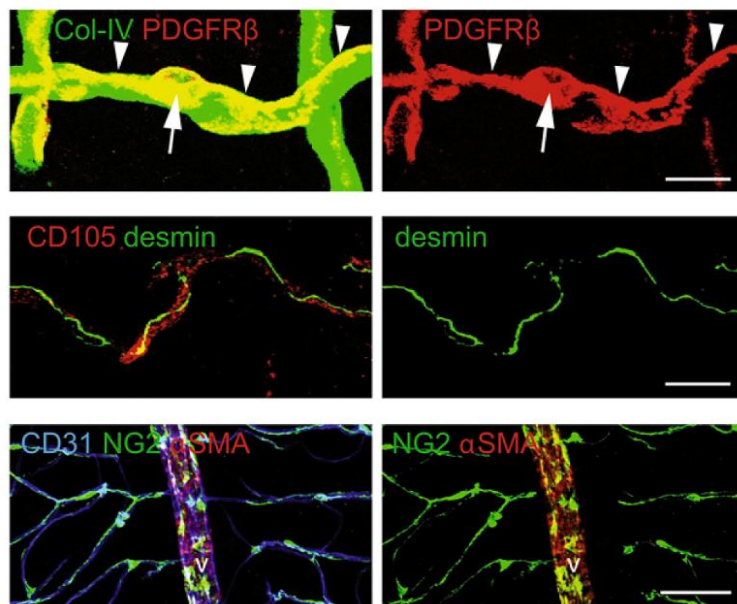


Figure 1. 9. PCs identification. Several markers are used to identify PCs but any of them is PC specific. In the upper panel the vascular BM of a brain capillary was identified by collagen IV (Col-IV, green) and PCs by PDGFR β (red) immunostaining. PC is well embedded in vessel BM, as seen by the yellow appearance on the merged image. The white arrow points to a typical PC cell body and the arrowheads indicate PC processes that stretch horizontally along the capillary. In the middle panel a tridimensional view of brain EC (CD105, red) and PCs (desmin, green). In the lower panel the triple immunostaining of endothelium (CD31, blue) and PCs (NG2, green) and vSMCs (α SMA, red) in the retina. vSMCs covering the vein (v) are positive for α SMA and occasionally also for NG2, whereas PCs surrounding the capillaries are α SMA negative and NG2 positive.

1.3. Signalling pathways implicated in PCs and in their paracrine regulation with the endothelium during sprouting angiogenesis

The paracrine and juxtacrine cross-talk between PCs and ECs is fundamental for angiogenesis and vessel stabilization. Therefore, several molecules and pathways are involved in this process allowing the correct vascular development (**Figure 1.10**) (Armulik et al., 2011; Caporali et al., 2016). The critical growth factors and signalling molecules involved in PCs biology and in their regulation with the endothelium are described below.

1.3.1. PDGF-B/PDGFR β

During angiogenesis the new formed vessel, susceptible to degradation, needs to be covered with PCs to be stabilized (Caporali et al., 2016). ECs starts to secrete platelet-derived growth factor beta (PDGF-B) which interacts with PDGFR β expressed on the surface of PC cells, triggering a cascade of events that leads to PC proliferation and migration into the new formed vessel (Betsholtz, 2004; Hoch and Soriano, 2003).

PDGF-B is not required for the initial induction of PCs but allows their expansion and spreading along the micro-vessels (Hellstrom et al., 1999). Knockout of the *PDGFB* or *PDGFR β* genes in mice results in identical phenotypes and into perinatal lethality due to vascular defects that rise from PC loss leading to endothelial hyperplasia and abnormal vascular morphogenesis (Crosby et al., 1998; Hellström et al., 2001a; Levéen et al., 1994; Lindahl et al., 1997; Soriano, 1994). Depletion of *PDGFB* specifically in ECs leads to reduction of PCs, showing that ECs are the main source of PDGF-B protein (Bjarnegård et al., 2004).

PDGF-B expression is only substantial at places of active angiogenesis (Hellstrom et al., 1999) and once secreted by tip cells it normally bonds to the extracellular matrix or on the cell surface by a C-terminal retention motif, which

1. Introduction

has affinity for heparin and heparin sulfate proteoglycans (HSPGs) (Abramsson et al., 2007; Gerhardt and Betsholtz, 2003; Kurup et al., 2006; Ostman et al., 1991). The location of PDGF-B in the cell surface or in the matrix-bound is essential for the correct signalling. Deletion of the retention motif (*PDGFB*^{ret/ret}) or the global reduction of N-sulfated heparan sulfate by knockout of N-deacetylase/N-sulfotransferase (NDST)-1 enzyme in mice, leads to hypoplasia and partial detachment of PCs (Abramsson et al., 2007; Lindblom et al., 2003).

To maintain a normal angiogenesis the interplay between PDGF-B and PDGFR β is essential. Moreover, in many pathologies this signalling pathway is compromised. In humans, null or loss of function mutations on both PDGF-B and PDGFR- β in heterozygosis leads to the onset of a pathology called primary familial brain calcification (PFBC), characterized by brain vessel calcifications, with accumulation of calcification deposits in PCs. Conversely, an increased expression of PDGF-B is associated with an increased angiogenesis in different type of tumours (reviewed by (Caporali et al., 2016)).

1.3.2. Sphingosine-1-phosphate

Sphingosine-1-phosphate (S1P) is secreted by PCs and it binds to a G-protein coupled receptor (S1P1-5) in ECs leading to adhesive, junctional and cytoskeletal changes and also affecting cellular proliferation, survival and migration (Allende and Proia, 2002). Therefore, S1P leads to PCs recruitment cooperating with PDGF-B/PDGFR β signalling. S1P-S1P1 receptor activation results in ECs adhesion to PCs promoting microtubule polymerization via Rac signalling and to the consequent trafficking of N-cadherin to polarized plasma membrane domains on ECs (Paik et al., 2004). Knockout of S1P1 (*edg1*) in mice resulted in PC depletion and as a consequence to an incomplete vascular maturation (Liu et al., 2000). Also, endothelial specific depletion of the receptor S1P1-5 leads to the same vascular defects as a global knockout, suggesting its endothelial-specific functioning (Allende et al., 2003).

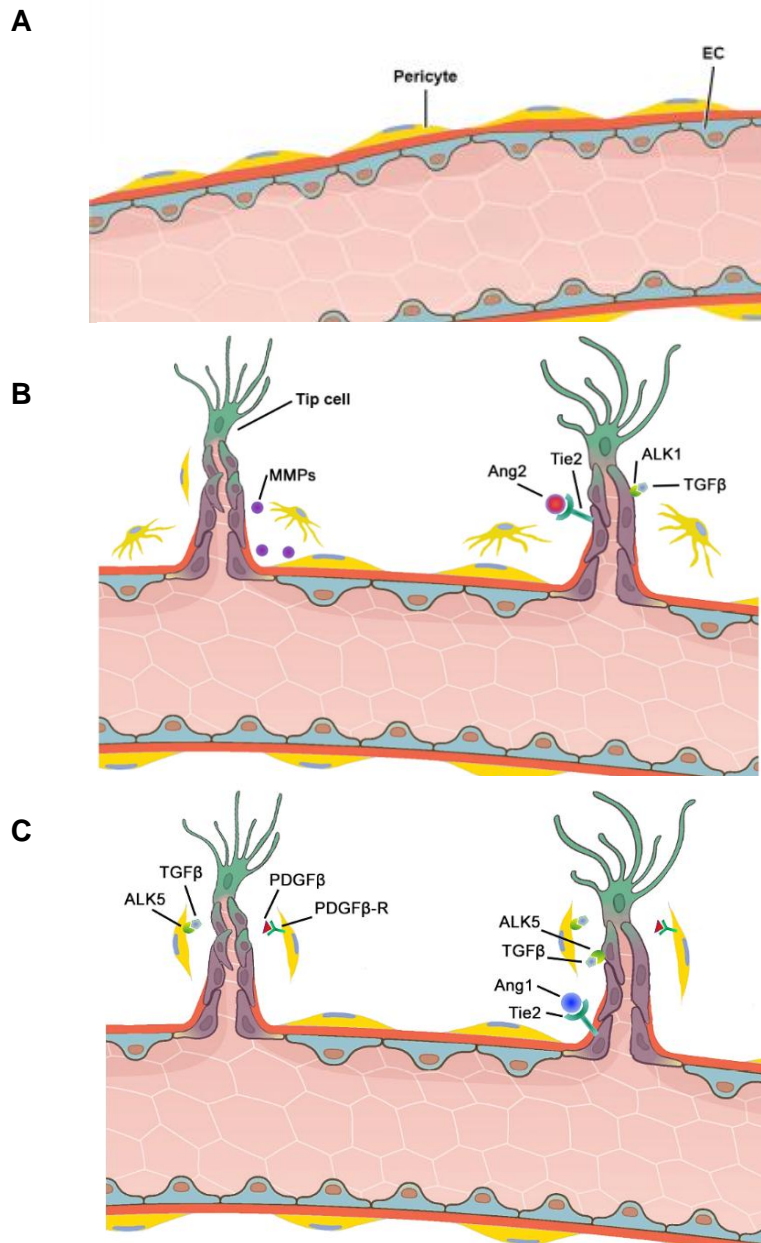


Figure 1.10. Signalling pathways regulating PCs and ECs cross-talk during the sprouting angiogenesis. (A) Before angiogenesis, PCs are attached to the long axis of capillaries, embracing ECs. (B) During the initial phase of vascular sprouting, angiogenic factors stimulate ECs to degrade the BM via secretion of MMPs. Activated PCs also produce several MMPs to support EC migration in the surrounding ECM. ANG-2-TIE2 and TGF β -ALK1 signalling contributes to the detachment of PCs from ECs. Detached EC from the pre-existing vessel is led by so-called endothelial tip cells, which become activated by stimulation of angiogenic factors. Neighbouring ECs follow the tip cell to form stalk cells, which elongate the newly formed vascular sprout by cell proliferation. (C) Since newly formed blood vessels are highly unstable with limited endothelial barrier integrity, ECs release chemokines, like PDGF β , to recruit PCs and initiate the vascular stabilization process. Recruited PCs further promote endothelial maturation and endothelial barrier formation by releasing paracrine factors, like Ang1 and TGF β , to suppress EC growth and migratory response. Vice versa, TGF β secreted by ECs binds to ALK5 in PCs, which inhibits PCs proliferation and stimulates the production of contractile and BM/ECM proteins (Adapted from (van Dijk et al., 2014)).

1.3.3. Angiopoietin-1 and 2

Angiopoietin-1 (Ang-1) is produced by perivascular cells in a region that is far from the leading edge of the new vessels, once secreted it stimulates the activation of its main receptor Tie-2 that is predominantly expressed in ECs (Armulik et al., 2011; Caporali et al., 2016; Ribatti et al., 2011). Tie-2 in ECs directly regulates adherent junctions reducing the phosphorylation of VE-cadherin and PECAM-1 (Gamble et al., 2000), leading to vascular maturation and stabilization. Also, Tie-2 activation can regulate PCs in a paracrine manner, stimulating ECs to secrete PDGF-B and TGF- β resulting in PC recruitment and vessel stabilization (Davis et al., 1996; Suri et al., 1996; Vontell et al., 2006). Ang-1 or Tie-2 loss of function causes mice to die at mid-gestation with cardiovascular problems (Dumont et al., 1994). These embryos present severe vascular defects, with the basement membrane of blood vessels poorly organized and reduced coverage and detachment of PCs (Patan, 1998; Suri et al., 1996). Mutations in *TIE-2* gene in humans also lead to venous malformation where loss of venous mural cells is shown (Vikkula et al., 1996).

Moreover, over-expression of Ang-2, a Tie-2 antagonist, results in PCs loss. Ang-2 is produced by ECs from the leading edge and acts autocrinally through interaction with Tie2 receptor, mediating PC loss and vessel destabilization (Hammes et al., 2004).

Vessel stabilization and maturation is dependent on the balance of Ang-1 and Ang2. The unbalance favouring Ang-2 leads to the impairment of angiogenesis, a common characteristic in pathological events such as diabetic retinopathy and tumour metastatisation (Durham & Herman, 2011).

1.3.4. Transforming growth factor- β

TGF- β is a cytokine implicated in many processes of the vascular development where it can have a pro- or anti-angiogenic role, depending on their context and concentration (Goumans et al., 2002; Vontell et al., 2006).

ECs and PCs express a latent form of TGF- β that can be activated upon contact of PCs with ECs by gap junction's formation between both cell types (Sato and Rifkin, 1989). Connexin-43 junction is expressed by ECs and PCs, and connexin-45 is MC specific. Mesenchymal cells deficient in connexin-43 when co-cultured with ECs do not complete MC differentiation and are able to produce latent TGF- β but not the activated molecule. Moreover, treatment with TGF- β restores the differentiation capacity and the production of the active molecule (Hirschi et al., 2003; Theis et al., 2001).

Also TGF- β receptors - activin receptor-like kinase (Alk)-1 and Alk-5 - are important regulators of the two cell types promoting opposite cellular events (Goumans et al., 2002, 2003; Oh et al., 2000). Activation of Alk-5 in mesenchymal cells leads to the phosphorylation of Smad2/3 leading to differentiation into MCs. On the other hand, activation of Alk-1 in ECs opposes this effect leading to the phosphorylation of Smad1/5 and inducing MCs proliferation and migration (Chen et al., 2003; Goumans et al., 2002; Ota et al., 2002). Additionally, Alk-1 signalling promotes EC proliferation and migration with Alk-5 involved in EC stabilization and maturation. However, a complex interaction between the two proteins has been suggested in this cell type, where Alk-1 inhibits Alk-5 but this last one is required for Alk-1 signalling. Alk-1 signalling is in this way more active in early phases of angiogenesis, stimulating cell proliferation and migration, and Alk-5 dominates in the latest phases, promoting cell differentiation, maturation and extracellular matrix production (Armulik et al., 2011).

Several knockout mutants related to the TGF- β signalling were described, *tgfb1* (Dickson et al., 1995), *alk1* (Urness et al., 2000), *alk5* (Larsson et al., 2001), *tgfbr2* (Oshima et al., 1996), *smad4* (Lan et al., 2007), *smad5* (Yang et al., 1999), and *endoglin* (Li et al., 1999), showing all embryonic lethality with severe vascular abnormalities, such as remodelling defects in the yolk sac vasculature, arterio-venous anastomoses, MCs formation deficiencies, and in some of them defective hematopoiesis (Armulik et al., 2011).

In humans, mutations in *ENDOGLIN*, *ALK1*, and *SMAD4* are related with the occurrence of a severe hereditary disorder, hereditary hemorrhagic telangiectasia (HHT), that is an autosomal-dominant disorder characterized by

1. Introduction

vascular malformations such as the formation of arterio-venous anastomoses (Berg et al., 1997; Gallione et al., 2004).

1.3.5. Other regulators

Other regulators have been also implicated in PCs functions during angiogenesis, promoting their recruitment, migration and proliferation or even maturation and stabilization.

HB-EGF, produced by ECs, have been implicated in PC migration, proliferation and protection of the cells from oxidative stress (Yu et al., 2012), leading to the activation of ErbB1, ErbB2 and ErbB4 receptors in MCs and as a result, cell migration is stimulated (Iivanainen et al., 2003; Stratman et al., 2010). Different *in vivo* studies have verified that PDGFB and EGF may collaborate in PC recruitment; HB-EGF inhibition also leads to reduced PC recruitment and vascular defects that remind PDGF-B/PDGFR β (Armulik, 2005; Armulik et al., 2011).

PDGFB-PDGFR β also leads to the activation of stromal cell-derived factor (SDF)-1 α promoting endothelial tube formation and maturation by stimulation of PC migration and vascular BM assembly (Song et al., 2009).

Shh signalling is also implicated in PC recruitment, by the activation of Patched (Ptc) receptor in these cells (Lindahl et al., 1997).

Notch signalling is critical for sprouting angiogenesis where it plays a major role on ECs (Chappell and Bautch, 2010; Sainson and Harris, 2008) however, it was also implicated in MCs regulation and in the interaction of both cells. Jagged-1 (Jag-1) expressed in ECs leads to the activation of Notch3 signalling in MCs promoting their maturation. Knockout mice of Notch3 presents a reduced expression of arterial vSMC markers, and also its over-expression in MCs leads to increased expression of certain vSMC markers (Domenga et al., 2004; Jin et al., 2008; Liu et al., 2009, 2010). During retinal angiogenesis Notch3 was also implicated in MCs recruitment and vessel maturation by a Ang-2 mediated mechanism (Liu et al., 2010). However this Ang-2 implication is not

clear, once other studies have implicated this protein as a vessel destabilizing factor (Hammes et al., 2004).

Ephrin-Eph receptor signalling was also implicated in MC biology, controlling PC migration and association with vessels probably by the regulation of focal adhesions. A MC-specific knockout of ephrin-B2 results in association defects of MCs with the vessels surrounded and abnormal extracellular matrix deposits (Foo et al., 2006).

Semaphorin-3-A (Sem3A) has also been related to vessel stabilization, promoting the increment of PCs coverage. This protein appears to work in synergy with TGF- β inducing vessel stability, by an unknown mechanism (Groppa et al., 2015). Down- regulation of this protein has been observed in different types of cancer with high metastatic potential, conferring poor prognosis to the patients (Jiang et al., 2015).

Also different cytokines are related to PCs and their paracrine communication with ECs promoting the correct vascular development. For instance, activation of NF- κ B in PCs leads to the up-regulation of different cytokines such as IL-8, IP-10 and RANTES stimulating ECs proliferation and promoting angiogenesis (LaBarbera et al., 2015).

1.4. PCs in cancer therapy

In normal tissues there is a balance between pro-angiogenic and anti-angiogenic factors that maintain tissue homeostasis and functions. However, in tumours, it was originally proposed that genetic (e.g., oncogenes) and epigenetic (e.g., hypoxia) mechanisms were deregulated, leading to an unbalance of these mechanisms promoting a more pro-angiogenic side. Aberrant tumour vessels promote tumour growth, metastasis and reduced efficacy of therapies especially in solid tumours, where the vessels are not able to adequately perfuse the tissue (Caporali et al., 2016). Therefore, vascular normalization constitutes, in theory, a good approach in order to prevent metastasis and increase oxygenation, thereby enhancing the effects of therapy

1. Introduction

and decreasing tumour volume (Cooke et al., 2012; Jain, 2009; Xian et al., 2006).

The first studies in tumoural PCs have shown increased coverage within the tumour vasculature, promoting tumour growth and resistance to anti-cancer agents (Bergers and Hanahan, 2008). Thus, traditional therapies with anti-angiogenic agents were directed to PCs (Meng et al., 2015) promoting the re-establishment of a normal structure and function of blood vessels (vascular normalization) (Jain, 2009, 2013). However, nowadays it is known that PC coverage of blood vessels in tumours is not homogenous (Eberhard et al., 2000). Some vessels, especially those surrounding the tumour, present high PC coverage in fact, creating a barrier that blocks the access to the immune system cells and to the therapeutic agents (Bergers and Hanahan, 2008). In contrast, highly metastatic tumours apparently show a reduced PC coverage, which causes a leakiness of the endothelial wall and cancerous cells extravasations and dissemination. In this case, a multi-target intervention acting on both angiogenesis and PC coverage, would be more beneficial for patients (Meng et al., 2015).

In the tumours with high PC coverage the inhibition of PC is an advantage. Therefore, several strategies were designed with the purpose of blocking PC function (Meng et al., 2015). Inhibition of PDGFR β or VEGFR alone seems to be insufficient in allowing cell-directed cancer therapies to penetrate the PC–EC shield. However, dual inhibition of VEGFR and PDGFR β reduces the protection to cancer cells and potentiates the effects of other therapies (Kłosowska-Wardęga et al., 2009; Taeger et al., 2011). It has been shown that this strategy is effective in both preclinical and clinical studies (Bergers and Hanahan, 2008).

In contrast, there are tumours with low PC coverage, where pro-angiogenic factors prevent PC coating of the vessel tips (Cooke et al., 2012; Greenberg et al., 2008; Korpisalo et al., 2008; Xian et al., 2006). This poor PC recruitment within the vessel leads to an excessive tumour angiogenesis, cancer cell extravasation, and further dissemination. Theoretically, multimodal therapy with agonists of PDGFR β , VEGFR and Tie-2 may reinforce PC–EC interactions, restricting vascular sprouting and preventing tumour angiogenesis (Meng et al., 2015).

1.5. Mouse models for studying vascular development in physiology and pathology

Several models are used to study angiogenesis, its mediators and new therapeutic targets. Frequently used *in vitro* models are: 1) the transwell chemotactic assays; 2) cell migration in scratch assays; 3) EC proliferation assays; 4) network formation in Matrigel®; and 5) three-dimensional angiogenesis assays such as the aortic ring. However, most of those *in vitro* tests focus on isolated steps of angiogenesis and do not fully recapitulate physiological conditions such as blood flow and the variety of EC's origin (Pitulescu et al., 2010). Therefore, to improve these limitations and attempt to accurately recapitulate angiogenesis, *in vivo* assays started to be used. The most common model systems for studying physiological and pathological angiogenesis are mouse and zebra-fish embryos, postnatal mouse retinas and a variety of tumour models (Pitulescu et al., 2010).

1.5.1. Retinal model

In the retina blood vessels, they undergo extensive changes during development. During gestation, the hyaloid vasculature supplies the inner eye and lens with nutrients and oxygen. Immediately after birth, these hyaloid vessels start to regress and a new vascular plexus starts to form rapidly on top of a pre-existing migratory astrocyte plexus (Fruttiger et al., 1996). Retinal astrocytes are the main VEGF-A source in response to local hypoxia, and thereby are crucial for retinal vascular development (Alon et al., 1995).

The mouse retinal vasculature develops from birth until postnatal day 7 (P7) (Figure 1.11), where the endothelial network extends gradually from the capillary ring at the optic nerve disc, sprouting radially toward the periphery. Sprouting, EC proliferation and migration initially lead to a primitive vascular plexus, which later undergoes substantial remodelling and matures vascular plexus, composed by a hierarchical vascular tree of arteries, veins and

1. Introduction

interconnecting capillaries (Adams and Alitalo, 2007; Pitulescu et al., 2010; Rocha and Adams, 2009).

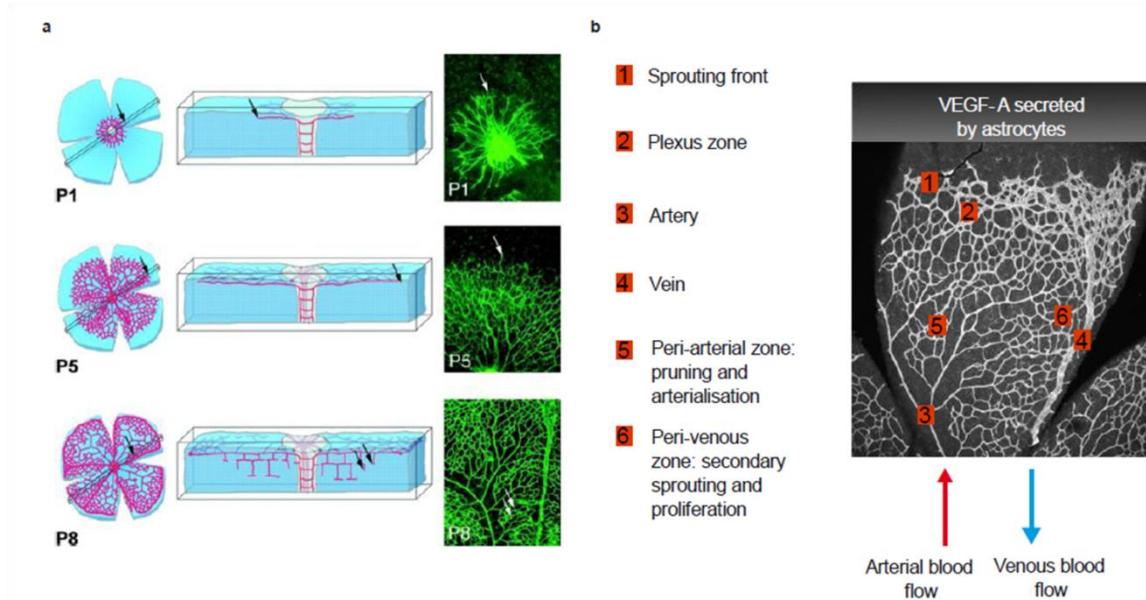


Figure 1.11. Figure 3.6 Growth of retinal blood vessels. (A). Schematic presentation of retina development and confocal images of isolectinB4 (green) labeled retinas are shown to the right. The top view shows a representative image of retinal vascular plexus at post-natal day 1 (P1), where the primary vascular network is growing in the fiber layer of the retina. White arrows in P1 and P5 images show sprouting happening towards the retinal periphery. At P8, sprouting occurs into deeper layers of the retina (arrows) (Gerhardt et al., 2003). (B). Summary of the differentiated zones within the developing retinal vascular plexus. (1) In the sprouting zone, directional extension of tip cells and filopodia promote vascular growth along a gradient of matrix-bound VEGF-A released by astrocytes in response to hypoxia. (2) Plexus zone, integrated by a perfused but primitive vascular bed. Limited sprouting occurs in this zone. Conversely, ECs located at this region are highly proliferative. (3) Artery zone, characterized for a high pressure blood flow. (4) Vein zone, characterized for a low pressure blood flow. (5) The peri-arterial zone is characterized for the presence of few side branches, as a consequence of strong pruning. The process of arterialisiation also takes place in the peri-arterial zone. (6) The peri-venous region is characterized to be a highly branched region, due to secondary sprouting and ECs proliferation (Adapted from (Roca and Adams, 2007)).

After the initial two-dimensional vascular growth period, sprouting into the deeper retinal layers begins and within the next 1–2 weeks, depending on the mouse strain, deep and intermediate vascular plexuses are completely formed (Figure 1.11 A). (Connor et al., 2009; Pitulescu et al., 2010) Thus, the retinas are very attractive models to study, both physiological and pathological

angiogenesis, as it allows to follow the processes in a single system at various stages of postnatal life (Connor et al., 2009). Therefore, vessel formation, maturation and specialization are examples of vascular processes that can be studied and analysed through immunostaining of the retina using several markers that mediate the vascular development (Figure 1.11 B) (Gerhardt et al., 2003).

Mouse genetics has allowed tissue-specific control of gene deletion, facilitating the study of different aspects of the angiogenic processes under genetically modified conditions. The Cre-loxP strategy is one of the best gene deletion techniques *in vivo*. This strategy involves the insertion of two loxP sites around a critical gene region that is recognized as a substrate by a site-specific DNA recombinase Cre leading to the deletion of the flanked DNA segment, generating a non-functional and inactivated allele. Temporal control of the deletion can be incorporated using tamoxifen-inducible versions of the Cre (CreERT) (Pitulescu et al., 2010). Consequently, the mouse retinal model combined with the advanced gene modification techniques, offer an excellent tool to uncover the contribution of a variety of genes in different aspects of vascular development (Pitulescu et al., 2010).

1.5.2. The RIP1-Tag2 transgenic mouse model

The Rip1Tag2 is a transgenic mouse model of pancreatic neuroendocrine tumours (PNETs) that is frequently used to study several aspects of tumour angiogenesis. In this model, the simian virus 40 large T-antigen (*Tag*) oncogene is expressed under the control of the rat insulin gene promoter (*Rip*), leading to the development of insulin-producing β -cell carcinoma (insulinoma) in the islets of Langerhans in the pancreas (Hanahan, 1985). In these animals a normal *Tag* oncogene expression starts within the pancreatic embryonic development, where it is expressed in all β -cells in the islets of Langerhans (approximately 400 islets in the pancreas). However, 4 weeks after birth the β -cells start to proliferate extensively, followed by hyperplasia and dysplasia of the islets (Bergers et al., 1999; Hanahan, 1985). Approximately 50% of the islets develop

1. Introduction

into hyperplastic and dysplastic islets during the first 5 weeks (Figure 1.12). Then, about 8-12% of these hyperplastic islands become angiogenic, presenting an active vasculature due to the induction of “angiogenic switch” (7-10 weeks after birth). This switch of angiogenesis in the Langerhans islets is characterized by EC proliferation and migration, vascular dilation and a micro-haemorrhage, leading to the reddish colour that these angiogenic islets present. A few weeks later (10-12 weeks of age) around 3% of the islets become encapsulated adenomas that are necessary for further development into invasive tumors (carcinoma). Therefore, approximately 25% of these adenomas progress to invasive carcinoma, highly vascularized, with hemorrhagic dilated vessels. These invasive carcinomas then start to metastasize, mainly to the liver and pancreatic lymph nodes. Finally, at approximately 13-15 weeks of age, mice die due to severe hypoglycemia (Bergers et al., 1999; Bill and Christofori, 2016; Hanahan, 1985).

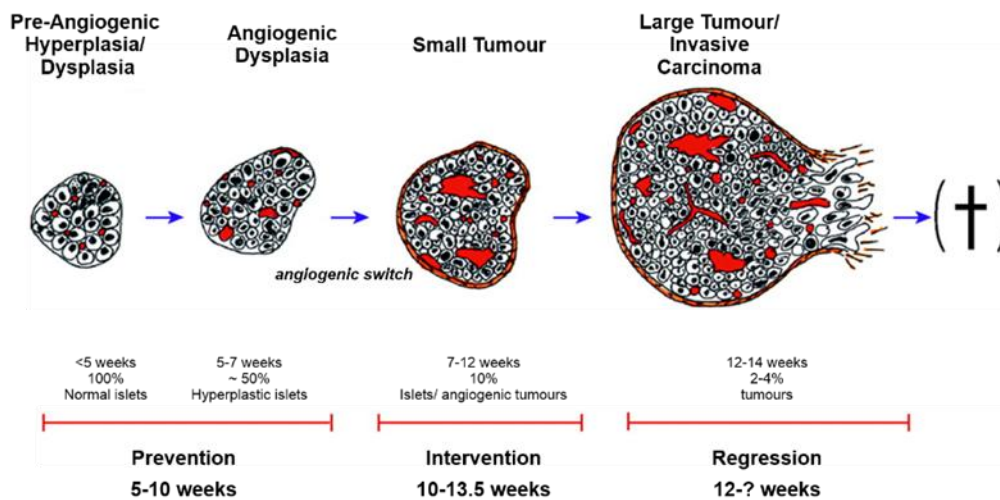


Figure 1.12. The tumour progression of RIP1-TAG2 mice model. In RIP1-TAG2 mice normal insulin-producing β cells of the pancreatic islets are converted into islet cell carcinomas under the influence of the SV40 T antigen (Tag). In this model the normal Langerhans islet express the Tag oncogene and are morphologically asymptomatic until 3 to 4 weeks of age. Hyperplastic islets then begin to appear stochastically displaying β -cell hyperproliferation and features of dysplasia and carcinoma *in situ*. Angiogenic islets arise from hyperplastic/dysplastic islets by switching on angiogenesis in the normally quiescent islet capillaries. Solid tumours arise at 10 weeks as small encapsulated tumours (adenomas) that progress by 12 to 13 weeks into large adenomas and (less frequently) invasive carcinomas, both of which are intensely vascularized by dilated hemorrhagic vessels (Adapted from (Bergers et al., 1999)).

Therefore, the Rip1Tag2 model has revealed important insights into the tumor progression, angiogenesis and metastasis. Moreover, the use of this model has allowed the validation of eligible biological or pharmacological anti-angiogenic compounds, some of which have been subsequently successfully implemented into clinical practice (Bergers et al., 1999; Bill and Christofori, 2016; Bill et al., 2015; Casanovas et al., 2005).

1.6. PI3K signalling pathway

Phosphoinositide 3-kinases (PI3Ks) signalling is a key regulator of different cellular processes including cell cycle progression, cell growth, survival, migration, and intracellular vesicular transport. Due to its clear importance at biological level, this pathway is also implicated in the aetiology and maintenance of various diseases, most prominently in cancer, overgrowth syndromes, inflammation and autoimmunity, with emerging potential roles in metabolic and cardiovascular disorders (Vanhaesebroeck et al., 2010, 2016).

PI3Ks are members of a conserved family of lipid kinases located in the cellular membrane that share a common and defining feature, which is their ability to phosphorylate the 3-hydroxyl group of the inositol ring of phosphatidylinositol (PtdIns) lipid substrates. There are three possible lipid substrates of PI3K: PtdIns, PtdIns-4-phosphate (PtdIns4P) and PtdIns-4,5-bisphosphate (PtdIns(4,5)P₂). These 3-phosphoinositides coordinate the localization and function of multiple effector proteins including: adaptor proteins, protein kinases (e.g. phosphoinositide-dependent kinase 1 and AKT/PKB) and nucleotide-exchange factors or GTPase-activating proteins (GAPs) for GTPases of the Rho, RAS and Arf families, resulting in their activation. These effector proteins bind the lipids through specific lipid binding domains: the pleckstrin homology (PH) domain, the phox homology (PX) domain and the FYVE domain (Vanhaesebroeck et al., 2010).

Based on their structure, substrate preference, distribution, mechanism of activation and functions PI3Ks in mammals are divided into three classes: class

1. Introduction

I, class II and class III (Figure 1.13) (Jiang and Liu, 2009; Vanhaesebroeck et al., 2010).

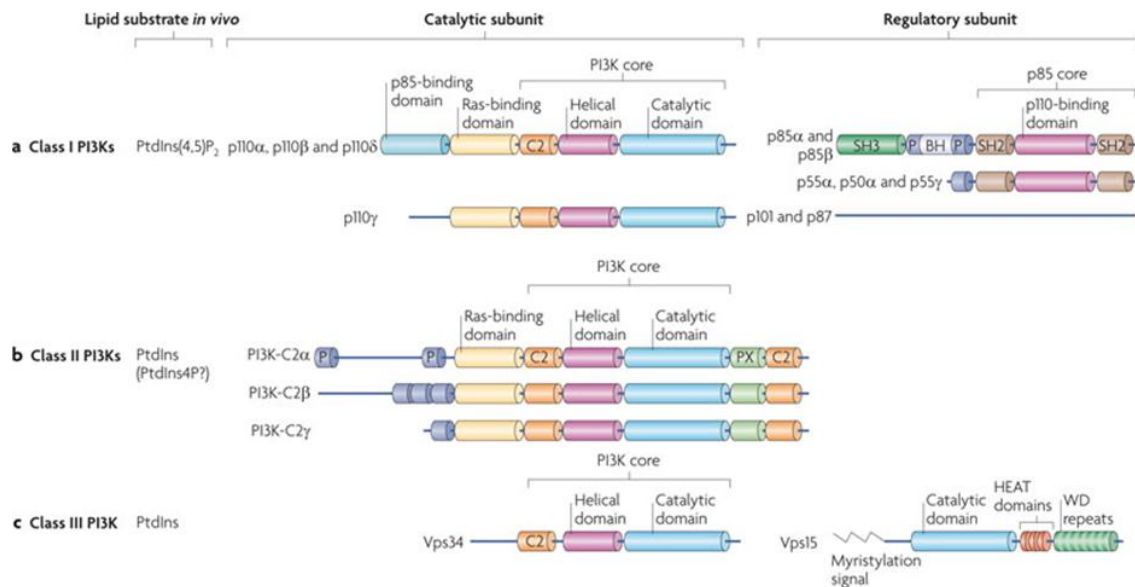


Figure 1.13. PI3Ks family. PI3K are divided into three classes based on their structural and biochemical characteristics. All PI3K catalytic subunits have a PI3K core structure formed by a C2 domain, a helical domain and a catalytic domain. (a) Class I PI3Ks are formed by a p85 regulatory subunit (for p110 α , p110 β and p110 δ) or p101 or p87 regulatory subunit (for p110 γ). All p85 isoforms have two Src homology 2 (SH2) domains and p101 and p87 lack this SH2 domains. (b) Class II PI3Ks lack regulatory subunits but have amino- and carboxy-terminal extensions to the PI3K core structure, which could mediate protein-protein interactions. (c) Class III PI3K has one catalytic member, vacuolar protein sorting 34 (Vps34) and binds Vps15. Vps15 consists of a catalytic domain (which is thought to be inactive), HEAT domains (which probably mediate protein-protein interactions) and WD repeats, which have structural and functional characteristics similar to a G β subunit (Vanhaesebroeck et al., 2010).

The class I PI3Ks works as heterodimers formed by a p110 catalytic subunit and a regulatory sub-unit. Depending on their ability to bind p85-type regulatory sub-units class I PI3Ks are subdivided into class IA (that binds to p85) and class IB (that does not bind to p85) (Graupera and Potente, 2013). The class IA is formed by three catalytic sub-units: p110 α , β and δ (encoded by three distinct genes: *PIK3CA*, *PIK3CB*, and *PIK3CD*, respectively). These isoforms can associate with any of the five regulatory sub-units: p85 α (and its splicing variants p55 α and p50 α , encoded by *PIK3R1*), p85 β (encoded by *PIK3R2*) and p55 γ (encoded by *PIK3R3*), collectively called p85-type regulatory

sub-units (Thorpe et al., 2015). On the other hand, class IB PI3Ks is composed of the solely p110 γ catalytic sub-unit (encoded by *PIK3CG*) and differs from the class IA PI3K by binding to one of the two regulatory sub-units p101 (encoded by *PIK3R5*) and p87 (also known as p84 or p87PIKAP, encoded by *PIK3R6*), which have no homology to p85 sub-unit. In mammalian cells, class I PI3Ks are present in all cell types, being p110 δ and p110 γ highly enriched in leukocytes (Graupera and Potente, 2013).

This class is mainly characterized by their catalytic activity in response to receptor tyrosine kinases (RTKs), G protein-coupled receptors (GPCRs) and RAS proteins, however it can also function as scaffolds for other proteins (**Figure 1.14**) (Jean and Kiger, 2014; Vanhaesebroeck et al., 2010).

The Class II PI3Ks is the least understood. Little is known about their mechanism(s) of action, specific downstream effectors and functional roles in cells, and exhibits relative resistance to PI3K inhibitors. In mammals this class counts with three isoforms: PI3K-C2 α , PI3K-C2 β and PI3K-C2 γ . PI3K-C2 α and PI3K-C2 β are expressed in a large amount of tissues (but not ubiquitous), whereas the expression of PI3K-C2 γ seems to be more restricted (Vanhaesebroeck et al., 2010). The class II are constitutively associated with intracellular membranes and unlike class I, it is only formed by a single catalytic sub-unit, lacking the binding site for regulatory sub-unit recruitment. These sub-units possess a RAS binding domain and a PI3K core domain, and are constitutively associated with intracellular membranes. In the absence of an activating signal, class II PI3Ks predominantly localize to endosomes where they generate PtdIns(3)P for effectors molecules through PX and FYVE binding domains. In addition RTKs and GPCRs have also been reported to activate class II PI3Ks (Figure 1.14) (Graupera and Potente, 2013).

Class III PI3Ks is formed by the only catalytic member, VPS34. VPS34 activity can be regulated by nutrients such as amino acids and glucose, and by GPCRs. (Vanhaesebroeck et al., 2010). This catalytic member, is constitutively bound to VPS15, a serine/threonine kinase, which acts as a regulatory sub-unit. The lipid kinase activity of VPS34 generates PtdIns(3)P and has been involved in vesicular trafficking, autophagy and nutrient signalling (**Figure 1.14**) (Graupera and Potente, 2013).

1. Introduction

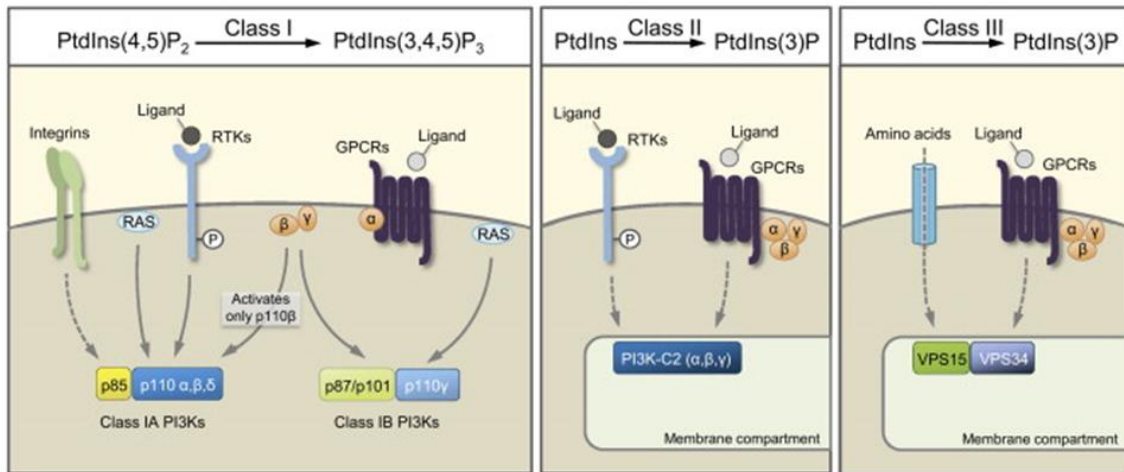


Figure 1.14. Classes of mammalian PI3Ks. Mammalian PI3Ks are grouped in three classes based on their structure and substrates characteristics. The Class I use PtdIns(4,5)P₂ as a substrate forming PtdIns(3,4,5)P₃ and consist of four catalytic subunits p110α, p110β and p110δ that are bound to the p85 regulatory subunit and p110γ connected with p101 or p87 regulatory subunit. PI3Ks can be activated by several extracellular stimuli, being that p110α and p110δ are preferentially activated by receptor tyrosine kinases (RTK), whereas p110β is activated by G-protein coupled receptors (GPCRs) and RTKs and p110γ is mainly activated by G-proteins. Class II and Class III PI3Ks are localized in membrane and produce PtdIns(3)P. Class II PI3Ks consist of a single p110-like catalytic subunit and VPS34 the only isoform in class III is constitutively bound to its regulatory subunit VPS15. The signals that activate class II and class III PI3Ks are not fully understood. It is thought that class II can be activated by RTKs and GPCRs, while class III can be regulated by GPCRs and nutrient availability (Graupera et al., 2013).

1.6.1. Class I PI3K

Class I as described previously can be divided into two different classes: class IA and class IB. Under basal conditions, class IA PI3Ks are thought to exist mainly as heterodimers, with the regulatory and catalytic sub-units constitutively bound to each other (Kok et al., 2009), and seems that both the catalytic (Yu et al., 1998a) and the regulatory sub-units (Brachmann et al., 2005a; Zhao et al., 2006) are unstable as monomers (Kok et al., 2009). Therefore, in quiescent cells, a pre-existing p85–p110 complex is cytosolic and p110-encoded PI3K activity is repressed. It is known that p85 regulatory sub-units at least have three regulatory functions: 1) the stabilization of the p110 catalytic sub-unit, avoiding their degradation, 2) the inactivation of their kinase activity in the basal state and 3) the recruitment to phosphorylated Tyr (pTyr)

residues in receptors and adaptor molecules (Mellor et al., 2012; Vanhaesebroeck et al., 2010). In response to upstream activating signals ligand-activated RTKs or GPCRs at the plasma membrane recruit the p85-p110 complex via two SH2 domains present in p85 that binds to specific phosphorylated tyrosine residues (Tyr-Y-X-X-Met motif) in activated receptors or associated adapter proteins. This binding allows the release of p85 from the complex leading to the activation of p110 proteins and their connection with lipid substrates in the membrane (Vanhaesebroeck et al., 2010). In the class IA PI3K, p110 α and p110 δ are more associated with RTKs and RAS protein whereas, p110 β can bind to both RTKs and to G $\beta\gamma$ sub-units of GPCRs and appears to act as an integrator of signalling through both pathways (Yuan and Cantley, 2010).

In the case of class IB, there is only one catalytic sub-unit p110 γ that can form two heterodimeric PI3K γ variants, p87-p110 γ and p101-p110 γ . The p101 and p84 regulate p110 γ signalling, being important in the relay of signals by G $\beta\gamma$ and RAS. These isoforms are encoded by two separate genes, and are highly expressed in leukocytes (Kok et al., 2009; S et al., 2005; Voigt et al., 2006). Moreover, they have a distinct tissue distribution, respond differentially to upstream signals and generate distinct pools of PIP₃. PIP₃ generated by p101-p110 γ , unlike that generated by p87-p110 γ , it is rapidly endocytosed to motile, microtubule-associated vesicles (Vanhaesebroeck et al., 2010).

The small GTPase RAS can be activated by tyrosin kinases and GPCRs leading to the activation of class I PI3K. In fact, RAS can promote signalling by p110 α and p110 γ through direct interaction with a RAS binding domain (RBD) found in p110 catalytic sub-units (Graupera and Potente, 2013; Vanhaesebroeck et al., 2010).

Class I PI3K activation leads to the phosphorylation of the phosphatidylinositol 4,5-bisphosphate (PIP₂) producing phosphatidylinositol 3,4,5-triphosphate (PIP₃) in the membranes in which they are activated (Graupera and Potente, 2013; Vanhaesebroeck et al., 2010). PIP₃ is mainly generated at the plasma membrane, however it might also be present in endosomes and the nucleus (Lindsay et al., 2006). PIP₃ coordinate the localization and function of multiple effector proteins, such as Ser/Thr and Tyr

1. Introduction

protein kinases (like AKT and BTK, respectively), adaptor proteins (such as GAB2) and regulators of small GTPase (GAPs and GEFs) (Lemmon, 2008; Vanhaesebroeck et al., 2001, 2010).

Moreover, PIP₃ signalling is regulated by the lipid phosphatases tensin homologue deleted on chromosome ten (PTEN) and Src-homology 2 (SH2) domain-containing inositol 5'-phosphatase (SHIP), which convert this lipid to phosphatidylinositol 4,5-bisphosphate (PtdIns(4,5)P₂) and phosphatidylinositol (3,4)-bisphosphate (PtdIns(3,4)P₂), respectively, and therefore functionally antagonizes PI3K activity (Parsons, 2004; Vanhaesebroeck et al., 2005).

1.6.1.1. Signalling inputs and isoform specificity

Class I PI3K catalytic isoforms have several similarities: 1) they share a conserved domain structure; 2) they use the same lipid substrates; and also 3) generate the same lipid products. However, despite the similarities its increasing evidence that they mediate PI3K signalling in different ways in both, physiological and pathological contexts.

Input through RTKs. Specific growth factor ligands connect with RTKs leading to their dimerization, activation and auto-phosphorylation of tyrosin-containing YXXM motifs. Class IA p110-p85 heterodimers cooperate with these activated receptors through the interaction of p85-SH2 domains with the phosphorylated YXXM motifs (Rameh et al., 1995; Yu et al., 1998a, 1998b). All class IA isoforms (PI3K α , PI3K β , and PI3K δ) can interact with activated RTKs. However, several pharmacological or genetic studies using isoform-selective inactivation strategies have shown that loss of p110 α activity was sufficient to block PI3K signalling after RTKs activation (Foukas et al., 2006; Graupera et al., 2008; Knight et al., 2006; Sopsakis et al., 2010; Utermark et al., 2012; Zhao et al., 2006), and that p110 β had only a slight effect after acute RTK activation (Ciraolo et al., 2008; Guillermet-Guibert et al., 2008a; Jia et al., 2008a). It has also been shown that p110 δ is the primary isoform downstream of RTKs in leucocytes (where they are mainly expressed), mast cells and macrophages (Ali et al., 2004; Geering et al., 2007; Papakonstanti et al., 2008). It was suggested

that the differential expression of the catalytic isoforms in a particular tissue might dictate which of these isoforms are dominant in mediating RTK signalling. However, differential expression does not completely explain the isoform specificity as in many tissues p110 β levels are comparable to, or even higher than, levels of p110 α (Geering et al., 2007).

In a study of Utermark *et al* it was described that while p110 α inactivation blocks normal mammary development and mammary tumorigenesis driven by polyoma middle T (PyMT) or HER2, p110 β inactivation increased mammary gland outgrowth and accelerated tumour formation driven by oncogenic RTKs. Biochemical analyses also showed that in p110 β knock-out cells, the activated RTKs had more bound to p110 α and higher associated lipid kinase activity. Moreover, the pharmacologically inactivation of p110 β could still compete with p110 α for binding sites on activated receptors, slightly reducing signalling and tumour growth. To explain this negative role a competition model was suggested: p110 α may have higher lipid kinase activity than p110 β when associated to RTKs. Thus, less-active p110 β competes with the more active p110 α for receptor-binding sites, leading to a decrease of lipid kinase activity associated with these receptors (Thorpe et al., 2015; Utermark et al., 2012).

The PI3K class-IB might also function downstream of RTKs through the regulatory isoform p87 in mouse myeloid cells mediating p110 γ activation (Schmid et al., 2011; Thorpe et al., 2015).

Input through GPCR. GPCRs are a family of receptors composed by seven-transmembranar domains that transmit their intracellular signalling through the allosteric activation of heterotrimeric G proteins. The G proteins are formed by G α and G $\beta\gamma$ sub-units (Thorpe et al., 2015). G $\beta\gamma$ sub-units directly activate p110 β and p110 γ , but not p110 α and p110 δ (Vanhaesebroeck et al., 2010). In fact, both p110 β and p110 γ isoforms have a similar region in the C2-helical domain linker that bind to G $\beta\gamma$ sub-units and that is not present in other class IA isoforms (Vadas et al., 2013). Abrogation of p110 β –G $\beta\gamma$ interaction, blocked p110 β -mediated signalling downstream of GPCRs, and leads to inhibition of proliferation and invasiveness in cancer cells (Zhao et al., 2003).

1. Introduction

In the p110 γ isoform, p101 regulatory sub-unit is the main regulatory isoform in GPCR signalling and both p110 γ and p101 interact directly with G $\beta\gamma$ heterodimers (Schmid et al., 2011; Thorpe et al., 2015). However, also p87 regulatory isoform can increase the activation response to G $\beta\gamma$ (Brock et al., 2003; S et al., 2005; Stephens et al., 1997). Different studies have shown that p110 γ -mediated signalling may contribute to tumorigenesis via GPCR dependent mechanisms (Schmid et al., 2011, 2013).

Although p110 δ does not directly interact with G proteins, unknown GPCRs can also activate Tyr kinases and RAS, which could in turn activate class I PI3K isoforms that are not directly responsive to G $\beta\gamma$ sub-units, such as p110 δ (Durand et al., 2009; Reif et al., 2004; Saudemont et al., 2009; Vanhaesebroeck et al., 2010).

Input through RAS and other small GTPases. All class I PI3K catalytic isoforms have an amino-terminal RAS-binding domain (RBD), allowing them to interact with RAS GTPases or other RAS super family members (Thorpe et al., 2015). Activated or oncogenic RAS protein can directly activate p110 α and p110 γ catalytic isoforms, and the RAS family member TC21 (also known as RRAS2) can also lead to p110 δ activation (Delgado et al., 2009; Rodriguez-Viciano et al., 2004).

Apparently, p85–p110 α complexes are only responsive to RAS following the activation of Tyr kinase pathways. The p85 regulatory sub-unit can inhibit RAS-mediated p110 α activation, and this blockade can only be released when the SH2 domains of p85 are connected with pTyr complexes (Jimenez et al., 2002).

In the case of p110 γ isoform, the association with RAS leads to the translocation of p110 γ to the membrane and increases its kinase activity (Kurig et al., 2009; Pacold et al., 2000). The activation of p110 γ through RAS seems to be mediated by the regulatory sub-unit p87 and not p101 (Kurig et al., 2009) in fact, disabling the RBD of p110 γ in mice blocks the responsiveness of p110 γ to GPCRs more than deleting the p101 regulatory sub-unit of p110 γ does (Suire et al., 2006).

Although p110 δ was shown to bind to RAS *in vitro* (Fritsch et al., 2013; Vanhaesebroeck et al., 1997), some studies indicated that p110 δ kinase activity was not stimulated by HRAS, NRAS or KRAS, but instead by RRAS and TC21. Also, *TC21-KO* mice had diminished PI3K activity and recruitment of p110 δ to T cell receptors (TCRs) and B cell receptors (BCRs), suggesting that p110 δ activity may be regulated by additional RAS sub-family members (Delgado et al., 2009).

In the case of the p110 β isoform, activation through RAS is less clear. *In vitro* studies suggested that the kinase activity of p110 β was not stimulated by any RAS subfamily members (Rodriguez-Viciano et al., 2004), instead this isoform is regulated by RAC1 and CDC42 RHO family GTPases (Fritsch et al., 2013). Direct interactions between the p110 β RBD and RAC1 are important for GPCR-mediated activation of p110 β , both G $\beta\gamma$ and RHO GTPase cooperate to promote p110 β -mediated signalling (Fritsch et al., 2013). Remarkably, RAC1 and CDC42 can also be activated downstream of PI3K by PtdIns(3,4,5)P₃-dependent guanine nucleotide exchange factors (GEFs) and GTPase activating proteins (GAPs) (Klarlund et al., 1997; Krugmann et al., 2002; Welch et al., 2002).

1.6.1.2. Signalling outputs and downstream effectors

Following activation, class I PI3Ks generate PIP₃ lipid at the plasma membrane, which will induce the recruitment and activation of several effector proteins that bind to the lipid through a pleckstrin homology (PH) domain (the most predominant), Phox (PX), C1, C2 and other lipid-binding domains, regulating many aspects of cell function. These effectors proteins include Ser/Thr and Tyr protein kinases (such as AKT and BTK, respectively), adaptor proteins (such as GRB2 associated binding GAB1 and GAB2, TAPP1, and DAPP) and regulators of small GTPases (GAPs and GEFs) (Vanhaesebroeck et al., 2001, 2010, 2012). Also PI3K can control intermediates that are not present at the cell membrane, but drive gene expression programs in the nucleus. This is the case of Forkhead box O (FOXO) transcription factors, that

1. Introduction

are directly regulated by PI3K activity through AKT dependent phosphorylation (Figure 1.15) (Graupera and Potente, 2013; Oellerich and Potente, 2012).

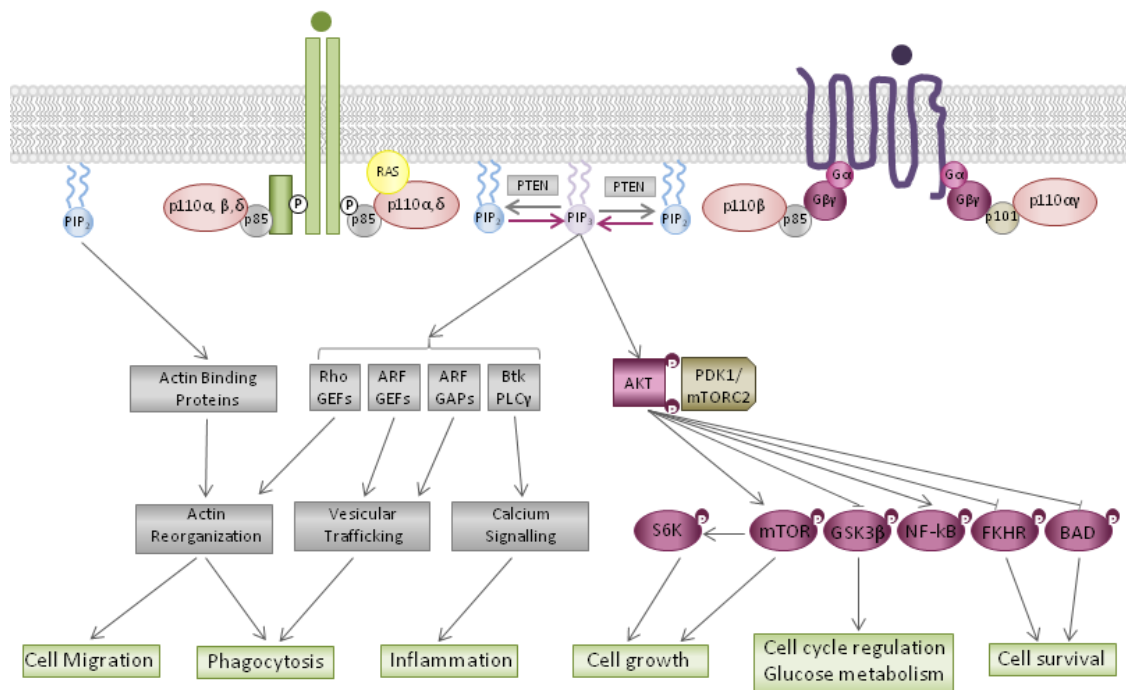


Figure 1.15. Downstream class I-PI3K signalling. Upon receptor tyrosine kinase (RTK) or G-protein coupled receptor (GPCR) activation, class I PI3Ks are recruited to the plasma membrane by interaction with phosphorylated YXXM motifs on RTKs or their adaptors, or with GPCR-associated Gβγ subunits. In the membrane they phosphorylate PIP₂ into PIP₃ leading to the activation of a number of AKT-dependent and AKT-independent downstream signalling pathways; these regulate several cellular functions, such as growth, metabolism, motility, survival. The PTEN lipid phosphatase removes the 3' phosphate from PIP₃ to inactivate class I PI3K signalling and thus regulating its effect.

AKT a close partner. The Ser/Thr kinase AKT is the major downstream mediator of the PI3K effects. To date, three AKT isoforms were described, which are encoded by different genes: the *AKT1* (*PKBα*), the *AKT2* (*PKBβ*) and the *AKT3* (*PKBγ*) (Alessi et al., 1996; Blume-Jensen and Hunter, 2001; Hennessy et al., 2005). Some evidence points out that these isoforms have differential effects: AKT1 promotes growth and survival whereas, AKT2 controls cellular invasiveness and mesenchymal characteristics (Dummler et al., 2006; Paz-Ares et al., 2009; Mundi et al., 2016).

The PH domain in the N-terminal region of AKT interacts with 3'-phosphoinositides, contributing to recruitment of AKT to the plasma membrane. The AKT recruitment results in conformational changes exposing two crucial

amino acids, the threonine 308 and the serine 473, which need to be phosphorylated to AKT activation. The threonine 308 is phosphorylated by the constitutively active phosphoinositide-dependent kinase 1 (PDK1), stabilizing the activation loop; whereas, PDK2 leads to the phosphorylation of the serine 473 in the hydrophobic C-terminal domain promoting the AKT full activation (Alessi et al., 1996; Blume-Jensen and Hunter, 2001; Hennessy et al., 2005). PDK1 itself is activated by PIP3, while PDK2 has been recently identified as a member of the mammalian target of rapamycin complex (mTORC) 2 (Hennessy et al., 2005; Sarbassov et al., 2005; Mundi et al., 2016). Phosphorylated AKT (p-AKT) represents the active form (Mundi et al., 2016). Following activation, AKT ultimately results in cell survival, proliferation, growth and metabolism, promoting the phosphorylation and consequent activation of a vast number of downstream effectors (Ji et al., 2014; Mundi et al., 2016).

AKT controls **cell survival** promoting the down-regulation of pro-apoptotic factors such as BAD, procaspase-9 and Forkhead (FKHR). In addition, several anti-apoptotic genes are also up-regulated upon AKT activation, including cyclic-AMP response element-binding protein (CREB), I κ B kinase (IKK) leading to the phosphorylation of I κ B (inhibitor of NF- κ B) that ultimately results in its proteasomal degradation and NF- κ B nuclear localization. Activation of AKT also leads to MDM2 phosphorylation and its translocation to the nucleus, where it decreased the tumour protein 53 (p53). The p53 protein is a tumour suppressor protein responsible for cell-cycle arrest and apoptosis. Thereby, reduced p53 levels upon AKT activation result in pro-growth and pro-survival signals (Carroll et al., 1999; Hennessy et al., 2005; McCann et al., 1995; Sherr and Weber, 2000). Also, PI3K/AKT signalling directly controls FOXOs transcription factors. In the absence of active PI3K/AKT, FOXOs localized in the nucleus promote cell cycle arrest, reactive oxygen species detoxification and programmed cell death. Upon PI3K activation, FOXO isoforms are directly phosphorylated by AKT protein, which results in their nuclear exclusion and proteasomal degradation (Graupera and Potente, 2013; Oellerich and Potente, 2012).

PI3K AKT-mediated also controls **cell growth** through the induction of insulin-stimulated protein synthesis by phosphorylating tuberous sclerosis 2 (TSC2) at serine 939 and thus activating mTORC1 signalling (Huang and

1. Introduction

Manning, 2008). When AKT phosphorylate TSC-2 inhibits its function, allowing the RAS homologue enriched in brain (RHEB) protein to activate mTORC1. This activation of mTORC1 leads to the phosphorylation of 4E-binding protein 1 (4E-BP1) and P70-S6 kinase 1, which are both crucial to ribosomal protein synthesis (Manning and Cantley, 2007). AKT can also directly activate mTORC1 independently of TSC-2 (Vander Haar et al., 2007), inducing the phosphorylation of proline-rich AKT substrate (PRAS40) and the subsequent activation of mTORC1, independently of TSC-2 (Bhaskar and Hay, 2007).

AKT can directly stimulate **cell proliferation** by preventing the nuclear localization of the cell-cycle arresters p27 and p21 and thus attenuating its cell-cycle inhibitory effects, such as apoptosis and senescence (Manning and Cantley, 2007; Sekimoto et al., 2004). Moreover, AKT-mediated phosphorylation of GSK-3A at Ser21 and GSK-3B at Ser9 results in inhibition of GSK-3 kinase activity (which controls cyclinD1 proteasome degradation), resulting in the up-regulation of cyclin D1 and consequent cell proliferation (Shimura et al., 2012). The AKT dependent inhibition of TSC-2 can also promote the stability of some cyclins and transcription factors that results into cell-cycle progression (Manning and Cantley, 2007).

AKT activity have been associated with **cell migration and invasion**, a mechanism that apparently is cell specific, in which AKT play different roles among the different cell types. In epithelial cells, activation of AKT1 leads to the degradation of the nuclear factor of activated T cells (NFAT) transcription factor by an unknown mechanism, resulting in the decreased epithelial cell migration (Irie et al., 2005; Yoeli-Lerner et al., 2005). Also loss of AKT1, but not AKT2, results in an increased activation of ERK1 and ERK2, which was found to be required for enhanced migration (Hutchinson et al., 2004). Mouse tumour models have suggested that AKT1 inhibits metastases (Hutchinson et al., 2004), whereas AKT2 promotes metastases (Arboleda et al., 2003). In fibroblasts, an opposite mechanism has been proposed, with AKT1 promoting migration and with AKT2 inhibiting it (Zhou et al., 2006). Similarly, in ECs, AKT1 but not AKT2 play an important role in migration through regulation of NO signalling pathway (Zhou et al., 2006). These facts demonstrate both the importance of crosstalk between the PI3K-AKT pathway and other pathways,

and also the AKT isoform specificity among the different cell types (Manning and Cantley, 2007).

Downstream signalling beyond AKT. AKT activation is usually concomitant with PI3K activation, however this is not always the case, and there are exceptions to this paradigm. Other PH domain-containing effector proteins in the class I PI3K signalling were identified, including GEFs and GAPs for small GTPases of the RHO, RAC, RAS and ADP-ribosylation factor (ARF) families, together with several protein kinases and signalling adaptors. These molecules can regulate PI3K-mediated signalling in an isoform dependent manner (Vanhaesebroeck et al., 2010, 2012). For example, RAC is positively regulated by all PI3K isoforms, RhoA is negatively regulated by p110 δ (Eickholt et al., 2007; Papakonstanti et al., 2008, 2008) and is not affected by p110 α (Graupera et al., 2008). Also, in 3T3-L1 adipocytes p110 β isoform function independent of AKT. Upon insulin stimulation on this cells, AKT phosphorylation still occurs after PIP₃ and PIP₂ substantial reduction due to p110 β inhibition (Knight et al., 2006). Moreover, there is no a strict correlation between p110 α mutations and the activation of AKT. Certain tumours with activating mutations in p110 α (encoded by *PIK3CA* gene) do not exhibit increased levels of AKT phosphorylation (Vasudevan et al., 2009). Therefore, the role of individual PI3K isoforms is not fully understood, and other effectors beyond AKT can also play pivotal roles in cell signalling transduction mediating important cellular processes.

1.6.1.3. Regulation by PTEN

Phosphatase and tensin homologue deleted on chromosome ten (PTEN) was first described as a tumour suppressor protein with a highly regulated gene transcription that contained an intrinsic tyrosine phosphatase activity (Li and Sun, 1997). In a variety of tumours, including those of the brain, breast, and prostate PTEN is frequently lost from a region of chromosome 10q23 (Li et al., 1997; Steck et al., 1997). Moreover, PTEN is one of the most frequently

1. Introduction

mutated genes in human cancer, and its inactivation occurs in several types of tumours (Carracedo et al., 2011).

PTEN function as both, a specific protein and a lipid phosphatase, and its primary cellular substrate is the second messenger PIP₃, which hydrolyzes to PIP₂ (Hopkins et al., 2014; Li and Sun, 1997; Stambolic et al., 1998). Therefore, PTEN antagonize PI3K-mediated signalling of growth, proliferation, survival and migration, by inhibiting PIP₃ dependent processes such as the membrane recruitment and activation of AKT. PTEN thus occupies a critical node for the inhibition of oncogenic transformation.

Apart from its lipid phosphatase activity, PTEN presents PIP₃-independent functions, such as the protein phosphatase activity that is critical for the inhibition of cellular migration, invasion and focal adhesion formation by dephosphorylate the focal adhesion kinase (FAK) (Leslie et al., 2007). Moreover, in glioma cells the protein phosphatase activity of PTEN is essential to induce PTEN phosphorylation and inhibit cellular migration (Raftopoulou et al., 2004) where it can be also involved in the regulation glioma cell migration by inhibition of Src family kinases (Dey et al., 2008). In addition, PTEN phosphatase activity blocks the phosphorylation of the nitrogen-activated protein kinase (MAPK), impairing its activation, leading to reduced levels of nuclear cyclinD1 and thus inhibiting cell-cycle progression (Planchon et al., 2008; Weng et al., 2001). PTEN also presents nuclear functions, where several proteins have been shown to affect PTEN nuclear localization, thereby impacting PTEN's ability to act in the nucleus and promote genomic stability (Mayo and Donner, 2002; Song et al., 2012).

Additionally to its function as a lipid and protein phosphatase, PTEN has also been proposed to exert other functions unrelated to its phosphatase activity. In pathological situations PTEN is down-regulated promoting methylation in thyroid, breast, lung, endometrial, ovarian, gastric, and brain tumours (Song et al., 2012), suggesting that these other functions of PTEN can also control several cellular processes. PTEN was also found silenced by the expression of a number of micro-RNAs and non-coding RNAs (Song et al., 2012).

PTEN ubiquitination by NEDD4-1 leads to PTEN nuclear import (Wang et al., 2007). In the nucleus, PTEN interacts with anaphase-promoting complex or cyclosome (APC/C) (Song et al., 2011), facilitating its association with its co-activator CDH1 that recognize and recruit specific targets of the APC/C complex for degradation. The APC/C targets include mitotic cyclins (cyclin A and B), mitotic kinases (Aurora kinases, PLK1, Nek2A), proteins involved in chromosome segregation (Securin, Sgo1), DNA replication proteins (Geminin, Cdc6), F-box protein (SKP2) and transcription factors (Ets2, FoxM1) (Manchado et al., 2010), therefore nuclear PTEN regulate cell-cycle progression.

1.7. PI3K and angiogenesis

Several studies have been published in the last decades revealing the importance of PI3K signalling during the vascular development, both in physiological and in pathological process. Moreover, PI3K affects not only ECs but also MCs, macrophages and immune cells, being the class I PI3K the most relevant and intensively study in this context. Therefore, class I PI3K isoforms are key integrators of angiogenic signalling. However, the isoform specificity in the different cell types and also the mechanisms in which the pro-angiogenic signals integrate PI3K signalling to achieve a correct cellular response, need to be further elucidated (Soler et al., 2015).

1.7.1. Class I PI3K and regulation of EC biology

Signal inputs of class I. Cell-based studies have demonstrated that PI3K signalling can be activated downstream of different proteins including: the VEGF family (namely VEGF-A and VEGF-C), the Ang1 and Ang2 proteins, VE-cadherin, Dll4, and ephrins, among others (Graupera and Potente, 2013).

VEGFs family is formed by three receptors (VEGFR1/FLT1, VEGFR2/FLK21 and VEGFR3/FLT4) and five ligands (VEGF-A, VEGF-B, VEGF-C, VEGF-D and PlGF) (Potente et al., 2011). PI3K can be active and

1. Introduction

signal transduce downstream of VEGFR2 (upon VEGF-A stimulation) and VEGFR3 (upon VEGF-C stimulation), but not VEGFR1 (upon PlGF stimulation), in a complex interplay between the two proteins. VEGFR2 and VEGFR3 use different cellular mechanisms, but both activate PI3K/AKT signalling (Dayanir et al., 2001; Gerber et al., 1998; Graupera and Potente, 2013; Mäkinen et al., 2001; Thakker et al., 1999). Upon VEGF-A stimulation, SRC kinases are activated by VEGFR2 leading to the phosphorylation of two Tyr-X-X-Met motifs and subsequent recruitment and activation of p85-p110 complex. Apparently, VEGFR3 activate PI3K upon VEGF-C stimulation in a RAS dependent manner, where this protein works as a connector between VEGFR3 and the p85-p110s once, VEGFR3 lack of a p85-binding motif (Graupera and Potente, 2013; Ruan and Kazlauskas, 2012; Wang et al., 2004). Therefore, the activation of PI3K/AKT pathway downstream of VEGF / VEGFRs signalling can control many aspects of ECs functions, including: cell migration, differentiation and proliferation (Graupera and Potente, 2013).

The ANG-TIE signalling also plays an important role in PI3K activation during vascular morphogenesis and maturation. This family is formed by two receptors (TIE1 and TIE2) and three ligands (ANG1, ANG2 and ANG3) (Augustin et al., 2009). ANG1, as previously described, is expressed mostly by PCs acting as an activator of TIE2 in ECs and is required for EC survival and vessel stabilization, being more active in quiescent vessels. On the other hand, ANG2 expressed in ECs acts as an antagonist of ANG1, leading to the vessel destabilization (Augustin et al., 2009). Both, ANG1 and ANG2 can activate PI3K/AKT, through unknown mechanisms that lead to the p85-p110s recruitment (Augustin et al., 2009; Kontos et al., 2002; Papapetropoulos et al., 2000; Saharinen et al., 2008). In the case of ANG1, activation of PI3K happens in more quiescent vessels promoting TIE2 activation and the formation of TIE2-TIE2 trans-association complexes at cell junctions (Fukuhara et al., 2008; Graupera and Potente, 2013; Saharinen et al., 2008). ANG2 can induce PI3K signalling via TIE2 (Papapetropoulos et al., 2000), and also can be regulated by activated PI3K/AKT signal that can reduce the levels of ANG2 expression through a FOXO1 (transcriptional activator of ANG2) inhibition dependent manner (Daly et al., 2004, 2006; Potente et al., 2005).

VE-cadherin can also activate PI3K signalling during the vascular development promoting the vessel stabilization by a FOXO1 dependent mechanism, promoting its inactivation and therefore the de-repression of a tight junction protein CLAUDIN5 (Taddei et al., 2008).

Signal outputs of class I. During angiogenesis PI3K activation in ECs is mostly linked to AKT activation and its downstream cellular response. Therefore, PI3K/AKT controls many cellular processes that are important for the correct vascular development, including cell survival, growth, proliferation and motility. PI3K signalling can also mediate angiogenesis by direct regulation of other effector proteins such as hypoxia inducible factor α (HIF-1 α and HIF-2 α), that in turn regulate the expression of VEGF and other angiogenic factors, which finally promote angiogenesis (Gordan et al., 2007; Jiang and Liu, 2009; Semenza, 2003; Wang et al., 1995). In addition, activated PI3K/AKT signalling promotes the activation of the endothelial nitric oxide (NO) synthase (eNOS) protein and the subsequent release of NO, which in turn can stimulate vasodilation, vascular remodelling and angiogenesis (Manning and Cantley, 2007).

Inside the *in vivo* models. Different studies in zebra-fish and mice have revealed essential functions of PI3Ks in vascular development (Lelievre et al., 2005; Nicoli et al., 2012). Most of them had characterized the specific roles of the different PI3K isoforms in angiogenesis (Graupera and Potente, 2013). EC-specific deletion of four (p85 α , p55 α , p50 α and p85 β), of the five class IA regulatory sub-units, results in embryonic lethality at mid-digestion due to defects in the vessel integrity. However, when a single allele of p85 α is maintained the embryonic lethality is rescued, meaning that the regulatory sub-units can compensate for each other's loss (Graupera and Potente, 2013; Yuan et al., 2008). On the other hand, the different catalytic sub-units have revealed distinct and non-redundant functions during the angiogenesis process. With regard to this, it has been described that p110 α isoform of PI3K is the only

1. Introduction

isoform absolutely required for a proper vascular development and remodelling (Graupera et al., 2008).

The first studies describing an essential role of p110 α in angiogenesis were carried out in mice with ubiquitous mutation of p110 α catalytic sub-unit. Constitutive inactivation of p110 α resulted in multiple vascular defects, including dilated vessels in the head, reduced branching morphogenesis in the endocardium, lack of hierarchical order of large and small branches in the yolk sac and impaired development of anterior cardinal veins. These vascular defects were similar to those in mice defective in the Tie2 signalling pathway. Indeed, Tie2 protein levels were significantly lower in p110 α -deficient mice. These findings strongly suggested an essential role of p110 α in vascular development (Lelievre et al., 2005).

Graupera *et al.* corroborate these data, also showing that ubiquitous or EC specific inactivation of p110 α , and not p110 β or p110 δ , led to embryonic lethality at mid-digestion due to severe defects in angiogenic sprouting and vascular remodelling. In contrast, vascular development in p110 β and p110 δ mutant mice was normal, viable and displayed no obvious vascular abnormalities, corroborating the unique role of p110 α among PI3K family in controlling angiogenic development and remodelling. The p110 α activity is high in ECs and preferentially induced by tyrosine kinase ligands (such as VEGF-A). In contrast, p110 β signals downstream of GPCR ligands such as SDF-1a, whereas p110 δ is expressed at low level and contributes only minimally to PI3K activity in EC. Thereby, it was seen that EC migration during angiogenic sprouting selectively required signalling through p110 α isoform, downstream of VEGF receptor activation. Specifically, p110 α was shown to control migration through up-regulation of the RHO-A-dependent signals required for tail release during cell motility. The RHO-A activity is regulated by ARAP3, a specific RHO-A GAP that is activated upon PIP₃ production. Both, the genetic deletion of ARAP3, or a knock-in mutation that make ARAP3 unable to bind PIP₃ leads to severe vascular defects, which are similar to the phenotypes observed upon p110 α inactivation (Graupera et al., 2008).

In zebra-fish it was also described that p110 α is the key isoform during vasculogenesis, promoting ventral migration of venous angioblasts and thus

allowing vein formation. This process can be blocked by p110 α -selective inhibitors (Herbert et al., 2009). Moreover, p110 α -PI3K signalling negatively mediated arterial morphogenesis, leading to the ERK1/2 MAP Kinase pathways activation, and arterial specification (Herbert et al., 2009). PI3K signalling also promotes tip cell migration and vessel branching during intersegmental vessel sprouting in zebra-fish embryos by a microRNAs (miRs) depending mechanism (Nicoli et al., 2012).

During the vascular development FOXOs family acts as negative regulator of endothelial angiogenic process. A PI3K/AKT activation leads to the phosphorylation of FOXOs, restraining its function and thereby promoting cell survival, proliferation and vessel growth (Daly et al., 2004; Goettsch et al., 2008; Potente et al., 2005). FOXO1 is the most relevant suppressor of EC growth and its inactivation causes early embryonic lethality in mice due to defective angiogenesis (Furuyama et al., 2004; Hosaka et al., 2004).

1.7.2. Class I PI3K and regulation of PCs biology

Little is known about the direct role that PI3K signalling plays in the regulation of PCs biology and so far, no studies have addressed the role of each PI3K isoform in PCs during angiogenesis *in vivo*. Most of the published work came from the *in vitro* experiments using vSMC.

The signalling cascade stimulated by PDGFR- β in PCs is critical for their recruitment into the growing vessels and for their proliferation, migration, and survival (Armulik et al., 2011). Once activated, distinct phosphorylated tyrosine residues of PDGFR- β are bound by specific Src homology 2 (SH2) domain-containing proteins, including PI3K. *In vitro* assays suggest that PI3K binding to the PDGFR- β leads to cell migration, differentiation, and proliferation improvements (Alimandi et al., 1997; Higaki et al., 1996; Kundra et al., 1994; Wennström et al., 1994). However, mutant mice (PDGFR $\beta^{F3/F3}$) carrying point mutations that inactivate both, PI3K and Phosphoinositide phospholipase C (PLC γ), have shown that loss in the binding of these molecules to PDGFR- β does not significantly disrupt the receptor function, especially when compared to

1. Introduction

the phenotype of PDGFR β ^{-/-} mice. Moreover, only when used mutant vSMCs, extracted from the PDGFR β ^{F3/F3} transgenic mice, the defects were evident leading to deregulation in migration and proliferation. These differences between *in vivo* and *in vitro* data may be due to the *in vivo* complexity where other compensatory signalling pathways can be somehow compensated for the loss of PI3K or PLC γ (Tallquist et al., 2000).

Another study of Vantler *et al.* has shown that p110 α and p110 δ , but not p110 β , are recruited to the activated PDGFR β in vSMC. Instead, p110 β is stimulated by GPCRs in those cells. Using specific Class IA inhibitors, PIK-75 (p110 α -specific), TGX-221 (p110 β -specific) and IC-87114 (p110 δ -specific) and genetic inactivation by specific siRNAs, they demonstrate that AKT phosphorylation, downstream of PDGFR β , is largely depended on p110 α activity. Therefore, only p110 α activity promotes proliferation, migration, and cell survival responses in vSMCs. Although p110 δ binds to the activated PDGFR β , its catalytic activity seems to be of minor importance once p110 δ -specific inhibition had no significant effect. vSMC-specific p110 α -deficient mice (sm-p110 α ^{-/-}) have also shown that p110 α is important for neointima formation and growth via SMC proliferation and migration, after balloon angioplasty (Vantler et al., 2015).

Other mediators were also implicated in PI3K signalling in vSMCs apart from PDGFR β /PDGFR β . Bai *et al.* have seen that VEGF produced by PCs in hypoxic conditions is a crucial factor in the cross-talk between these cells and ECs during angiogenesis. Therefore, exposure of PCs to sodium cyanide (NaCN) and glucose deprivation resulted in increased expression of VEGF via activation of MAPKs and PI3K/AKT signalling pathways, which in turn promotes the activation of NF- κ B transcription factor, resulting in increased expression of VEGF and subsequent increase in the permeability of ECs (Bai et al., 2015). Brain PCs are also activated by TNF- α which - when phosphorylated - leads to the activation of several proteins, including p42/p44 MAPK, p38 MAPK, JNK and PI3K-AKT, resulting in the secretion of MMP-9 that regulates PCs migration (Takata et al., 2011). Activation of GPCR-PI3K pathways interferes with cell cycle proteins in vSMC. The thrombin receptor activation in vSMCs leads to the subsequent activation of PI3K and reduced levels of p27^{Kip1} (family member of

cyclin-dependent kinase inhibitor (CDKI)), and thus increasing cellular proliferation (Seasholtz et al., 2001).

In vSMC, p110 α , p110 β , and surprisingly also p110 δ isoforms, are widely expressed compared to p110 γ (Vantler et al., 2015). However, p110 α appears to be the key isoform mainly engaged by RTKs, and possibly p110 β can mediate GPCR signalling in this cells.

1.7.3. PTEN regulation during angiogenesis

During the vascular development PI3K signalling is mainly regulated by lipid phosphatases. The class I PI3K is mainly regulated by the 3-phosphatase PTEN, as described previously, which converts the PIP₃ into PIP₂ antagonizing its effect. The balance between PI3K and PTEN determines the intracellular level of PIP₃ and its intracellular activity (Graupera and Potente, 2013).

Constitutive homozygous PTEN deletion in mice (PTEN^{-/-}) resulted in early embryonic lethality (E9.5). Otherwise, mice carrying heterozygous PTEN loss (PTEN^{+/-}) could undergo embryogenesis but developed different types of cancer and autoimmune diseases. PTEN deletion in different types of tissues using the Cre-loxP system revealed increased activation of AKT and ERK signalling pathways in the targeted cells, associated with hiper-proliferation that in some tissues culminate in hyperplasia and carcinoma development (Suzuki et al., 2008).

In Zebra-fish embryos, lacking functional PTEN (ptena^{-/-}ptenb^{-/-}) also displays increased angiogenesis (associated with excessive sprouting and filopodia formation resulting in hyperbranching), which is related to PI3K hyper-activation associated with increased pAKT and VEGF levels (Choorapoikayil et al., 2013). Moreover, this hyperbranching phenotype is rescued by treatment with the PI3K-specific inhibitor LY294002 (Choorapoikayil et al., 2013).

Mice lacking PTEN specific in ECs (Tie2Cre-PTEN^{Flox/Flox}) died during embryogenesis (E11.5) due to bleeding and cardiac failure, caused by impaired recruitment of MCs to blood vessels, and cardiomyocytes to the endocardium

1. Introduction

(Hamada et al., 2005a; Suzuki et al., 2008). These vascular abnormalities were partially rescued by a (co-) deletion of p85 α and p110 γ indicating that PTEN desphosphorylates PIP₃ produced by RTKs and GPCRs. Loss of PC in these mice is associated with overexpression of Ang-2 protein, and is not related with defects in PDGFB/PDGFR β or with TGF- β signalling pathways (Hamada et al., 2005).

Tie2CrePTEN^{+/-} mice, which presented a constitutive heterozygous loss of PTEN in ECs, could successfully go through embryogenesis, but displayed increased vascularisation associated with enhanced angiogenesis both in physiological and pathological conditions. Also, *in vitro* assays using Tie2CrePTEN^{+/-} ECs revealed increased proliferation and migration (Suzuki et al., 2008).

PdgfbCreERT2;PTEN^{flox/flox} mice also leads to the specific inactivation of PTEN in ECs however, this deletion was induced postnatally revealing that PTEN have PI3K-dependent and independent functions, in which Dll4/Notch signalling arrest stalk cell proliferation by inducing the expression of PTEN. Currently, the tip cell phenotype is usually associated with high levels of Delta-like 4 (Dll4), which activate Notch in neighbouring stalk cells, preventing them from becoming a new tip cell. Consequently, PTEN inactivation in ECs results in ECs stalk cells numbers unbalancing, which culminate in vascular hyperplasia, due to a failure in this Notch-induced proliferation arrest. Moreover, no PC dissociation were observed in this study (Serra et al., 2015). As follows, a major role of PTEN in ECs appear to be the suppression of EC proliferation and growth, however, up to now, EC proliferation is only arrested when all class I PI3K are inactivated while, specific blocking of each one of PI3K isoforms does not interfere with EC proliferation. Therefore, it is possible that PTEN regulates EC proliferation and growth independent of its lipid phosphatase activity (Graupera and Potente, 2013).

Different studies have also demonstrated that PTEN plays an important role in MCs regulation, both in physiology and in pathology. The majority of these studies were, however, as it has been happening for PI3K, developed in a vSMC context (Hamada et al., 2005). PTEN activity is correlated with significant alterations in vSMC growth rate during vascular development and after

experimental vascular injury (Garl et al., 2004; Mourani et al., 2004) and its inactivation leads to constitutive AKT activation (Hamada et al., 2005). Using a SM22 α -CrePTEN^{flox/flox}, it was shown that deletion of PTEN specific in vSMC resulted in widespread vSMC hyperplasia due to increased proliferation. This downregulation was associated with increased AKT phosphorylation in the major vessels, hearts, and lungs of mutant mice. Therefore, PTEN depletion results in hypoxia-inducible factor (HIF)-1 α -mediated production of the chemokine stromal cell-derived factor (SDF-1 α), which induces an autocrine SMC growth loop, and increases progenitor cell migration through a paracrine signalling mechanism. Moreover, this mutant exhibits many features associated with pathological vascular remodelling, including remarkable SMC hyperplasia as well as vascular recruitment of progenitor cells, suggesting that an alteration in SMC - PTEN signalling serves as one of the initiating keys driving to pathological vascular remodelling (Nemenoff et al., 2008).

1.8. PI3K and cancer

Several pathological conditions are related to PI3K signalling deregulation, leading to different type of signal events associated with cellular transformation, cancer, and metastasis (Okkenhaug et al., 2016). In cancer, this pathway is frequently up-regulated as a consequence of oncogenic RTK and RAS, amplification or mutational activation of *PIK3CA*, and/or inactivation of the tumour suppressor PTEN. In fact, cancer genetic studies suggest that in human tumours: the *PIK3CA* gene is the second most frequently mutated oncogene, and PTEN is among the most frequently mutated tumour suppressor genes (Brachmann et al., 2005b; Okkenhaug et al., 2002).

1. Introduction

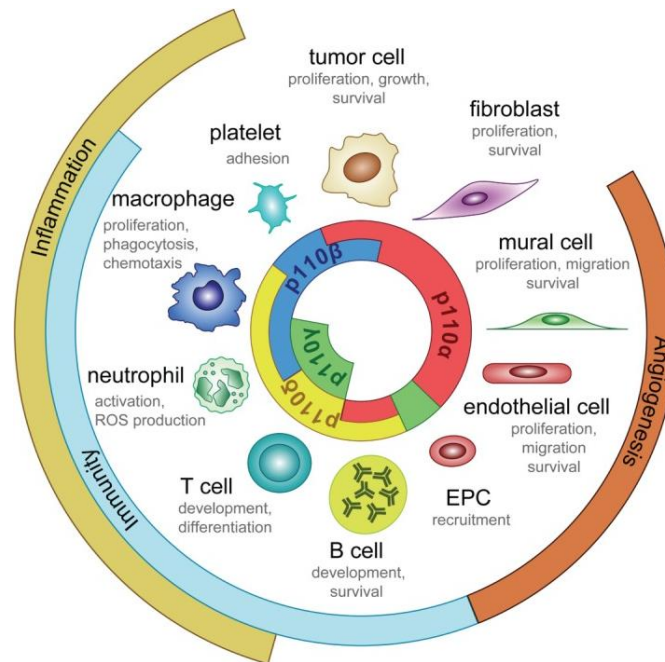


Figure 1.16. Isoform-specific roles of class I PI3Ks. Schematic illustration of isoform specific roles of class I PI3K isoforms in normal physiology and cancer (Soler et al., 2015).

Moreover, PI3K signalling is also important in the regulation of tumour stroma functions. Classically, the stroma includes the vasculature, infiltrating immune cells, fibroblasts and connective tissue. PI3K activity thus, hypothetically can have an important role in the regulation not only on cancer cells but also in their microenvironment (Figure 1.16) (Geudens and Gerhardt, 2011; Hirsch et al., 2014a; Murillo et al., 2014; Soler et al., 2013).

In this context, different strategies, that are currently being tested in clinical trials, were designed to interfere with PI3K cascade, including pan-class I PI3K inhibitors, isoform-selective PI3K inhibitors, rapamycin analogs (rapalogues), active-site mTOR inhibitors, dual PI3K mTOR inhibitors, and AKT inhibitors, that interfere not only with cancer cells itself but also, with the tumour stroma (Soler et al., 2015). However, counterbalancing this opportunity, the challenge is targeting enzymes that are also active and have crucial roles in normal cells and tissues (Hennessy et al., 2005).

The initial results from pre-clinical and clinical trials, despite some solid tumours, are showing limited single agent activity of PI3K inhibitors (Okkenhaug et al., 2016). These limitations may be due to several reasons (reviewed by (Okkenhaug et al., 2016)): 1) lack of selectivity, insufficient target inhibition, off

target effects, intrinsic and acquired drug resistance, and lack of tolerability to the different PI3K inhibitors (Toska and Baselga, 2016). Isoform-selectivity PI3K inhibitors seem to be safer than pan-PI3K inhibitors (Mayer et al., 2016). Also, a transient administration of the drugs affecting PI3K, with periods of interruption, increased their therapeutic index, maintaining the same efficacy (Yang et al., 2016). 2) Although pan-class I PI3K inhibitors are less well tolerated, quite often they are more efficient, once the effect of isoform-selective class I PI3K inhibitors can be compensated by other PI3K isoform, as it was observed by activation of PI3K β upon selective blockade of PI3K α (Costa et al., 2015) and vice versa (Schwartz et al., 2015) 3) Cancer cells can easily resist to PI3K inhibition, by increasing intrinsic feedback mechanisms, which may overlap with those promoted by the PI3K inhibitors, upon short-term inactivation. Also, they can develop genetic resistance upon long-term PI3K blockade (Juric et al., 2015; Wei et al., 2016). 4) Inhibition of PI3K in cancer cells *in vitro* is more cytostatic than cytotoxic. This can reflect the fundamental role of PI3K in these cells, working more as a growth factor/nutrient sensor, in which cells with blocked PI3K signalling are in a more quiescent status, but not necessarily dead (Okkenhaug et al., 2016). 5) Also, cancer cells can activate PI3K in many ways (Josephs and Sarker, 2015; Weigelt and Downward, 2012). Although the specific mutations, such as *PIK3CA* amplification/mutation, bring some predictive value in determining the sensitivity to PI3K inhibitors, this correlation is not always absolute and linear, seeing that other genetic parameters also affect this response (Fritsch et al., 2014). Consequently, combination therapies are being developed and evaluated in both preclinical and clinical settings, and will be necessary to maximize clinical efficacy of PI3K inhibitors (Thorpe et al., 2015).

1.8.1. PI3K in tumour vasculature

Tumours need new blood vessels to grow and spread, therefore many antiangiogenic therapies have been documented in multiple preclinical models of cancer (Fang et al., 2007; Hu et al., 2005; Kong et al., 2009; Murillo et al.,

1. Introduction

2014; Schnell et al., 2008; Soler et al., 2013; Yuan et al., 2008). Several of these antiangiogenic treatments rely on the use of PI3K inhibitors, which can modulate the vasculature directly by the inhibition of ECs, or indirectly by inhibition of the angiogenesis promoting tumour-associated myeloid cells and VEGF production by tumour cells (Figura 1.17). (Okkenhaug et al., 2016).

The pan-class I PI3K inhibitors used in high doses have revealed that continued PI3K inhibition results in reduced total intra-tumour vessel area, reduced vessel function (Fang et al., 2007; Hu et al., 2005; Kong et al., 2009; Murillo et al., 2014; Schnell et al., 2008; Soler et al., 2013; Yuan et al., 2008), antitumor activity, and also a smaller antiangiogenic impact than VEGF-targeted therapies (Pàez-Ribes et al., 2009; Soler et al., 2016), indicating that high doses of PI3K inhibitors have less impact on vessel eradication than VEGF-targeted therapies (Pàez-Ribes et al., 2009). Interestingly, low doses of PI3K inhibitors leads to vessel normalization, associated with either reduced or no changes in vessel density (Fokas et al., 2012; Qayum et al., 2009, 2012). These vessels are more functional and thus, they had additional capacity to deliver chemotherapy to the tumour (Qayum et al., 2012). The direct vascular effects of low doses-PI3K inhibitors on tumour angiogenesis appears to improve vessel function, enhance drug delivery and potentially also increase the influx of antitumor immune cells to improve immunotherapy (Okkenhaug et al., 2016).

Apart, from the use of pan-PI3K, several studies addressed the isoform-specific PI3K inhibition. Given that tumour cells express all 4 class I PI3K isoforms, pan-class I PI3K inhibitors are expected to offer higher effectiveness. However, it was described that the uses of these agents present off-target effects. Therefore, isoform-selective PI3K inhibitors may have the ability to block the relevant target with fewer side effects (Jia et al., 2009; Rodon et al., 2013)

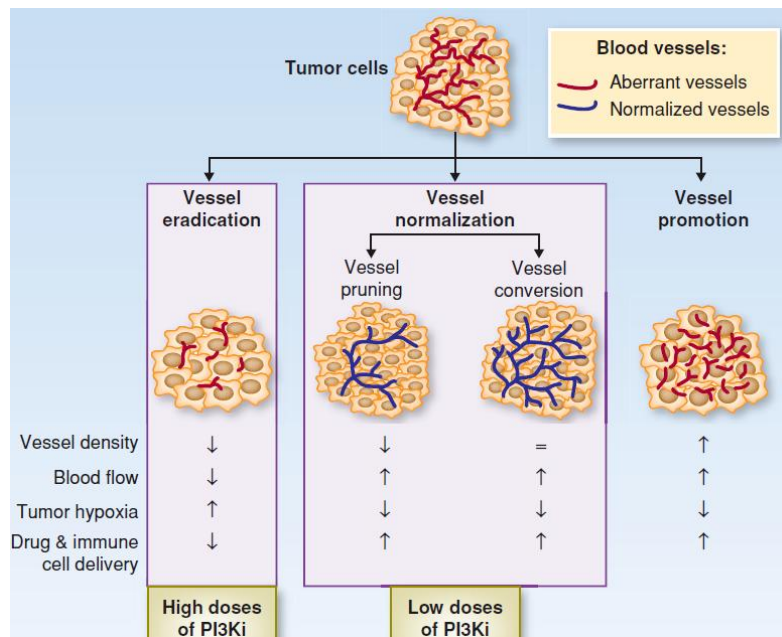


Figure 1.17. Vascular targeting strategies in cancer with PI3K inhibitors. PI3K inhibitors (PI3Ki), at high doses can induce a mild vessel eradication response, whereas at low doses they can lead to vessel normalization, associated with either reduced or no changes in vessel density. The vessel eradication aimed to reduce the tumour vasculature. The problems with this strategy is that there is a reduced chemotherapy delivery to the tumour and induction of hypoxia, which can accelerate tumour progression; vessel normalization, aimed at improving vascular perfusion and oxygenation, allowing enhanced drug delivery and immunotherapy; the vessel promotion strategy is based on stimulating vessel growth, together with promotion of vasodilatation, and is aimed at enhancing delivery of chemotherapy and other anticancer agents to the tumour (Adapted from (Okkenhaug et al., 2016)).

Apparently, several studies have shown that block p110 α selectively have the same antiangiogenic properties that the pan-PI3K inhibition, suggesting that p110 α -selective agents may be a better antiangiogenic option due to their reduced toxicity, and also that this isoform is the most important one for the tumour vasculature development. However, also the inhibition of the other class I isoforms have shown positive insights affecting the microenvironment (Soler et al., 2015). Thus, blocking p110 γ isoform leads to decreased tumour growth by inhibiting recruitment of inflammatory cells (Schmid et al., 2013). Moreover, inhibiting p110 δ suppresses the function of regulatory T cells, allowing cytotoxic T-cell responses to tumours (Ali et al., 2014), leading to a reduction in the tumour growth and metastasis. Another strategy is the use of dual inhibitors, such as p110 α/δ inhibition, affecting directly the vasculature and their microenvironment. However, hypothetically this strategy may result in immune

1. Introduction

suppression once, upon p110 δ inhibition, p110 α compensates for B cell development in the bone marrow and B cell survival in the spleen. An alternative would be to use p110 α -selective and p110 δ -selective inhibitors sequentially, which would offer the advantage of inhibiting each isoform individually without inducing immune suppression (Soler et al., 2015).

2. Objectives

PCs have gained increased attention as important regulators of vascular development, participating in vessel formation, stabilization and maturation. As a result, new therapies aim to target these cells to promote or inhibit angiogenesis. Several signalling pathways have been implicated in PC regulation and in their intercellular communication with the EC. Although signalling through p110 α /PI3K is critical for the correct vascular development, little is known about the direct role that PI3K signalling plays in the regulation of PCs biology during angiogenesis. Thus, the aims of my PhD are:

1. Study PC physiology and differentiation during sprouting angiogenesis.
2. Address the relevance and specificity of PI3K isoforms in the regulation of PCs biology in physiological angiogenesis.
3. Investigate the relevance of PI3K signalling regulation by PTEN in PCs during physiological angiogenesis.
4. Investigate the role of PI3K in PCs during pathological angiogenesis.

3. Materials and Methods

3.1. Mouse experiments

3.1.1. Mouse care

All mice analysed in this work were kept in individually ventilated cages and cared for according to the guidelines and legislation of the Catalan DARP (Departament d' Agricultura, Ramaderia i Pesca), with procedures accepted by the Ethics Committees of IDIBELL-CEEA.

3.1.2. Genetically modified mice and inducible genetic experiments

To investigate the role of p110 α , p110 β and PTEN inactivation specific in PCs during physiological angiogenesis we have used different transgenic mice models available in the laboratory (**Table 3.1**).

➤ p110 α and p110 β inactivation in PCs:

❖ **p110 α ^{D933A} and p110 β ^{D931A} mice:** These mice present a germline mutation in the ATP binding site that change DFG motif to a AFG motif (knock-in strategy) in the *Pik3ca* and *Pik3cb*, respectively. This point mutation inactivates p110 α and p110 β kinase function but p110 α ^{D933A} and p110 β ^{D931A} proteins are not degraded. In contrast to gene deletion, this approach preserves signalling complex stoichiometry and avoids possible compensation from other p110 isoforms (Foukas et al., 2006). Homozygous of p110 α ^{D933A/D933A} mice die at embryonic day 10 (Graupera et al., 2008) while p110 β ^{D931A/D931A} mice also presents embryonic lethality at different points of the embryonic development (Guillermet-Guibert et al., 2015). The heterozygous p110 α ^{D933A/WT} mice are

viable and only present a slight retardation in the vascular development that overcomes. Adult $p110\alpha^{D933A/WT}$ mice show similar vasculature compared to wild-type mice. The heterozygous $p110\beta^{D933A/WT}$ are also viable but showed reduction in the fertility.

❖ **$p110\alpha^{Flox/Flox}$ and $p110\beta^{Flox/Flox}$ mice:** In an attempt to circumvent the embryonic lethality exhibited by $p110\alpha$ and $p110\beta$ homozygous mutants (Graupera et al., 2008; Guillermet-Guibert et al., 2008b) and to study the specific role of $p110\alpha$ and $p110\beta$ specific in PCs we have used a tamoxifen-inducible PC Cre line, *Pdgfr β (BAC)-CreERT2* transgenic mouse line (Chen et al., 2016a) (kindly provided by Ralf Adams laboratory), in which the Cre is only active in PCs after 4-OH tamoxifen administration. Therefore, these models have allowed the postnatally depletion of $p110\alpha$ and $p110\beta$ specifically in PCs by 4-OH tamoxifen administration (knock-out strategy). With this model we would expect to have full deletion of $p110\alpha$ and $p110\beta$; however, total deletion of both isoforms depend on the efficiency of recombination and the absence of $p110\alpha$ and $p110\beta$ proteins could lead to possible compensations by the other PI3K members (Utermark et al., 2012).

❖ **$p110\alpha^{D933A/flox}$ and $p110\beta^{D931A/flox}$ mice:** For the majority of the experiments of this work we have used *PDGFR β (BAC)-CreERT2;p110 $\alpha^{D933A/flox}$* and *Pdgfr β (BAC)-CreERT2; p110 $\beta^{D931A/flox}$* mice. Both of these models present one allele with the constitutive kinase-death mutation D933A or D931A and other allele with $p110\alpha$ or $p110\beta$ floxed under the expression of CreERT2 specifically in PCs. After 4-OH tamoxifen administration we obtained a *Pdgfr β (BAC)-CreERT2; p110 $\alpha^{D933A/i\Delta PC}$* mice and a *Pdgfr β (BAC)-CreERT2; p110 $\beta^{D931A/i\Delta PC}$* mice, where only inactive $p110\alpha^{D933A}$ and $p110\beta^{D931A}$ protein are expressed. The advantage of this model is that we get full inactivation of the isoforms without changes in the signalling complex stoichiometry and without compensations from other PI3K family members.

3. Materials and Methods

For experiments with the p110 α and the p110 β isoform, breeding were set up between p110 α ^{D933A/flox} mice and a Pdgfr β (BAC)-CreERT2;p110 α ^{flox/flox} mice in the case of p110 α inactivation; and the p110 β ^{D931A/flox} mice were crossed with Pdgfr β (BAC)-CreERT2;p110 β ^{flox/flox} to allow p110 β inactivation in PCs. In this way we could obtain as offspring the principal transgenic mice models used in this thesis work. **In the case of p110 α inactivation:** p110 α ^{flox/flox} (referred as Control), p110 α ^{D933A/flox} (referred as heterozygous), Pdgfr β (BAC)-CreERT2;p110 α ^{flox/flox} (also referred as PC specific inducible knock-out) and Pdgfr β (BAC)-CreERT2;p110 α ^{D933A/flox} (principal model of study). **For the p110 β inactivation:** p110 β ^{flox/flox} (referred as Control), p110 β ^{D931A/flox} (referred as heterozygous), Pdgfr β (BAC)-CreERT2;p110 β ^{flox/flox} (also referred as PC specific inducible knock-out) and Pdgfr β (BAC)-CreERT2;p110 β ^{D931A/flox} (principal model of study).

The Pdgfr β (BAC)-CreERT2 transgenic mice incorporate Cre recombinase protein fused to the mutant form of the human estrogen receptor (ERT2) that is insensitive to estrogen but is responsible to the artificial ligand 4-OH tamoxifen. CreERT2 is expressed under the PC-specific promoter PDGFR β . Consequently, Cre-mediated recombination and deletion of floxed p110 α and p110 β can be induced in PCs expressing PDGFR β upon 4-OH tamoxifen administration. As a consequence, in the absence of 4-OH tamoxifen, the CreERT2 protein remains in the cell cytoplasm sequestered by the heat shock protein 90 (Hsp90) whereas, in the presence of 4-OH tamoxifen, the CreERT2 is translocated to the nucleus to mediate loxP-specific recombination events. In the absence of Cre-ERT2 upon 4-OH tamoxifen administration, floxed p110 α and p110 β cannot be recombined and therefore, p110 α ^{flox/flox} and p110 β ^{flox/flox} mice were used as control.

To verify the Pdgfr β (BAC)-CreERT2 specificity for the PCs in the retina the Pdgfr β (BAC)-CreERT2;p110 α ^{flox/flox} mice was crossed with a *Rosa26-eYFP* transgenic mice allowing the detection of Cre activity by the YFP expression signal (Srinivas et al., 2001); and also the Pdgfr β (BAC)-CreERT2;p110 α ^{D933A/flox} mice that only express one allele flox was crossed with *Rosa26-mTmG* fluorescent reporter line, which allows the detection of Cre activity by recombination-induced expression of membrane-bound green

fluorescent protein (GFP) and inactivation of the red fluorescent protein Tomato expression (Muzumdar et al., 2007). The recombination was induced upon 4-OH tamoxifen administration in mice at postnatal (P) day 1 and P2 and the retinas isolated at P6.

➤ **PTEN inactivation in PCs:**

To investigate the loss of PTEN in PCs, PTEN^{Flox/Flox} mice (Suzuki et al., 2001) were also bred to the Pdgfrβ(BAC)-CreERT2 transgenic mice. For experiments, breeding were set up between Pdgfrβ(BAC)-CreERT2-PTEN^{Flox/Flox} and PTEN^{Flox/Flox} thus, obtaining a similar proportion of PDGFRβ(BAC)-CreERT2;PTEN^{Flox/Flox} (also referred as Cre positive) and PTEN^{Flox/Flox} (also referred as Cre negative that was used as control) within the offspring. Therefore, in this mouse model the Cre mediated recombination and deletion of PTEN in PCs expressing *PDGFRβ* can be activated upon 4-hydroxytamoxifen (4OH-tamoxifen) administration.

Table 3.1. Mouse lines

Mouse Line	Description	Source
p110α ^{D933A}	<i>Pi3kca</i> knock-in mouse (carrying a germline mutation in the DFG motif of the p110α ATP binding site) that express a kinase-dead p110α ^{D933A} protein. Homozygous lethal at E10.5. It is viable in heterozygosity.	(Foukas et al., 2006)
p110β ^{D931A}	<i>Pi3kcb</i> knock-in mouse (carrying a germline mutation in the DFG motif of the p110β ATP binding site) that express a kinase-dead p110β ^{D933A} protein. Homozygous lethal at different types of the embryonic development and is viable in heterozygosity.	(Guillermet-Guibert et al., 2015)
p110α ^{flox/flox}	<i>Pi3kca</i> conditional knock-out mouse.	(Graupera et al., 2008)

3. Materials and Methods

p110β^{flox/flox}	<i>Pi3kcb</i> conditional knock-out mouse.	(Guillemet-Guibert et al., 2008)
p110α^{D933A/flox}	One <i>Pi3kca</i> allele is carried the germline mutation in DGF motif of the of the p110 α ATP binding site that express a kinase-dead p110 α ^{D933A} protein. Second <i>Pi3kca</i> allele is floxed.	In this study
p110β^{D931A/flox}	One <i>Pi3kcb</i> allele is carried the germline mutation in DGF motif of the of the p110 β ATP binding site that express a kinase-dead p110 β ^{D931A} protein. Second <i>Pi3kca</i> allele is floxed.	In this Study
PTEN^{flox/flox}	PTEN conditional knockout mouse.	(Suzuki et al., 2001)
Pdgfrβ(BAC)-CreERT2	Tamoxifen-inducible Cre recombinase expression under <i>PDGFRβ</i> PC specific promoter.	(Chen et al., 2016)
Rosa26-mTmG	Expression of membrane-bound green fluorescent protein (GFP) and inactivation of the red fluorescent protein Tomato expression after Cre-recombinase activity.	(Muzumdar et al., 2007)
Rosa26-eYFP	Expression of eYFP protein after Cre-recombinase activity.	(Srinivas et al., 2001)

3.1.3. RIP1-Tag2 mice

To investigate the role of p110 β in a pathological condition the RIP1-Tag2 tumoral mice model (Hanahan, 1985) were backcrossed onto the C57/BL6 background for >10 generations and WT littermates used as controls (kindly provided by Oriol Casanovas laboratory).

3.1.4. Induction of Cre mediated gene deletion

Cre activity and gene deletion were induced by intraperitoneal injections of 4-OH tamoxifen (Sigma, #H7904). 25 mg of 4-OH tamoxifen powder were dissolved in ethanol to obtain a working solution of 10mg/ml. The solution was aliquoted under sterile conditions and stored at -20°C. New born mice were injected at specific postnatal days with 25 µg/pup/day of 4-OH tamoxifen.

Remarkably, 4-OH tamoxifen solution needed to be previously homogenized to avoid precipitates. A Hamilton syringe (Hamilton Company, #80087) was used for injection. Pups derived were injected with 4-OH tamoxifen at postnatal days 1 (P1) and P2 and tissue of interest was collected at P6 and P9.

3.1.5. Mouse genotyping

3.1.5.1. Tissue digestion

New born mice were weaned once they turned 3-weeks old. Upon weaning tail biopsies were kept for genotyping. Tissue was lysated with 600 µl of 50 mM NaOH (Sigma). Samples were incubated at 100°C for 15 min and were vortexed and kept at room temperature (RT) until they reached 50-70°C. To neutralize the samples, 100 µl of 1M Tris HCl pH 7.4 (Sigma) were added to each sample. Samples were vortexed, centrifuged at maximum speed for 1 min and kept at 4°C until samples were processed for DNA amplification.

3.1.5.2. PCR

Polymerase chain reactions (PCR) were performed using two different protocols referred as PCR reaction I and PCR reaction II (**Table 3.2**).

3. Materials and Methods

❖ PCR reaction I (to a final volume of 30 µl): 2 µl DNA sample, 15.75 µl H₂O, 3 µl MgCl₂ 15mM (diluted from MgCl₂ 50 mM Ecogen, #MG-110C), 3 µl of 10X reaction buffer without Mg (Ecogen), 3 µl of 10M primer pool (forward+reverse), 3 µl dNTPs and 0.35 µl Ecotaq DNA polymerase (Ecogen, #BT-314106).

❖ PCR reaction II (to a final volume of 25 µl): 1.5 µl DNA sample, 15.875 µl H₂O, 2.5 µl 10X Titanium taq reaction buffer, 2.5 µl of 10 M primer pool (forward+reverse), 2.5 µl dNTPs and 0.125 µl 50X titanium taq polymerase (Clontech, #K1915- y).

Mastercycler (Eppendorf) was used to perform PCRs. PCR reactions were then separated on a 2% agarose (Sigma) gel diluted in TAE buffer 1X (from a TAE 50X stock: 242 g Tris base (Sigma), 57.1 ml acetic acid glacial (Panreac) and 100ml EDTA 0.5 M pH8 (Gibco, #15575) in dH₂O) with ethidium bromide (Sigma).

Table 3.2. PCR conditions and primers

Gen	PCR type & Primers	Program	Type
p110α	ma36:5'-CCTAAGCCCTTAAAGCCTTAC-3' ma47:5'-ACTGCCATGCAGTGGAGAAGCC-3'	1. 94°C_3 min 2. 94°C_30s 3. 65°C_30s 4. 72°C_30s 5. 2-4 for 39 cycles 6. 72°C_7 min 7. 16°C_hold	II
p110β	b11:5'-CTTAGGGAAGAGCGAGGA-3' Bseq2:5'-AAGAAGTATGTACACCTCTCT-3' NeoF2:5'-CTGTCATCTCACCTTGCTCC-3'	1. 94 °_3min 2. 94 °C_30s 3. 60 °C_30s 4. 72 °C_30s 5. go to 2 39 times 6. 72 °C_7min	II
PTEN	FW:5'-ACTCAAGGCAGGGATGAGC-3' RV:5'-GCCCGATGCAATAAATATG-3'	1. 94 °C_2min 2. 94 °C_30s	II

3. Materials and Methods

		<p>3. From 65°C to 55°C. 0.5°C/Cycle_1min 4-72 °C_1min 5. From 2 to 4 x 20 cycles 6. 94 °C_30s 7. 55°C_ 1min 30s 8. 72°C_1min 30s 9. From 6 to 8 x 20 cycles 10. 72°C_5min 11. 4 °C_hold</p>	
PDGFRβ (BAC)-CreERT2	<p>CRE1: 5'-GCCTGCATT ACCGG CGATGC AACGA-3'</p> <p>CRE2:5'GTGGCAGATGGCGCGGCAACAC CA TT-3'</p> <p>IL-2 FW: 5' - CTAGGCCACAGAATTGAAAGATCT-3'</p> <p>IL-2 RV: 5'- GTAGGTGGAAATTCTAGCATCATCC-3'</p>	<p>1. 94°C_3min 2. 94°C_30s 3. 65°C_30s 4. 72°C_30s 5. 2-4 for 39 cycles 6. 72°C_7 min 7. 16°C_hold</p>	I
Rosa26-mTmG	<p>Primer 1: 5'-CTC TGC TGC CTC CTG GCT TCT-3'</p> <p>Primer 2:5'- CGA GGC GGA TCA CAA GCA ATA-3'</p> <p>Primer 3:5'- TCA ATG GGC GGG GGT CGT T-3'</p>	<p>1. 94°C_5 min 2. 94°C_30 s 3. 65°C_30 s 4. 72°C_30 s 5. 2_4 for 39 cycles 6. 72°C_7 min 7. 16°C_hold</p>	II
Rosa26R-YFP	<p>R1:5'- AAA GTC GCT CTG AGT TGT TAT-3'</p> <p>R2: 5'-GCG AAG AGT TTG TCC TCA ACC-3'</p> <p>R3: 5'-GGA GCG GGA GAA ATG GAT ATG-3'</p>	<p>1. 94°C_ 2 min 2. 94°C_ 30 s 3. 65°C_30 s 4. 50°C_30 s 5. 2_4 for 40 cycles 6. 72°C_ 40 s 7. 72°C_5 min 8. 16°C_hold</p>	II
RIP1-Tag2	<p>Tag:5' GCTCAAAGTTCAGCCTGTCC-3'</p> <p>5' GGTGGGTTAAAGGAGCATGA-3'</p> <p>β2-globulina:5' ATTCACCCCACTGAGACTG-3'</p> <p>5' TGGAGGAAGCTCAGGAAAGA-3'</p>	<p>1. 94°C_ 3 min 2. 94°C_30 s 3. 65°C_ 30 s 4. 72°C_30 s 5. repetir 2_4 durant 39 cicles 6. 72°C_ 7 min</p>	II

3. Materials and Methods

3.1.6. Postnatal mouse retina isolation and staining

3.1.6.1. Eyes extraction and retina isolation

Pups were sacrificed by decapitation and eyes were quickly removed using scissors and forceps. Eyes were fixed in a solution of 4% paraformaldehyde (PFA, Sigma, #15.812-7) in phosphate-buffered saline (PBS) for 45 min at 4°C. Then eyes were washed in PBS followed by dissection of retinas. The procedure of retina isolation was done with the help of a binocular dissecting microscope (Carl Zeiss). Briefly, eyes were collected in a clean culture dish filled with PBS and the cornea was incised with the help of a needle. Using micro-scissors (Fine Science Tools, #15000-10), the cornea was cut and removed. Next, the iris was also removed using two forceps (Fine Science Tools, #11252-00) and the outer layer of the eye, the sclera and the pigmented retina layer started to be separated. The outer layer should be dissected carefully, in small increments, to avoid damaging the retina layer beneath. At this point, the lens and the vitrous humor, which appear as a single jelly-like structure need to be removed. Finally, the hyaloids vessels were carefully detached from the inner side of the eye using fine movements. Isolated retinas were fixed for 1h at 4°C and were kept in PBS at 4°C until they were processed for immunofluorescence (IF). Procedure details are shown in Figure 3.1.

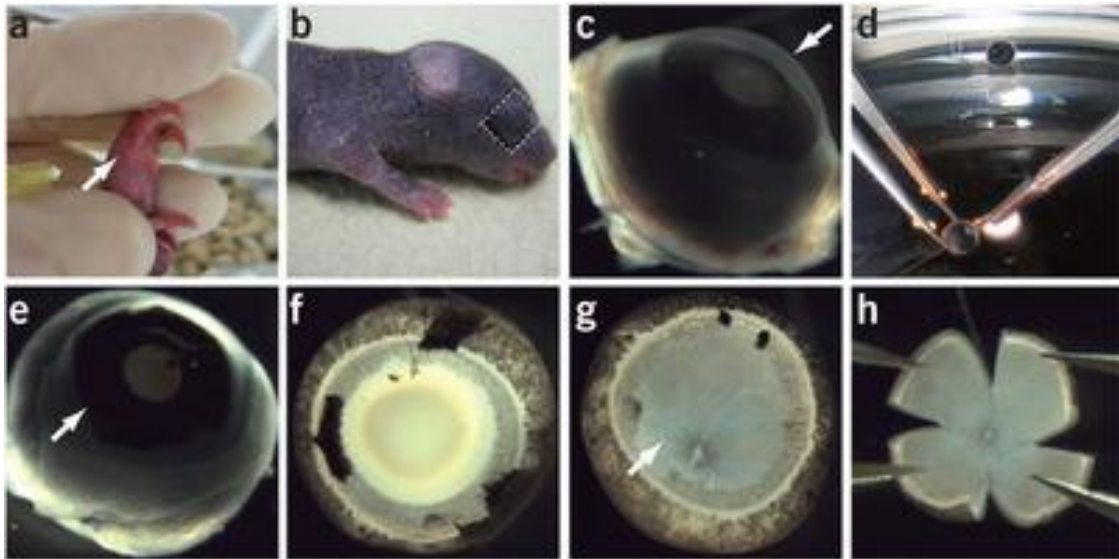


Figure 3.1. Tamoxifen injection, eye isolation and retina dissection. a, Intra-gastric tamoxifen injection in a P1 and P2 mouse pup. b, Image showing where to make the incisions around the eye of the pup. c, Dissected eyeball from a P6, P7, P10 or P15 pup. Arrow points to the cornea surface. d, Overview of cornea dissection. e, Eyeball without cornea. Arrow indicates dissected cornea. f, Image showing eye without sclera, choroid, cornea layers, pigmented layers and without the iris. g, Dissected eye without lens. Arrow shows hyaloid vessels. h, Retina with four radial incisions. Figure modified from (Pitulescu et al., 2010).

3.1.6.2. Staining of whole-mount retinas

3.1.6.2.1. Immunofluorescence staining with primary antibodies

Retinas were blocked with permeabilization buffer (1% bovine serum albumin (BSA, Sigma), 0.3% Triton X-100 in PBS) ON at 4°C with gentle rocking. Then, retinas were incubated with primary antibodies in appropriate dilutions (**Table 3.3**) in permeabilization buffer ON at 4°C with gentle rocking. The following day, primary antibodies were removed and retinas were washed 3 times (10 min each) with PBT buffer (0,1% Tween-20 in PBS). Retinas were further incubated 30min at RT in Pblec buffer (1% Triton X-100, 1 mM CaCl₂, 1 mM MgCl₂ and 1 mM MnCl₂ in PBS pH6.8) and then, they were incubated ON

3. Materials and Methods

at 4°C or 2h at RT with the appropriate dilution of secondary antibodies (**Table 3.4**). Conjugated isolectin-B4 and NG2 were added together with the secondary antibodies in the appropriate dilution (**Table 3.3**). Then, retinas were washed 3 times, 10 min each with PBT. After antibody staining, retinas were post-fixed in 4% PFA for 2min. At the end, between 4-5 incision were made in the retinas to flat mount them on glass slides using Mowiol (Calbiochem, #475904) with DAKO (Sigma) as mounting medium. All the incubations were done in 2 ml tubes (Eppendorf).

Table 3.3. List of primary antibodies used for immunofluorescence in mouse

Antibody	Conj	Host	Dilution	Company	Catalogue#
CD31	-	Rat	1:100	BD Pharmingen	550274
Desmin	-	Rabbit	1:100	Abcam,	15200
Erg 1,2,3	-	Rabbit	1:100	Santa Cruz	sc-353
Erg 1,2,3	-	Rabbit	1:400	Abcam	ab92513
p-S6	-	Rabbit	1:100	Cell Signalling	2215S
Collagen IV	-	Rabbit	1:50	Millipore	AB756P
Cleavage caspase-3	-	Rabbit	1:100	Cell Signalling	9664
Isolectin GS-IB4	488	-	1:300	Mol. probes	121411
Isolectin GS-IB4	568	-	1:300	Mol. probes	121412
Isolectin GS-IB4	647	-	1:300	Mol. probes	132450
NG2	-	Rabbit	1:100	Millipore	AB5320
NG2	488	-	1:100	Millipore	AB5320A4

Table 3.4. List of secondary antibodies used for immunofluorescence in mouse

Antibody	Conj	Dilution	Company	Catalogue#
Goat anti-rabbit	Alexa Fluor 488	1:300	Invitrogen	A11008
Goat anti-rabbit	Alexa Fluor 568	1:300	Invitrogen	A11011
Goat anti-rat	Alexa Fluor 488	1:300	Invitrogen	A11006
Goat anti-rat	Alexa Fluor 568	1:300	Invitrogen	A11077
Goat anti-rat	Alexa Fluor 633	1:300	Invitrogen	A21094
Goat anti-mouse	Alexa Fluor 488	1:300	Invitrogen	A11001
Goat anti-mouse	Alexa Fluor 568	1:300	Invitrogen	A21236
Goat anti-mouse	Alexa Fluor 633	1:300	Invitrogen	A11031

3.1.6.2.2. *In vivo* proliferation assay by EdU detection

EdU is a synthetic analogue of thymidine, and therefore, it can be incorporated into DNA during S phase. The Click-iT EdU Imaging Kit (Invitrogen, #C10337 and #C10340) was used for EdU injection and detection. To determine the number of proliferating ECs and PCs in the growing retinal vasculature, baby mice were injected intraperitoneally with 60 µl of component A from the kit (diluted to 0.5 mg/ml in 50% DMSO: 50% PBS) 2h before they were sacrificed for retina extraction as described in **section 3.1.6.1**. Then, the reaction for EdU detection was performed following the instructions the Click-iT Imaging Kit. Briefly, each pair of retinas were incubated for 1h at RT with gentle rocking in 100 µl of EdU detection solution (8,6 µl)of 10X Click-iT EdU reaction buffer in 77,4 µl of H₂O (component D), 4 µl of CuSO₄ (component E), 1 µl of 10X azyde-conjugated Alexa-Fluor in 9 µl of H₂O (component F) and 0,24 µl of alexa 633 (component B)). Retinas were washed twice with PBS and then, they

3. Materials and Methods

were incubated with permeabilization buffer ON at 4°C with gentle rocking. Thereafter, retinas were incubated in appropriate dilution of Erg 1,2,3 antibody (Table 3.3) in permeabilization buffer ON at 4°C with gentle rocking. The day after, retinas were washed 3 times with PBT at RT, followed by 30 min incubation with Pblec buffer at RT. Secondary antibody against Erg1,2,3 and isolectin-B4 were incubated ON agitating at 4°C in appropriate dilutions (Table 3.4). Retinas were washed 3 times (10 min each) with PBT and postfixed for 5 minutes with 4% PFA at RT. Finally, they were flat-mounted on glass slides using Mowiol with DAKO. Quantification of proliferative PCs and ECs was done as describe in 3.1.8

3.1.7. Confocal imaging

Leica TCS SP5 confocal microscope was used. Images were taken with objectives: 10x, 20x, 40x (oil) and 63x (oil) objectives. All images are maximal z-stack projections (unless specified otherwise). Images were processed using Volocity, Fiji and Adobe Photoshop CS5.

3.1.8. Methods used for quantifying vessel features

3.1.8.1. Radial expansion

The migratory length of the vascular plexus was analyzed by measuring the total length of the retinal vasculature from the optic nerve towards the retinal periphery (**Figure 3.2**). Four measurements were taken from each retina. The average distance of vessel migration per retina was used in comparisons between animals of different genotypes. Images for the radial expansion quantification were taken with the 4x objective of the Nikon 801 microscope.

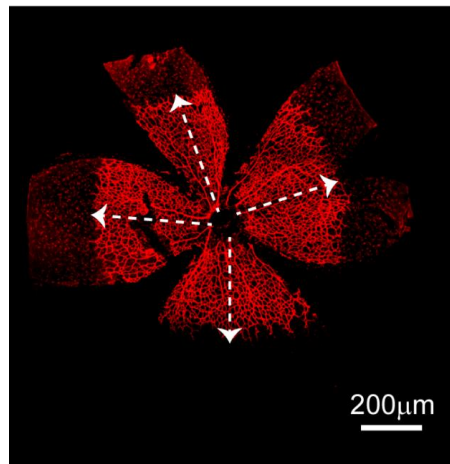


Figure 3.2. Radial Expansion.

3.1.8.2. Vascular branching

The number of branch points per field of $10^4 \mu\text{m}^2$ behind the vascular sprouting front or in the capillary area was quantified as shown in **Figure 3.3**. Six images of the sprouting front or of the capillary area were taken from each retina and, at least five retinas per genotype were analyzed. Quantified images were taken with the 40x objective.

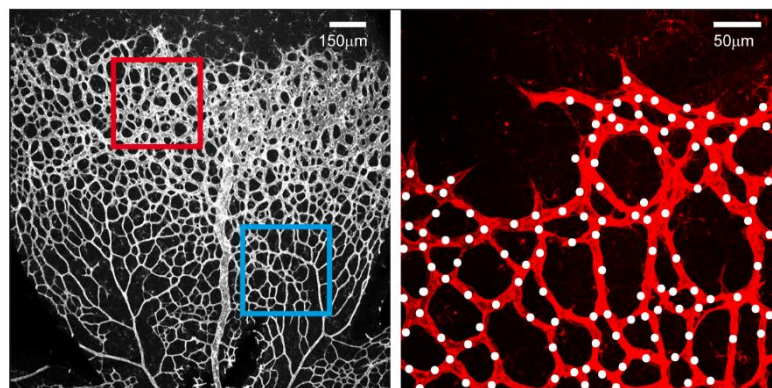


Figure 3.3. Branching Points.

3. Materials and Methods

3.1.8.3. Number of sprouts

The number of sprouts was expressed as number of sprouts per $1\mu\text{m}$ of the perimeter of the sprouting front. For this, the total vessel length of the sprouting front was determined using images taken with the 40x objective with the proper scale set up, as shown in **Figure 3.4**. Thereafter, the number of sprouts present throughout the sprouting membrane were quantified. Six images of the sprouting front were taken from each retina and at least four retinas per genotype were analyzed. Graphs represent the number of sprout in $1\mu\text{m}$ of sprouting front.

3.1.8.4. Filopodia quantification

The number of filopodia in the perimeter of the sprouting front was quantified (**Figure 3.4 highlight**). The number of filopodia/ μm distance was plotted. Six images of the sprouting front were taken from each retina and at least four retinas per genotype were analyzed.

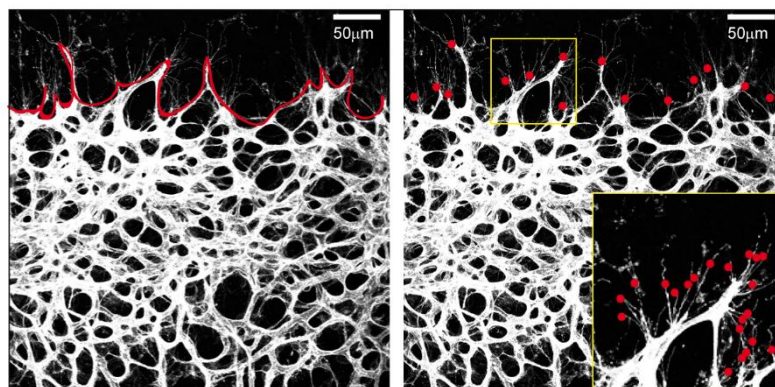


Figure 3.4. Number of Sprouts and Filopodia.

3.1.8.5. PC coverage

The quantifications were done using the Image J software in images taken with the 40x objective and the proper scale set up. PC coverage was quantified

as NG2 or Desmin positive area per isolectin-B4 positive area as shown in **Figure 3.5**. For that, first the channels were splitted from maximal z-stack projections. The isolectin-B4 channel and the NG2 or desmin channel thereafter were used to establish the vascular area by setting a manual threshold and by manually “add selection”. Six images of the sprouting front and remodelling plexus were taken from each retina and at least four retinas per genotype were analyzed. Graphs represent the percentage of NG2 or Desmin positive area per isolectin-B4 area.

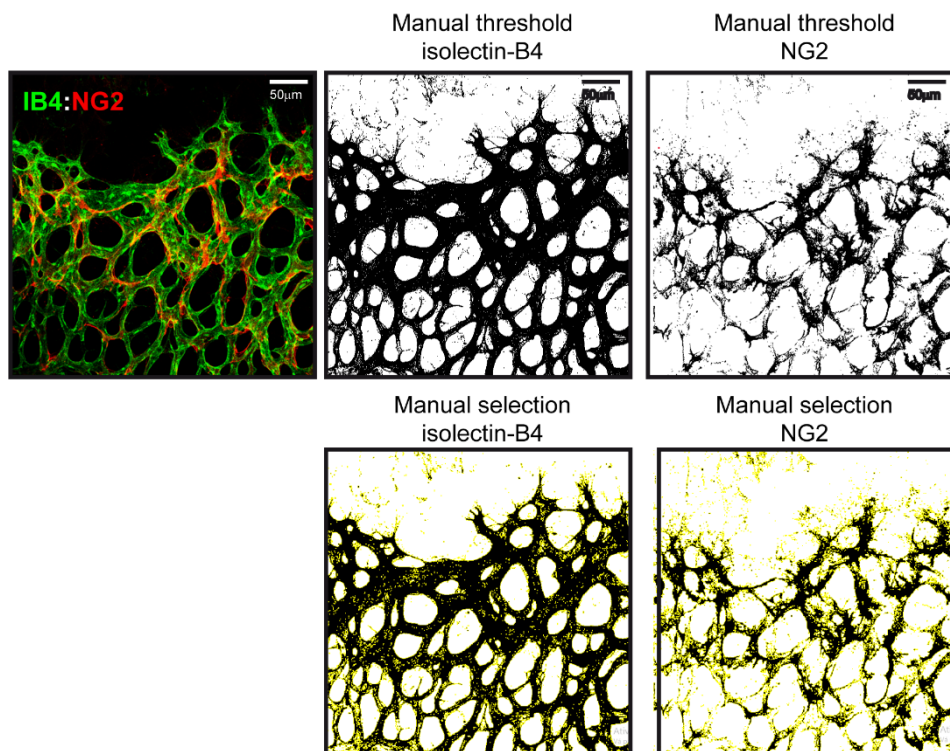


Figure 3.5. PC coverage in the vessel area.

3.1.8.6. Quantification of proliferative PCs

A field of 100 µm x 100 µm (**Figure 3.6, yellow square**) was determined in the vascular sprouting front and remodelling plexus of images taken with the 40x objective from retinas stained for EdU, NG2 and isolectin-B4. The number of EdU+ (blue – yellow stars) was divided by the total number of PCs NG2 (red) within this visual field and was represented as % of proliferative PCs. For WT retinas the number of EdU+ cells in the NG2 area within the field was quantified

3. Materials and Methods

and represented as number of proliferative PCs. At least three images of both, the sprouting front and remodelling plexus were taken from each retina and at least four retinas per genotype were analysed.

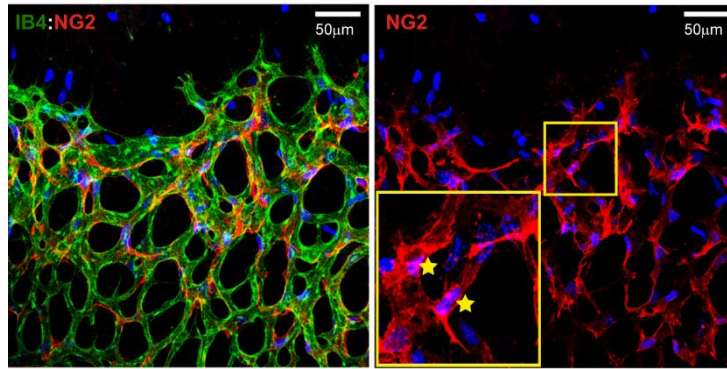


Figure 3.6. PC proliferation.

3.1.8.7. Quantification of proliferative ECs

A field of 100x100 µm (**Figure 3.7, yellow square**) was determined behind the vascular sprouting front and remodelling plexus of images taken with the 40x objective from retinas stained for EdU, Erg1,2,3 and isolectin-B4. The number of Edu+ (green) were divided by the total number of Erg+ (red) EC nuclei within this visual field of 100x100µm and was represented as % of proliferative ECs. In the case of WT retinas EC proliferation was quantified as the number of EdU+ (green) per isolectin-B4 positive area in the field. At least three images of both, the sprouting front and remodelling plexus were taken from each retina and at least four retinas per genotype were analyzed.

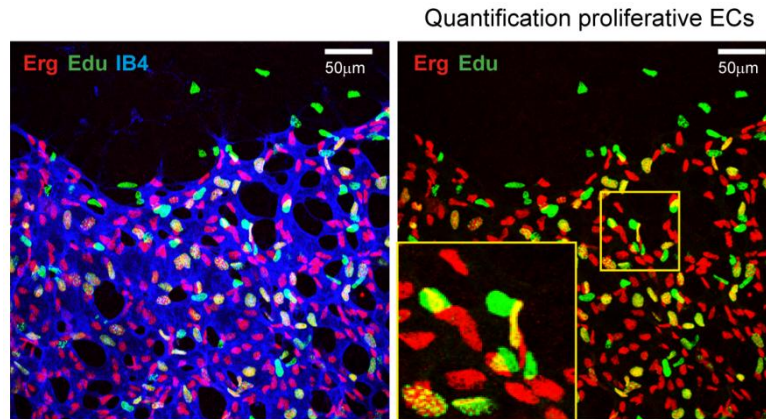


Figure 3.7. Number of proliferative EC

3.1.8.8. Quantification of collagen IV staining intensity

The quantification was done using the Image J software in images taken with the 40x objective and proper scale set up. The total intensity of collagen IV staining over the isolectin-B4 positive area was quantified as shown in **Figure 3.8**. For that, first the channels were splitted from maximal z-stack projections. The isolectin-B4 channel was used to establish the vascular area by setting a manual threshold to have a binary image. Isolectin-B4 positive area was used as template to measure the intensity of the collagen IV staining in this area. Area and integrated density parameters were measured. Then, to calculate the corrected total fluorescence (CTF) the following formula was used:

- $CTF = \text{Integrated Density} - (\text{Area selected for Isolectin-B4 positivity} \times \text{Mean fluorescence of background readings})$.

The background readings were taken from three areas close to the vasculature but negative for isolectin-B4. The average of the CTF of different retinas is the value represented in the graphs named as integrated density.

3. Materials and Methods

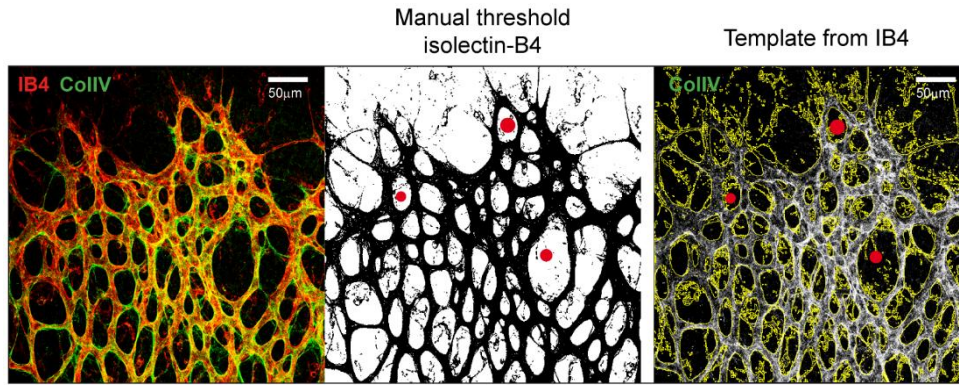


Figure 3.8. Collagen IV integrate density.

3.1.9. Pharmacological inactivation of p110 β *in vivo* using the RIP1-Tag2 model

To study the role of p110 β in a pathological condition the KIN-193 was used to pharmacologic inhibits p110 β in the RIP1-Tag2 mice model. The RIP1-Tag2 mice used for this study were provided by Dr. Oriol Casanovas IDIBELL-ICO. When the animals reached the 12 weeks of age, they were randomly distributed within the treatment and control groups. Both males and females were used in the same proportion since females generally have less tumour burden and survive less than males. The KIN-193 was kindly provided by Dr. Violeta Serra VHIO's. RIP1-Tag2 mice were treated daily by oral gavage starting at 12 weeks of age until 16 weeks of age with KIN-193 [(10 mg/kg/d) MedChemexpress (Shanghai, China)] and vehicle [0.5% (w/v) methylcellulose and 0.2% (w/v) polysorbate 80 in deionized water].

The animals were sacrificed by cervical dislocation and the pancreas with the tumours, the spleen and liver were collected and stored in paraffin or OCT.

3.1.9.1. Evaluation of the animal status and determination of endpoint survival

To evaluate the animal survival we took into account the animal condition in the endpoint. This endpoint was determined because the pharmacological

treatment period had arrived to the end or the animal was presenting illness or suffering signs. In the end of the study, a survival curve was performed to evaluate the efficiency of the pharmacological treatment and the overall survival of the animal. The pancreas and liver of the animal were collected in the endpoint to evaluate the antitumor, the angiogenic and the metastatic effect of the pharmacological treatment (**Figure 3.9**).

3.1.9.2. Determination of pancreatic tumour number and burden of RIP1 –Tag2

The pancreas of the animals were surgically isolated and the tumour number and burden were determined. In the end of the study the average per animal of the tumour number and burden were calculated and the treated group (KIN-193) and the vehicle were compared.

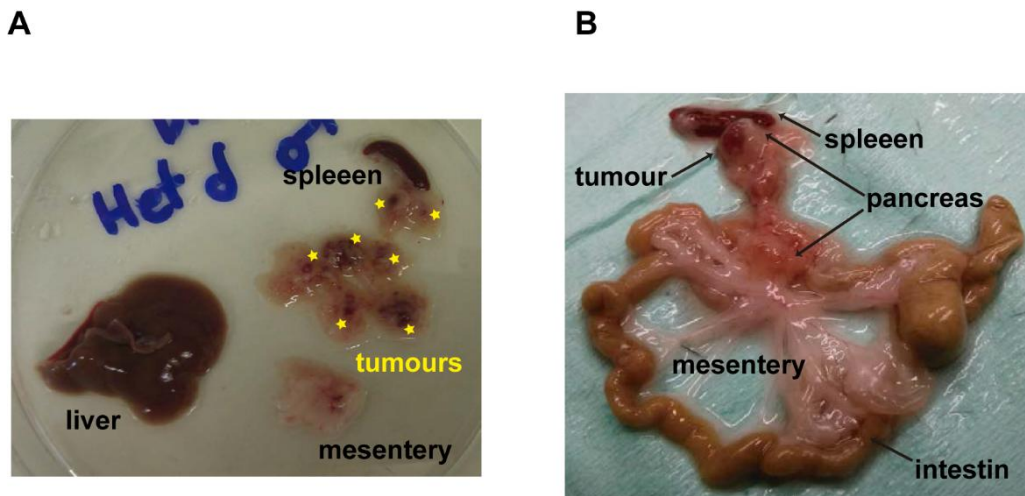


Figure 3.9. RIP1-Tag2 tumoral model. (A) Image of pancreas with multiple tumours, the mesentery and the liver. (B) The pancreas it is well connected with the spleen and the mesentery.

The tumour burden, expressed as mm^3 , was calculated by the sum of all individual tumour volume collected for each mouse. To calculate the volume of each tumour the formula for a spheroid was applied (**Figure 3.10**).

3. Materials and Methods

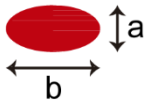
$$V_a = \Sigma (\pi/6 \times a^2 \times b)$$
A diagram of a red ellipsoid. A horizontal double-headed arrow below the ellipsoid is labeled 'b', representing its width. A vertical double-headed arrow to the right of the ellipsoid is labeled 'a', representing its height.

Figure 3.10. Formula to determine the tumour volume (V_a).

3.1.9.3. Determination of the hemorrhagic phenotype of the tumours

In order to determine the grade of effectiveness of the KIN-193, we evaluated the colour of each tumour present in the pancreas of each animal where three colour degrees were considered: red (fully haemorrhagic), pink and white. Thereafter, we calculated the percentage of each of the three phenotypes and we compared to the total number of tumours per animal.

3.1.9.4. Determination of macro-metastasis in liver and mesentery

We also analysed whether the animal had secondary tumours in other organs that were not the pancreatic ones, focusing mostly on the liver, which is the organ more affected with metastasis in the RIP1-Tag2 mice model. We also focus on the mesenteric lymph nodes once they become enlarged and change colour (darker) when they are infiltrated. We also registered the presence or absence of mesenteric lymph nodes infiltrations and its size and colour. Moreover, the RIP1-Tag2 mice can also present carcinoids in the intestine however, this was not considered as metastasis once the presence of carcinoids is not caused by the beta cells but rather by cells that secrete glucagon.

3.1.9.5. Immunodetection of proteins

3.1.9.5.1. Immunohistochemistry

The tumour tissue was preserved in paraffin blocks and cut into sections of 5µm of thickness, using a microtome, then transferred to poly-lysine slides and the subsequent detection of proteins was performed by immunohistochemistry.

First, the sections were deparaffinised and rehydrated using a battery xylol and ethanol, thereafter the antigen retrieval was performed using a pressure cooker with sodium citrate at pH = 6. The samples were left to cool in citrate for 20 minutes. Then, the endogenous peroxidases were inactivated by a solution of 3% H₂O₂ in distilled H₂O (H₂O_d) for 10 minutes and washed with PBS 1X - 0.05% Triton X-100 (PBS-T) during other 10 minutes. Thereafter, samples were incubated for 1 hour at room temperature (RT) in a blocking solution with 5% goat serum diluted in 1X in a humid chamber. The sections were then incubated overnight with the primary antibody diluted in the blocking solution at 4°C (**Table 3.5**). In the next day, samples were washed 3 times with PBS-T for 10 minutes and incubated in horseradish peroxidase (HRP) conjugated secondary antibody (Dako) for 90 minutes at RT. The samples were washed again 3 times with PBS-T for 10 minutes, and finally revealed with diaminobenzidine (Dako) according to the different antibodies, whereas the negative control did not react. Subsequently, samples were washed with tap water to stop the reaction and were stained with hematoxylin. Finally, the samples were re-dehydrated with ethanol and xylol battery and mounted slides with mounting medium.

3.1.9.5.2. Immunofluorescence

The fresh tumour tissue preserved in OCT at -80 ° C were cut into sections of 5µm using the cryostat and transferred to the poly-lysinate slides and the subsequent detection of proteins by immunofluorescence was

3. Materials and Methods

performed. The samples were fixed with acetone (kept at -20 ° C) for 10 minutes at 4°C. After leaving the samples drying to remove all the acetone, the sections were washed 3 times with PBS 1X for 10 minutes. Thereafter, the sections were blocked using blocking solution consisting of 5% goat serum in 1X PBS for 1 hour at RT in a humid chamber. After that, the sections were incubated with primary antibody diluted in blocking solution ON at 4°C (**table 3.5**). In the next day, the samples were washed with PBS and incubated with the secondary antibodies diluted at 1/200 (**Table 3.4**) in blocking solution in a humid chamber, protected from light for 90 minutes at RT. The samples were washed 3 times with PBS and incubated with DAPI to 1/5000 in PBS for 5 minutes. The sections were finally mounted with mounting medium consisting mowiol and Dako.

Table 3.5. List of primary antibodies used in RIP1-Tag2 studies

Antibody	Host	Assay	Dilution	Company	Catalogue#
CD31	rat	IF	1:100	BD Pharmigen	550274
Desmin	rabbit	IF	1:150	Abcam	Ab15200
Tag	rabbit	IF/IHC	1:10.000	Homemade (Pàez-Ribes et al., 2009)	-

3.1.9.6. Immunohistochemistry and immunofluorescent analysis

The different analysis and parameters evaluated were based on a number of samples (N) with a minimum of five animals per group and a minimum of 3 tumours per group. In the RIP1-Tag2 mice tumours were considered individual data.

3.1.9.6.1. Vascular analysis

In the vascular analysis the number of vessels and PCs was determined using the CD31 and desmin marker, respectively. The quantifications were made using 20x images, taken with a Nikon-80I, and four images were analyzed for each tumour and a minimum of four tumours were considered. For the vessels analysis the data are represented as number of vessels (CD31+) by section, and for the PCs the data are represented as the number of PCs (Desmin+) per number of vessels (CD31+).

3.1.9.6.2. Micro-metastasis analysis

The presence of tumour cells in the liver or lymph nodes was assessed by T-antigen (Tag) immunostaining in either OCT or paraffin embedded. The incidence of liver/lymph node metastasis was determined by scoring for presence or absence in each animal from a minimum of 10 mice per group (**Figure 3.11**).

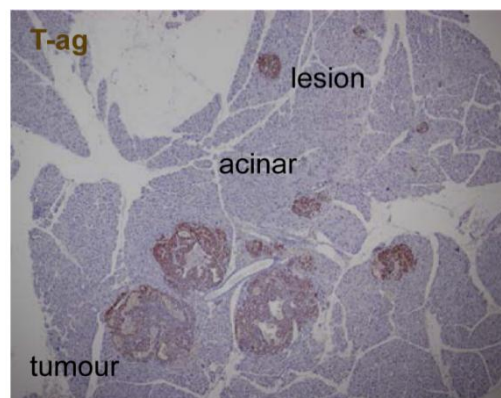


Figure 3.11. Immunohistochemistry image with T-antigen staining.

3.2. Cell Culture

3.2.1. Culturing of mouse brain PC cells

To isolate PCs from the brain we followed the protocol described by Tigges., et al (Tigges et al., 2012). First, we have done the coating of two wells of a 12-well plate with 500 µl of 2% collagen type 1 (BD Biosciences 354249) for at least 2 h at 37 °C (we have previously dissolved 200 µl of high concentration collagen type 1 in 10 ml of PBS). Then, six mice were sacrificed by cervical dislocation, shortly before their brains were extracted and placed in cold Hank's balanced salt solution (Gibco) containing 1% penicillin/streptomycin (P/S, Gibco). The olfactory bulb, cerebellum and medulla were dissected away and the rest of the brain was minced thoroughly with a sterilized razor blade. The minced brain tissue was washed once with the Hank's balanced salt solution and then washed by centrifuging in a 15 ml falcon tube centrifuge at 1200 rpm for 5 min and incubated in an enzymatic solution (Worthington LK003150), containing 30 U/ml papain and 40 µg/ml DNase I in Earl's Balanced Salt Solution (EBSS) avoiding vigorous mixing for 70 min at 37 °C (To reconstituted one papain vial with 250 µl of EBSS-DNase and add 3.75 ml of EBSS for a final volume of 4 ml).

After incubation the digested brain tissue was homogenized by passing it 10 × through an 18 gauge needle and subsequently 10 × through a 21 gauge needle. The homogenized brain cells were then mixed with 1.7 volumes of 22% bovine serum albumin (BSA) in phosphate buffered saline (PBS) in 15 ml Falcon and centrifuged at 4000 rpm for 10 min. The lipid layer on top of the vial was carefully removed, and the cell pellet was re-suspended in 5 ml of EC growth medium (ECGM) consisting of Hams F12, supplemented with 10% FBS, Heparin, ascorbic acid, l-glutamine, penicillin/streptomycin (all from Sigma, St. Louis, MO) and EC growth supplement (ECGS) (EBM-2 basal medium (Lonza CC-3156) + EGM-2 Bulletkit (Lonza CC-4176), and centrifuged for 5 min at 1200 rpm. Subsequently, the cells were re-suspended in ECGM and plated on two wells of a 12-well plate coated with collagen I. After 20 h, cells were washed

3 times with PBS and fresh ECGM added. Cells were grown in ECGM, with the medium changed every 3 days. After 7–9 days, the cells reach confluence, and the cultures were harvested with trypsin and passed 1:2 onto fresh collagen-coated 12-well plates. Cells were grown to confluence and then passed again as described previously. During the first two passages, the cells were kept in ECGM; following the third passage, cells were maintained in PC medium (ScienCell 1201): basal medium + 2% FBS and supplements (included) containing 2% FBS.

3.2.2. Culturing of mouse lung EC (mLECs)

3.2.2.1. EC isolation from mouse lungs

3.2.2.1.1. Tissue digestion

The WT mice were sacrificed by cervical dislocation and their lungs were removed and kept in ice cold Hank's balanced salt solution (Gibco) containing 1% penicillin/streptomycin (P/S, Gibco). Once in the cell culture primary hood, lungs were minced with a scalpel. Then, lung pieces were poured through a 40 µm cell strainer, placed on a 50 ml Falcon tube, to remove blood constituents. Tissue pieces were digested in 5ml 4U/ml of dispase II (Gibco,#17105-041) for 1h at 37°C. Thereafter, the suspension containing lung pieces was homogenized by pipetting up and down to release single cells from the tissue pieces. Then, DMEM (Lonza, #BE12-604F) containing 10% of inactivated FBS (Gibco, #10270-106) and 1% P/S was added to the cell suspension and the homogenate was filtered through a 40 µm cell strainer, placed on a 50ml. A pellet containing mouse cells was obtained by centrifugation (5min 1200rpm). The pellet was washed twice with PBS/BSA (PBS containing 0.5% BSA (diluted from PAA, #K11-022), performing a 5 min centrifugation (1200rpm) after every wash.

3. Materials and Methods

3.2.2.1.2. First selection

The resulting cell pellet from the last centrifugation was re-suspended in 100µl of PBS/BSA. Previously, we have prepared magnetic beads coated with VEcadherin (BD Pharmigen, #555289) used to isolate specifically ECs from the lung homogenate. 6µl/lung of magnetic beads were placed into a 1.5ml eppendorf and were washed five times with PBS/BSA using a Dynal magnet (Dynal, MCP-S). After the last wash, magnetic beads were re-suspended in 6µl of PBS/BSA and finally, 1.25µl/lung of VE-cadherin antibody were added. The mixture of magnetic beads and VE-cadherin was incubated 1h at RT with gentle shaking. Magnetic beads were then washed four times with PBS/BSA using a magnet for cell separation. Then, 100 µl of PBS/BSA were added into the eppendorf and the mixture was homogenized and transferred to incubate with the 100 µl of cell suspension for 30 min at RT. Then, magnetic beads were washed four times with PBS/BSA using a magnet for cell separation. After the final wash, magnetic beads coupled with ECs were re-suspended in F-12 complete medium containing: DMEM F-12 (Gibco, #21041-025), supplemented with 20% of inactivated FBS (Gibco, #10270-106), 4 ml of EC growth factor (Promocell, #C-30140) and 1% P/S. Then, the suspension was seeded on 12-well culture dishes coated with 0.5% gelatine (Sigma) in sterile H₂O (this moment is considered as passage 0 (P₀)). The following day, the wells were carefully washed twice with PBS/BSA and F-12 complete medium was replaced. The medium was changed every second day.

3.2.2.1.3. Second selection

Once the cells had been in culture for 7 days, they were re-purified by removing the culture medium and incubating the cells for 1h with a solution containing VE-cadherin antibody-coated magnetic beads (prepared as described in 3.2.2.1.2). After 1h of incubation at RT, cells were trypsinized and centrifuged for 5 min at 1200 rpm. Then, the pellet was washed three times with PBS/BSA and finally re-suspended in DMEN F-12 complete medium. Cells

were seeded on 12-well culture dishes coated with 0.5% gelatine in sterile H₂O. The following day, the wells were carefully washed twice with PBS/BSA and DMEN F-12 complete medium was replaced. From here on, cells were cultured and split following standard procedures, always guaranteeing a confluence of at least 70% and never exceeding from passage 5.

3.2.3. Co-cultures of PCs and mLECs

3.2.3.1. Migration Assay

For the migration assay co-cultured, first, four 8 μ M PET filters of the transwells (Falcon, #35097) were pre-coated with Gelatin 0.5%, and let it dry overnight in the hood. In the same day 4 wells of a 24-well plate were coated with 2% of collagen type I during at least 2 hours and WT PCs were seeded (re-suspended in 600 μ L of PC medium) to reach a 100% of confluence (0.8×10^5 cells/well). In the next day, the PET filters were first re-hydrated and incubated with DMEM to balance the pH and then WT mLECs were seeded carefully (re-suspended in 150 μ L) to obtain a monolayer (0.5×10^5) with the different conditions (**Figure 3.12**): (1) as a negative control, EC monoculture (without PCs (PC -)) in DMEM-F12 starving medium condition (SM - without growth factors and FBS) was used; (2) ECs were co-cultured with the PC (PC +) in DMEM-F12 starving medium (SM - without growth factors and FBS); as positive controls, we have used (3) the EC monoculture (PC -) in their optimal culture conditions (DMEM-F12 EC complete medium (with growth factors and FBS) - CM); and 4) ECs and PCs co-cultured (PC +) in EC optimal culture conditions DMEM-F12 EC complete medium (with growth factors and FBS) - CM).

The PCs were watched twice with PBS1x and the same mediums conditions were used. The ECs were placed on the top and incubated during 72 hours. Then the medium was aspirated and washed carefully two times with PBS. Therefore, 0.5% crystal violet staining solution was used for each well and incubated for 20 min at room temperature. Then, the transwell was carefully washed again four times with PBS1x to remove the excess of crystal violet and

3. Materials and Methods

cotton swaps were used in the upper part of the PET filter to remove the ECs that did not migrate. Then filters were removed from the transwell using a blade and mounted with Mowiol with DAKO for posterior microscopy analysis

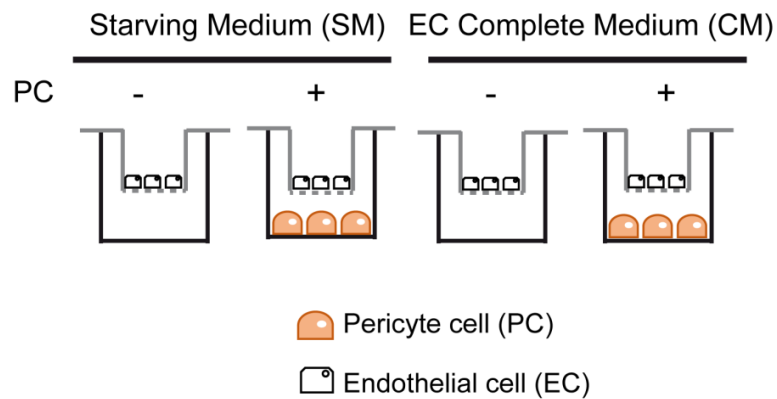


Figure 3.12. Migration assay for EC-PC co-cultures.

3.2.3.2. Proliferation Assay

For the co-cultured migration assay first four 0.4 μ M PET filters of the transwells (Corning[®] 24 Well HTS Transwell[®], # EK-680170) were pre-coated with collagen type I 2%, and let it dry overnight in the hood. In the next day, the PET membranes were first re-hydrate and incubated with DMEM to balance the pH and then the PCs were seeded carefully (re-suspended in 150 μ L of PC medium) to obtain a monolayer (0.5×10^5). In the next day, 4 wells of a 24-well plate with cover sleeps were coated with 0.5% of gelatin during 30 minutes and WT ECs were seeded (re-suspended in 600 μ L with the different conditions) to reach a 30% of confluence (0.3×10^5 cells/well). The PC in the transwells were then washed two times with PBS1x and placed in the ECs with the same different conditions described in 3.2.3.1 (**Figure 3.13**): (1) as a negative control, EC monoculture (without PCs (PC -)) in DMEM-F12 starving medium condition (SM - without growth factors and FBS) was used; (2) ECs were co-cultured with the PC (PC +) in DMEM-F12 starving medium (SM - without growth factors and FBS); as positive controls, we have used (3) the EC monoculture (PC -) in their

optimal culture conditions (DMEM-F12 EC complete medium (with growth factors and FBS) - CM); and 4) ECs and PCs co-cultured (PC +) in EC optimal culture conditions (DMEM-F12 EC complete medium (with growth factors and FBS) - CM). The cells were incubated during 24hours. And the BrdU stained was performed in the ECs as described in the 3.2.4.5 section.

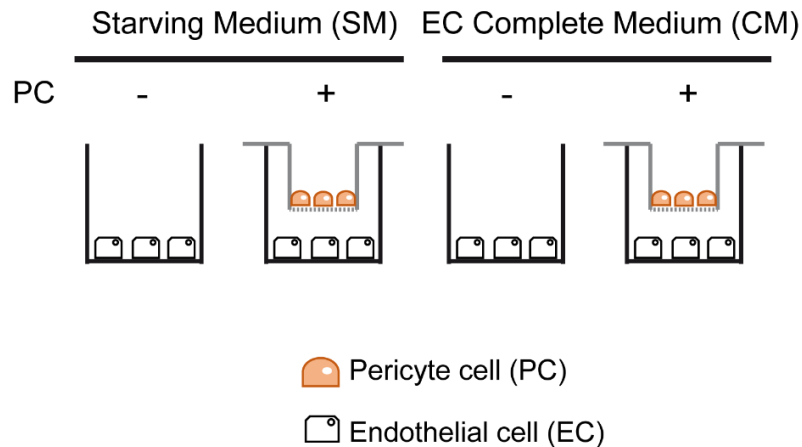


Figure 3.13. Proliferation assay for EC-PC co-cultures.

3.2.4. Pharmacological treatments in PCs

To evaluate the inhibition of the PI3K pathway *in vitro*, different types of PI3K inhibitors were used namely: the pan-PI3K - **GDC-0941** (1.0 μM); the p110 α specific - **GDC0326** (1.0 μM); the p110 β specific - **TGX-221** (0.5 μM); and the p110 δ specific - **D030** (IC-87114) (0.5 μM) or vehicle (DMSO) (**Table 3.6**).

3.2.4.1. PCs migration assay upon PI3K specific inhibition (wound healing assay)

First, a 6-well plate was coated with 2% of collagen type I during at least 2 hours, thereafter WT PCs were seeded into PCs medium to reach a 100% of confluence in order to obtain a monolayer of cells (0.2×10^6 cells/well). The next

3. Materials and Methods

day, using a (yellow) pipette tip a straight scratch was made, simulating a wound. Then the cells were washed twice with PBS1x and the mediums with the different inhibitors added, namely the p110 α -specific **GDC0326** (1.0 μ M); the p110 β -specific **TGX221** (0.5 μ M); and the vehicle (DMSO). Photos were taken immediately after wound (time 0h) and after 18h (time 18h).

3.2.4.2. PCs proliferation assay upon PI3K specific inhibition

First, a 24-well plate was used with the cover slips and coated with 2% of collagen type I during at least 2 hours, thereafter WT PCs were seeded into PCs medium to reach a 30% of confluence (0.3×10^5 cells/well) with the different medium conditions using the different inhibitors, namely the p110 α -specific **GDC0326** (1.0 μ M); the p110 β -specific **TGX221** (0.5 μ M); and the vehicle (DMSO) and incubated during 24hours. The next day the BrdU assay was performed as described in the section 3.2.4.5.

Table 3.6. PI3K inhibitors used *in vitro*

Name	Isoform Specificity	Work Concent,	IC50
GDC-0941	pan-PI3K	1.0 μ M	3 nM p110 α , 33 nM p110 β , 3nM p110 δ and 75nM p110 γ
GDC0326	p110 α	1.0 μ M	(KI*: 0.2 nM p110α , 133nM p110 β , 20 nM p110 δ and 51 nM p110 γ)
TGX-221	p110 β	0.5 μ M	5 nM p110β (5 μ M p110 α , 210 nM p110 δ i >10 μ M p110 γ)
D030 (IC-87114)	p110 δ	0.5 μ M	0.5 μM p110δ (75 μ M p110 β /p110 α and 29 μ M p110 γ)

* KI (inhibitory constant): for the GDC0326 we did not have access to the IC50, therefore the KI values are represented. The KI refers to the affinity of a particular drug; indicates the concentration of inhibitor required to hold 50% of the receptors for a particular therapeutic target. The IC50 is the average of the highest inhibitory concentration, indicates the concentration required to inhibit 50% of a process.

3.2.4.3. PCs viability assay using MTS assay upon PI3K specific inhibition

PCs were seeded in 96-well culture plates (2000cells/100µl culture medium per well) with the different medium conditions using the inhibitors: p110α-specific **GDC0326** (1.0 µM); the p110β-specific **TGX221** (0.5 µM); and the vehicle (DMSO). The next day, 20µl of MTS reagent (Promega, CellTiter 96 Aqueous Non Radioactive Proliferation Assay, #G5421) were added to each well 4h before the desired end-point. Cells were incubated with MTS compound at 37°C for 4h and absorbance was recorded at 490nm. If pharmacological treatments were required for the experiment, drugs were incorporated at the desired concentrations before cells were seeded into the 96-well plates.

3.2.4.4. PCs treatment to Western immunoblotting

First, a 6-well plate was coated with 2% of collagen type I during at least 2 hours, thereafter WT PCs were seeded into PCs medium to reach a 50% of confluence (0.1×10^6 cells/well). The next day, the mediums with the different inhibitors were added, namely the p110α-specific **GDC0326** (1.0 µM); the p110β-specific **TGX221** (0.5 µM); the p110δ-specific **D030** (0.5 µM); the pan-PI3K **GDC0941** (1.0 µM) and the vehicle (DMSO). Treatments were made during 2 hours and the protein lysates and the immunoblotting were made as described in the section **3.2.5**.

3.2.4.5. Immunofluorescence of cultured PCs and mLECs

For this purpose, 10µM BrdU (Amersham) was incorporated to the cell culture medium and was incubated for 2h. Then cells were rinsed three times with PBS and fixed with 4% PFA for 20min. Two more washes with PBS were performed after fixation and thereafter cells were permeabilized with PBS-0.2% Triton X-100 for 5min, treated with HCl 2N for 10min and blocked for 45min at

3. Materials and Methods

RT in PBS containing 3% BSA. BrdU incorporated in DNA was immunodetected by incubation with a mouse monoclonal anti-BrdU (BD Bioscience, #347580) incubated 1:50 in PBS containing 3% BSA, ON at 4°C in wet chamber. The following day, cover-slips were washed three times (5min each with TBS-T), and secondary antibody (Molecular Probes, goat anti-mouse 488 #A-11001) was incubated at the appropriate dilution (1:200) in PBS containing 3% BSA, for 1h at RT. Cover-slips were then washed three times with TBS-T, adding DAPI (1µg/ml) in the last one. A final wash with PBS was performed before mounting the cover-slips on microscope slides using Mowiol as mounting medium. Immunofluorescence was visualized with a Nikon microscope 801 (20x lens). For analysis, the number of BrdU positive cells per field was rectified by the total number of cells present at the field (DAPI positive).

3.2.5. Protein extraction and Western immunoblotting

3.2.5.1. Protein lyses and sample processing

For Western blot analysis, PCs and mLECs were lysed with lysis buffer B (150 mM NaCl, 1mM EDTA, 50 mM Tris-HCl pH 7.4 and 1% Triton X-100 in H₂O) supplemented with 1mM DTT, 2 mg/ml aprotinin, 1 mM pepstatin A, 1 M leupeptin, 10 g/ml TLCK, 1 mM PMSF, 50 mM NaF, 1 mM NaVO₃ and 1 µM okadaic acid. Lysates were collected in a 1.5ml eppendorf and were kept on ice for 15min. Then, lysates were centrifuged for 15min, at maximum speed at 4°C. Supernatants were collected in a new ice-cold 1.5ml eppendorfs and were kept frozen at -80°C until processed for experiment. The protein content of the samples was quantified using the BCA protein assay kit (Pierce) following the instructions recommended by the manufacturer. Protein samples were then diluted in sample buffer 4X (250 mM Tris-HCl pH 6.8, 40% glycerol, 8% SDS, 0.04% bromophenol blue and 250mM DTT in H₂O) in a proportion of 3 volumes of protein sample: 1 volume of 4X SDS sample buffer. Samples were heated at 100°C for 5 min and spinned for 30sec to recover all the volume.

3.2.5.2. Protein electrophoresis and membrane transference

Samples were resolved on 8%, 10% or 12,5% SDS poly-acrylamide gels. SDS-PAGE gels were composed of a stacking part (4% acrylamide, 125mM Tris-HCl pH 6.8, 0.4% SDS, 0.1% ammonium persulfate (APS) and 0.1% tetramethylethylenediamine (TEMED) in H₂O) and a resolution part (10% acrylamide, 375mM Tris-HCl pH8.8/0.4% SDS, 0.1% APS and 0.1% TEMED in H₂O). Samples were run for 1- 2h at 130V with running buffer 1X (25mM Tris, 192 mM glycine and 0.1% SDS in H₂O). Thereafter, proteins separated in the acrylamide gels were transferred generally onto PVDF membranes (Roche) previously activated in methanol (Emsure). For the detection of MYPT were used nitrocellulose membranes (Roche). Gel to membrane transference was performed at 4°C at 250 mA for 2h in Transfer buffer 1X (25mM Tris, 192mM glycine and 20% methanol). After transference, membranes were washed for 5min in 1X TBS (For 500mL of TBS 10x: 6g Tris, 43.85 g NaCl, pH7.5) containing 0.05% Tween (referred as TBS-T). Membranes were then incubated for 1h at RT with TBS-T containing 5% of milk. Membranes were washed twice (5min each time) with TBS-T and incubated ON at 4°C with incubation solution (2% BSA in TBS-T with 0.02% sodium azide) containing the desired primary antibody at the appropriate dilution. Table 3.8 details primary antibodies used for immunoblotting. The following day, membranes were washed three times (10min each) with TBST and were incubated for 1h at RT with 5% milk in TBS-T containing the appropriate dilution of secondary antibodies (Table 3.9). Upon incubation with secondary antibody, membranes were washed three times (10min each) with TBS-T and protein detection was performed by enhanced chemiluminescence (ECL) following the protocol described in Table 3.10. Quantification of band intensities by densitometry was carried out using the Image J software.

3. Materials and Methods

Table 3.7 Reducing agents, phosphatase and protease inhibitors used for the different lysis buffers

Product	Company-Catalogue #
DL-Dithiothreitol (DTT)	Sigma ; #D0632
Aprotinin	Sigma ; #A6279
Pepstatin A	Sigma ; #P4265
Leupeptin	Sigma ; #L2884
Na-p-tosyl-L-lysine chloromethyl ketone (TLCK)	Sigma ; #T7254
Phenylmethylsulfonylfluoride (PMSF)	Sigma ; #P7626
Sodium fluoride (NaF)	Sigma ; #S7920
Sodium orthovanadate (NaVO ₃)	Sigma ; #S6508
Okadaic acid	Cayman Chemical Company; #10011490

Table 3.8. Primary antibodies used for immunoblotting

Antibody	Host	Company	Dilution	Catalogue #
VE-cadherin	Goat	Santa Cruz	1:200	sc-6458
PTEN	Rabbit	Cell Signalling Technology	1:1000	9559
β-actin	Mouse	ABCCAM	1:25000	49900
p-akt (S473)	Rabbit	Cell Signalling Technology	1:2000	4060
p-S6 (Ser240/244)	Rabbit	Cell Signalling Technology	1:1000	2215S
PDGFRβ (cd140b)	Rat	eBioscience	1:500	14-1402-82
p110α	Mouse	Home made Monoclonal Antibody U3A	1:10	(Klippel et al., 1994)
p110β	Rabbit	Santa Cruz	1:300	sc-602

3. Materials and Methods

p1105	Rabbit	Santa Cruz	1:500	sc-7176
pan-p85	Rabbit	Upstate	1/5000	06-195
p-Erk	Rabbit	Cell Signalling Technology	1/1000	. 9102
t-Akt	Rabbit	Cell Signalling Technology	1/1000	9272
t-Erk1/2	Rabbit	Cell Signalling Technology	1/1000	9102
Desmin	Rabbit	Abcam	1:1000	Ab15200
Tubulin	Mouse	Sigma	1:25000	T6074

Table 3.9. Secondary antibodies used for immunoblotting

Antibody	Host	Company	Dilution	Catalogue #
Anti-Rabbit HRP	Swine	DAKO	1:5000	P 0399
Anti-mouse HRP	Rabbit	DAKO	1:5000	P 0260
Anti-goat HRP	Rabbit	DAKO	1:5000	P 0160

Table 3.10. ECL protocol

Solution A	Solution B
5ml 1M Tris pH8.5 45ml H2O 110µl 90mM coumaric acid (Sigma) 250 µl 250mM luminol (Sigma)	110 µl H2O2 30% 900 µl H2O
*Solutions A and B need to be mixed in a 1:3 ratio	

4. Results

Part I – PI3K in PCs during physiological angiogenesis

4.1. PCs during vascular development

4.1.1. PCs differentiation during vessels maturation

The first aim of the study was to investigate PCs biology during angiogenesis using mice retinas at different time points of their development. For this purpose, we collected *wild type* (WT) mice retinas at the following time points: at **postnatal day 3 (P3)**, where the vascular plexus is growing through sprouting angiogenesis and the vasculature looks immature – at this time point it is difficult to distinguish arteries and veins; at **postnatal day 6 (P6)**, where two different areas can be distinguished: 1) the sprouting front area, where the plexus is immature, similarly to the P3 retinas (P6a); 2) and the distal area close to the optic nerve, where vessels remodelling and regression started to occur (P6b). At this time point it is already possible to differentiate a well- established hierarchical vascular tree of arteries, veins and capillaries; and at **postnatal day 9 (P9)**, where primary plexus is mature and stable and has reached the retinal periphery. Vessels undergo extensive remodelling and regression similarly to what is happening in the P6b retinal area (**Figure 4.1**). This strategy allowed the characterization of PC differentiation from an immature (Angiogenic Front) to a mature (Remodelling Plexus) vasculature.

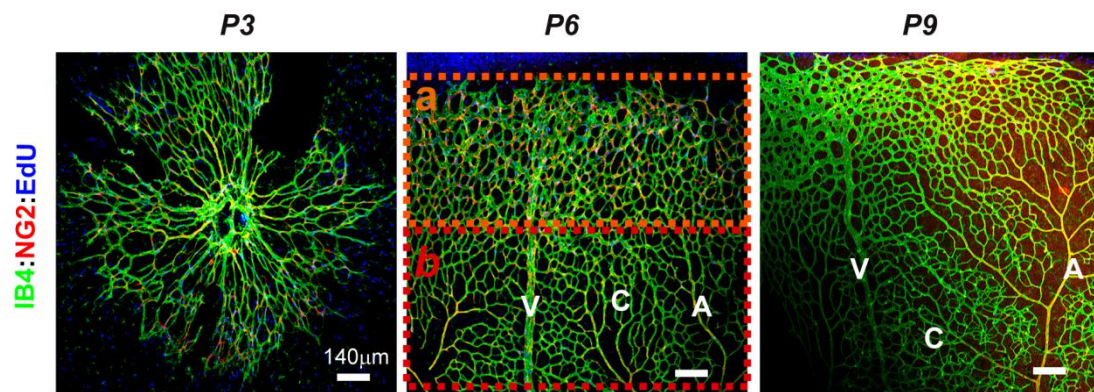


Figure 4.1. Vessel maturation during the sprouting angiogenesis. Whole-mount WT retinas at P3, P6 and P9 of the retinal vessel development, stained for isolectin-B4 (green), NG2 (red) and EdU (blue). The P3 retinas are in active sprouting angiogenesis and the plexus is very immature, where it is not possible to distinguish between vessel types; at P6 we can define two areas in the same preparation: a) sprouting angiogenesis area; and b) the remodelling and stabilization area. We can already differentiate between arteries (A), veins (V) and capillaries (C); at P9 all the plexus is mature and stable.

To understand PCs behaviour during retinal angiogenesis, we decided to analyse different parameters in the growing vasculature.

First, we analysed the PCs coverage per vessel area using the well-defined PC marker NG2, a transmembrane chondroitin sulfate proteoglycan expressed by PCs during the retinal development, together with the vessel marker isolectin-B4. Our quantification revealed that: 1) PC coverage increased over time; and 2) the remodelling areas (P6b and P9) showed more PC coverage, when compared with those areas where sprouting angiogenesis is taking place (P3 and P6a) (**Figure 4.2**). We also noticed that PCs change their morphology during vessel maturation. In areas, where active angiogenesis is taking place, PCs have a retracted shape, presenting multiple protrusions connected with the vessel (**Figure 4.3, yellow arrows**) but the cell body is less connected with the blood microvessels. On the other hand, PCs in the remodelling areas have a more elongated shape and are well-ensheathed within vessels by multiple contact points (**Figure 4.3**).

Next, we quantified the percentage of proliferative PCs at the same time points of the vascular development by injecting EdU (a S-phase marker) at P3,

4. Results

P6 and P9. The number of EdU positive PCs in a $10^4 \mu\text{m}^2$ area was determined after co-labelling with the PC marker NG2 and isolectin-B4. Interestingly, we detected that at early time points, where sprouting angiogenesis occurs, there was a higher number of PCs proliferating (P3 ad P6a), while in the areas of remodelled vasculature, PCs proliferation decreased (P6b and P9) (**Figure 4.4 A-C**). In addition, quantifying the EdU positive cells in the isolectin-B4 positive zone within a $10^4 \mu\text{m}^2$ area, we detected higher proliferative rates of ECs located at the sprouting front of P6 retinas (P6a). Similarly to the patterns of PC proliferation, we observed a dramatic reduction of the ECs proliferation in the remodelling area (P6b and P9). Although both, PCs and ECs proliferate at P3, we detected higher levels of proliferation in PCs when compared with those of the ECs, suggesting that PCs expand first than ECs (**Figure 4.4 A-B-D**).

Taken together, we found that during vessel formation in the retina PCs differentiate along with the vessels maturation. Active and immature PCs are associated with angiogenic sprouts during the early phases of vascularisation where they acquired a retracted position and start to proliferate even earlier than ECs. Quiescent and mature PCs, concomitant with EC quiescence, appear in later stages of vascular development allowing the correct remodelling of the plexus.

4.1.2. Collagen IV and vascular stabilization

PCs recruitment to ECs is necessary to stimulate vascular basement membrane matrix assembly, a key step in vascular maturation and stabilization. One of the several components that form the basement membrane matrix is collagen IV secreted by both, ECs and PCs (Stratman and Davis, 2012).

Thus, following the same strategy used for the Figures 4.2-4.4, we collected WT retinas at P3, P6 and P9 and we stained them with collagen IV and isolectin-B4. We found an increase in collagen IV deposition during vessel maturation with the remodelling plexus areas (P6b and P9) showing increased collagen IV expression when compared with the sprouting front zones (P3 and P6a) (**Figure 4.5**). These data corroborate the importance of collagen IV

secretion during the remodelling angiogenesis, which facilitates the vascular stabilization.

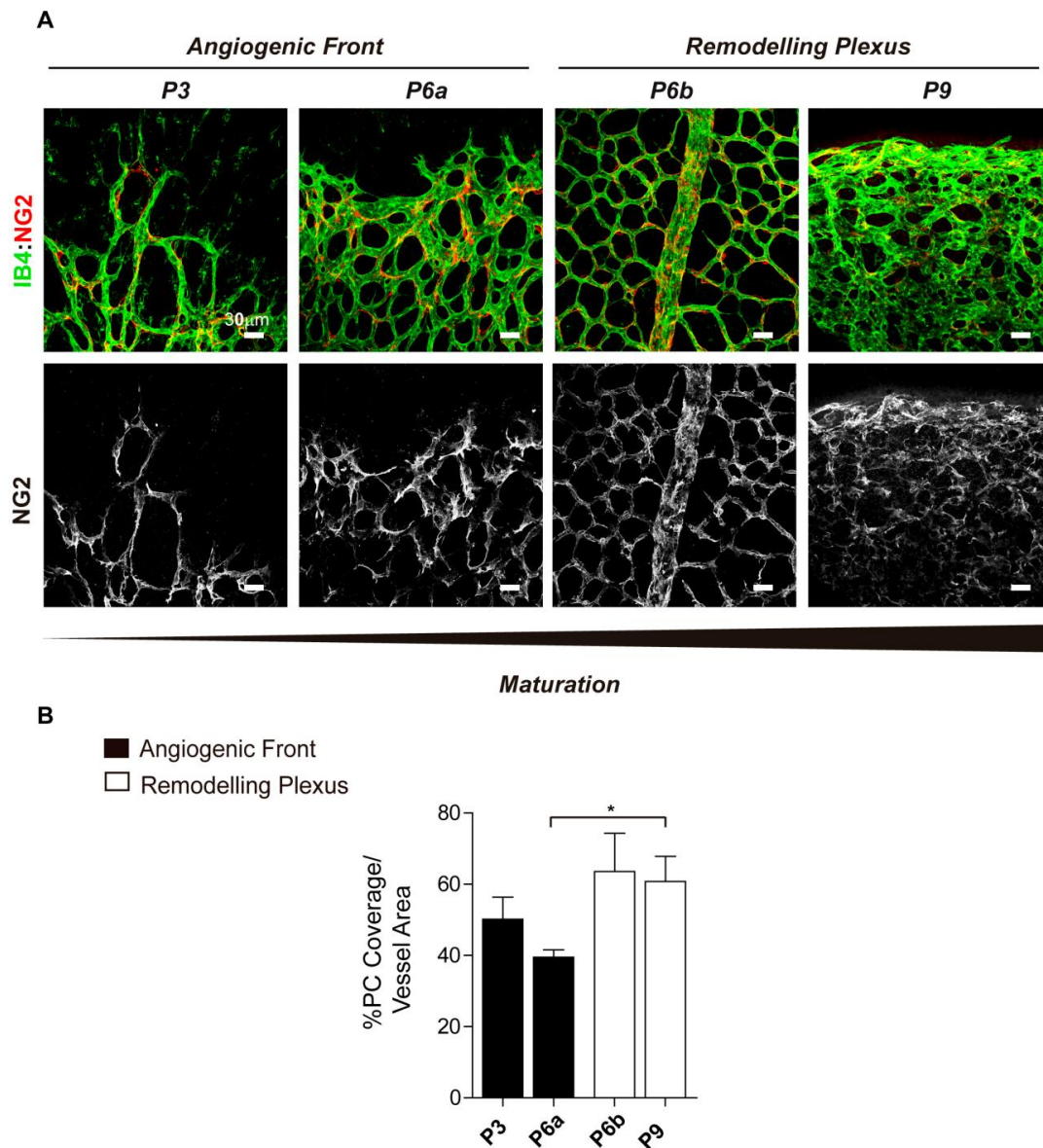


Figure 4.2. PC coverage of vessels increases during maturation. (A) Confocal images of WT retinas at P3 and P6a during the active sprouting angiogenesis (angiogenic front); and at P6b and P9 during vessel remodelling and maturation (remodelling plexus). The retinas are stained with isolectin-B4 (green) and NG2 (red). (B) Quantification of PC coverage shows increased coverage of vessels along the retinal maturation. $N \geq 3$ retinas for each condition. Error bars are standard error of the mean. * $P < 0.05$ was considered statistically significant. Statistical analysis was performed by Mann-Whitney test.

4. Results

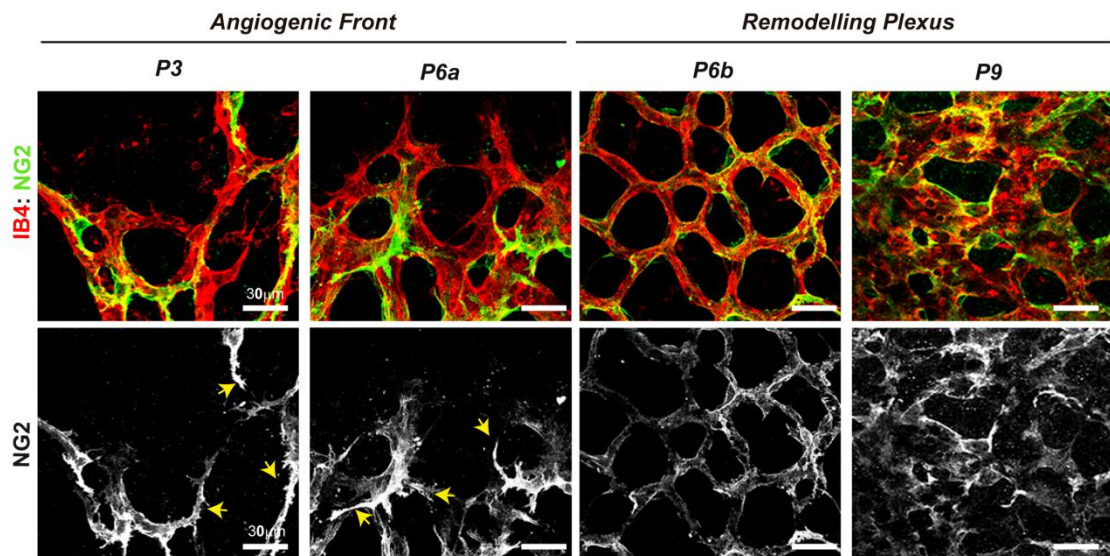


Figure 4.3. PCs change their morphology during the maturation. Confocal images of WT retinas at P3 and P6a during the active sprouting angiogenesis (angiogenic front); and at P6b and P9 during vessel remodelling and maturation (remodelling plexus) showing the PC morphology changes during vessel maturation. The yellow arrows represent the PCs protrusions. The retinas are stained with islectin-B4 (red) and NG2 (green).

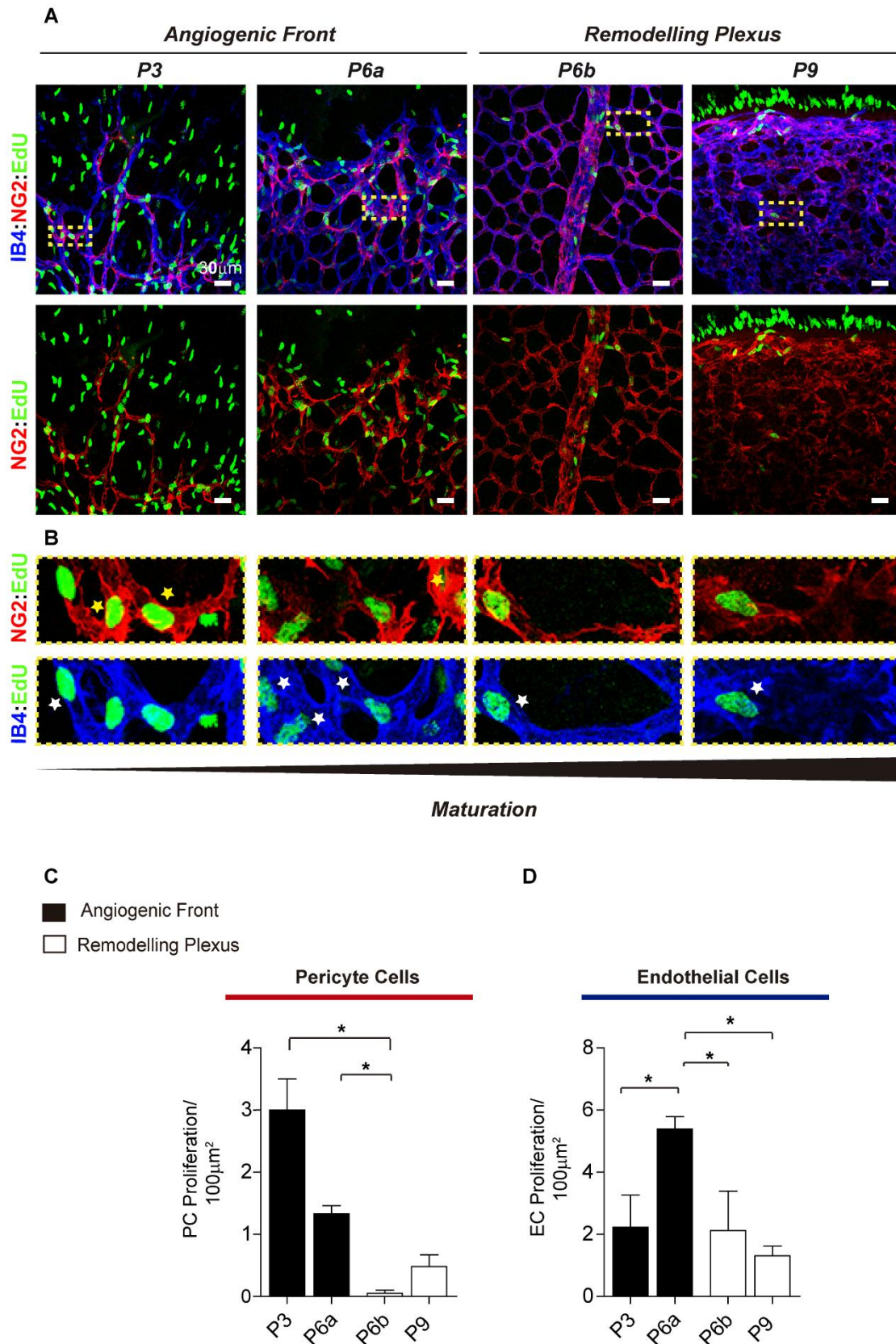


Figure 4.4. PC and EC proliferation decreases during maturation. (A) Confocal images of WT retinas at P3 and P6a during the active sprouting angiogenesis (angiogenic front); and at P6b and P9 during vessel remodelling and maturation (remodelling plexus). Retinas were injected with EdU 2h before isolation and were stained with isolectin-B4 (blue), NG2 (red) and

4. Results

the EdU (blue). **(B)** Zoom of zone selected in A highlighting the NG2 and IB4 proliferation (EdU positive cells). Yellow stars indicate proliferative PCs (NG2+/EdU+) and white stars indicate proliferative ECs (IB4+/EdU+). **(C)** Quantification of PC proliferation – number of EdU positive PC in the NG2 positive area per $10^4\mu\text{m}^2$ of vessel area. $N \geq 3$ retinas for each condition. **(D)** Quantification of EC proliferation - EdU positive cells in isolectin-B4 positive area per $10^4\mu\text{m}^2$. $N \geq 3$ retinas for each condition. Error bars are standard error of the mean. * $P < 0.05$ was considered statistically significant. Statistical analysis was performed by Mann-Whitney test.

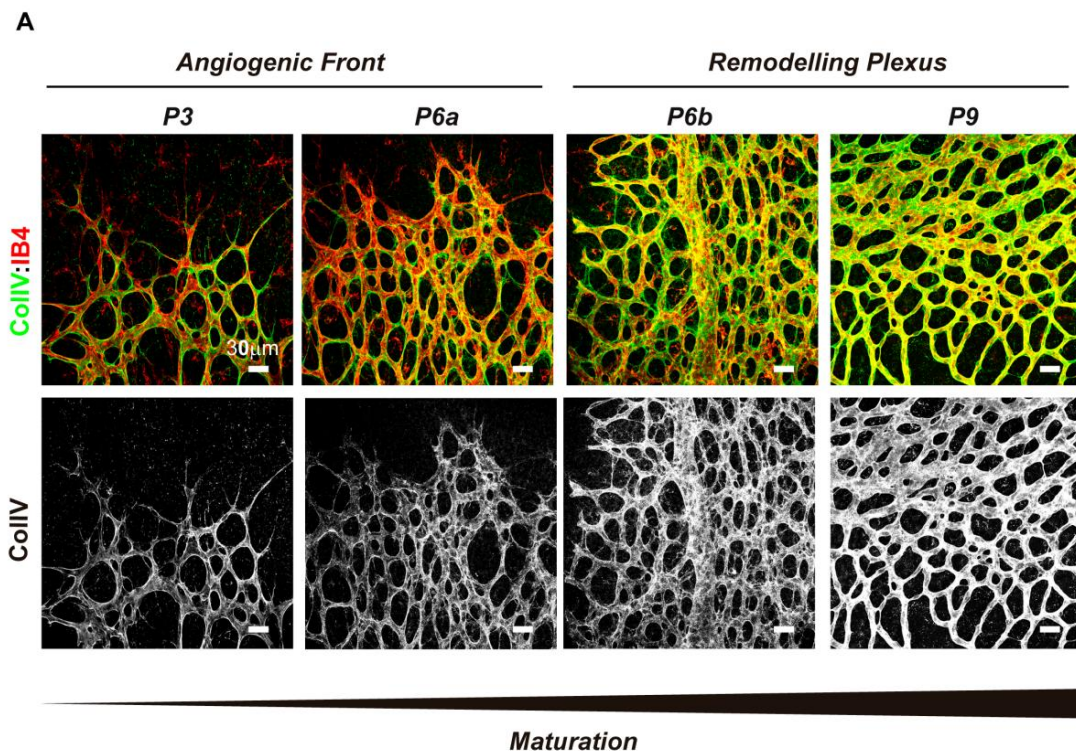


Figure 4.5. Deposition of collagen IV increases during maturation. (A) Confocal images of WT retinas at P3 and P6a during the active sprouting angiogenesis (angiogenic front); and at P6b and P9 during vessel remodelling and maturation (remodelling plexus). Retinas are stained with isolectin-B4 (red) and collagen IV (green).

4.1.3. PCs promote EC proliferation and migration

Our retina data suggests that PCs functions may have impact on the ECs regulation, especially proliferation. To test that, we have co-cultured PCs and ECs using the transwells system and analysed the effects of PCs on ECs proliferation and migration *in vitro*.

First, we have isolated PCs and ECs from WT mice and the purity of the culture was assessed by western blot using both, PCs and EC markers. The PDGFR β and desmin are well-established PC-specific markers and thus were used to identify PCs. The VE-cadherin marker is EC-specific and was used to identify ECs. PCs were shown to be PDGFR β and desmin positives and VE-cadherin negative at passage 6 (P6). Moreover, PCs conserved the same expression profile even after 16 passages (P16), demonstrating the purity of the primary cell culture even after several passages. On the other side, ECs were VE-cadherin positive and PDGFR β and desmin negative (**Figure 4.6**).

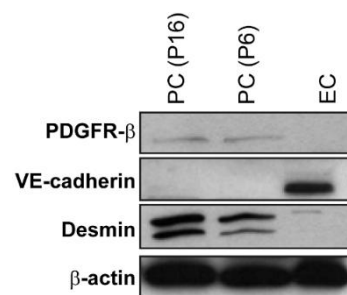


Figure 4.6. Characterization of WT PCs and ECs. Expression of PC markers - PDGFR β and Desmin - and the EC marker - VE-cadherin - in PC and EC WT. For PCs we have used different cell passages(P), namely P16 and P6, to confirm the purity of the primary cell culture after several passages.

Moreover, co-culture systems of PCs and ECs were established in order to analyse if PCs signalling interferes with EC proliferation and/or migration. For the proliferation experiments, PCs were first seeded onto transwell filters with a 0.4 μ m pore size membranes, which only allow the diffusion of soluble factors; after 24 hours ECs were plated in a 24-well plate onto cover slips in a 30% of confluence and the transwells with the PCs were placed on the top of the ECs

4. Results

as described in the material and methods section (3.2.3). The cells were co-cultured for 24 hours. In order to analyse if PCs regulate ECs proliferation, four different conditions were established as represented in **Figure 4.7A**: 1) as a negative control ECs were seeded without PCs (PC -) in starving medium (SM); 2) to see the effect of PCs on ECs proliferation, PCs were placed on the top of ECs (PC+) and co-cultured in starving medium (SM); and as positive controls we have used 3) the ECs monoculture (PC -) in their optimal culture conditions (EC complete medium-CM); and 4) ECs and PCs co-cultured (PC +) in EC optimal culture conditions (EC complete medium-CM). Our results suggested that ECs in the presence of PCs (PC+SM) increased their proliferation, since experienced increase in BrdU incorporation was detected when compared with the ECs alone (PC- SM) (**Figure 4.7 B-C**). These results suggested that PCs communicate with the ECs stimulating their proliferation through paracrine signalling.

For the migration assays, PCs were first plated in a 24 well plate to obtain a monolayer. After 24h, ECs were seeded onto transwell filters with an 8.0 μ m pore membrane, which allows the migration of the cells through the pores, and placed on the top of the PCs as described in the section material and methods section (3.2.3). The cells were co-cultured for 72 hours. To analyse if PCs regulate ECs migration, we again used four different conditions as represented in **Figure 4.8A**: 1) as a negative control, EC monoculture (PC -) in the transwell in starving medium condition was used; 2) to see the effect of PCs on ECs migration, ECs were placed on the top of PC (PC +) and co-cultured in starving medium (SM); as positive controls, we have used 3) the EC monoculture (PC -) in their optimal culture conditions (EC complete medium - CM); and 4) ECs and PCs co-cultured (PC +) in EC optimal culture conditions (EC complete medium - CM). We have detected a slight increase of ECs in the lower part of the transwell filter, after crystal violet staining, when co-cultured with the PCs (PC+SM) compared with the ECs alone (PC-SM), suggesting that PCs also impact on ECs migration (**Figure 4.8B-C**). These results suggested that PCs regulate ECs inducing their migration by paracrine communication.

Overall, our data suggested the existence of an interplay between PCs and ECs where PCs apparently regulate by paracrine signalling ECs proliferation and migration.

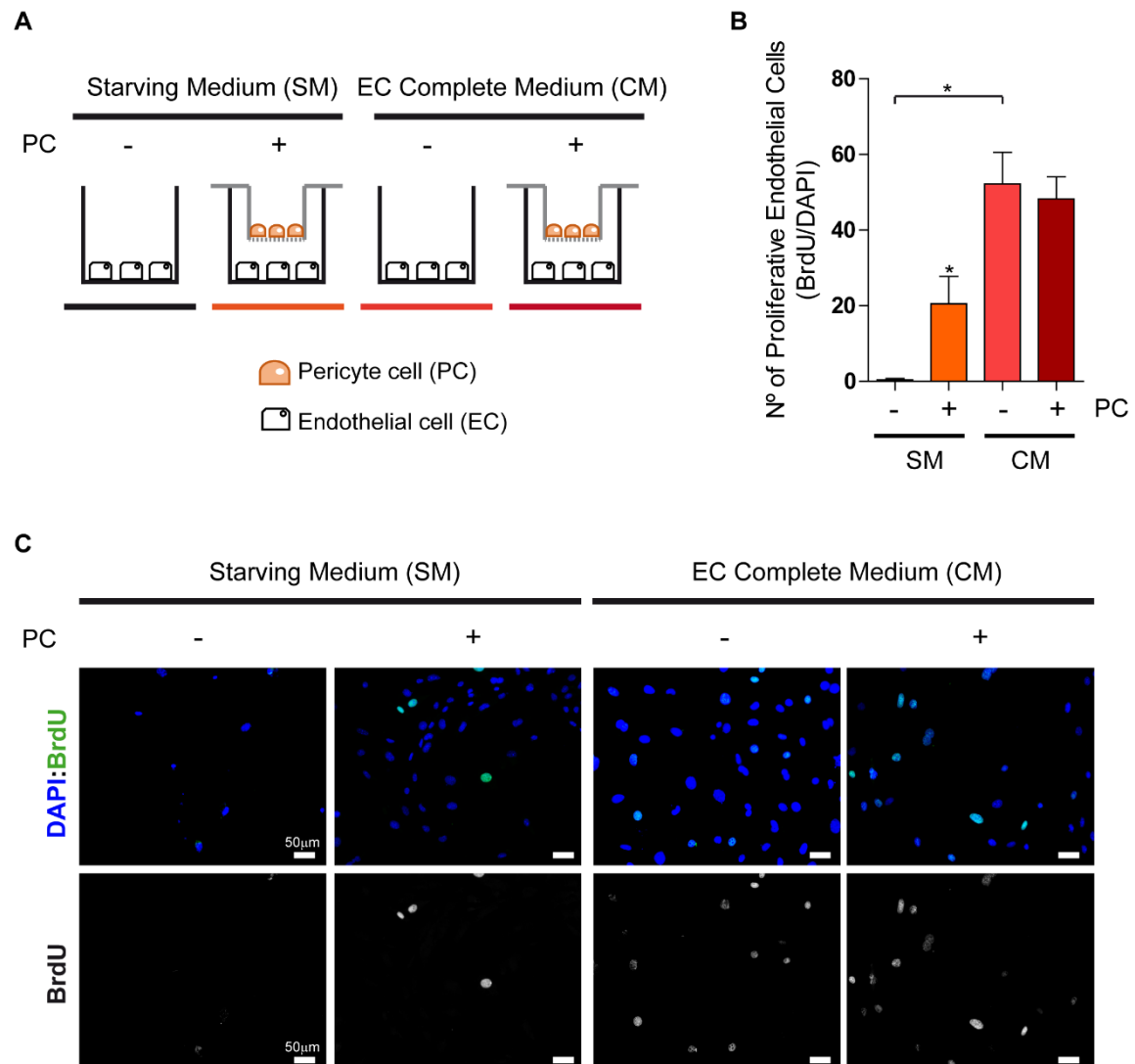


Figure 4.7. EC in co-culture with PCs increased the BrdU incorporation. (A) Schematic representation of experimental conditions used with the transwells filters. Four conditions were established: black line – ECs in monoculture (PC-) with starving medium (SM); orange line – ECs co-cultured with PCs (PC+) in starving medium (SM); pink line- ECs in monoculture (PC-) in normal growing conditions (EC complete medium - CM); brown line – ECs co-cultured with PCs (PC+) in ECs normal growing conditions (EC complete medium - CM). (B) Quantification of the percentage of proliferative ECs in the different culture conditions shown in A. (C) Representative images of ECs in the different cultures conditions shown in A. After 24h of co-culture ECs were labelled *in situ* in the co-culture with BrdU and then fixed and immunostained for BrdU (Green) and DAPI (blue). Error bars are standard error of the mean. Mean of at least four independent experiments is shown. * $P < 0.05$ was considered statistically significant. Statistical analysis was performed by Mann-Whitney test.

4. Results

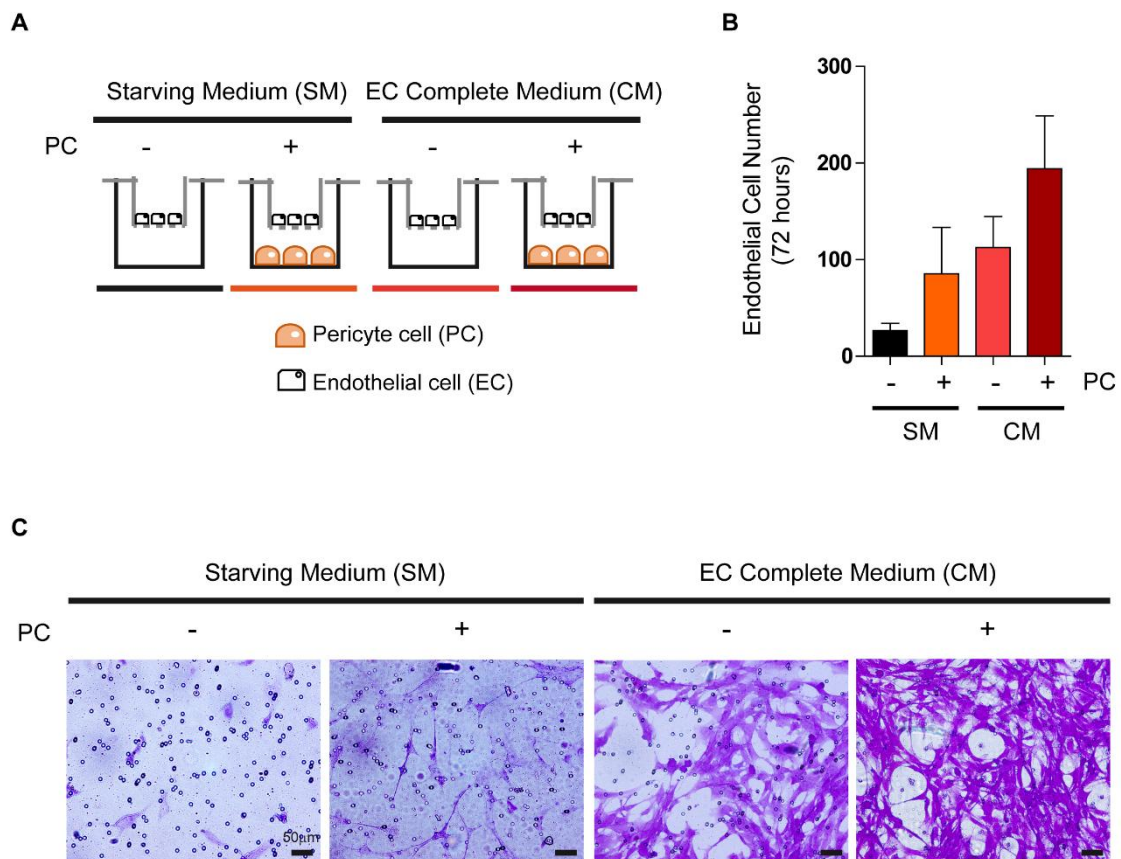


Figure 4.8. EC in co-culture with PCs increased migration (A) Schematic representation of experimental conditions used with the transwells filters. Four conditions were established: black line – ECs in monoculture (PC-) with starving medium (SM); orange line – ECs co-cultured with PCs (PC+) in starving medium (SM); pink line- ECs in monoculture (PC-) in normal growing conditions (EC complete medium - CM); brown line – ECs co-cultured with PCs (PC+) in ECs normal growing conditions (EC complete medium - CM). (B) Quantification of the number of migrate ECs in the different culture conditions shown in A. (C) Representative images of transwell filters with ECs in the different cultures conditions shown in A. After 72h of co-culture ECs were fixed and stained with crystal violet (purple). Error bars are standard error of the mean. Mean of at least four independent experiments is shown. Statistical analysis was performed by Mann-Whitney test.

4.2. PI3K regulation of PCs – *in vivo* and *in vitro* studies

4.2.1. PI3K activity during angiogenesis

Next, we investigated the level of pS6, which serves as a read out of PI3K activity, in P6 WT mice retinas. We have focused our attention at P6 retinas as at that time point it allows the detection in the same sample of both, the active sprouting area and the remodelling and stabilization area. We found increased levels of pS6 in the active sprouting angiogenesis areas, when compared with those areas in remodelling, where pS6 levels were almost undetectable (**Figure 4.9 A-B**). In addition, it seems that the pS6 level is also enriched in the PCs. In the Figure 4.9 C there are highlighted (yellow arrows) isolectin-B4 negative areas in close proximity with vessels (PC localization) that look like PCs expressing pS6 protein. PI3K activity is thus increased in the places of active angiogenesis where the new vessels are being formed and apparently could be regulating both, the ECs and the PCs in the vessel.

Previous data from our laboratory identified p110 α -PI3K isoform as an important regulator of ECs migration during the sprouting angiogenesis (Angulo-Urarte A., et al unpublished data; Graupera et al., 2008). Moreover, our retina data suggested that PI3K activity is likewise enriched in PCs, and since during the angiogenesis the crosstalk between ECs and PCs is fundamental to the proper vascular development (Caporali et al., 2016), we questioned whether PI3K signalling (mainly p110 α) has possible effects on PCs functions such as migration, proliferation and viability.

4. Results

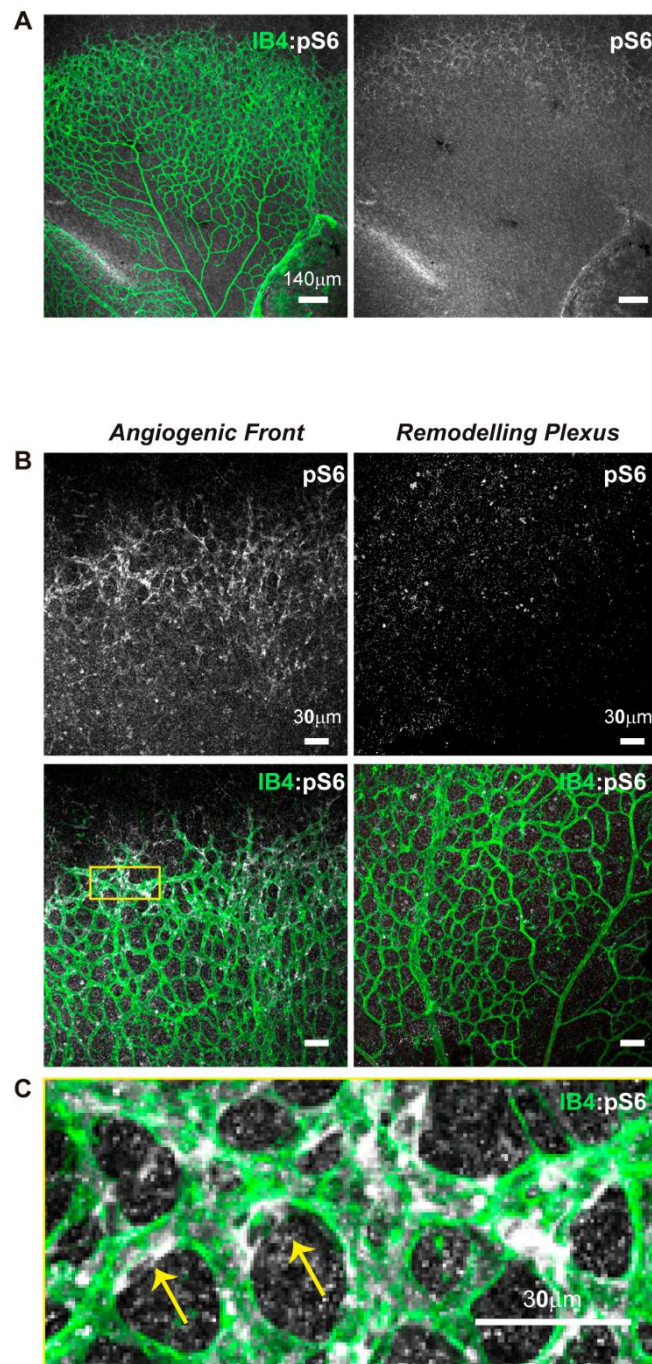


Figure 4.9. PI3K activity is upregulated during the sprouting angiogenesis. (A) Whole-mount confocal images of WT retinas at P6 stained with isolectin-B4 (green) and pS6 (grey). (B) Higher magnification images of P6 WT retinas in the angiogenic front and in the remodelling plexus showing increased levels of p-S6 in the angiogenic front. (C) Zoom of zone selected in B highlighting the pS6 levels in the vessels. Yellow arrows indicate a possible pS6 enrichment in PCs.

4.2.2. PCs express all class IA isoforms

Data from our laboratory and others have demonstrated isoform selectivity stimulating PI3K signalling in the regulation of both, the ECs and vSMCs. Interestingly, in these two cell populations' p110 α seems to be the major isoform (Graupera et al., 2008; Vantler et al., 2015). Therefore, we hypothesized that this isoform would also be essential for PCs regulation and function.

First, we analysed the expression of class IA PI3K isoforms in WT PCs. We found that WT PCs express all class IA catalytic isoforms, p110 α , p110 β and p110 δ , as well the regulatory sub-unit p85 (**Figure 4.10**). Although, p110 δ expression is believed to be restricted to leukocytes, we found that PCs also express p110 δ . Vantler *et al.*, also described that vSMC express all class IA-PI3K isoforms, including p110 δ (Vantler et al., 2015).

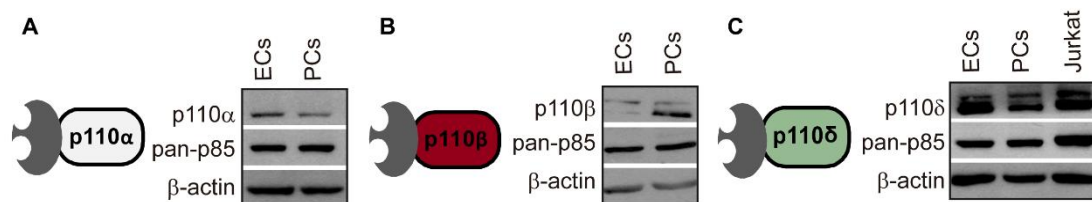


Figure 4.10. PC cells express all class IA-PI3k isoforms. Analysis by Western Blot of the catalytic class IA PI3K isoforms expression in WT PCs, namely the (A) p110 α , (B) p110 β and (C) p110 δ . We have also detected that PCs express the class IA regulatory subunit p85. EC (ECs) and jurkat cells were used as positive controls.

4.2.3. p110 α -PI3K regulates AKT phosphorylation

Next, we used a battery of isoform selectivity inhibitors (**Table 4.1**) to reveal which isoform account to PI3K signalling in PCs and accessed the pAKT (Ser473) level, as readout of PI3K activity. Among all the class IA-PI3K isoforms, only p110 α inactivation substantially reduced the pAKT levels (**Figure**

4. Results

4.11), suggesting that p110 α isoform regulates AKT activation like it happens with vSMCs and ECs (Graupera et al., 2008; Vantler et al., 2015).

Table 4. 1. PI3K inhibitors.

Name of Inhibitor	Isoform Specificity
GDC-0941	pan-PI3K
GDC0326	p110 α
TGX-221	p110 β
D030	p110 δ

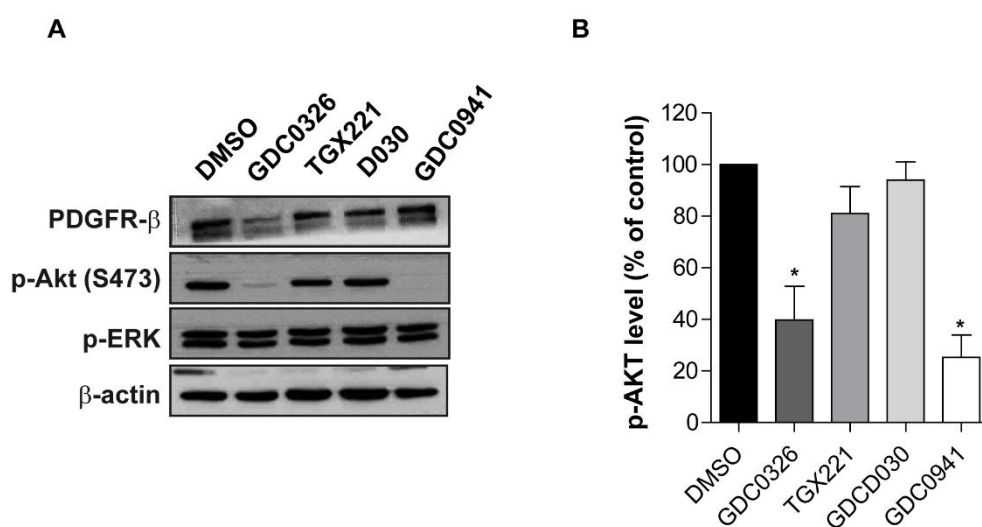


Figure 4.11. Only p110 α -PI3K inactivation in PCs reduced the levels of pAKT. PCs were treated with isoform-specific PI3K inhibitors: a p110 α -specific GDC0326 (1.0 μ M), a p110 β -specific TGX221 (0.5 μ M), a p110 δ -specific D030 (0.5 μ M), a pan-PI3K (1.0 μ M) and DMSO (control) during 2h. (A) Thereafter cells were lysed and immunoblotted using the indicated antibodies. PDGFR- β as a control of the PCs culture specificity, pAKT (S473) as readout of PI3K activity and p-ERK as readout of MAPK signalling. (B) Graphs represent the relative immunoreactivity of pAKT (S473) normalized to β -Actin of the representative experiments in (A). The results are expressed as the percentage of control (DMSO). Error bars are standard error of the mean. Mean of at four independent experiments is shown. *P<0.05 was considered statistically significant. Statistical analysis was performed by Mann-Whitney test.

4.2.4. PI3K regulates PCs cells in an isoform dependent manner

Next, we assessed the cell migration, viability and proliferation of PCs upon pharmacological inhibition of p110 α and p110 β . PCs were treated with GDC0326 (p110 α -specific inhibitor) and TGX221 (p110 β -specific inhibitor) and DMSO (control). By performing a wound-healing assay (migration assessment) and a MTS assay (viability assessment), we found that p110 α inactivation, but not p110 β , leads to a reduction in cell migration (**Figure 4.12A-B**) and viability (**Figure 4.12C**), respectively. However, inhibition of p110 β , but not p110 α , results in the reduction of PCs proliferation detected by BrdU incorporation (**Figure 4.13**), demonstrating that in these cells also p110 β , and not only p110 α , acts as a positive regulator, controlling cell proliferation.

Taking together, these observation revealed that p110 α and p110 β are involved in the regulation of PC biology. Our data also suggests that migration and survival of PCs are regulated by the p110 α in an AKT axis while p110 β regulates PC proliferation independent of AKT.

4. Results

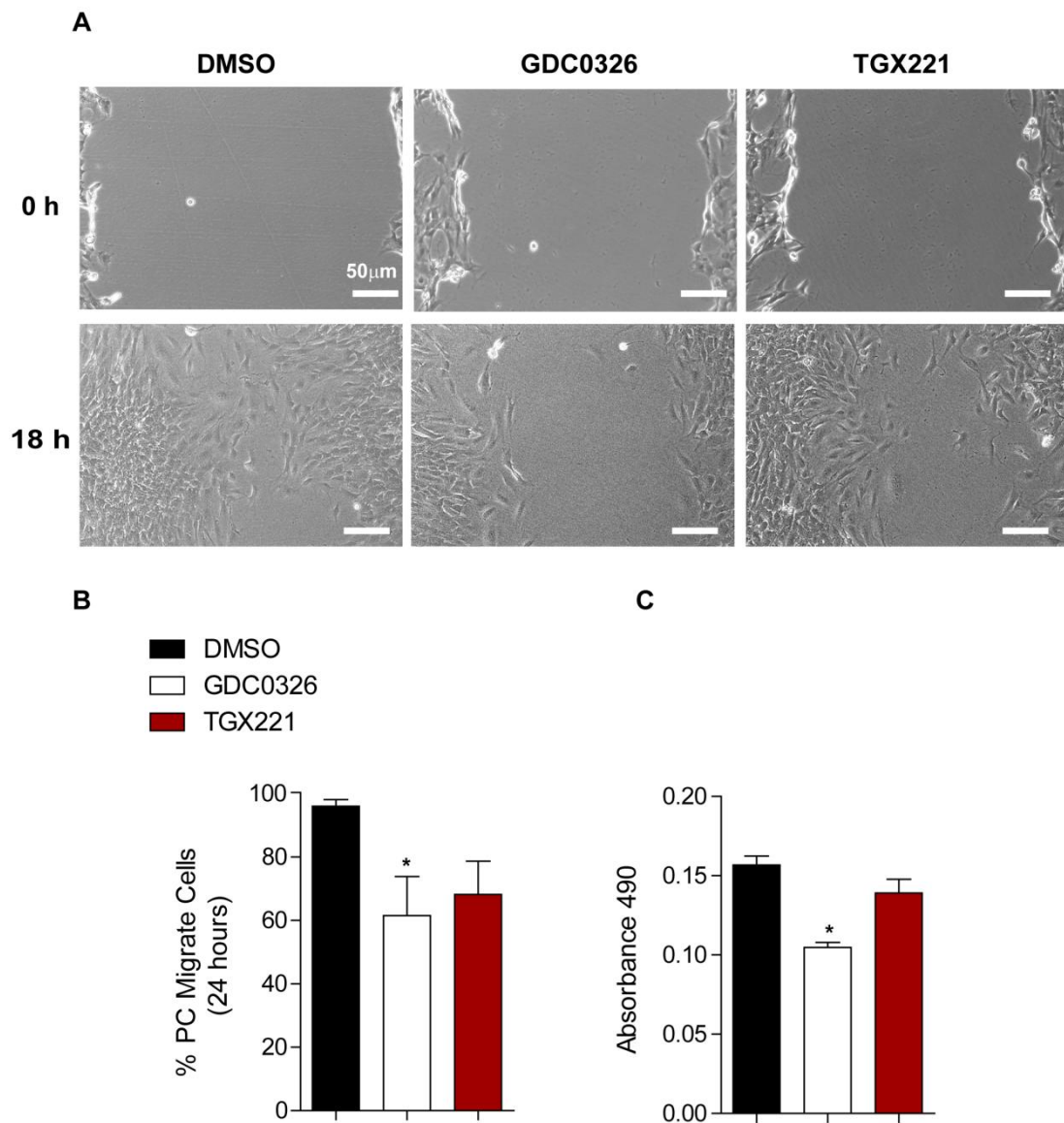


Figure 4.12. The p110 α -PI3K regulates PC viability and migration. PCs were treated with isoform-specific PI3K inhibitors: a p110 α -specific GDC0326 (1.0 μ M), a p110 β -specific TGX221 (0.5 μ M) and DMSO (control) during 18h. (A) Representative phase contrast images of PCs monolayers, immediately and 18h hours after scratching (B) Quantification of the percentage of migrate PCs in the different culture conditions shown in (A). (C) Quantification of PC viability using the MTS viability assay (absorbance 490). Error bars are standard error of the mean. Mean of at least four independent experiments is shown. *P<0.05 was considered statistically significant. Statistical analysis was performed by Mann-Whitney test.

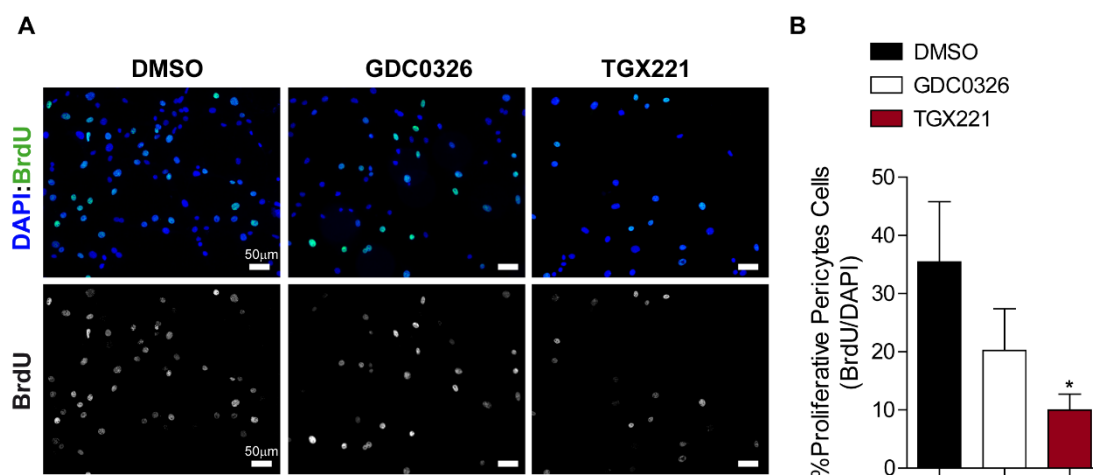


Figure 4.13. The p110 β -PI3K isoform regulates PC proliferation. (A) Representative images of PCs after 24h treatment with isoform-specific PI3K inhibitors: a p110 α -specific GDC0326 (1.0 μ M), a p110 β -specific TGX221 (0.5 μ M) and DMSO (control). The PCs were labelled *in situ* with BrdU and then fixed and immunostained for BrdU (Green) and DAPI (blue). (B) Quantification of the percentage of proliferative PCs in the different culture conditions shown in (A). Error bars are standard error of the mean. Mean of at least four independent experiments is shown. *P<0.05 was considered statistically significant. Statistical analysis was performed by Mann-Whitney test.

4.2.5. PI3K controls PCs biology in a isoform-dependent manner during sprouting angiogenesis – The model selection

The *in vitro* results suggested that PI3K signalling is important for regulation of PCs fundamental functions in an isoform-dependent manner and that both, p110 α and p110 β isoforms are implicated in PCs regulation with p110 α involved in PC migration and p110 β controlling PC proliferation. Since, PCs are key mediators of sprouting angiogenesis, we sought to validate whether PI3K also relies on PC functions during sprouting angiogenesis *in vivo* using the mouse retina model as a tool and the Cre/loxP as a system that allows the specificity of the genetic inactivation (Albanese et al., 2002; Bouabe and Okkenhaug, 2013).

For this purpose, we took advantage of the tamoxifen inducible Pdgfr β (BAC)-CreERT2 transgenic mice, which in the retina have been shown to be restrictedly expressed in MCs (Chen et al., 2016b).

4. Results

In order to inactivate p110 α and p110 β in PCs we combined one allele flox and other allele kinase-death. This strategy proved to be the more efficient based on two observations: 1) the full depletion of p110 α may lead to compensation of other isoforms (Graupera., et al. unpublished data); and 2) the comparison of the vascular phenotypes upon two floxed alleles approach versus the flox/kinase-death alleles approach in ECs, revealed that the last one exhibits a more efficient recombination and more reproducible and penetrant phenotypes (Angulo-Urarte., et al. unpublished data).

A disadvantage of the combinatory strategy is that one of the alleles has a kinase-death protein that is constitutively expressed and that could affect the PCs specificity. However, in the study of Angulo-Urarte et al. it was found that the expression of this allele is not interfering significantly with the p110 α -specific roles in ECs (Angulo-Urarte et al unpublished data).

Therefore, the Pdgfr β (BAC)-CreERT2;p110 α ^{flox/D933A} (**p110 α ^{D933A/i Δ PC}**) and the Pdgfr β (BAC)-CreERT2;p110 β ^{flox/D931A} (**p110 β ^{D931A/i Δ PC}**) transgenic mice were generated to specifically inactivate p110 α and p110 β isoforms, respectively, in PCs upon 4-hydroxytamoxifen (4-OH) administration.

4.2.6. The efficiency of PDGFR β (BAC)-CreERT2

First, we started to analyse the efficiency of the Pdgfr β (BAC)-CreERT2 promoter. The recombination of the floxed gene was primarily tested by crossbreeding the Pdgfr β (BAC)-CreERT2; p110 α ^{flox/flox} mice with a *Rosa26-eYFP* transgenic mice allowing the detection of Cre activity from YFP fluorescence signal (Srinivas et al., 2001). The recombination was induced by injection of 4-OH in mice at P1 and P2 and the retinas were isolated at P6. Immunofluorescence analysis of the retinas has shown YFP positive signal, demonstrating the efficacy of the recombination. In addition, co-labelling with desmin revealed that YFP expression is concomitant with desmin positive cells, which validate the specificity of the Pdgfr β (BAC)-CreERT2 to PCs in the retina model (**Figure 4.14**).

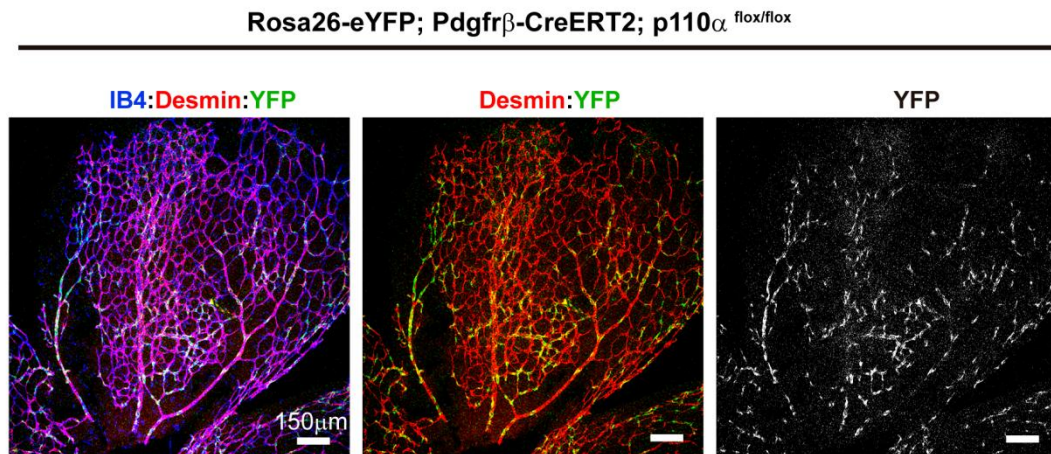


Figure 4.14. Efficient induction and specificity of Pdgfr β -CreERT2. Cre expression detected by YFP (green) positive signal in the PC nuclei in P6 retinas of Rosa26-eYFP; Pdgfr- β (BAC)-CreERT2;p110 α ^{flox/flox} after 4-OH injections at P1 and P2 and the retinas isolated at P6. The retinas were co-stained with isolectin-B4 (blue) and the PC marker Desmin (red).

Moreover, we further confirm the specificity and efficiency of our promoter using the *Rosa26-mTmG* fluorescent reporter line, which allows the detection of Cre activity by recombination-induced expression of membrane-bound green fluorescent protein (GFP) and inactivation of the red fluorescent protein Tomato expression (Muzumdar et al., 2007). Therefore, the Pdgfr- β (BAC)-CreERT2;p110 α ^{flox/D933A} mice expressing only one floxed allele were crossed with *Rosa26-mTmG* fluorescent reporter line. Similarly, the 4-OH were administrated at P1 and P2 and the retinas isolated at P6.

Even with only one floxed allele, using the NG2 marker, it was possible to observe that a high percentage and that only NG2 positive cells showed GFP expression. Therefore, Pdgfr β (BAC)-CreERT2 has shown to be a highly efficient and specificity for PCs in the retina mouse model (**Figure 4.15**).

Taking together, these analysis further validate the PDGFR β promotor, which in the retina only recombines into the PCs population with a high ratio of efficiency.

4. Results

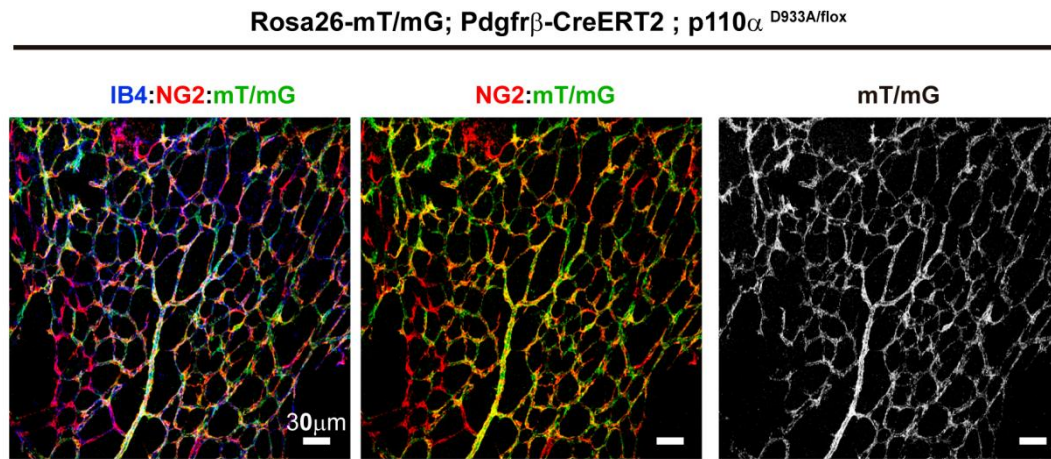


Figure 4.15. Efficient induction and specificity of Pdgfr β -CreERT2. The Cre expression was detected by GFP (green) positive signal in PC in P6 retinas of Rosa26-mT/mG; Pdgfr- β (BAC)-CreERT2;p110 α ^{D933A/flox} even with only one allele floxed. The 4-OH tamoxifen injections were performed at P1 and P2 and the retinas isolated at P6 were so-stained with isolectin-B4 (blue) and the PC marker NG2 (red). The Cre-recombination of the Rosa26-mT/mG promotor induces the expression of membrane – bound green fluorescent protein (GFP) and the inactivation of the red fluorescent protein tomato.

4.2.7. p110a-PI3K isoform does not regulate PCs biology during sprouting angiogenesis

We first focus on the study of PCs coverage in the Pdgfr β (BAC)-CreERT2;p110 α ^{D933A/flox} mice (**p110 α ^{D933A/iAPC}**). To validate our genetic strategy choice (described at the section 4.3.1), in our first analysis we included the following controls: **(1)** the full deletion mice Pdgfr β (BAC)-CreERT2;p110 α ^{flox/flox} (**p110 α ^{iAPC/iAPC}**); **(2)** the **p110 α ^{WT/D933A}** mice that have one allele constitutively expressed and a kinase death form of p110 α (**p110 α ^{D933A}**); and the **(3)** **p110 α ^{flox/flox}** mice without Cre-activity that was used as a control. From now on, unless otherwise stated, pups were injected at P1 and P2 and the retinas isolated at P6.

Although, we found PI3K activity increased in the sprouting front of WT retinas, we sought to analyse both areas: the sprouting front (Angiogenic Front) and the remodelling area (Remodelling Plexus) of the P6 retinas, as it was previously described. These strategies allowed the study of the PI3K impact on

the active and in the quiescent vasculature since PCs are important in both cases.

Using the NG2 marker to stained PCs and isolectin-B4, we found that partial inactivation of p110 α (p110 $\alpha^{WT/D933A}$) did not impact on PC coverage in the angiogenic front, when compared with the control (p110 $\alpha^{flox/flox}$). Moreover, full depletion of p110 α in PCs (p110 $\alpha^{i\Delta PC/i\Delta PC}$) or the combined strategy (p110 $\alpha^{D933A/i\Delta PC}$) also did not show any difference in PC coverage compared to the control (**Figure 4.16**). In addition, we did not detect any change in PCs coverage in the remodelling area when used p110 $\alpha^{D933A/i\Delta PC}$ compared with control (**Figure 4.17**) or p110 $\alpha^{WT/D933A}$ and p110 $\alpha^{i\Delta PC/i\Delta PC}$ mice models (data not shown).

To confirm our results, we have used the well-established cytoskeleton marker of PCs – desmin – and the vessel marker isolectin-B4, and we did not detected differences in PCs coverage in the p110 $\alpha^{D933A/i\Delta PC}$ mice in the angiogenic front (**Figure 4.18A-B**) or even in the remodelling plexus (**Figure 4.18A-C**). Thus, p110 α isoform apparently does not regulate PCs coverage of the endothelium in both, the angiogenic and the remodelling areas.

Next, we assessed the PCs' morphology using the co-labelling isolectin-B4 and NG2 in the angiogenic front and the remodelling plexus of the retina and we did not find any evident morphological change in the p110 $\alpha^{D933A/i\Delta PC}$ PC compared with the control (**Figure 4.19**).

We also analysed the impact of p110 α on PCs proliferation using the p110 $\alpha^{D933A/i\Delta PC}$ mice. For this, EdU proliferative staining and NG2 marker were used in the recombined P6 retinas. We quantified the percentage of EdU positive cells in PCs (NG2⁺) in the angiogenic front and in the remodelling area and we did not detected differences in PC proliferation upon p110 α inactivation in the angiogenic front (**Figure 4.20**) nor in the remodelling plexus (**Figure 4.21**), which suggests that p110 α does not regulate PCs proliferation.

Taken together, this data has shown that, surprisingly, p110 α does not have an impact on PC coverage, proliferation or even morphological changes during the sprouting angiogenesis in the mouse retina.

4. Results

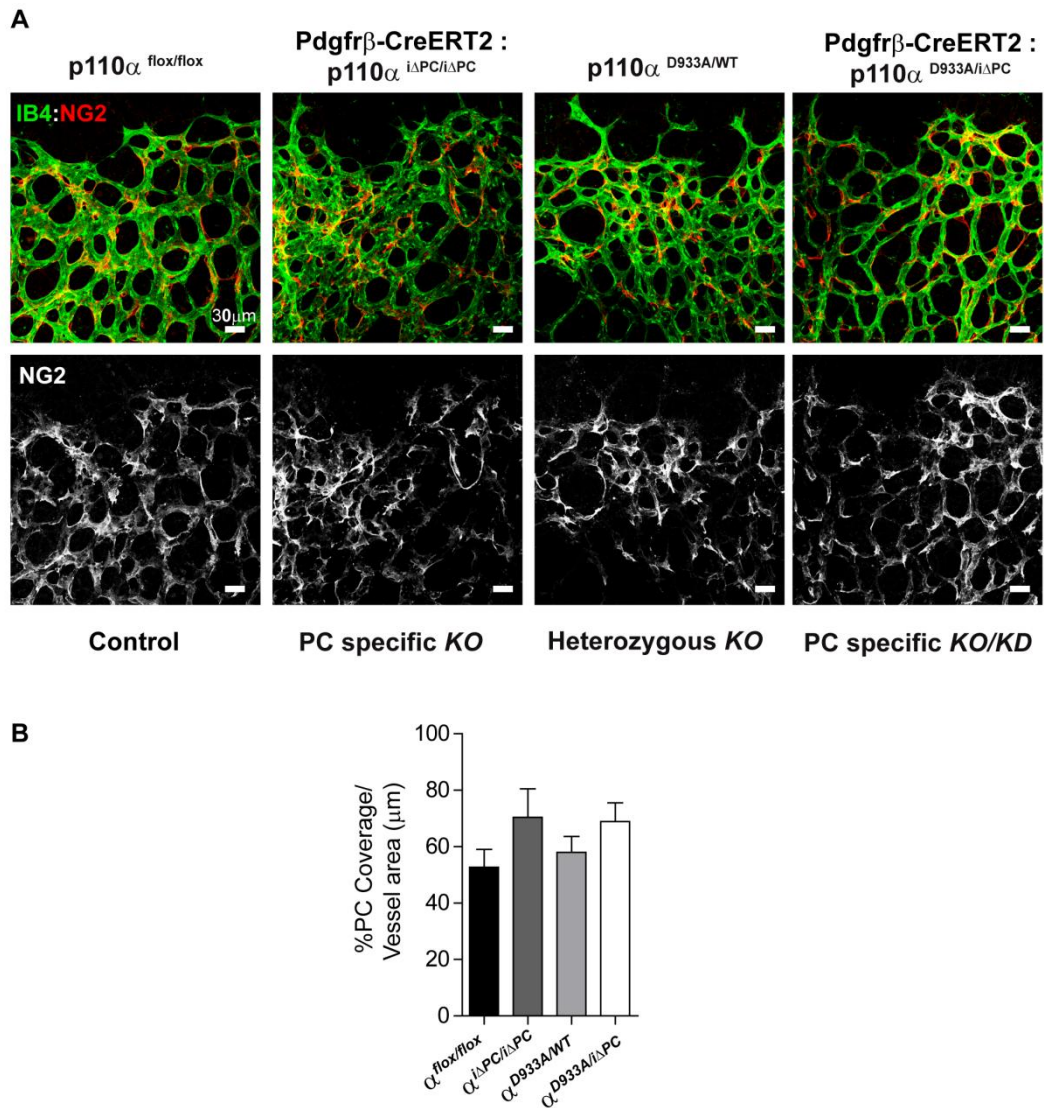


Figure 4.16. $p110\alpha$ inactivation did not affect PC coverage using NG2 marker in the sprouting front of the retina. (A) Confocal images of P6 retinas injected with 4-OH tamoxifen at P1 and P2 and stained with isolectin-B4 (green) and NG2 (red) (B) Quantification of PC coverage per vessel area in the P6 retinas of the respective genotypes. $N \geq 4$ retinas for each condition. Error bars are standard error of the mean. Statistical analysis was performed by Mann-Whitney test.

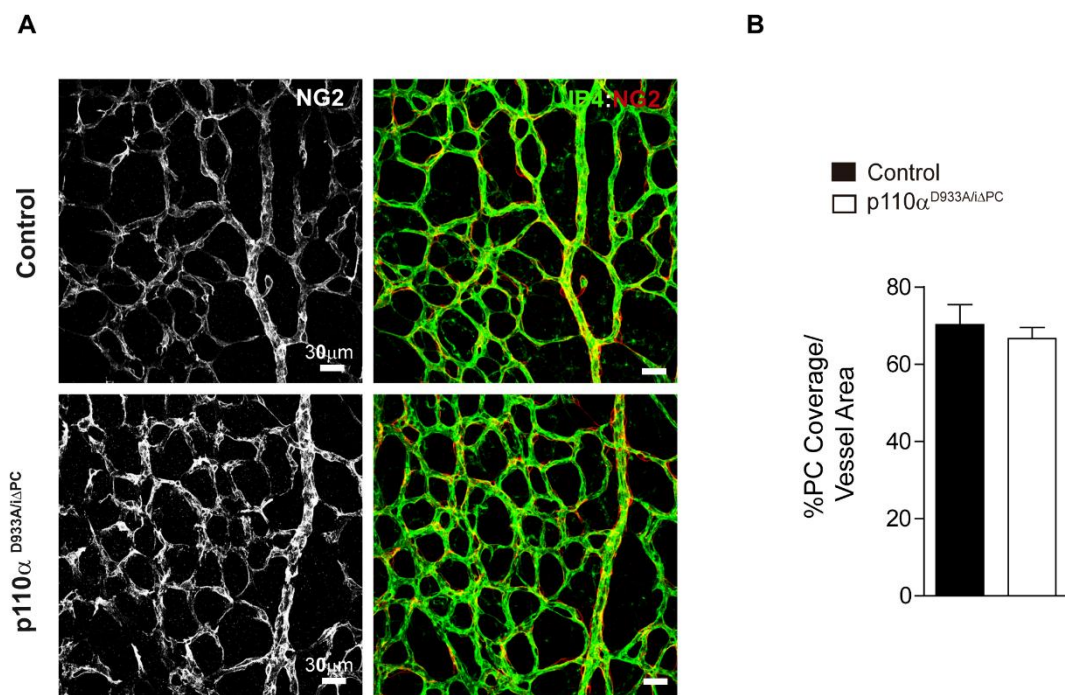


Figure 4.17. p110 α inactivation did not affect PC coverage using the NG2 marker in the remodelling plexus of the retina. (A) Confocal images of P6 retinas injected with 4-OH tamoxifen at P1 and P2 and stained with isolectin-B4 (green) and NG2 (red) (B) Quantification of PC coverage per vessel area in P6 retinas of the p110 $\alpha^{D933A/i\Delta PC}$ compared with the control (p110 $\alpha^{flox/flox}$). $N \geq 4$ retinas for each condition. Error bars are standard error of the mean. Statistical analysis was performed by Mann-Whitney test.

4. Results

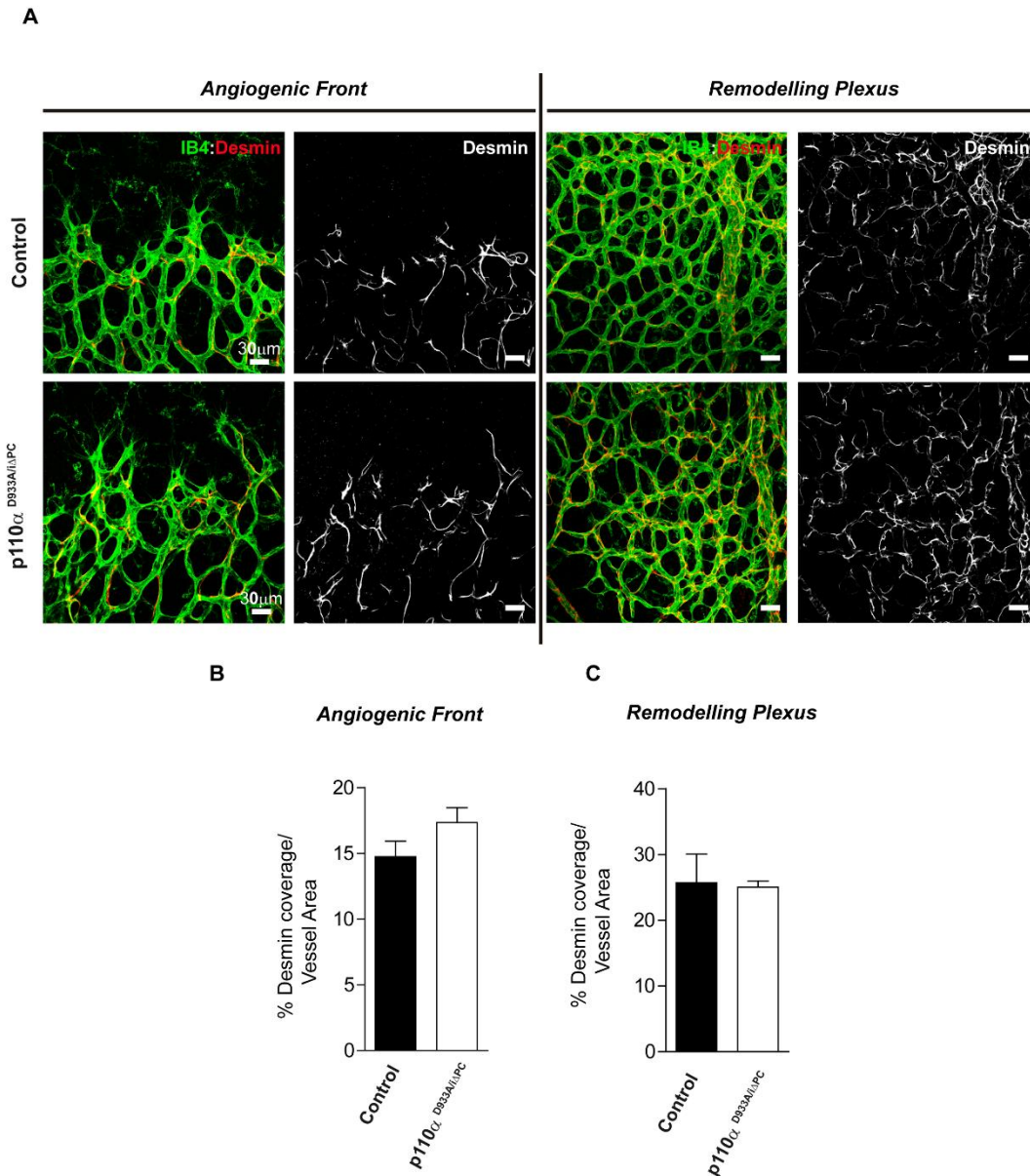


Figure 4.18. $p110\alpha$ inactivation did not affect PC coverage using desmin marker. (A) Confocal images of P6 retinas injected with 4-OH tamoxifen at P1 and P2 and stained with isolectin-B4 (green) and Desmin (red) in both areas, the angiogenic front and the remodelling plexus (B) Quantification of PC coverage per vessel area in P6 retinas of the $p110\alpha^{D933A/i\Delta PC}$ compared with the control ($p110\alpha^{flox/flox}$) in the sprouting front. (C) Quantification of PC coverage per vessel area in P6 retinas of the $p110\alpha^{D933A/i\Delta PC}$ compared with the control ($p110\alpha^{flox/flox}$) in the remodelling plexus. $N \geq 4$ retinas for each condition. Error bars are standard error of the mean. Statistical analysis was performed by Mann-Whitney test.

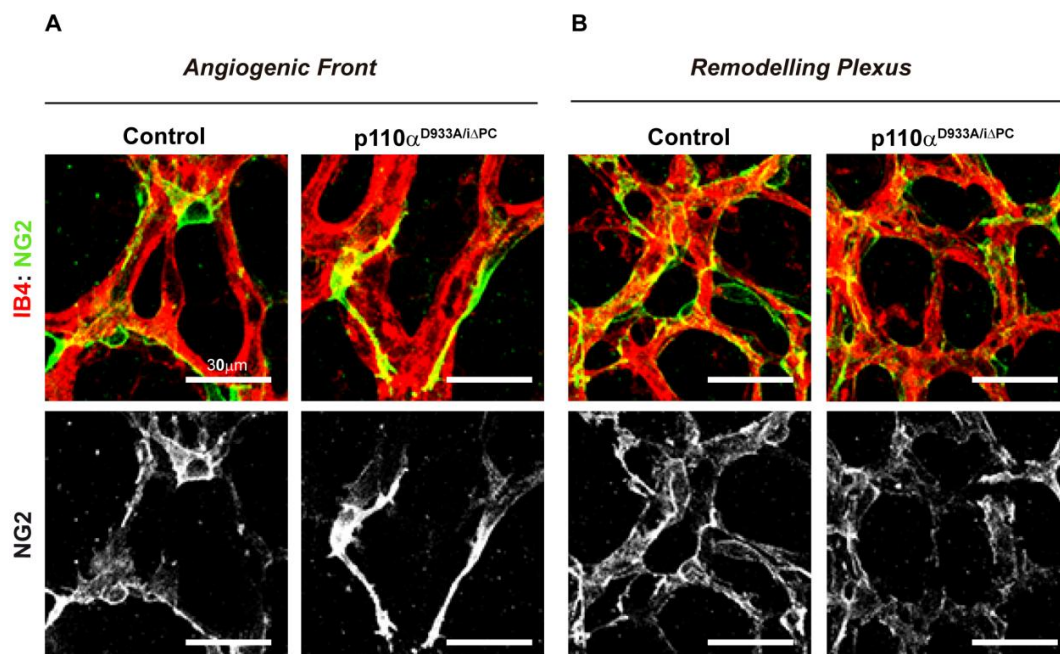


Figure 4.19. p110 α inactivation did not affect PC morphology (A) Confocal images of P6 retinas of the p110 $\alpha^{\text{D933A}/\Delta\text{PC}}$ and the respective control (p110 $\alpha^{\text{floxed/floxed}}$), injected with 4-OH tamoxifen at P1 and P2 and stained with isolectin-B4 (green) and NG2 (red) in both areas, the angiogenic front and the remodelling plexus.

4. Results

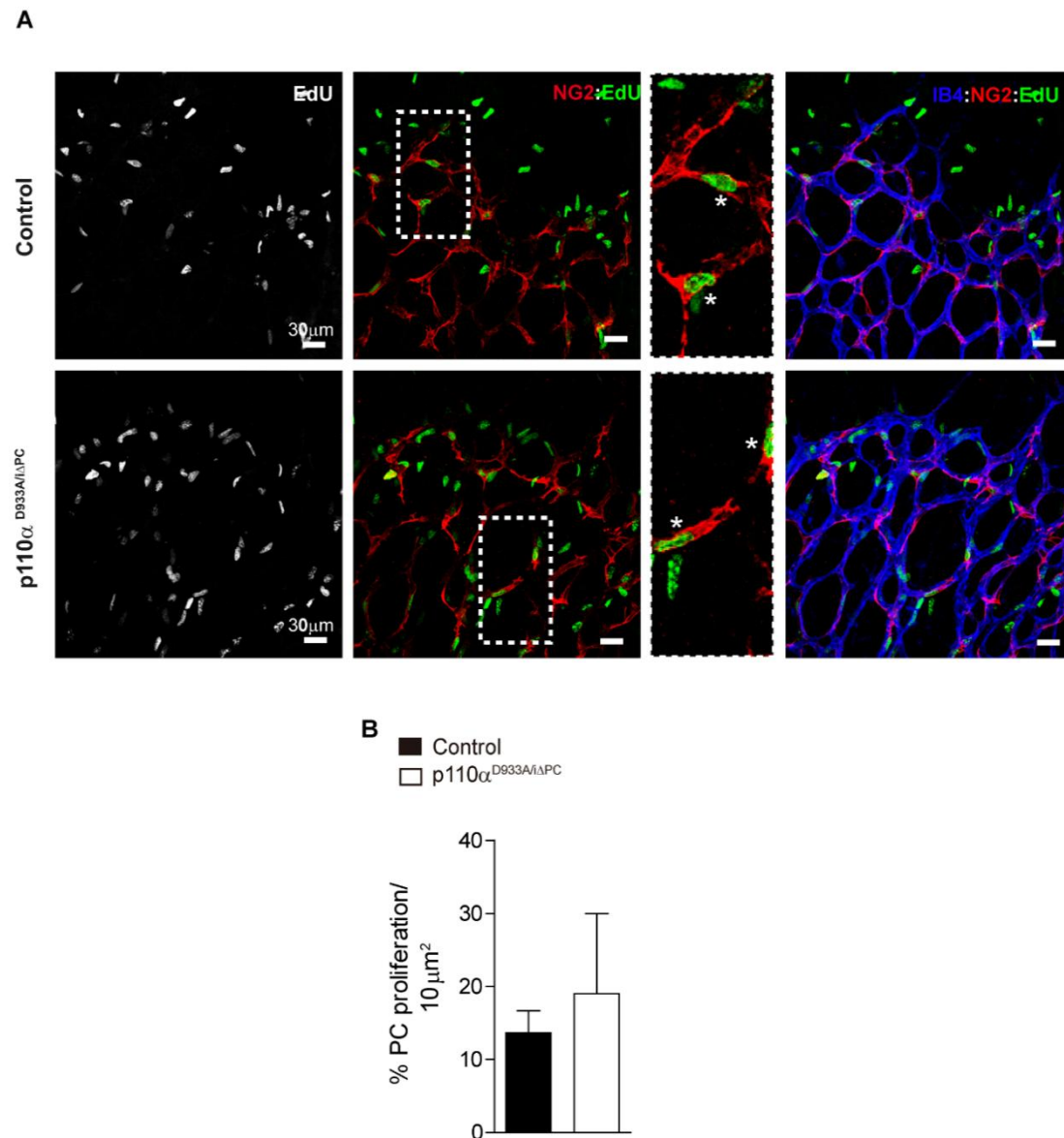


Figure 4.20. $p110\alpha$ inactivation did not affect PC proliferation in the angiogenic front (A) Confocal images of the angiogenic front of P6 retinas injected with 4-OH tamoxifen at P1 and P2. Retinas were injected with EdU 2h before isolation and were stained with isolectin-B4 (blue), NG2 (red) and the EdU (green). (B) Quantification of PC proliferation - EdU positive PCs per total number of PCs in a $10^4 \mu\text{m}^2$ area in P6 retinas of the $p110\alpha^{D933A/\Delta PC}$ compared with the control ($p110\alpha^{lox/lox}$). $N \geq 4$ retinas for each condition. Error bars are standard error of the mean. Statistical analysis was performed by Mann-Whitney test.

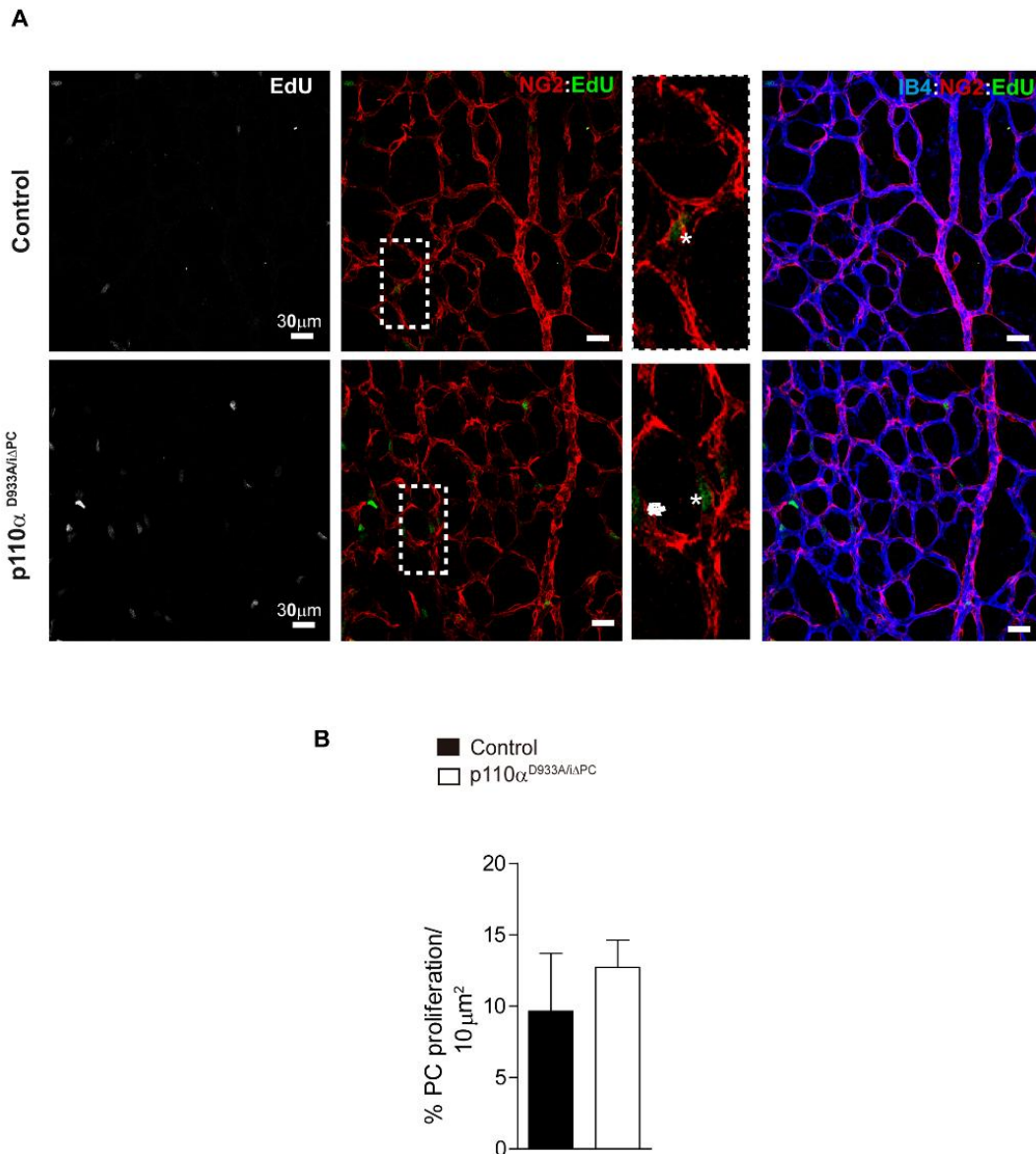


Figure 4.21. p110 α isoform inactivation did not affect PC proliferation in the remodelling plexus (A) Confocal images of the remodelling plexus of P6 retinas injected with 4-OH tamoxifen at P1 and P2. Retinas were injected with EdU 2h before isolation and were stained with isolectin-B4 (blue), NG2 (red) and the EdU (green). (B) Quantification of PC proliferation - EdU positive PCs per total number of PCs in a $10^4\mu\text{m}^2$ area in P6 retinas of the p110 $\alpha^{\text{D933A/i}\Delta\text{PC}}$ compared with the control (p110 $\alpha^{\text{fllox/fllox}}$). $N \geq 4$ retinas for each condition. Error bars are standard error of the mean. Statistical analysis was performed by Mann-Whitney test.

4. Results

4.2.8. p110 β -PI3K isoform is the key regulator of PCs biology during sprouting angiogenesis

The p110 β isoform regulates PCs proliferation *in vitro* therefore, using the same strategy as for p110 α isoform, the impact of p110 β on PCs *in vivo* sprouting angiogenesis was also investigated.

As for p110 α , to study how p110 β affects PCs and to validate the efficiency of our mice strategy, we first assessed the PCs coverage. For this purpose, we have quantified the PC coverage per vessel area in our combined strategy using the $\text{Pdgr}\beta(\text{BAC})\text{-CreERT2;p110}\beta^{\text{D931A/flox}}$ (**p110 $\beta^{\text{D931A/i}\Delta\text{PC}}$**) and to validate our model we have also used: **(1)** the full deletion mice $\text{Pdgr}\beta(\text{BAC})\text{-CreERT2;p110}\beta^{\text{flox/flox}}$ (**p110 $\beta^{\text{i}\Delta\text{PC/i}\Delta\text{PC}}$**); **(2)** the p110 $\beta^{\text{WT/D933A}}$ mutant mice carrying one kinase death allele expressed in all cell types (**p110 β^{D933A}**) and the **(3)** p110 $\beta^{\text{flox/flox}}$ negative for Cre-activity used as a control.

Using the co-staining of NG2 with isolectin-B4, we observed that the constitutive inactivation of p110 β (p110 $\beta^{\text{WT/D931A}}$) did not affect PCs coverage per vessel area in the angiogenic front, when compared to the control (p110 $\beta^{\text{flox/flox}}$). Moreover, we have not detected any differences in PCs coverage upon p110 β full inactivation (p110 $\beta^{\text{i}\Delta\text{PC/i}\Delta\text{PC}}$) in the angiogenic front. However, when used the combined strategy taking advantage of the p110 $\beta^{\text{D931A/i}\Delta\text{PC}}$ mice model, a significant reduction in PCs coverage has been observed (**Figure 4.22**). It seems that specific inactivation of p110 β in PCs results in reduced coverage of PC in the vessels. A slight reduction of PCs coverage was also observed in the remodelling area in the p110 $\beta^{\text{D931A/i}\Delta\text{PC}}$ mice when compared to the controls (**Figure 4.23**).

Surprisingly, p110 β and not p110 α , regulates PCs coverage mainly at the sprouting front. These results also suggested that the partial inactivation of p110 β in a constitutive manner does not impact on the retinal PCs and that the total deletion of p110 β specifically in PCs quite likely leads to compensatory effects by the other isoforms, since differences in PC coverage were not observed. Therefore, the most efficient approach is the inactivation of p110 β

using the combined strategy, which helps to avoid the possible compensatory effects of p110 β full deletion.

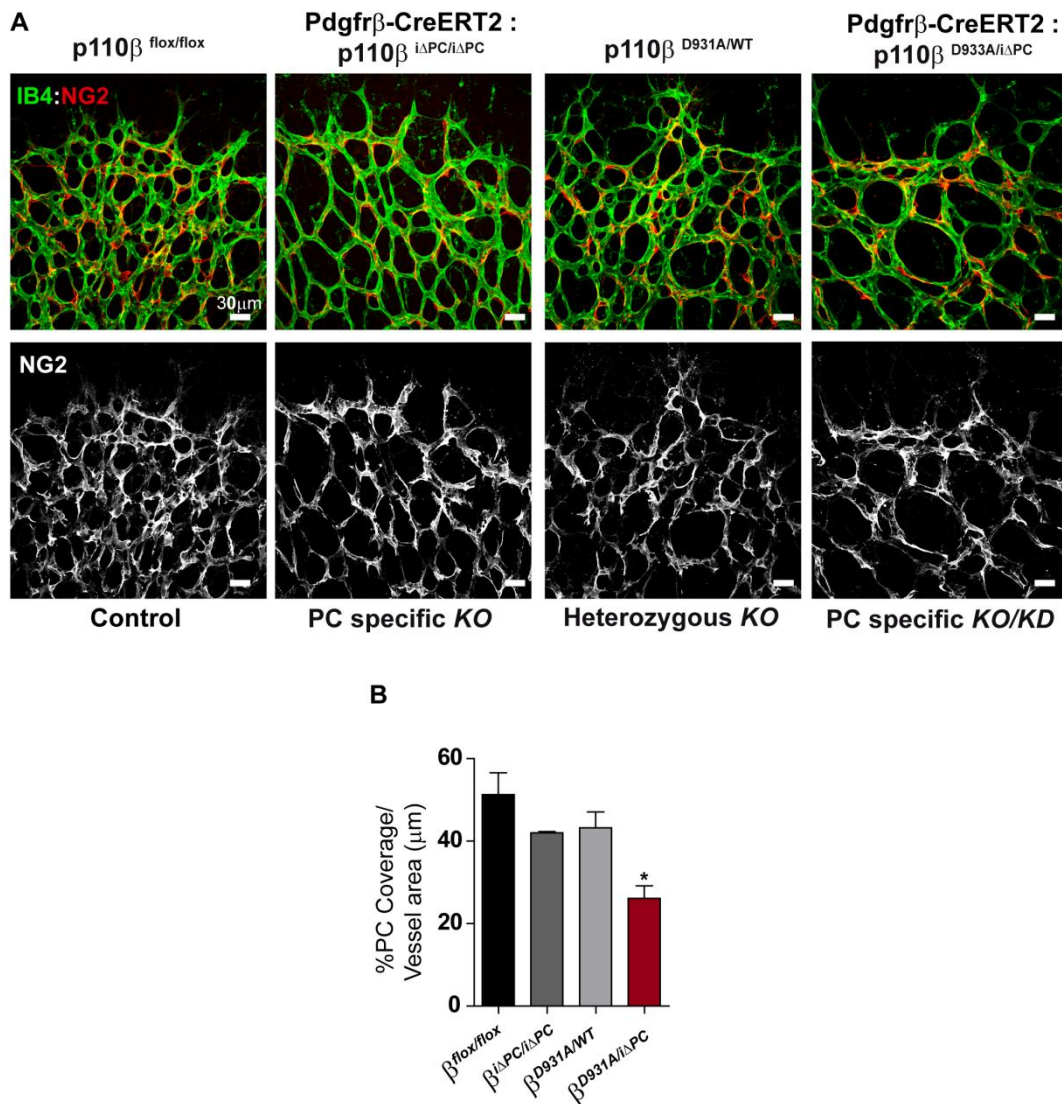


Figure 4.22. p110 β inactivation impacts on PC coverage using NG2 marker in the sprouting front of the retina. (A) Confocal images of P6 retinas injected with 4-OH tamoxifen at P1 and P2 and stained with isolectin-B4 (green) and NG2 (red) (B) Quantification of PC coverage per vessel area in the P6 retinas of the respective genotypes. N \geq 4 retinas for each condition except for p110 $\beta^{i\Delta PC/\Delta PC}$ n=2 retinas. Error bars are standard error of the mean. *P<0.05 was considered statistically significant. Statistical analysis was performed by Mann-Whitney test.

4. Results

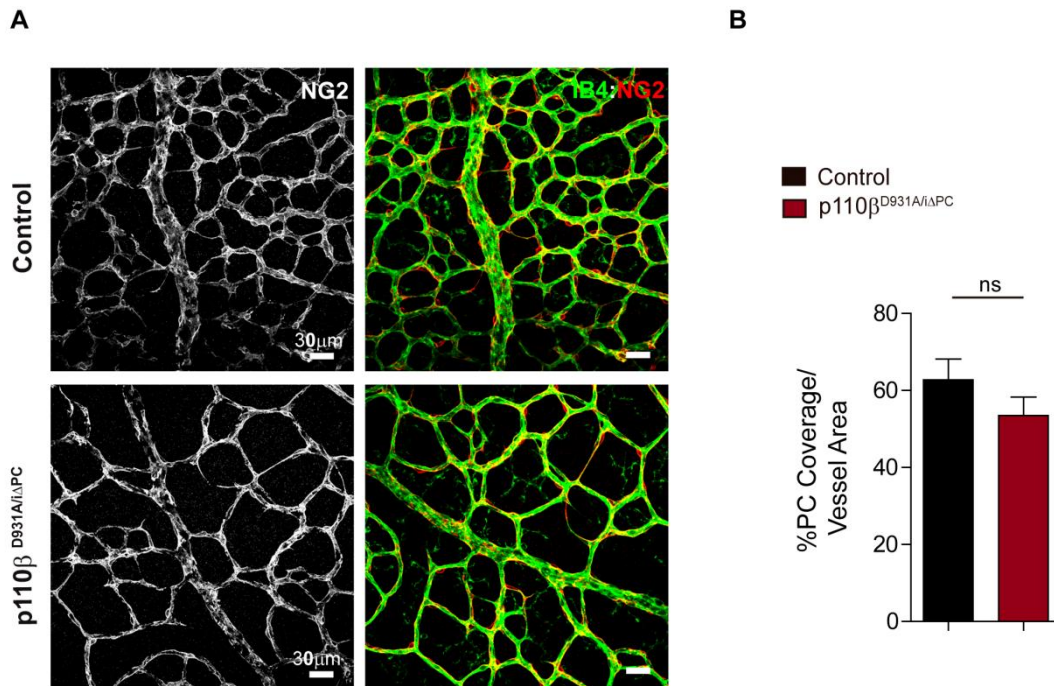


Figure 4.23. p110β inactivation slight reduced PC coverage in the remodelling plexus of the retina when used the NG2 marker. (A) Confocal images of P6 retinas injected with 4-OH tamoxifen at P1 and P2 and stained with isolectin-B4 (green) and NG2 (red) (B) Quantification of PC coverage per vessel area in P6 retinas of the p110β^{D931A/iΔPC} compared with the control (p110β^{flox/flox}). N ≥ 4 retinas for each condition. Error bars are standard error of the mean. Statistical analysis was performed by Mann-Whitney test.

To confirm our data with the NG2 marker, we also quantified PCs coverage using the desmin marker co-stained with isolectin-B4 in the angiogenic front and in the remodelling areas of p110β^{D931A/iΔPC} mice. The coverage of desmin-positive cells in the vessels in contrast to what we observed using NG2, was not altered after p110β inactivation in P6 mouse retinas in both areas of the retinas. (**Figure 4.24 A,B,C,D**). Although, not clear at the moment we think that the differences between NG2 and desmin markers can be related with the maturation grade of the PC. It was described that in retinas a mature PC presents NG2 expression, and not desmin, more restricted to the albuminal cell bodies (Hughes and Chan-Ling, 2004).

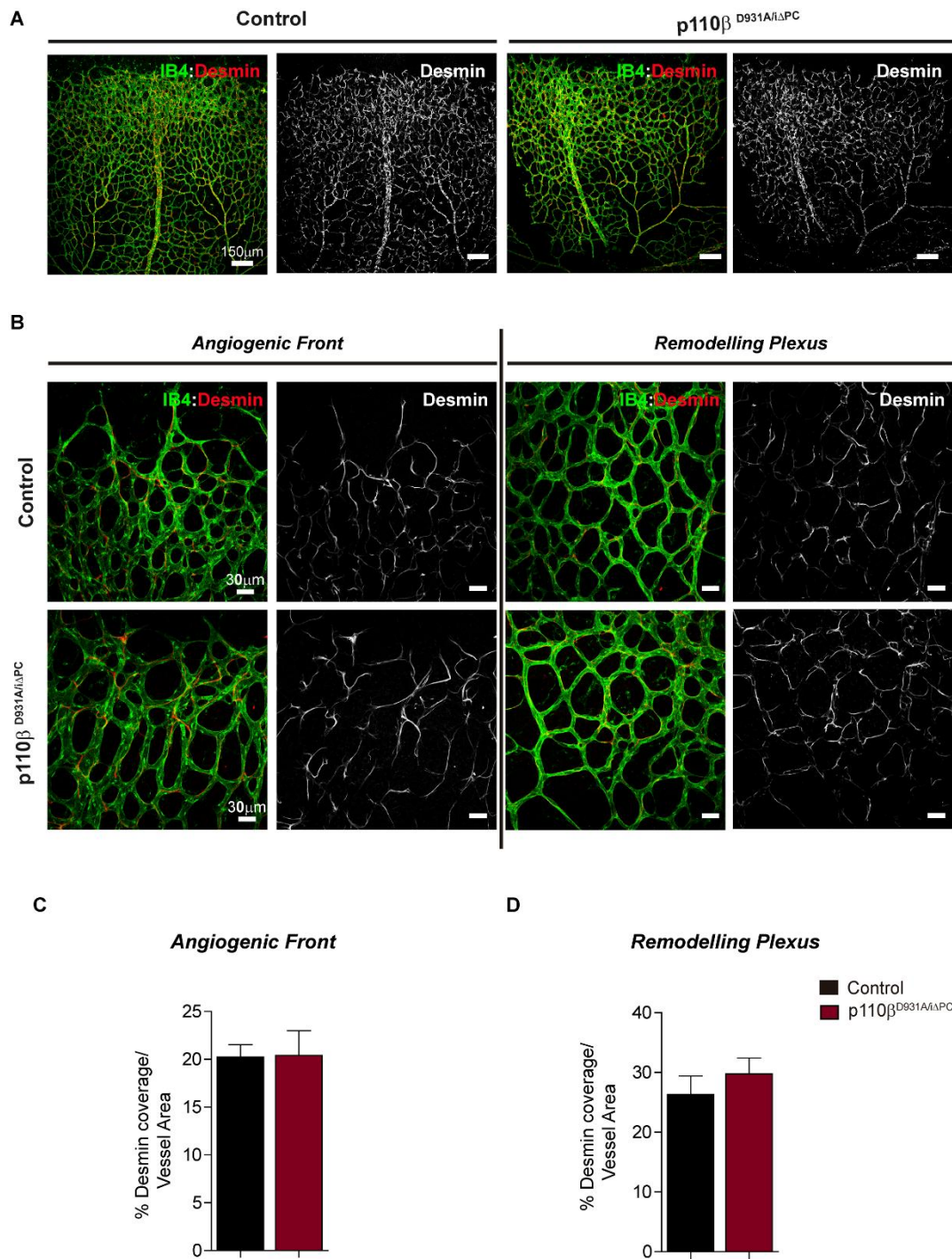


Figure 4.24. $p110\beta$ inactivation did not affect PC coverage using desmin marker. (A) Whole-mount of P6 retinas injected with 4-OH tamoxifen at P1 and P2 and stained with isolectin-B4 (green) and desmin (red) of the $p110\beta^{D931A/i\Delta PC}$ and respective control ($p110\beta^{flox/flox}$). (B) High magnification confocal images of the angiogenic front and remodelling plexus of the $p110\beta^{D931A/i\Delta PC}$ and respective control ($p110\beta^{flox/flox}$). (C) Quantification of PC coverage per vessel area in P6 retinas of the $p110\beta^{D931A/i\Delta PC}$ compared with the control ($p110\beta^{flox/flox}$). $N \geq 4$ retinas for each condition. Error bars are standard error of the mean. Statistical analysis was performed by Mann-Whitney test.

4. Results

During maturation, PCs exhibits several morphological changes and since we have detected that PCs from the p110 β mutant present defects in the coverage of the vessels, we hypothesised that their morphology could also be altered. Using high magnification images of PCs from p110 β ^{D931A/i Δ PC} mice it was possible to detect that these PCs, in the angiogenic front, were more elongated, thinner and they also presented less cytoplasmic protrusion compared to the control (**Figure 4.25A**). Moreover, in the remodelling plexus, these PCs also appeared to be thinner when compared to the PCs from the control (**Figure 4.25B**).

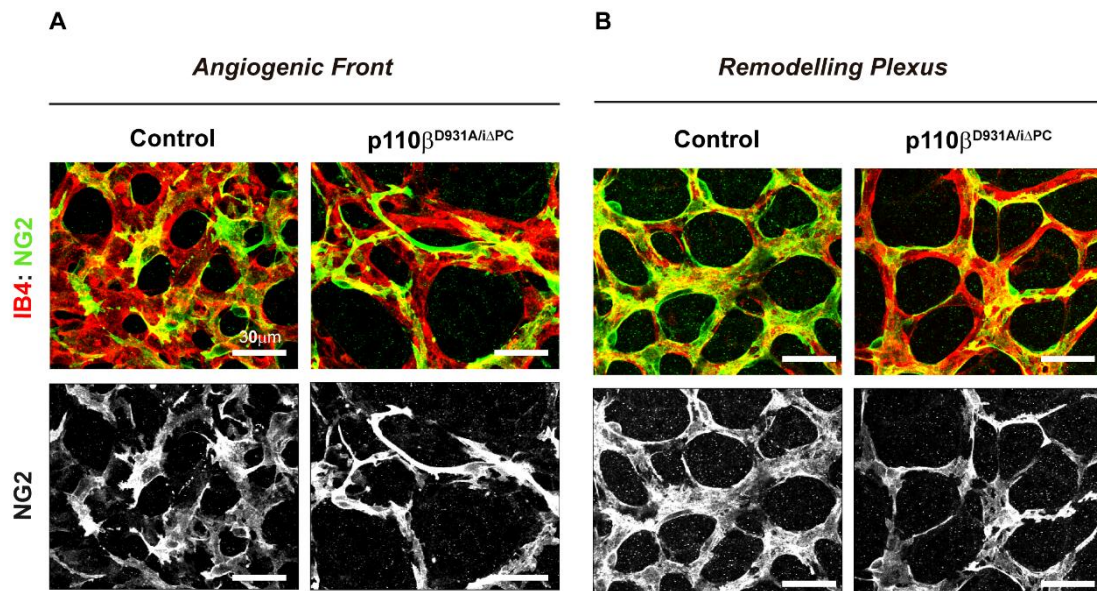


Figure 4.25. PCs morphology changes after p110 β inactivation (A) Confocal images of P6 retinas of the p110 β ^{D931A/i Δ PC} and the respective control (p110 β ^{flox/flox}), injected with 4-OH tamoxifen at P1 and P2 and stained with isolectin-B4 (green) and NG2 (red) in both areas, the angiogenic front and the remodelling plexus. We have detected that PC morphology changes upon p110 β inactivation acquiring a more elongated and thinner shape when compared with the control.

Next, we investigated the impact of p110 β inactivation on PCs proliferation using p110 β ^{D931A/i Δ PC} mice. After p110 β inactivation, the percentage of proliferative PCs was quantified using the co-staining with EdU and NG2 markers. We observed reduced PC proliferation in the p110 β ^{D931A/i Δ PC}, when compared to the control, not only in the sprouting area (**Figure 4.26**) where

PI3K activity is higher, but also in the remodelling plexus (**Figure 4.27**), demonstrating that p110 β is essential for PCs proliferation in both circumstances - the more active and the more quiescent plexus.

Together, this data suggests that p110 β isoform, but not p110 α , is the key regulator of PCs function during the sprouting angiogenesis regulating PC coverage, morphology and proliferation.

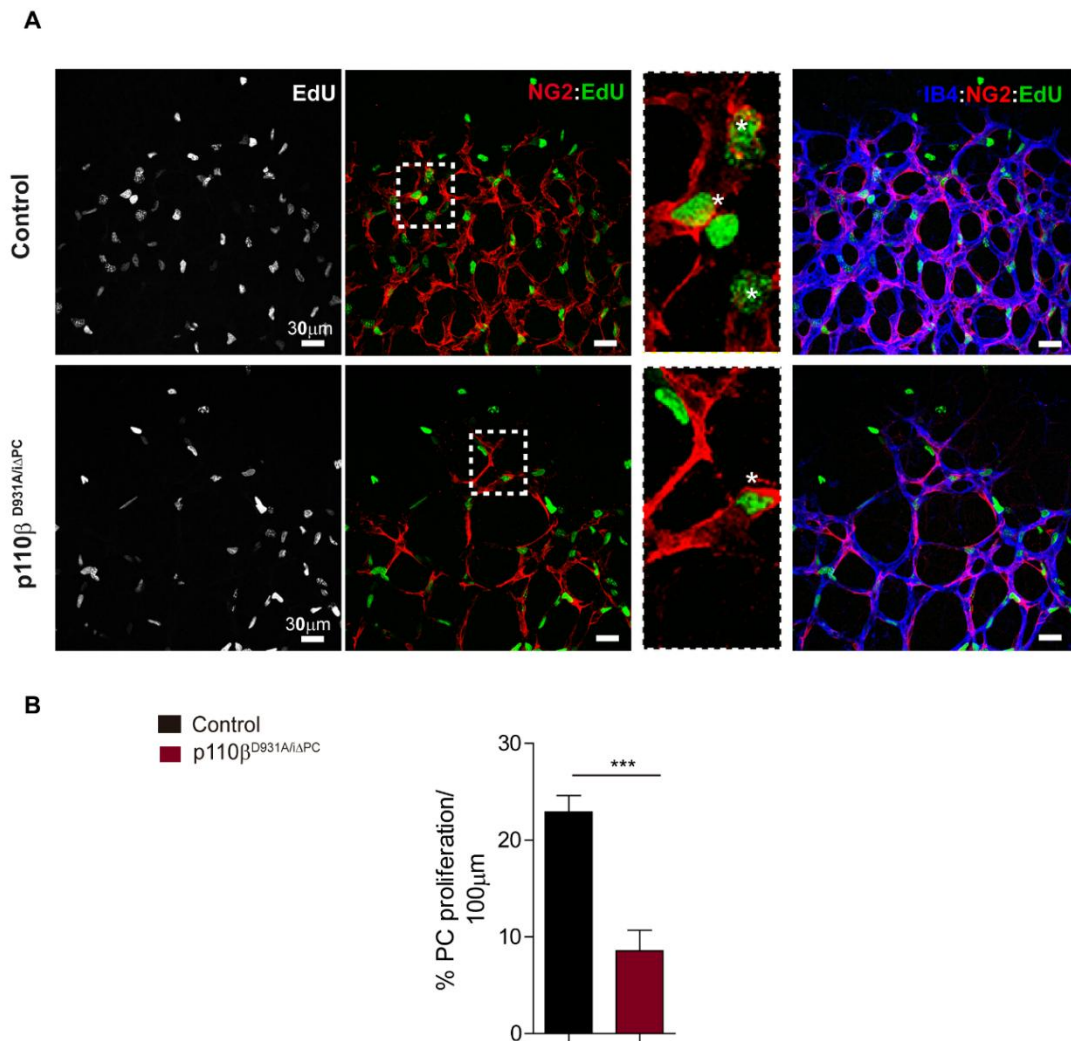


Figure 4.26. p110 β inactivation leads to PC proliferation arrest in the angiogenic front (A) Confocal images of the angiogenic font of P6 retinas injected with 4-OH tamoxifen at P1 and P2. Retinas were injected with EdU 2h before isolation and were stained with isolectin-B4 (blue), NG2 (red) and the EdU (green). (B) Quantification of PC proliferation - EdU positive PC cells per total number of PC cells in a 10⁴ μm^2 area in P6 retinas of the p110 $\beta^{\text{D931A}/\Delta\text{PC}}$ compared with the control (p110 $\beta^{\text{fllox/fllox}}$). N \geq 4 retinas for each condition. Error bars are standard error of the mean. ***P<0.001 was considered statistically significant. Statistical analysis was performed by Mann-Whitney test.

4. Results

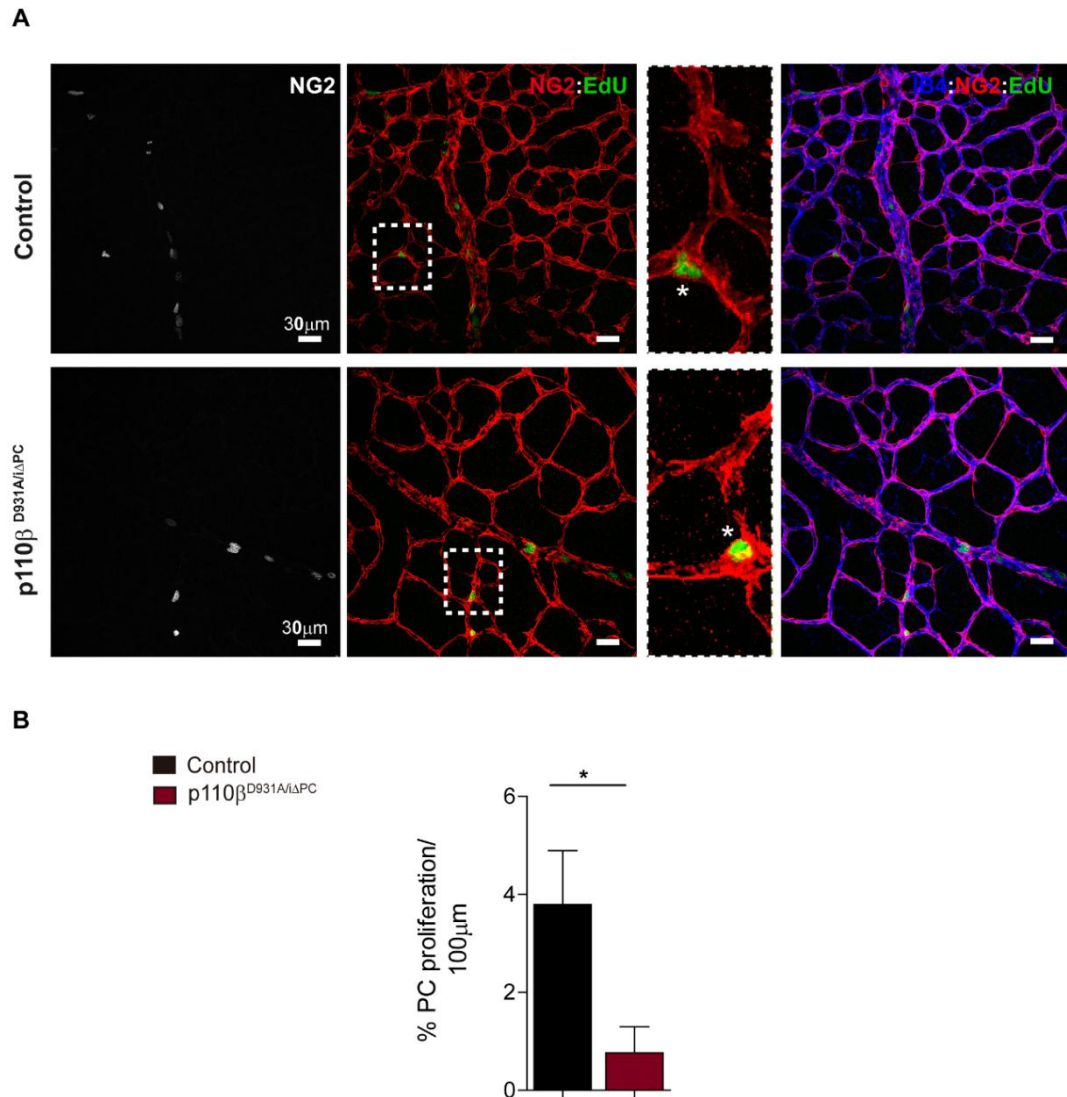


Figure 4.27. p110 β inactivation leads to PC proliferation arrest in remodelling plexus (A) Confocal images of the angiogenic font of P6 retinas injected with 4-OH tamoxifen at P1 and P2. Retinas were injected with EdU 2h before isolation and were stained with isolectin-B4 (blue), NG2 (red) and the EdU (green). (B) Quantification of PC proliferation - EdU positive PC cells per total number of PC cells in a $10^4 \mu\text{m}^2$ area in P6 retinas of the $p110\beta^{D931A/\Delta PC}$ compared with the control ($p110\beta^{flx/flx}$). $N \geq 4$ retinas for each condition. Error bars are standard error of the mean. * $P < 0.05$ was considered statistically significant. Statistical analysis was performed by Mann-Whitney test.

4.3. Paracrine regulation of ECs by PI3K signalling in PCs

PCs interact with ECs for tissue homeostasis and regeneration. This interaction can be done by direct contact between both cell types by diverse junctional structures that allow the diffusion of several molecules. However, most of PCs and ECs communication events are exerted by paracrine mechanisms that are determinants in the regulation of angiogenesis and vessel stabilization (Caporali et al., 2016). Given that p110 β is implicated in PC regulation during sprouting angiogenesis we predicted that this pathway is also regulating the PCs and ECs interaction previously described.

4.3.1. p110 α inactivation in PCs leads to defects in EC motility

We have seen that inactivation of p110 α in PCs does not interfere with PC coverage or proliferation. However, we have analysed even though possible defects of the vasculature since the cross-talk between PCs and ECs could be compromised.

First, we have quantified the expansion of the vascular plexus to the periphery of the P6 retinas, using the isolectin-B4 vessel marker. For this study, we have used once again the four genotype models to validate our mice strategy: **(1)** the p110 α ^{WT/D933A} mice were used to exclude any kind of effects of the constitutive point mutation; **(2)** p110 α ^{iAPC/iAPC} mice were used to analyse the effects of the complete deletion of p110 α in PCs; **(3)** the combined strategy p110 α ^{D933A/iAPC} that maintains the signalling complex stoichiometry, avoiding deregulation of PI3-kinase signalling, and also prevents possible combinatory effects as explained previously, and the **(4)** p110 α ^{flox/flox} mice without Cre activity used as a control.

We have seen that the full deletion of p110 α in PCs or the constitutive inactivation of p110 α using the p110 α ^{iAPC/iAPC} and the p110 α ^{WT/D933A}, respectively, did not show any differences in the radial expansion of the

4. Results

vessels. However, $p110\alpha^{D933A/\Delta PC}$ mice showed a significant reduction in the expansion of the plexus (**Figure 4.28**).

Although, the specific inactivation of $p110\alpha$ in PCs was not regulating PC coverage or proliferation, it seems to affect the communication between PCs and ECs, leading to defects in the expansion of the plexus. Additionally, we measured the radial expansion in $p110\alpha^{D933A/\Delta PC}$ retinas at P9, but we did not detect any differences when compared to the control (**Figure 4.29**). This data suggests that $p110\alpha$ inactivation on PCs leads to a delay in EC migration, but not to complete cell motility arrest.

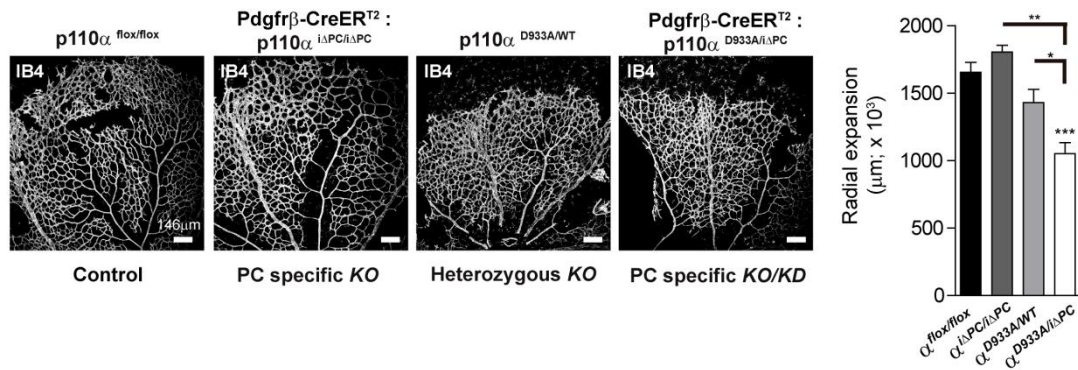


Figure 4.28. $p110\alpha$ inactivation in PCs results in radial expansion arrest in P6 retinas. (A) Whole-mount of P6 retinas injected with 4-OH tamoxifen at P1 and P2 and stained with isolectin-B4. (B) Quantification of radial expansion of blood vessels in P6 retinas of respective genotypes. $n \geq 3$ retinas for each genotype. Error bars are standard error of the mean. * $P < 0.05$, ** $P < 0.01$ and *** $P < 0.001$ was considered statistically significant. Statistical analysis was performed by Mann-Whitney test.

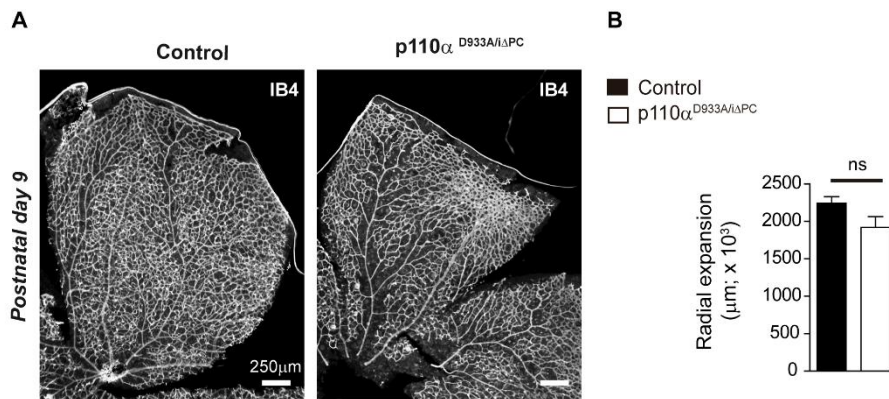


Figure 4.29. p110 α inactivation in PCs did not result in radial expansion defects in P9 retinas. (A) Whole-mount of P9 retinas injected with 4-OH tamoxifen at P1 and P2 and stained with isolectin-B4. (B) Quantification of radial expansion of blood vessels in P9 retinas of respective genotypes. $n \geq 4$ retinas for each genotype. Error bars are standard error of the mean. Statistical analysis was performed by Mann-Whitney test.

Despite of reduced expansion of the plexus we did not observe any other obvious defects in the vasculature in the p110 $\alpha^{D933A/i\Delta PC}$ mice, including defects in the number of branching, the number of tip cells, tips length or filopodia in the migrating vascular front (**Figure 4.30**). Similarly, in the more mature plexus of the retina we did not find differences in the number of branching points in the p110 $\alpha^{D933A/i\Delta PC}$ mice, when compared to the respective control littermates (**Figure 4.31**). ECs proliferation was also assessed using the EdU staining in combination with the EC nuclear marker ERG and the vessel marker isolectin-B4. We did not find any defects in EC proliferation in the p110 $\alpha^{D933A/i\Delta PC}$ mice in both areas of P6 retinas, the sprouting front (**Figure 4.32**) and the remodelling plexus (**Figure 4.33**). Apparently, the inactivation of this isoform only leads to a delayed expansion of the plexus that could be explained by defective interactions between both cell types.

4. Results

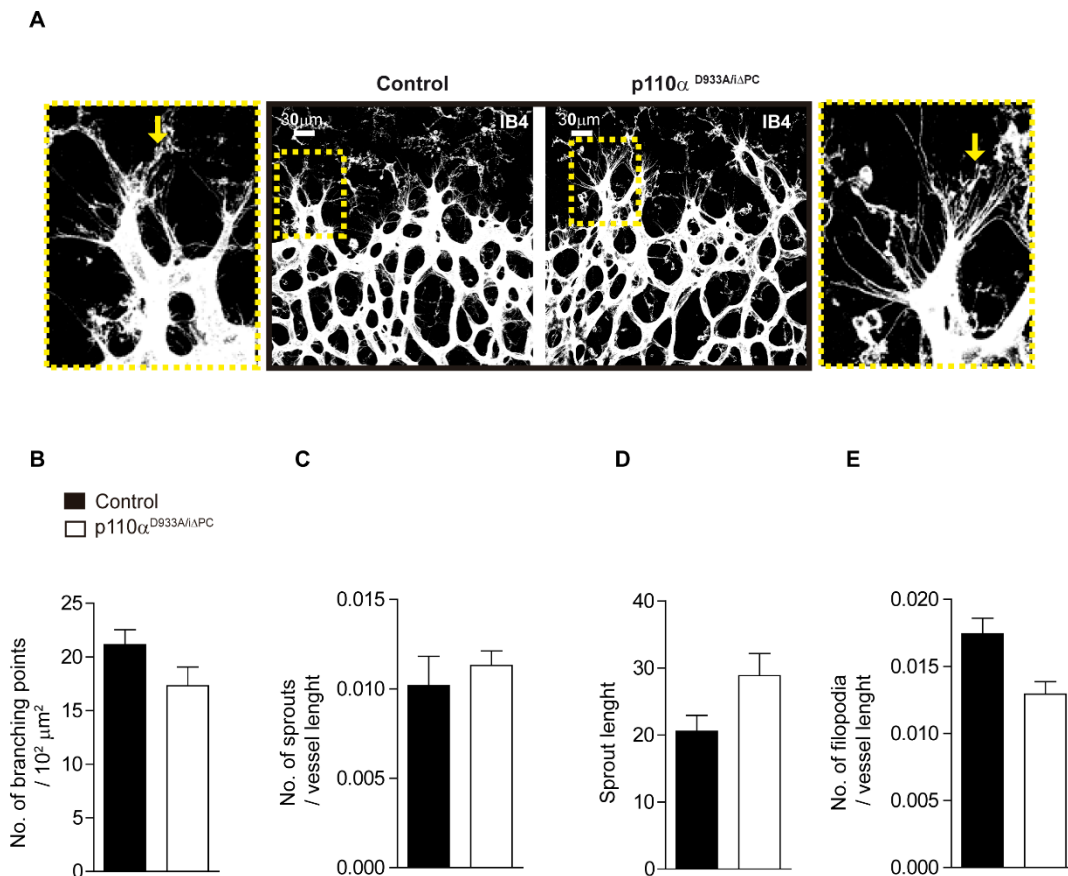


Figure 4.30. p110 α inactivation do not affect the vascular density, sprouts or filopodia in the vascular front of the retina. (A) Confocal images at the angiogenic front of P6 p110 α ^{D933A/iΔPC} mice retinas and respective control (p110 α ^{flox/flox}), upon 4-OH tamoxifen injection at P1 and P2. Isolectin-B4 staining was performed. The yellow squares are zoom of the confocal images highlighting the sprout cell and the yellow arrows indicating the filopodia. (B) Quantification of the number of branch points in the sprouting front area of p110 α ^{D933A/iΔPC} mice and control. (C) Quantification of number of sprouts per vessel length of p110 α ^{D933A/iΔPC} mice and control. (D) Quantification of Sprout length of p110 α ^{D933A/iΔPC} mice and control. (E) Quantification of filopodia number per vessel length in the p110 α ^{D933A/iΔPC} mice and control. n \geq 4 retinas for each genotype. Error bars are standard error of the mean. Statistical analysis was performed by Mann-Whitney test.

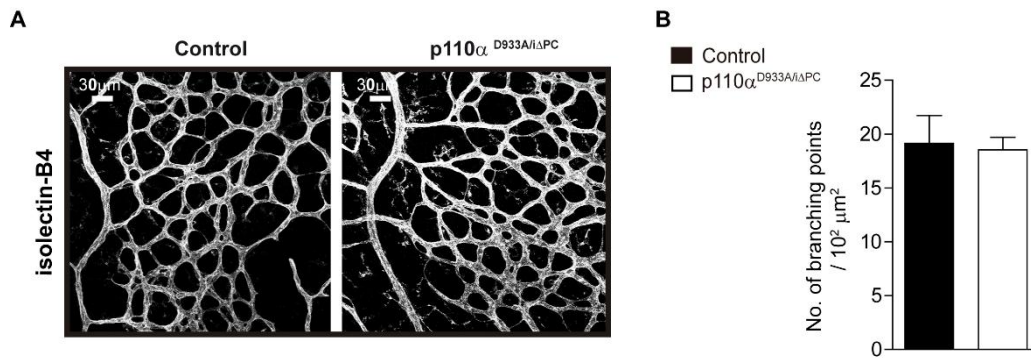


Figure 4.31. p110 α inactivation do not affect the vascular density in the remodelling plexus. (A) Confocal images at the remodelling plexus of P6 p110 α ^{D933A/iΔPC} mice retinas and respective control (p110 α ^{flox/flox}), upon 4-OH tamoxifen injection at P1 and P2. Isolectin-B4 staining was performed. (B) Quantification of the number of branch points in the remodelling area of p110 α ^{D933A/iΔPC} mice and control. $n \geq 4$ retinas for each genotype. Error bars are standard error of the mean. Statistical analysis was performed by Mann-Whitney test.

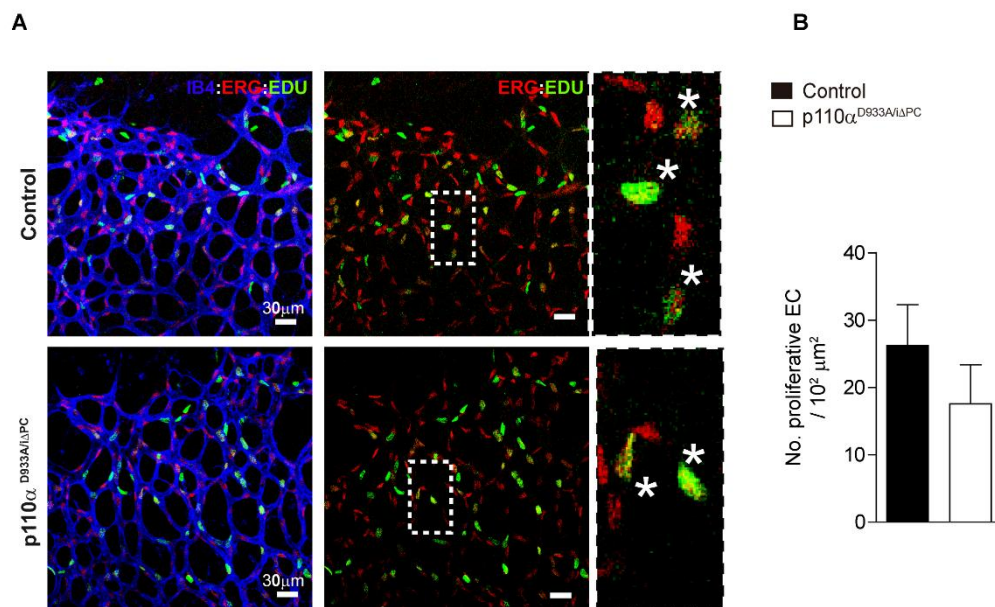


Figure 4.32. p110 α inactivation do not affect the EC proliferation in the sprouting front. (A) Confocal images of the angiogenic front of P6 retinas injected with 4-OH tamoxifen at P1 and P2. Retinas were injected with EdU 2h before isolation and were stained with isolectin-B4 (blue), ERG (red) and the EdU (green). (B) Quantification of EC proliferation - EdU positive cells per total number of EC (ERG positive) in a 10⁴ μm² area- in P6 retinas of the p110 α ^{D933A/iΔPC} compared with the control (p110 α ^{flox/flox}). $N \geq 4$ retinas for each condition. Error bars are standard error of the mean. Statistical analysis was performed by Mann-Whitney test.

4. Results

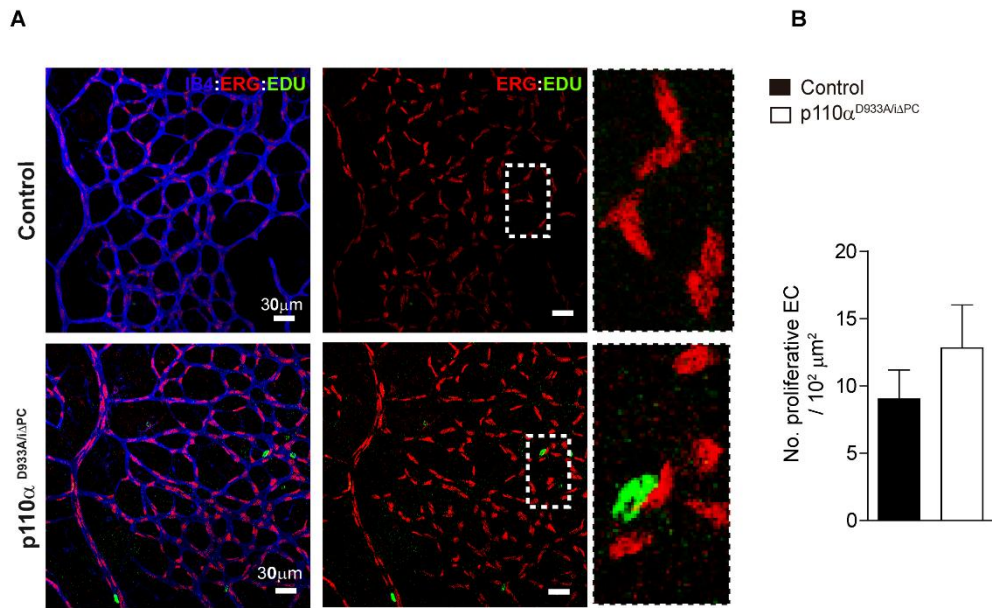


Figure 4.33. p110 α inactivation do not affect PC proliferation in the remodelling plexus. (A) Confocal images of the remodelling plexus of P6 retinas injected with 4-OH tamoxifen at P1 and P2. Retinas were injected with EdU 2h before isolation and were stained with isolectin-B4 (blue), ERG (red) and the EdU (green). (B) Quantification of EC proliferation - EdU positive cells per total number of EC (ERG positive) in a $10^4\mu\text{m}^2$ area- in P6 retinas of the p110 $\alpha^{\text{D933A/i}\Delta\text{PC}}$ compared with the control (p110 $\alpha^{\text{flox/flox}}$). $N \geq 4$ retinas for each condition. Error bars are standard error of the mean. Statistical analysis was performed by Mann-Whitney test.

4.3.2. p110 β inactivation in PCs leads to severe vascular defects

Next, we started to investigate the possible effects of inactivation of p110 β in PC in the vasculature. First, we wanted to analyse the radial expansion of P6 retinas and to exclude that these defects were due to the constitutive inactivation of p110 β four genotypic groups were studied: (1) the combined strategy using the p110 $\beta^{\text{D931A/i}\Delta\text{PC}}$ mice, (2) the full inactivation of p110 β in PCs using the p110 $\beta^{\text{i}\Delta\text{PC/i}\Delta\text{PC}}$, (3) the constitutive kinase-death mutant p110 $\beta^{\text{WT/D931A}}$ and the control without Cre-activity p110 $\beta^{\text{flox/flox}}$. We have only detected radial expansion defects in the p110 $\beta^{\text{D931A/i}\Delta\text{PC}}$ mice, indicating that these defects are due to specific p110 β inactivation in PCs (**Figure 4.34**). Additionally, the P9 mouse retinas of p110 $\beta^{\text{D931A/i}\Delta\text{PC}}$ were also analysed and no differences in the radial expansion were found, when compared to the control (**Figure 4.35**).

Therefore, p110 β inactivation in PCs causes delay in the EC migration but not full migration arrest, as seen before in p110 α mutants.

We also assessed the vascular density of p110 β ^{D931A/ Δ PC} in the sprouting front area, where we have seen less vascular density when compared to the control, however, no changes in the formation of sprouts, sprouts length or filopodia were detected in the perimeter of the sprouting front (**Figure 4.36**). Apparently, the effects seen in the vessel migration or density are not due to defects in the cells at the leading edge of the retina. Similarly, the vascular density of the remodelling area was slightly reduced in p110 β ^{D931A/ Δ PC} mice, when compared to the control (**Figure 4.37**), further demonstrating that PC-EC cross-talk upon p110 β inactivation in PC is affecting not only the sprouting and immature front of the retina, but also the more mature plexus.

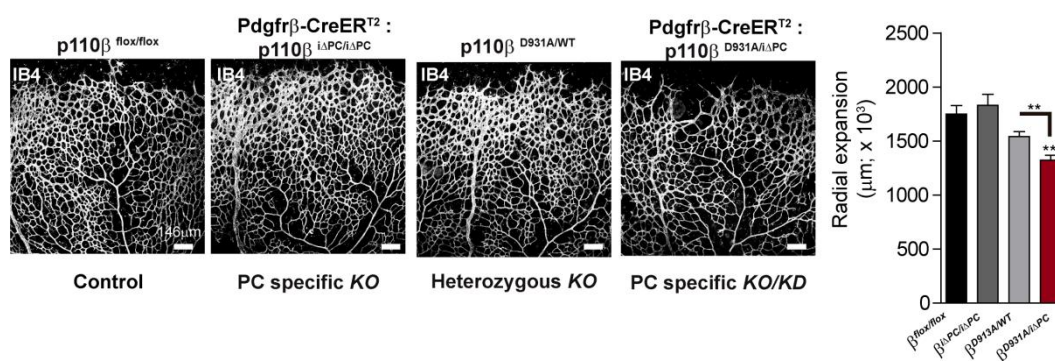


Figure 4.34. p110 β inactivation in PCs results in reduced radial expansion in P6 retinas. (A) Whole-mount of P6 retinas injected with 4-OH tamoxifen at P1 and P2 and stained with isolectin-B4. (B) Quantification of radial expansion of blood vessels in P6 retinas of respective genotypes. $n \geq 4$ retinas for each genotype. Error bars are standard error of the mean. ** $P < 0.01$ was considered statistically significant. Statistical analysis was performed by Mann-Whitney test.

4. Results

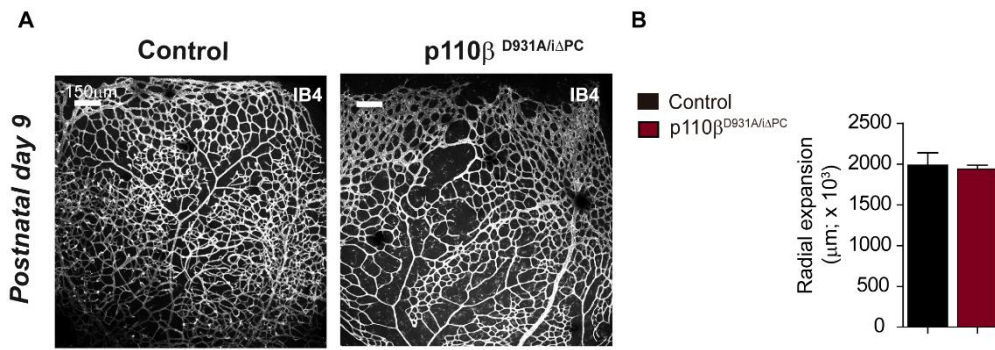


Figure 4.35. p110β inactivation in PCs do not affect radial expansion in P9 retinas. (A) Whole-mount of P9 retinas injected with 4-OH tamoxifen at P1 and P2 and stained with isolectin-B4. (B) Quantification of radial expansion of blood vessels in P9 retinas of respective genotypes. $n \geq 4$ retinas for each genotype. Error bars are standard error of the mean. Statistical analysis was performed by Mann-Whitney test.

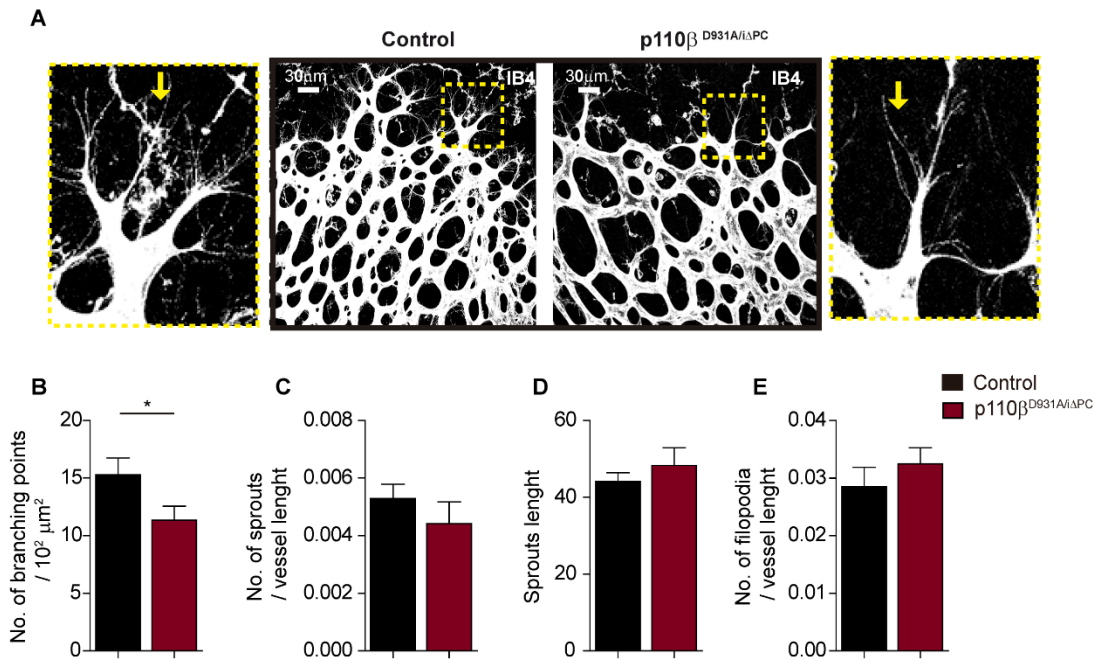


Figure 4.36. p110β inactivation leads to reduced vascular density but not impacts in the sprouts or filopodia in the vascular front of the retina. (A) Confocal images at the angiogenic front of P6 p110β^{D931A/iΔPC} mice retinas and respective control (p110β^{flox/flox}), upon 4-OH tamoxifen injection at P1 and P2. Isolectin-B4 staining was performed. The yellow squares are zoom of the confocal images highlighting the sprout cell and the yellow arrows indicating the filopodia. (B) Quantification of the number of branch points in the sprouting front area of p110β^{D931A/iΔPC} mice and control. (C) Quantification of number of sprouts per vessel length of p110β^{D931A/iΔPC} mice and control. (D) Quantification of Sprout length of p110β^{D931A/iΔPC} mice and control. (E) Quantification of filopodia number per vessel length in the p110β^{D931A/iΔPC} mice and control. $n \geq 4$ retinas for each genotype. Error bars are standard error of the mean. * $P < 0.05$ was considered statistically significant. Statistical analysis was performed by Mann-Whitney test.

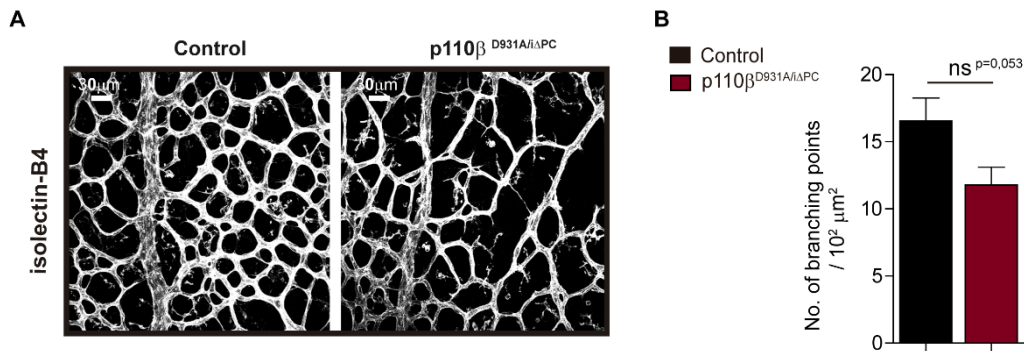


Figure 4.37. p110β inactivation in PCs results in reduced vascular density in the remodelling plexus. (A) Confocal images at the remodelling plexus of P6 p110β^{D931A/iΔPC} mice retinas and respective control (p110β^{flox/flox}), upon 4-OH tamoxifen injection at P1 and P2. Isolectin-B4 staining was performed. (B) Quantification of the number of branch points in the remodelling area of p110β^{D931A/iΔPC} mice and control. $n \geq 4$ retinas for each genotype. ^{ns}P < 0.053 and only *P < 0.05 was considered statistically significant. Error bars are standard error of the mean. Statistical analysis was performed by Mann-Whitney test

To discern whether the reduced vascular density of p110β inactivation in PC were due to failure in the EC proliferation, we have used the EdU staining together with ERG (EC-specific nuclear marker) and isolectin-B4 in the P6 mutant retinas. A significant decrease in the EC proliferation was observed in both, the angiogenic front (**Figure 4.38**) and in the remodelling plexus (**Figure 4.39**) of the p110β^{D931A/iΔPC} mice. Additionally, we analysed cell death to determine whether the observed defects were only a consequence of a cell arrest or whether a cell death could also be involved. Staining for cleaved caspase-3 to evaluate EC apoptosis showed no differences between control and the p110β^{D931A/iΔPC} retinas (**Figure 4.40**).

The p110β inactivation in PC leads to ECs migration and proliferation arrest, both of which resemble a more mature vascular plexus. During the maturation, there is an abundant collagen IV deposition as previously described using the WT retinas. Therefore, we have assessed the levels of this protein in the P6 retinas of the p110β^{D931A/iΔPC} mice, which showed higher deposition of collagen IV in both the sprouting area and the remodelling plexus, when compared to the control (**Figure 4.41**).

4. Results

Taking together, p110 β inactivation affects not only the PCs, but also leads to defects in the paracrine regulation of the endothelium resulting in severe vascular defects that resemble a more quiescent phenotype and mature vasculature.

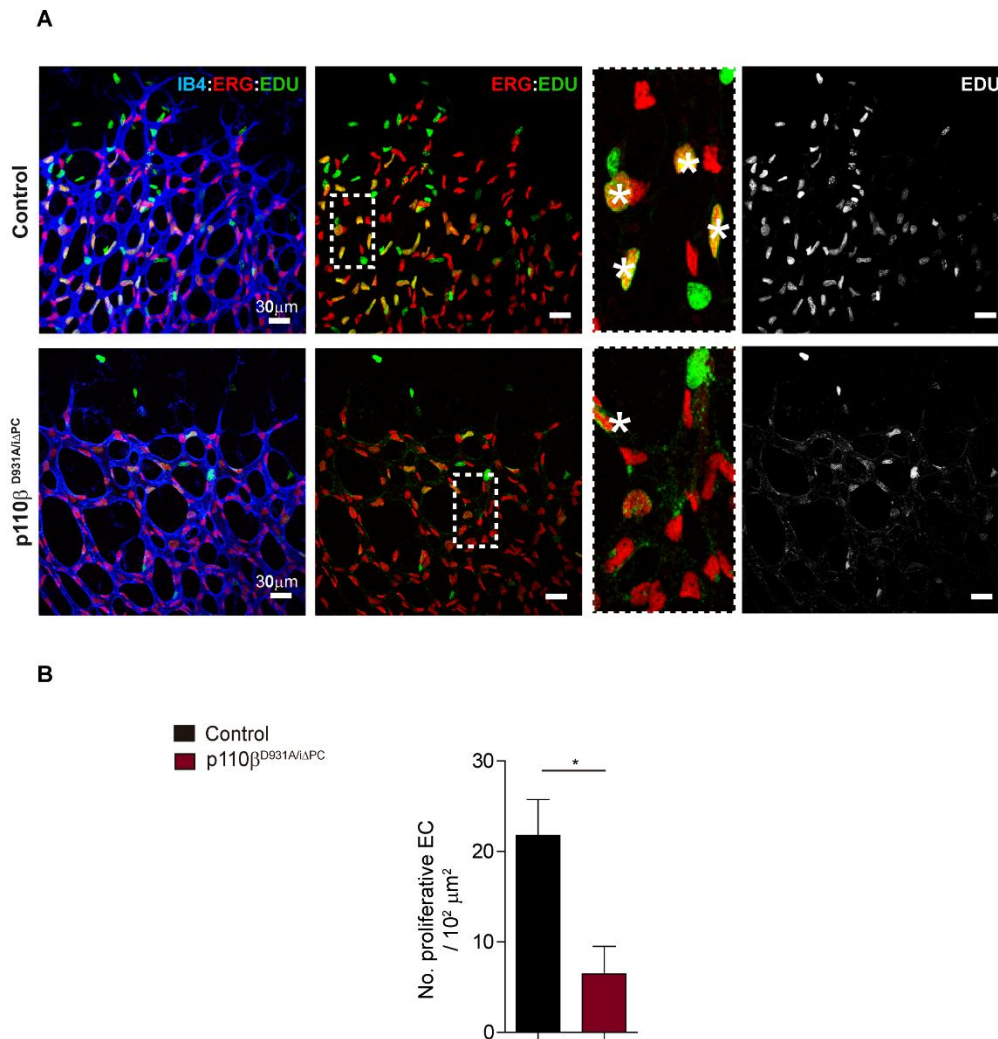


Figure 4.38. p110 β inactivation in PCs resulted in EC proliferation arrest in the sprouting front. (A) Confocal images of the angiogenic front of P6 retinas injected with 4-OH tamoxifen at P1 and P2. Retinas were injected with EdU 2h before isolation and were stained with isolectin-B4 (blue), ERG (red) and the EdU (green). **(B)** Quantification of EC proliferation - EdU positive cells per total number of EC (ERG positive) in a 10⁴μm² area- in P6 retinas of the p110 $\beta^{D931A/i\Delta PC}$ compared with the control (p110 $\beta^{fllox/fllox}$). N \geq 4 retinas for each condition. Error bars are standard error of the mean. *P <0.05 was considered statistically significant. Statistical analysis was performed by Mann-Whitney test.

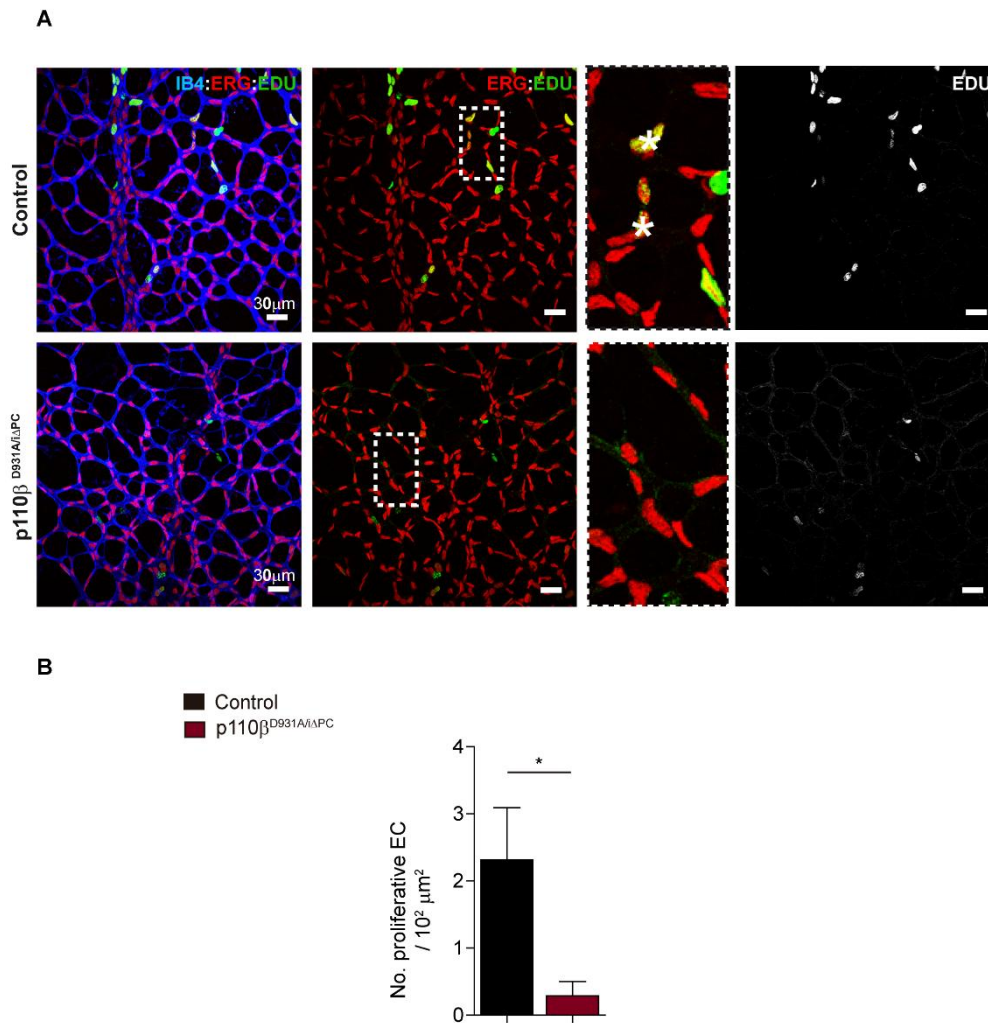


Figure 4.39. $p110\beta$ inactivation in PCs resulted in EC proliferation arrest in the remodelling plexus. (A) Confocal images of the angiogenic front of P6 retinas injected with 4-OH tamoxifen at P1 and P2. Retinas were injected with EdU 2h before isolation and were stained with isolectin-B4 (blue), ERG (red) and the EdU (green). **(B)** Quantification of EC proliferation - EdU positive cells per total number of EC (ERG positive) in a $10^4 \mu\text{m}^2$ area- in P6 retinas of the $p110\beta^{\text{D931A/i}\Delta\text{PC}}$ compared with the control ($p110\beta^{\text{floxed/floxed}}$). $N \geq 4$ retinas for each condition. Error bars are standard error of the mean. * $P < 0.05$ was considered statistically significant. Statistical analysis was performed by Mann-Whitney test.

4. Results

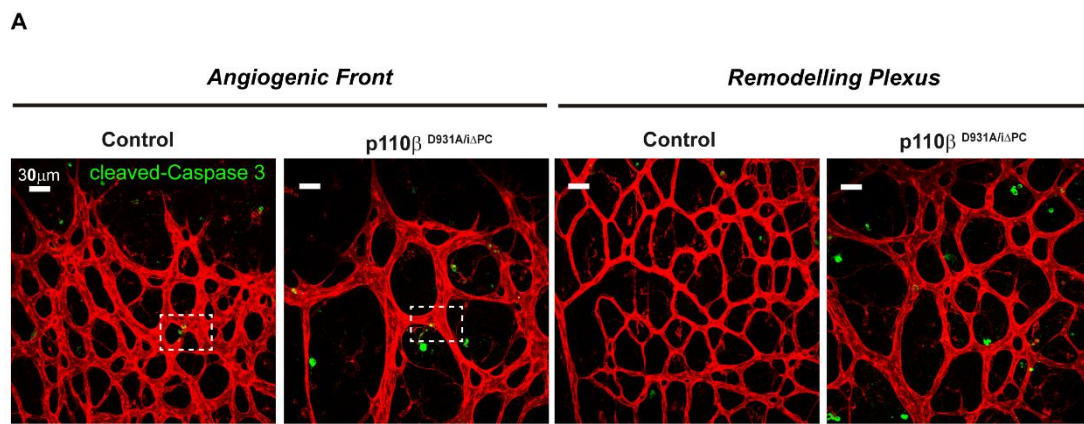


Figure 4.40. p110 β inactivation in PCs did not affect cell death in the vasculature. (A) Confocal images of the angiogenic front and remodelling plexus of P6 retinas injected with 4-OH tamoxifen at P1 and P2. Retinas were stained with isolectin-B4 (red) and cleaved-Caspase 3 (green).

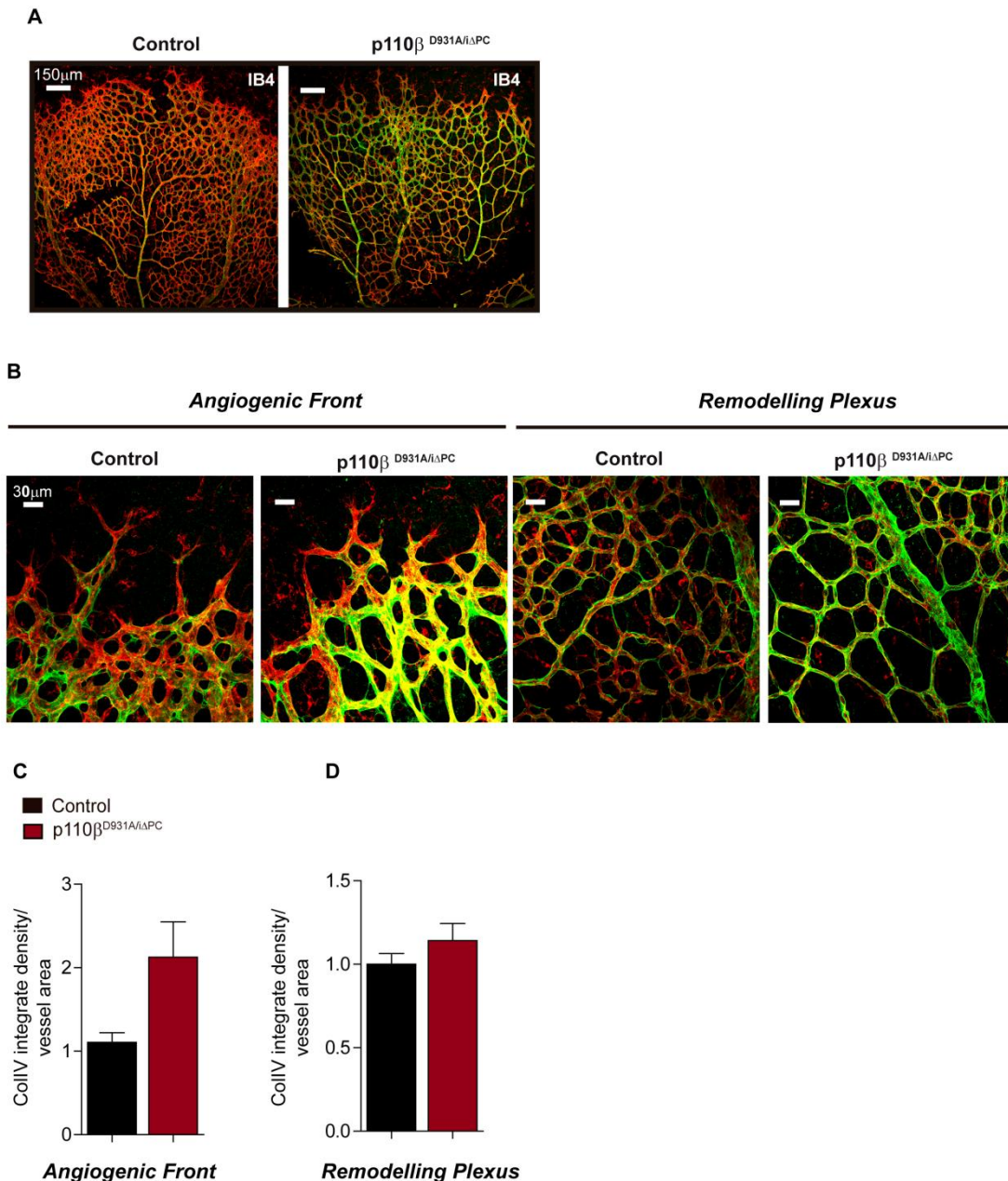


Figure 4.41. $p110\beta$ inactivation leads to increased deposition of collagen IV in angiogenic front. (A) Whole-mount of P9 retinas injected with 4-OH tamoxifen at P1 and P2 and stained with isolectin-B4 (red) and collagen IV (green). (B) High magnification confocal images of the angiogenic front and remodelling plexus of $p110\beta^{D931A/\Delta PC}$ and respective control ($p110\beta^{flx/flx}$). (C) Quantification of collagen IV integrate intensity in vessel area of the angiogenic front area. The $p110\beta^{D931A/\Delta PC}$ results in increased deposition of collagen IV in the sprouting front (but not statistically significant). N=3 retinas for each condition. (D) Quantification of collagen IV integrate intensity in vessel area of the remodeling plexus area. The $p110\beta^{D931A/\Delta PC}$ results in no changes in collagen IV in the remodelling plexus. N=3 retinas for each condition. Error bars are standard error of the mean. Statistical analysis was performed by Mann-Whitney test.

4.4. PTEN regulates PI3K function in PCs during the sprouting angiogenesis (ongoing experiments)

To further understand how PI3K pathway regulates PCs functions during the sprouting angiogenesis, we also inactivated PTEN specifically in PCs. PTEN is the major regulator of PI3K class I signalling acting as a lipid phosphatase, dephosphorylating the PIP3 lipids into PIP2 and thereby, counterbalancing the PI3K signalling effect (Vanhaesebroeck et al., 2010). Moreover, PTEN in ECs is required in a cell-autonomous and dose-dependent manner for the control of vascular density and vessel growth (Serra et al., 2015). For this purpose, we have used the tamoxifen-inducible PC-specific Cre line (Pdgfr β (BAC)-CreERT2) in combination with loxP-flanked alleles to genetically inactivate PTEN (PTEN^{i Δ PC}) in retinal PCs (ongoing experiments).

Analysis of P6 PTEN^{i Δ PC} retinas, using the NG2 and isolectin-B4, showed increased PC coverage in the sprouting front area, when compared to the control (**Figure 4.42A-B**). In contrast, in the remodelling plexus of the retina we have detected a slight reduction in the PC coverage (**Figure 4.42C-D**).

Data from our laboratory has shown that PTEN turnover is low and its ECs-specific inactivation leads to dramatic vascular defects that are maintained and increased over time (Serra et al., 2015). Thus, we next analysed the P9 retinas that, in agreement with the previous findings, showed an even stronger phenotype where PTEN^{i Δ PC} present more PCs coverage in the sprouting front when compared to the controls (**Figure 4.43A-B**). In contrast, no differences were detected in the remodelling plexus (**Figure 4.43C-D**). It seems then that PTEN controls PC coverage only in the immature plexus of the retina.

We have also seen that PCs in P9 retinas present an aberrant morphology, when compared with the control. They are larger and the cell body is more retracted, presenting more protrusions. In contrast, PC from control retinas are more elongated, thinner and the cell body is highly connected to the endothelium (**Figure 4.44**).

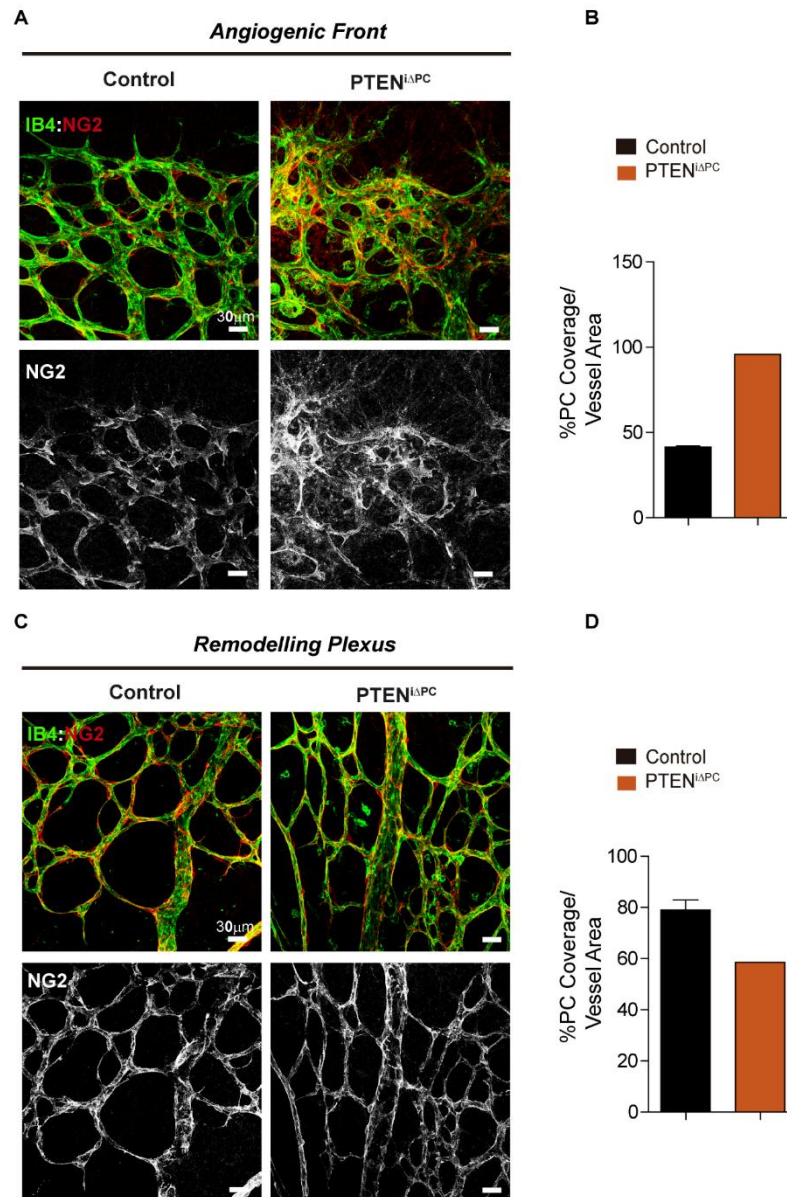


Figure 4.42. PTEN inactivation results in increased PC coverage in the angiogenic front and slight reduced PC coverage in the remodelling plexus of the P6 retina. (A) Confocal images of the angiogenic front area of P6 retinas injected with 4-OH tamoxifen at P1 and P2 and stained with isolectin-B4 (green) and NG2 (red) (B) Quantification of PC coverage per vessel area in P6 retinas of the PTEN^{iΔPC} (N=1 retina) compared with the control (N=2 retinas). (C) Confocal images of the remodelling plexus area of P6 retinas injected with 4-OH tamoxifen at P1 and P2 and stained with isolectin-B4 (green) and NG2 (red) (B) Quantification of PC coverage per vessel area in P6 retinas of the PTEN^{iΔPC} (N=1 retina) compared with the control (N=2 retinas). Error bars are standard error of the mean.

4. Results

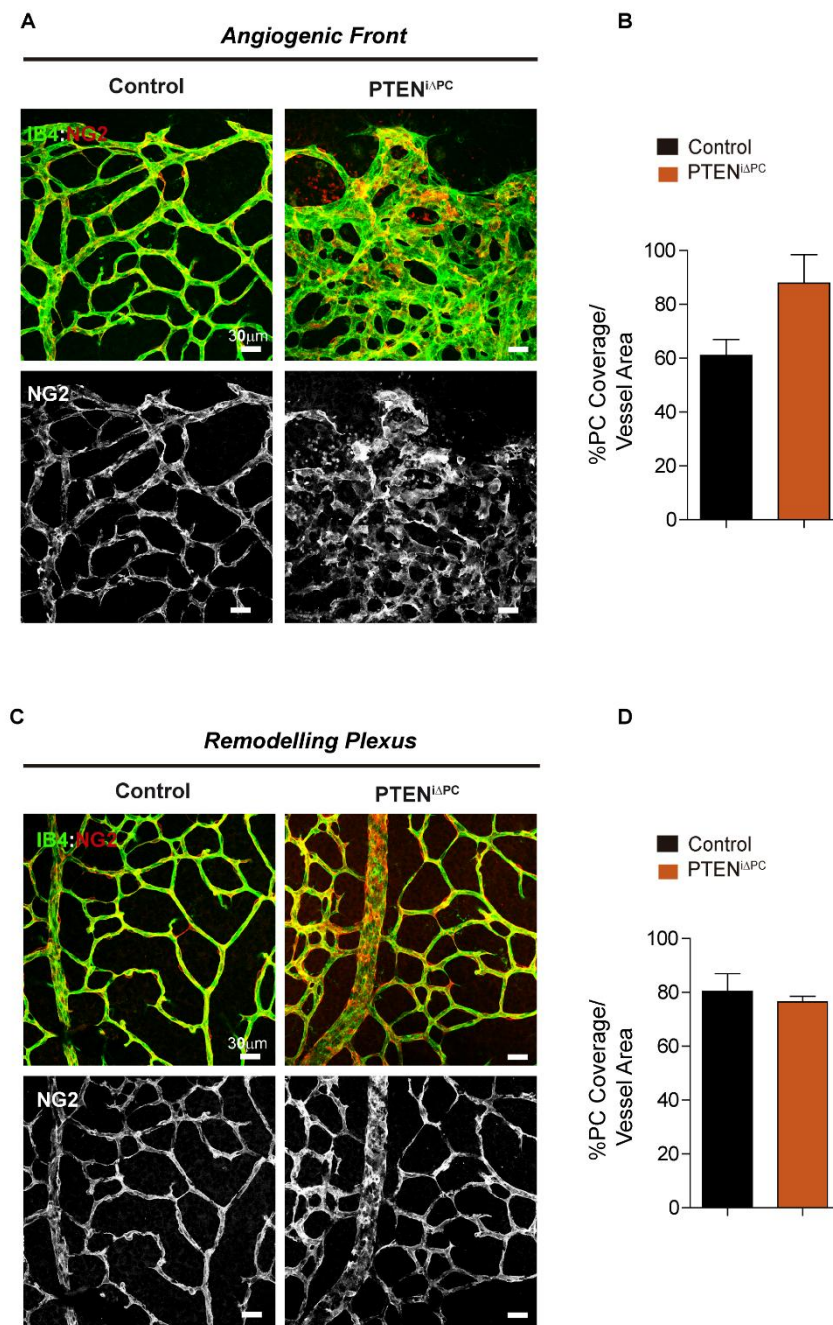


Figure 4.43. PTEN inactivation results in increased PC coverage in the angiogenic front and no changes in in the remodelling plexus of the P9 retina. (A) Confocal images of the angiogenic front area of P9 retinas injected with 4-OH tamoxifen at P1 and P2 and stained with isolectin-B4 (green) and NG2 (red) (B) Quantification of PC coverage per vessel area in P9 retinas of the $PTEN^{iAPC}$ compared with the control. (C) Confocal images of the remodelling plexus area of P6 retinas injected with 4-OH tamoxifen at P1 and P2 and stained with isolectin-B4 (green) and NG2 (red) (B) Quantification of PC coverage per vessel area in P9 retinas of the $PTEN^{iAPC}$ compared with the control. $n \geq 4$ retinas for each genotype. Error bars are standard error of the mean. Statistical analysis was performed by Mann-Whitney test.

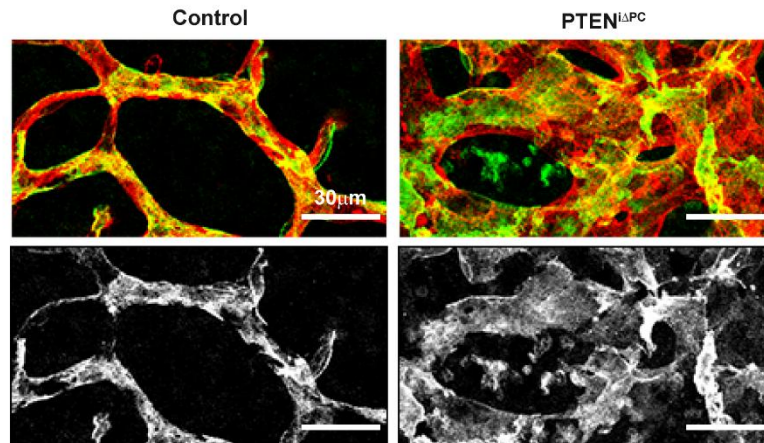


Figure 4.44. PCs morphology changes after PTEN inactivation. (A) Confocal images of P9 retinas of the $PTEN^{i\Delta PC}$ and the respective control, injected with 4-OH tamoxifen at P1 and P2 and stained with isolectin-B4 (green) and NG2 (red) in the angiogenic front. We have detected that PC morphology changes upon PTEN inactivation acquiring a more a larger shape, with the cell body more retracted, when compared with the control.

We further investigated the impact of $PTEN^{i\Delta PC}$ mice on the vasculature and as we detected a stronger phenotype in PCs at postnatal day 9, we focused our attention at this time point of the retinal development. Analysis of P9 retinas revealed reduced radial expansion of the vasculature in the $PTEN^{i\Delta PC}$ mice, when compared to the control thus, PTEN inactivation in PCs also affects EC expansion of the plexus (**Figure 4.45**). Interestingly, when observing all the retinal plexus it was possible to identify that the vascular defects were particularly found in the sprouting frontal zone, suggesting once more that PTEN regulates the immature PCs located at active sprouting areas.

Analysis of higher magnification images of $PTEN^{i\Delta PC}$ retinas showed increased vascular density in the sprouting front, (**Figure 4.46**). In contrast, in the remodelling area no significant differences were detected in the vasculature (**Figure 4.47**).

4. Results

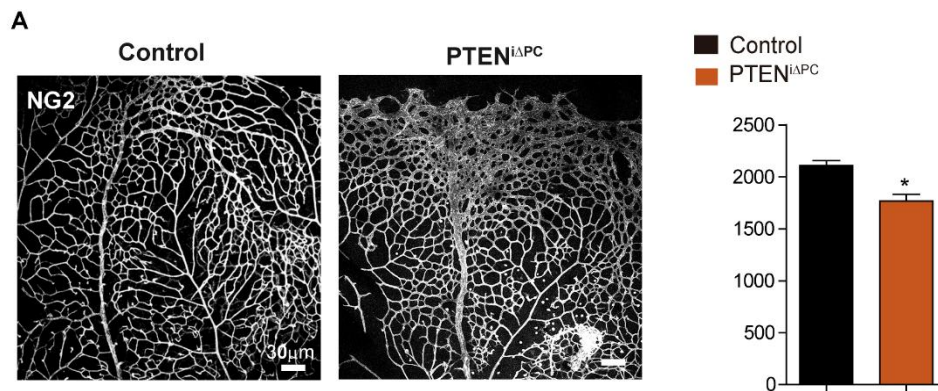


Figure 4.45. PTEN inactivation in PCs results in reduced expansion of the plexus in P9 retinas. (A) Whole-mount of P9 retinas injected with 4-OH tamoxifen at P1 and P2 and stained with isolectin-B4. (B) Quantification of radial expansion of blood vessels in P9 retinas of respective genotypes. $n \geq 4$ retinas for each genotype. Error bars are standard error of the mean. * $P < 0.05$ was considered statistically significant. Statistical analysis was performed by Mann-Whitney test.

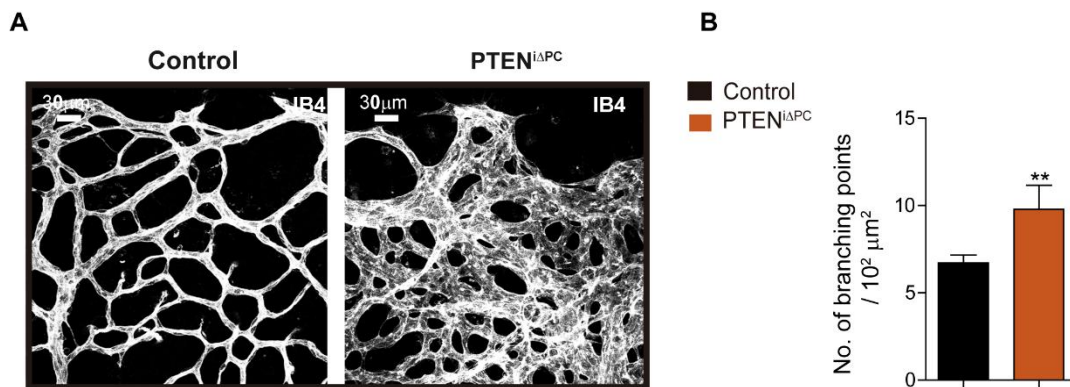


Figure 4.46. PTEN inactivation results in higher vascular density in the angiogenic front area. (A) Confocal images at the angiogenic front area of P9 PTEN^{iAPC} mice retinas and respective control, upon 4-OH tamoxifen injection at P1 and P2. Isolectin-B4 staining was performed. (B) Quantification of the number of branch points in the remodelling area of PTEN^{iAPC} mice and control. $n \geq 4$ retinas for each genotype ** $P < 0.01$ was considered statistically significant. Error bars are standard error of the mean. Statistical analysis was performed by Mann-Whitney test.

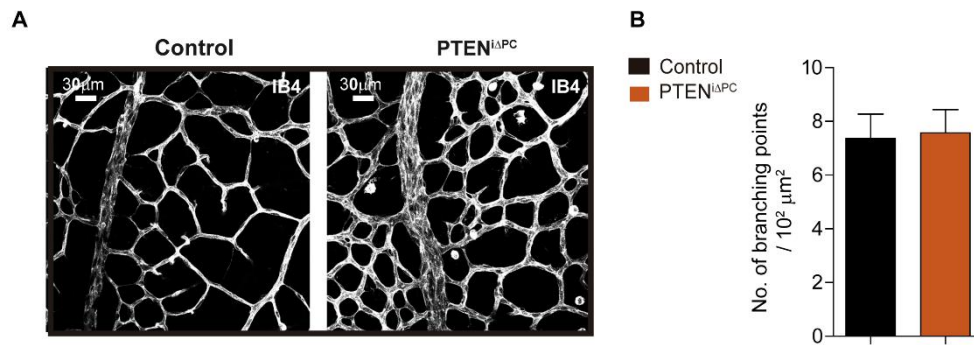


Figure 4.47. PTEN inactivation do not changed the vascular density in the remodelling plexus area. (A) Confocal images at the remodelling plexus of P9 PTEN^{ΔPC} mice retinas and respective control, upon 4-OH tamoxifen injection at P1 and P2. Isolectin-B4 staining was performed. (B) Quantification of the number of branch points in the remodelling area of PTEN^{ΔPC} mice and control. $n \geq 4$ retinas for each genotype. Error bars are standard error of the mean. Statistical analysis was performed by Mann-Whitney test

Taken together, PTEN inactivation in PCs leads to aberrant PCs morphology and increased PC coverage. These dramatic changes in the PCs upon PTEN inactivation also have impacts on the vasculature, resulting in impaired cell migration and increased vascular density.

Our data suggests that in PCs p110 β can be regulated by PTEN, since inactivation of both isoforms in these cells results in opposite effects. The p110 β inactivation leads to more quiescent PCs and consequently a mature vasculature whereas, PTEN inactivation results in an aberrant and active PCs and a more immature vasculature.

Part II – PI3K in PCs during pathological angiogenesis

4.5. Investigating the role of PI3K in PCs during tumoral angiogenesis

PCs are a ubiquitous part of the tumour microenvironment and have been proven to be multifaceted cells with an ability to significantly influence tumour development thus, different therapies have been developed to target these cells. However, whereas targeting ECs or fibroblasts might represent a therapeutic advantage, targeting PCs has shown different therapeutic effects, depending on the type of tumour (Armulik et al., 2011; Meng et al., 2015).

Our data suggested a key role of p110 β in the regulation of PCs proliferation and since PI3K pathway is implicated in the regulation and progression of different types of tumours, we sought to investigate the therapeutic benefit of inhibiting the p110 β isoform in the RIP1-Tag2 mouse model.

4.5.1. p110 β impacts on tumour PCs and impairs tumour progression

To study the impact of p110 β inactivation, the RIP1-Tag2 mice were treated daily by oral gavage, starting at 12 weeks of age until 16 weeks of age with KIN-193 (p110 β inhibitor) or vehicle. The RIP1-Tag2 is a transgenic mouse model of pancreatic neuroendocrine tumours (PNETs) that synchronously progress from incipient neoplasia to invasive carcinoma. The tumours develop spontaneously from the β -cells of the pancreatic islets of Langerhans as a result of expression of the SV40 large and small T-antigen under the control of the insulin promoter (Bill et al., 2015; Soler et al., 2015).

The treatment with KIN-193 in the tumour-bearing RIP1-Tag2 mice leads to a slight decrease in the overall survival of the animals (**Figure 4.48A-B**). However, p110 β inactivation also prevents tumour burden (**Figure 4.48D**), but

not tumour number (**Figure 4.48C**), when compared to the vehicle-treated animals. Moreover, *in vivo* treatment with KIN-193 led to a decrease of red-tumours and pink and white tumours were also detected when compared to the controls. The WT or vehicle-treated tumours of the RIP1-Tag2 mice only present red-coloured tumours thus, the decreased number of red-coloured tumours in the KIN-193 treated mice suggests an impact on the tumour vascularisation in these animals (**Figure 4.48E**). Thereby, we assessed the tumour vasculature upon KIN-193 treatment using the CD31 marker for vessels and the desmin to mark the PCs. We have seen that treated tumours showed no differences in the vessels number, but a significant reduction in the PCs number (**Figure 4.49**).

4.5.2. p110 β inhibition does not affect the metastatic potential

Although inactivation of p110 β using the KIN-193 inhibitor has an impact on the tumour burden and vascularisation affecting essentially PCs, a slight decrease in the overall survival of the treated animal has been observed. Therefore, we hypothesized that p110 β inactivation using the KIN-193 inhibitor leads to an enhanced metastatic potential and thus, affects the overall survival of the animals. However, we have not seen increased metastasis in both, lymph nodes or liver (**Figure 4.50**). This data leads us to speculate that other mechanisms could affect the overall survival of the animals and further studies need to be done.

4. Results

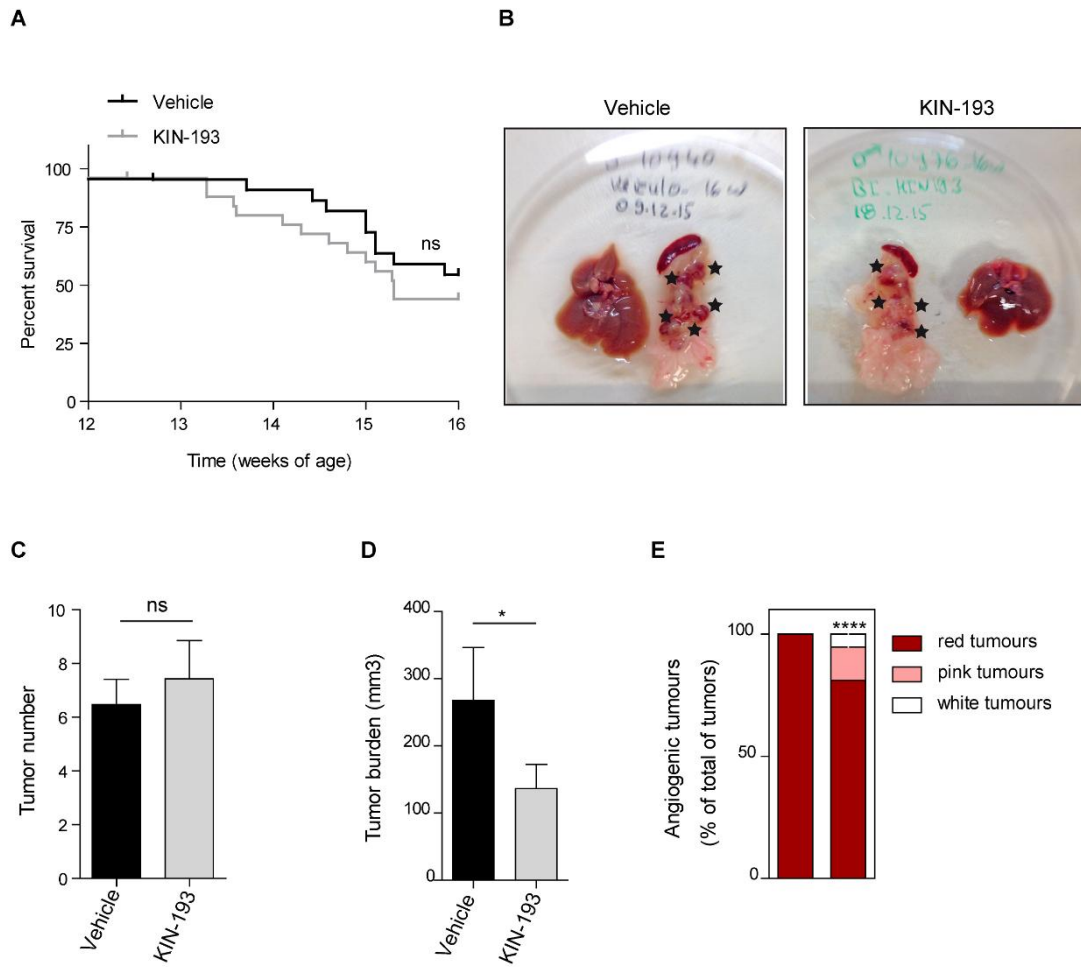


Figure 4.48. Pharmacological inhibition of p110 β -Class I PI3K in RIP1-Tag2 leads to a slight reduction of overall survival but impairs tumour progression. RIP1-Tag2 mice (12 weeks) treated daily with vehicle (n=21) or KIN-193 (10 mg/kg, n =27) for 4 weeks. **A)** Kaplan–Meier survival curve of the 4 weeks treatment. Statistical analysis was made with Log Rank test. **B)** Gross pathology images of excised pancreas and liver. Black arrow heads indicate the tumours. **C)** Total number of tumours. **D)** Total tumour burden analysis. **E)** Quantification of the percentage of "red, pink and white" tumours per mouse. Error bars are standard error of the mean. *P <0.05 and ****p < 0.0001 was considered statistically significant. Statistical analysis was performed by Mann-Whitney test.

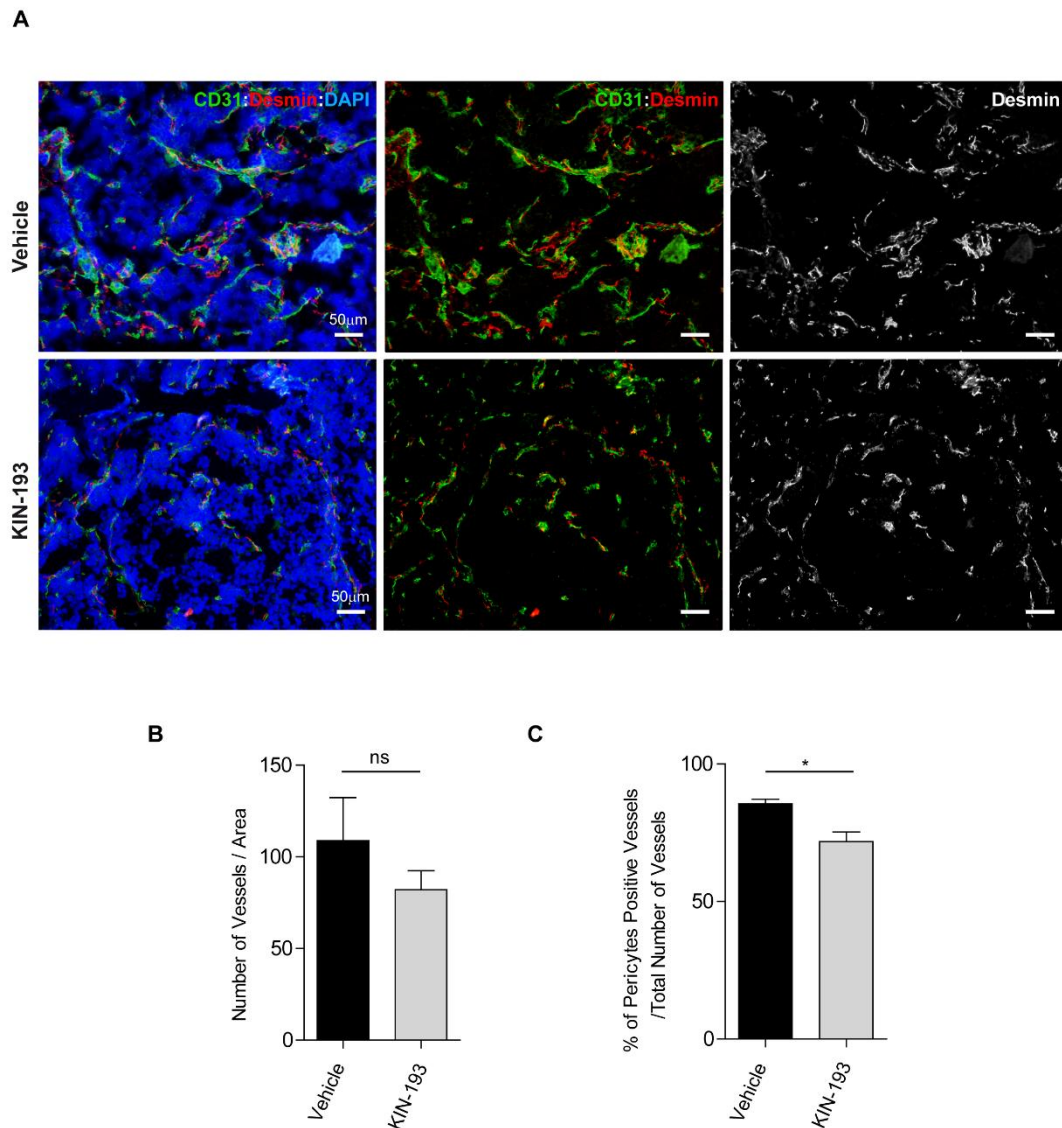


Figure 4.49. Pharmacological inhibition of p110 β -Class I PI3K in RIP1-Tag2 leads to PC depletion. RIP1-Tag2 mice treated daily with vehicle or KIN-193 for 4 weeks. **A)** Representative images of immunostaining for CD31 (green), Desmin (red) and DAPI (blue), of tumor sections. **B)** Quantification of number of vessels (CD31) per tumour area. **C)** Quantification of the percentage of vessels covered with PCs per total number of vessels. Error bars are standard error of the mean. *P < 0.05 was considered statistically significant. Statistical analysis was performed by Mann-Whitney test.

4. Results

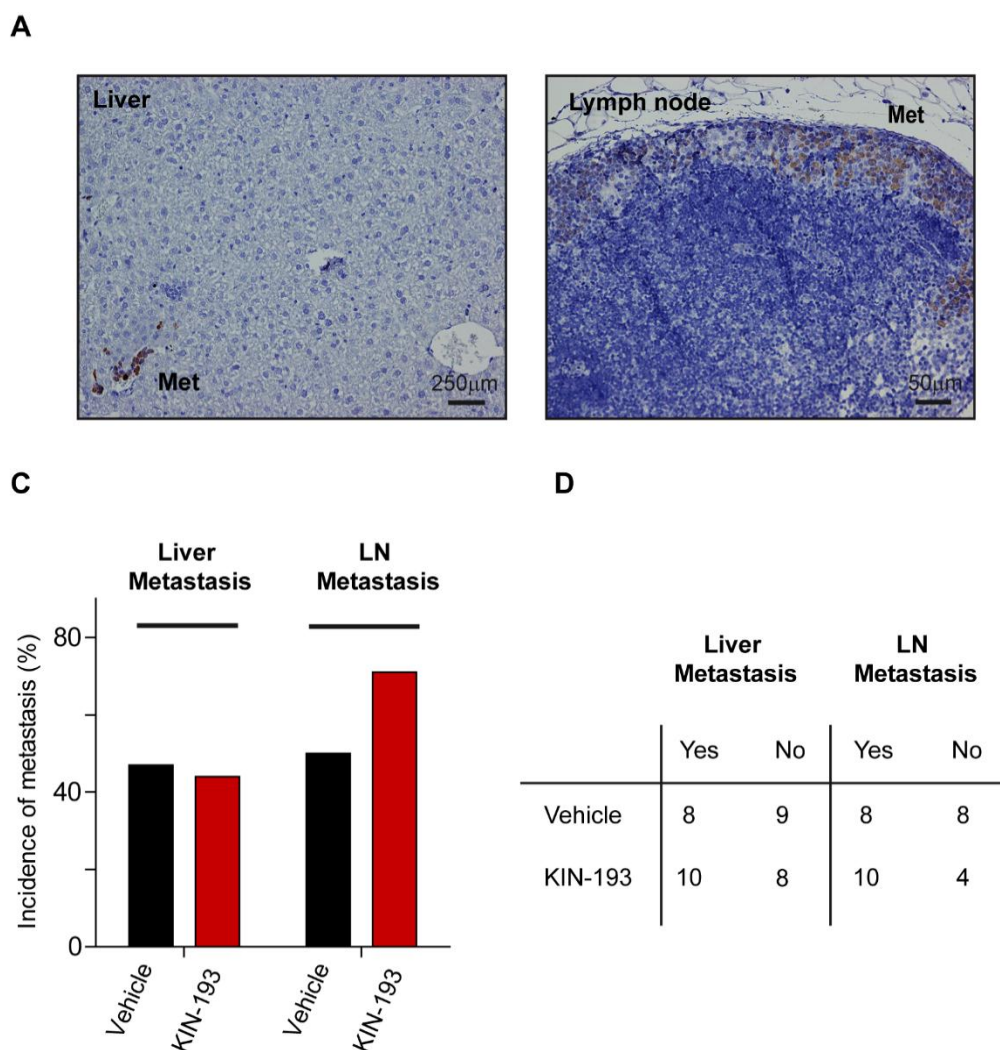


Figure 4.50. Pharmacological inhibition of p110 β -Class I PI3K in RIP1-Tag2 does not affect metastasis. RIP1-Tag2 mice treated daily with vehicle or KIN-193 for 4 weeks. (A) Histologic analysis of liver and lymph node metastasis (Met) in RIP1-Tag2 mice treated with vehicle or KIN-193 for 4 weeks starting at 12 weeks of age. Paraffin-embedded sections were immunohistochemical stained for the tumor marker SV40 T antigen (brown). (B) Quantification of the incidence of animals with microscopic liver micrometastasis and microscopic lymph node metastasis in the control (black bars) and KIN-193–treated (red bars) treatment arms. (C) Contingency table relating the number of animals in each treatment/metastasis case. KIN-193–treated mice did not show differences in the incidence of liver or lymph node metastasis. Error bars are standard error of the mean. Statistical analysis was performed by the χ^2 test.

5. Discussion

PCs are specialized MCs located at the abluminal surface of capillary blood vessels, which control the vascular development and stabilization (Armulik, 2005). They are intimately associated with the ECs, by sharing the same BM, and communicating with them via physical contact or by paracrine signalling (Caporali et al., 2016). These interactions are important for vessel formation, maturation, remodelling and maintenance (Gerhardt and Betsholtz, 2003). During the angiogenesis, activated PCs in the parental vessels swell, shorten their processes and project into the perivascular spaces. Thereafter, the BM is disrupted resulting in PC detachment from the vessel wall allowing ECs proliferation (Gutiérrez R. and Varela H, 1992a). The growing new vessel needs to be covered by PCs to be stabilized and preventing to be degraded. Therefore, PCs are recruited again to the microvessels, suppressing ECs growth and promoting their stabilization (Armulik et al., 2011; Ribatti et al., 2011).

In many pathologies, blocking angiogenesis would be beneficial (e.g. cancer, retinopathies and rheumatoid arthritis) whereas in others, the promotion of angiogenesis represents an advantage (e.g. myocardial infarction, stroke and hypertension). PCs have recently emerged as a therapeutic target to promote or inhibit angiogenesis thus, the basic understanding of PCs biology is fundamental to develop PC-related therapies (Stapor et al., 2014).

5.1. PCs differentiate during the retinal development

Although, the role of ECs during sprouting angiogenesis is well characterised (Hughes and Chan-Ling, 2004), the physiology and differentiation of PCs in this process is not fully understood. The retina is an ideal system to study PC development in the microcirculation, since it is possible to observe

several stages of PC differentiation from the more mature central retina, into the immature distal vascular plexus (Hughes and Chan-Ling, 2004).

We have investigated different aspects of PC biology in the growing vasculature of mouse retinas. A number of important observations were noticed: (1) PCs are closely associated with the ECs at very early time points of vessel development (P3); (2) PCs start to proliferate earlier than ECs and both cells become quiescent during the vascular remodelling; (3) PC coverage becomes more widespread during vessel maturation; (4) PC morphology changes through different stages in the retinal development.

In agreement with our findings, other authors showed that PCs are in close association with the ECs at the sprouting front in rat mesentery (Nehls et al., 1992) and in pancreatic tumours (Morikawa et al., 2002). Furthermore, Hughes *et al.* have shown PC involvement in the early vessel development (P0) of rat retinas (Hughes and Chan-Ling, 2004)

It is not fully understood whether PCs develop by division of pre-existing cells and/or by differentiation from immature mesenchymal cells (Armulik et al., 2011). Our study shows, for the first time, that PCs in the retina vasculature expands at very early time points through cell proliferation, which progressively decreased during vascular maturation. According to our findings, it has been previously shown that PCs proliferate during angiogenesis in the CNS, which is characterized by a seeming lack of immature mesenchyme (Armulik et al., 2011; Stapor et al., 2014). This suggests that new PCs could develop mainly by proliferation of the pre-existing ones. However, this observation requires further investigation and lineage tracing studies would be a good approach.

Interestingly, our results also indicate that PCs population expands first than the ECs, which suggests that PCs proliferation is required to activate ECs. In fact, PCs were shown to regulate ECs proliferation during the angiogenesis (Armulik et al., 2011; Stapor et al., 2014). It would therefore be interesting to study PCs and ECs proliferation at additional early time points of the retinal development, confirming this observation.

Dore-Duffy *et al.*, described that PCs from the CNS present a heterogeneous morphological pattern along the capillaries. The most common

5. Discussion

association between PCs and the microvessels is one in which PCs encircling the capillary, with broad and continuous projections that cover a large surface area of the microvessel. A second pattern also shows PCs wrapping around the capillary but the area is more defined and smaller and the PC projections are finger-like in shape. The third pattern was attributed to active and migrating PCs that normally are found in the early stages of angiogenesis or in pathological conditions. At this point the PCs orientation in the microvessel involves a retraction of projections. The fourth pattern shows that PCs are positioned longitudinally in a polar fashion along the microvessel, which may reflect PCs migrating along the vessel or PCs transition (Dore-Duffy and Cleary, 2011). Anatomically and developmentally, the retina is known as an extension of the CNS (London et al., 2013). Likewise, we observed that in the retina microvessels PCs also present morphological changes along the vessel development. PCs in the sprouting front of the retina have a retracted shape, with multiple protrusions connected with the endothelium, which resembles the third type of PC found in the CNS. Conversely, in the remodelling areas, PCs showed a more elongated shape with tight connections with the endothelium, similarly with the first and the second morphological pattern described.

Moreover, for vessel stabilization a BM has to be formed. There is a co-requirement of ECs and PCs to assemble and maintain the vascular BM matrix (Stratman and Davis, 2012). Collagen type IV is one of the major BM components that self-assemble to confer structural stability (Pöschl et al., 2004). We found an increase in the collagen IV deposition concomitant with vessel maturation, suggesting that its presence is associated with a more mature phenotype. Interestingly, this finding highlights the importance of PCs to both forming and stabilizing the new vasculature. It would be interesting to investigate other BM components, such as laminin, and fibronectin, which are also necessary for the correct BM assembly (Stapor et al., 2014).

Overall, our data suggests that PCs extend through different states, which contribute to the regulation of vessel development. Immature and proliferative PCs are present in areas of active sprouting angiogenesis, promoting vessel growth. These PCs are less connected with the vessels, present a retracted shape and possibly are required to activate ECs proliferation. In contrast,

mature and quiescent PCs are found in more mature vessels promoting their stabilization. These PCs are well connected with the endothelium, which promotes ECs quiescence and contributes to the collagen IV deposition. Stapor *et al.*, have also described transient PCs phenotypes during capillary sprouting in the brain, suggesting that subpopulations perform specific angiogenic functions. They found a transient expression of class III β -tubulin in brain PCs, typically associated with the earlier phases of sprouting angiogenesis (Stapor *et al.*, 2014). Therefore, it is reasonable to assume that different PCs populations can co-exist in the retina. Future studies using a PC-specific reporter line and other PC-specific markers would be useful in attempt to investigate different PCs populations in the retinal vasculature.

5.2. PCs control EC migration and proliferation *in vitro*

PCs can rapidly differentiate *in vitro* to other cell types, which make the study of PCs biology even more challenging. In the past years, different approaches have been developed to isolate and establish a pure PC culture (Boroujerdi *et al.*, 2014; Bryan and D'Amore, 2008; Tigges *et al.*, 2012). We used a protocol described by Tigges *et al.*, which allows to culture stable and pure PCs even after several passages (Tigges *et al.*, 2012).

PCs and ECs mostly communicate by paracrine signalling pathways. This crosstalk is determinant in the regulation of angiogenesis and vessel stabilization. (Caporali *et al.*, 2016). Co-cultures studies that prevented physical contact, but allowed diffusion of soluble factors, or the use of PCs conditioned mediums above the ECs, are inconclusive. There are studies where these type of co-cultures do not interfere with the ECs (Orlidge and D'Amore, 1987), whereas others claim that PCs can secrete molecules that stimulate the proliferation and migration of ECs (Watanabe *et al.*, 1997). Additionally, those studies involving PC-EC directed physical interaction have shown that PCs have an antiproliferative effect on ECs. (Orlidge and D'Amore, 1987; Sato and Rifkin, 1989)

5. Discussion

Given that our retina data suggest that PCs regulate ECs, we aimed to analyse if cultured PCs paracrine controls ECs. Using transwells co-cultures systems of PCs and ECs, avoiding the direct contact between both cell types, we found that PCs when co-culture with ECs stimulate their proliferation and slight impact in the EC migration. In agreement with the retinas, these results suggest that PCs can promote ECs activation by the secretion of different molecules, and possibly ECs quiescence by PC-EC direct contacts. Therefore, it is tempt to speculate that in retinas the active PCs at the sprouting angiogenesis possibly promote ECs proliferation by paracrine mechanisms. In contrast, PCs at the remodelling angiogenesis lead to the ECs quiescence possibly by direct contact communication.

5.3. Class IA-PI3K selectively regulates PCs biology *in vitro*

The PI3K family is important in almost all aspects of cellular biology including metabolic control, immunity, angiogenesis and cardiovascular homeostasis. Moreover, this signalling pathway is one of the most frequently deregulated pathways in cancer. Among all classes of PI3K the class IA is the best understood, being implicated in the regulation of several cell functions like migration, proliferation and survival (Vanhaesebroeck et al., 2010). Data from our laboratory have identified the p110 α /PI3K isoform as the major driver of PIP3 production in ECs during angiogenesis. Ubiquitous or EC-specific inactivation of p110 α /PI3K leads to embryonic lethality at mid-gestation due to severe defects in angiogenic sprouting and vascular remodelling (Graupera et al., 2008). Moreover, pharmacologic inactivation of p110 α *in vitro* ECs leads to cell migration defects (Soler et al., 2016). Similarly, p110 α signalling in vSMC has been shown to regulate the vascular remodelling (Vantler et al., 2015).

Therefore, we sought to validate whether p110 α is also critical to regulate PC functions. We observed that WT PCs express all class IA isoforms. The p110 α and p110 β isoforms are ubiquitously expressed, whereas p110 δ expression was found to be mainly enriched in leucocytes (Vanhaesebroeck et al., 1997). However, similarly to our data also vSMC expresses all class IA

isoforms including p110 δ (Vantler et al., 2015) and low expression levels of p110 δ were found in other cell types (Geng et al., 2004; Graupera et al., 2008; Puri et al., 2004; Sawyer et al., 2003)

Different studies have described vSMC (Caglayan et al., 2011; Dell et al., 2006; Nishishita and Lin, 2004) or even PCs (Arimura et al., 2012; Bai et al., 2015; Liu et al., 2007) autonomous functions with PI3K-AKT activation. The study of Vantler *et al.*, is the only one that goes further and implicates p110 α isoform has the single regulator of vSMC functions, such as proliferation, migration and survival, beyond PDGFR β -PDGFB signalling and in an AKT dependent mechanism (Vantler et al., 2015). During angiogenesis the ECs secrete PDGF-B, which binds with the PC-specific receptor PDGFR β causing receptor dimerization, autophosphorylation and activation. Several SH2 domain-containing proteins bind to distinct phosphorylated tyrosine residues, including PI3K, regulating PC survival, migration, apoptosis, proliferation and differentiation (Betsholtz, 2004; Sweeney et al., 2016).

We observed that pharmacological inhibition of p110 α (GDC0326), but not inhibition of p110 β (TGX221) or p110 δ (GDCD030) in cultured PCs led to reduced AKT phosphorylation. Moreover, we also found that only inactivation of p110 α , and not p110 β , impairs PCs migration and viability like occurs in vSMC (Vantler et al., 2015). However and surprisingly, in contrast to vSMCs, only p110 β inactivation leads to reduced PC proliferation. In vSMCs p110 α appears as the only regulator of vSMC functions (proliferation, migration and viability), and p110 β does not show biological implications (Vantler et al., 2015). Our data together with Vantler *et al.* suggest that different types of MCs (vSMC and PCs) show different regulation by the PI3K members. Although at the moment, these differences between PCs and vSMCs are not fully understood, it is reasonable to assume that different mediators can regulate PCs biology.

Our results suggest that in PCs p110 α isoform seems to control cell motility in an AKT dependent mechanism. Probably related with RTKs signalling activation such as PDGFB-PDGFR β , like occurs with vSMC (Vantler et al., 2015). It has also been shown that PDGF-B induced cell growth and anti-apoptotic responses through AKT in cultured brain PCs. Furthermore, PDGF-B in PCs significantly increased the expression of nerve growth factor (NGF) and

5. Discussion

neurotrophin-3 (NT-3) mediated by AKT (Arimura et al., 2012). Would be therefore interesting, to study if PDGFB stimulation in PCs affect p110 α /AKT activation, stimulating their biological responses of migration and viability.

On the other hand, p110 β isoform controls PC arrest in a mechanism that could be AKT independent. However, AKT-dependent mechanisms cannot be excluded at the moment based on two observations: First, the detection of p-AKT by WB was made after 2h of incubation with the p110 β inhibitor. On the other hand, in the proliferation experiments we have used 24 hours of incubation. Thus, possibly to inactivate p110 β in PCs a large exposure to its specific-inhibitor is required. Another explanation is that the AKT studies were made in basal conditions and perhaps to trigger p110 β response there is a need of a stimulus.

Although it is not clear, which upstream signal regulates p110 β in PCs, different signalling pathways could be involved stimulating both, AKT - dependent and -independent functions. In line with this, it is well-known that the noncanonical TGF β signalling can activate PI3K-AKT, inducing epithelial-mesenchymal transition (Chaudhury and Howe, 2009). Moreover, PI3K- TGF β signalling have been implicated in the proliferation and differentiation of brain PCs (Sweeney et al., 2016). Other mediators such as, insulin and the epidermal growth factor could also activate p110 β signalling in PCs. In fibroblasts these growth factors promote cell proliferation in a p110 β AKT-independent mechanism (Jia et al., 2008b).

Different studies have point p110 α as the major PI3K isoform of RTKs signalling, with a minimal contribution of p110 β (Foukas et al., 2006; Knight et al., 2006). It has also been shown that PDGFB -PDGFR β signalling is not involved in p110 β biological functions in different cell types (Hooshmand-Rad et al., 2000; Park et al., 2003; Roche et al., 1998). Likewise, in vSMC activation of p110 β isoform is dependent of GPCRs signals resulting in AKT activation (Vantler et al., 2015). These observations, indicate that p110 β in PCs could act downstream of GPCRs. Actually, in different cell types it has been shown that p110 β -AKT are activated downstream of GPCRs (Graneß et al., 1998; Guillermet-Guibert et al., 2008a; Kubo et al., 2005; Kurosu et al., 1997; Maier et al., 1999; Roche et al., 1998). Further studies using a broader range of ligands

will be essential to determine the molecular mechanism beyond p110 β responses in PCs.

5.4. Class IA-PI3K selectively regulates PCs biology during sprouting angiogenesis

PCs are ideally located at the interface between the endothelium and the surrounding tissue playing an active role during the angiogenesis. Several PCs functions relevant for angiogenesis have been proposed: (1) PCs detect the physiological needs of the tissue and the presence of angiogenic stimuli, (2) sense the hemodynamic forces within the vessel, (3) deposit or degrade extracellular matrix, (4) control by paracrine mechanisms and by contact-dependent signals the EC proliferation and differentiation, and (5) are able to contact many ECs at the same time allowing the integration of the signals along the vessel length (Trost et al., 2016). PI3Ks are key regulators during the angiogenesis process, responding to several environmental signals to regulate many cellular processes that are central to vascular growth and maintenance (Graupera and Potente, 2013).

There are no available good antibodies to detect the PI3K isoforms or even AKT by immunofluorescence thus, the pS6 staining is often used as a readout of PI3K activity (Hutchinson et al., 2011; Roux et al., 2007). Our results revealed that pS6 levels are stronger in the areas of active sprouting angiogenesis when compared with the more mature plexus, where the levels of pS6 are almost undetectable.

Therefore, our next aim was to study the role of PI3K signalling in PCs biology during the sprouting angiogenesis. Namely, the p110 α and the p110 β isoforms, since both are controlling PCs functions *in vitro*. To selectively inactivate p110 α and p110 β isoforms in retinal PCs we have used a tamoxifen-inducible Pdgfr β (BAC)-CreERT2 transgenic mouse line (Chen et al., 2016b). We have crossed this line with the transgenic mice p110 α ^{D933A/flox} and p110 β ^{D931A/flox} to selectively inactivate p110 α (p110 α ^{D933A/i Δ PC}) and p110 β (p110 β ^{D931A/i Δ PC}) in PCs, respectively. In the p110 α ^{D933A/i Δ PC} and p110 β ^{D931A/i Δ PC}

5. Discussion

mice one allele allows the selective inactivation of the isoforms in PCs upon 4-OH administration, but the other allele presented a constitutive inactivating mutation (p110 α ^{D933A} and p110 β ^{D931A}). Consequently, half of the protein is expressed but inactive. This strategy has shown to be efficient in maintaining the stoichiometry of the protein (Foukas et al., 2006; Graupera et al., 2008) and possibly avoids the compensatory effects of other PI3K isoforms (Utermark et al., 2012).

The phosphorylation of S6 is associated with the activation of PI3K/AKT/mTOR signalling pathway. However, this is not the only signalling that PI3K can activate. Therefore, we have characterized the p110 α ^{D933A/i Δ PC} and p110 β ^{D931A/i Δ PC} mutants in both areas, the sprouting area where the active angiogenesis is taking place and the more mature plexus that undergoes in stabilization and maturation. For that we have used the P6 retinas that are an intermediate point of the retinal development, allowing to study in the same preparation both processes, the sprouting and remodelling.

Although, our *in vitro* results revealed that p110 α in PCs controls cell motility and viability, somewhat unexpectedly, our retina data show that the genetic inactivation of p110 α (p110 α ^{D933A/i Δ PC}) does not regulate PC coverage, morphology or proliferation. On the other hand, p110 β inactivation (p110 β ^{D931A/i Δ PC}) results into reduced PC coverage in the angiogenic front and also a slight reduction in the remodelling plexus, when used the NG2 marker. Moreover, our results show that PCs coverage was not affected with the p110 β full inactivation specifically in PCs (p110 β ^{i Δ PC}) or in the constitutive inactivation (p110 β ^{D931A}) when compared with the control (p110 β ^{flox/flox}). These results further demonstrate the efficiency of our strategy, which avoids the possible compensation problems inherent to the p110 β full deletion, as explained previously. Furthermore, and in agreement with our *in vitro* data, we found that p110 β inactivation is not only affecting the coverage but also the proliferation of the PCs in both areas of the plexus. Together these data suggest that the coverage of the new plexus is mainly achieved by expanding the PC through proliferation and not by migration of PC from other locations. Furthermore, our data also highlight that opposed to what has been described in ECs and vSMC

(where PI3K signalling is mainly driven by p110 α), p110 β isoform is the key regulator of PCs biology in the vascular development of the retina.

Unexpectedly, our data show that the PCs coverage assessed by the cytoskeleton marker desmin is not altered in p110 β mutants retinas compared to the control. This finding is surprising, given that NG2 staining revealed reduced PC coverage and also the PCs proliferation arrest suggests a smaller number of PCs. Although it is not clear at the moment, the differences between NG2 and desmin, it is tempting to speculate that the *PDGFR β* promoter is in the retinas not homogenous and only targets specific PC sub-population. This observation would imply that different types of PCs populations could co-exist in the retina vasculature. In this particular case the existence of NG2+/Desmin- PCs populations. In fact, this concept is not new and Kurz *et al.*, have also described that several types of PCs may co-exist in the same vascular bed. They found that desmin and α SMA markers are not mutually exclusive in most of the PCs in the chicken chorioallantoic membrane (Kurz *et al.*, 2008). Therefore, future studies using the Pdgfr β (BAC)-CreERT2 transgenic mice in a WT background could help to better understand the possible existence of sub-populations of PCs in the retina vasculature. This strategy would allow to investigate if the recombined PCs are always Desmin+/NG2+, or other PCs population could also co-exist.

The differences seen with the two PCs markers could also be explained by the fact that NG2 mediates signalling through PI3K. NG2 has been shown to promote PCs recruitment during angiogenesis (Cattaruzza *et al.*, 2013; Huang *et al.*, 2010). Moreover, in the NG2 knock-out retina PCs proliferation is compromised (Ozerdem and Stallcup, 2004). These observations lead us to speculate that p110 β inactivation in PCs could affect NG2 functions inducing PC proliferation arrest.

Additionally, it was described by Hughes and Chan-Ling., that PC maturation is characterized by the gradual restriction of NG2 expression, and not desmin, to the albuminal cell bodies. In the normal development of the retina at P15 the desmin filaments from PCs start to be distinguished by NG2 positive cell bodies. In adult retina, NG2 labelling became further restricted to the soma, resulting in the adult-PC phenotype (Hughes and Chan-Ling, 2004).

5. Discussion

Our differences between the NG2 and desmin markers could be therefore associated with a different maturation status of the PC in the p110 β ^{D931A/ Δ PC} retinas. The p110 β inactivation in this perspective result in a more mature PC with the NG2 marker differently expressed to Desmin one. Actually, we also observed morphological changes in the PCs of p110 β ^{D931A/ Δ PC} mice. These PCs are more elongated and thinner when compared with the control, which resembled the more mature PC described previously in the WT retinas. We previously described that PCs during vessel maturation change their morphology. Our results showed that in WT retinas a retracted PC and less connected with the vessel is correlated with higher ratios of PCs proliferation whereas, a more elongated shape and more connection with the vessel wall leads to vascular stability and cell quiescence. These observations, suggest that p110 β isoform is not only important for PCs proliferation but also regulates PCs morphology promoting an active PC status.

In summary, our data show, that p110 β is the major regulator of PCs biology during the sprouting angiogenesis and its inactivation results into PC coverage defects, cell proliferation arrest and morphological changes, which resemble a more mature PC.

5.5. Inactivation of PI3K in PCs lead to severe vascular defects

Our results suggest that p110 β isoform is the major regulator of PCs functions during the sprouting angiogenesis. Interestingly, we observed that p110 β inactivation in PCs is not only affecting these cells autonomously but also impacts on the ECs, suggesting that PI3K regulates PCs and ECs cross-talk.

It is well-known that during angiogenesis PC and EC communication it is fundamental for the correct vascular development (Gerhardt and Betsholtz, 2003). However, the majority of the *in vivo* studies came from ECs autonomous effects that subsequently affect the PCs population (Bjarnegård et al., 2004; Caporali et al., 2016; Lindblom et al., 2003; Liu et al., 2000). Up to date, there are not many *in vivo* studies showing that PCs defects impact on the ECs population. The study of Liu *et al.*, also correlate MCs autonomous defects

with a compromised vasculature. They show that Notch3^{-/-} mutant mice (Notch3 is MC-specific) present defects in the investment of MCs which results in an abnormal vascular development in the retina (Liu et al., 2010).

Unexpectedly, we have found that reduced PCs coverage and proliferation leads to ECs hypoplasia and ECs proliferation arrest. Our results show that p110 β inactivation in PCs (p110 β ^{D931A/ Δ PC}) results in a reduced number of branching points and less EC proliferation in both, the sprouting front and the remodelling plexus of the retina. Additionally, we found that these differences are not related with increased cell death, since the cleaved caspase 3 staining in the p110 β ^{D931A/ Δ PC} mice do not show any difference when compared with the control. We also detected delayed in the expansion of the plexus in the p110 β ^{D931A/ Δ PC} mice, which is not related with defects in the cells at the very sprouting front of the retina since the sprouts and filopodia are not affected.

This observation is somewhat at odds with previous reports where the absence of PCs is accompanied by EC hyperplasia *in vivo* (Armulik et al., 2010; Daneman et al., 2010; Hellström et al., 2001b; Kofler et al., 2015; Uemura et al., 2002). Although not clear at the moment, these differences can be in part explained because PI3K is mediating NG2 functions in PCs. In fact, Ozerdem *et al.*, also described that NG2 knock-out retinas under hypoxic conditions result in PCs and ECs proliferation arrest (Ozerdem and Stallcup, 2004). Moreover, these divergences could be also related with the maturation status of PCs. Our results suggests that p110 β inactivation results in a more mature PC, which is characterized by a less proliferative – quiescent cell, that is well connected with the endothelium. As described previously, the NG2 staining during the maturation gradually becomes more restricted to the PC body, which reflects a more mature PC. Moreover, in these PCs the desmin filaments are distinguished from the more restricted NG2 expression (Hughes and Chan-Ling, 2004). These observations suggest that the differences detected in PC coverage with the NG2 marker are not related with less recruitment of PCs but rather implicated with the status of PC maturation. Thereafter, it is reasonable to speculate that more mature PCs result into more mature vasculature, which is characterized, like we observed, by ECs

5. Discussion

quiescence. Furthermore, we have also detected an increase in collagen IV deposition in the $p110\beta^{D931A/i\Delta PC}$ mice. The BM matrix production by both cells, PCs and ECs is a fundamental requirement for vessel maturation and stabilization (Stratman and Davis, 2012). These observations further demonstrated that $p110\beta$ inactivation on PCs could thus promote a more mature plexus.

Our results show that PI3K controls PCs biology not only in an autocrine fashion way, but also, is involved in their paracrine communication with the ECs. Thus, it would be interesting to find the molecular mechanism that is mediating PI3K signalling in PCs and in their cross-talk with the ECs. Our observations led us to speculate that PI3K signalling could mediate NG2 functions. As described previously, NG2 is involved into PC recruitment and PC-EC interactions. Additionally, NG2 knock-out retinas resemble our $p110\beta^{D931A/i\Delta PC}$ retinas and present PC and EC proliferation arrest, which results in hypovascularization.

Moreover, although PI3K signalling in vSMC is activated downstream of PDGFB-PDGFR β signalling our *in vitro* data suggest that in PCs other mechanism(s) is/are involved. Our $p110\beta^{D931A/i\Delta PC}$ retinas came to re-inforce this idea and also suggest that $p110\beta$ in PCs is not mediating signalling through PDGFB-PDGFR β . PDGFB-PDGFR β signalling defects in the retina vasculature are not similar to what we observed upon $p110\beta$ inactivation. In general impaired PDGFB-PDGFR β signalling results in PC recruitment failure and reduce PC coverage, which results into vascular hyperplasia, atypical vascular morphogenesis and formation of microaneurysms (Abramsson et al., 2007; Betsholtz, 2004; Hellström et al., 2001b; Lindahl et al., 1997; Lindblom et al., 2003; Trost et al., 2016). Using an anti-PDGFR β antibody Ogura *et al.*, also mimicked several aspects of diabetic retinopathy such as the inhibition of PC recruitment to the vessels, leading to vessel hyperpermeability, hyperperfusion and neoangiogenesis. These vessels formed aneurism-like structures with actively proliferating ECs (Ogura et al., 2017). Therefore, as suggested previously other pathways could be involved in $p110\beta$ -PI3K signalling in the PCs and in their cross-talk with the ECs.

Although, $p110\alpha^{D933A/i\Delta PC}$ mice did not reveal any alterations on PCs when compared with the control, we have seen that the vasculature is affected. We found that inactivation of $p110\alpha$ in PCs results, as $p110\beta$, in delayed expansion

of the retinal plexus, without affecting the sprouts and filopodia. Moreover, we observed that p110 α inactivation is not affecting the vascular density or EC proliferation in the sprouting front of the retinas. To confirm that the expansion defects were PC dependent we also analysed the p110 α ^{D933A} (full constitutive inactivation) and the p110 α ^{i Δ PC} (full deletion of p110 α specific in PCs) mice and we did not detect any difference when compared with the control (p110 α ^{flox/flox}).

PCs have been implicated as active mediators of ECs remodelling by an endosialin (CD248) receptor dependent mechanism. The endosialin receptor is expressed by PCs associated with newly forming but not stable quiescent vessels. The endosialin^{-/-} mice do not present defects in PC coverage and have normal vascular sprouting however, results in a vessel regression defects that lead to increased vessel density (Simonavicius et al., 2012). This led us to speculate that in the p110 α ^{D933A/i Δ PC} mice a similar process could be occurring. However, analyses of the vasculature in the remodelling plexus area of p110 α ^{D933A/i Δ PC} retina did not show any defects. The vasculature seems normal and no differences in the number of branches or in EC proliferation were detected. The defect in the radial expansion, often used as readout of EC migration could be due to the PC migration. We have seen that *in vitro* inactivation of p110 α impacts on PC migration, which additionally could interfere with the endothelium. Moreover, the radial expansion defects were recovered and P9 retinas did not show any difference comparing with the control what makes the p110 α isoform not crucial for PCs functions during sprouting angiogenesis. The p110 β inactivation also results in radial expansion defects suggesting that the expansion defects are not isoform-specific but rather a common aspect of PI3K inactivation in PCs.

Summing up, surprisingly we have found that p110 β isoform, and not p110 α , is the key regulator of PC biology during the sprouting angiogenesis and its inactivation leads to PC arrest and to a more mature PC morphology. This PC defects also impacts in the endothelium leading to a more quiescent plexus promoting EC proliferation arrest and BM components deposition. It is therefore, reasonable to assume that p110 β -PI3K in PCs is essential for active and immature angiogenesis promoting cell proliferation.

5. Discussion

5.6. PTEN opposes PI3K signalling in PCs during the sprouting angiogenesis

The PTEN is a dual lipid/protein phosphatase often underexpressed in cancer (Hopkins et al., 2014; Leslie et al., 2009; Song et al., 2012), whose the main activity is to dephosphorylate PtdIns(3,4,5)P3 at the 3'-position counterbalancing PI3K signalling. Recent studies have shown that p110 β , but not p110 α , has essential roles in tumorigenesis in PTEN-null mouse models and cell lines (Jia et al., 2008b; Wee et al., 2008). Therefore, we hypothesized that PTEN could also control p110 β functions in PCs during the sprouting angiogenesis. To study the PTEN signalling in PCs we have crossed the tamoxifen-inducible Pdgfr β (BAC)-CreERT2 transgenic mouse line (Chen et al., 2016b) with a PTEN^{flox/flox} mice (Suzuki et al., 2001), which leads upon 4-OH tamoxifen injection to the deletion of PTEN specifically in PCs (PTEN^{i Δ PC}).

Our preliminary results show, so far, that PTEN inactivation on PCs results in increased PC coverage (NG2 staining) in the angiogenic front of the retinas. Interestingly, these defects are amplified during the maturation. This observation goes in accordance with data from our laboratory describing that PTEN turnover is low and its EC-specific inactivation leads to dramatic vascular defects that are maintained and increased over time (Serra et al., 2015). The remodelling area of the P6 -PTEN^{i Δ PC} retinas showed less PC coverage than controls however in P9 retinas these differences were no longer detected. This observation suggests that PTEN inactivation in PCs is affecting more the PCs located in the active sprouting area than the PCs located into remodelling zones. Additionally, PTEN inactivation leads to changes in the PC morphology, which result in a more retracted shape, with more protrusions and less connection with the endothelium. These changes resemble a more immature PC. It thus reasonable to speculate that PTEN inactivation in PCs oppose to p110 β inactivation, since in the latter we observed less PC coverage and a more mature PC morphology.

Moreover, like with p110 β inactivation, also PTEN loss of function in PCs results in severe vascular defects, which are also maintained and increased overtime. Analyses of P9 retinas revealed more vascular density in the

sprouting angiogenesis, reflected by a significant increase in the number of branching points. Furthermore, the remodelling plexus was not affected. Inactivation of PTEN on PCs also leads to less expansion of the vascular plexus.

These preliminary results further suggest that PTEN opposes to the p110 β inactivation on PCs cells, promoting a more immature plexus. In fact, it was described that under normal growth conditions, the activity of p110 β is antagonized by PTEN, which controls the levels of PIP₃. However, in conditions where PTEN expression or activity is lost, the activity of p110 β is no longer countered by the phosphatase activity of PTEN, leading to high levels of PIP³ and downstream signalling (Dbouk and Backer, 2010). Additionally, PTEN has been shown to function downstream of anti-migratory GPCRs (Dbouk and Backer, 2010; Sanchez et al., 2005). This suggests that PTEN might also be acting as a negative regulator of p110 β activation downstream of GPCRs, regulating PC proliferation.

Notch signalling has also been also implicated by different studies in the regulation of PCs and in the PCs and ECs interaction. Mice deficient for Notch3 display reduced arterial vSMC coverage and impaired vSMC maturation (Domenga et al., 2004; Henshall et al., 2015; Liu et al., 2010). Also in zebrafish, Notch3 has been implicated in assuring PC coverage and vessel integrity (Wang et al., 2014). *In vitro* studies have shown that Notch signalling promotes PC survival and adhesion to ECs (Arboleda-Velasquez et al., 2014; Schulz et al., 2015). Moreover, in *Notch1*^{+/-}; *Notch3*^{-/-} mice, a combined deficiency of Notch1 (EC specific) and Notch3 (PC specific) model, was observed altered PC interaction with the endothelium and reduced PC coverage of the retinal vasculature. These defects additionally result into vascular hyperplasia, and failure in the vascular BM formation (Kofler et al., 2015). Data from our laboratory has also shown that EC deletion of PTEN results in vascular hyperplasia due to a failure to mediate Notch-induced proliferation arrest (Serra et al., 2015). These findings led us to speculate that PTEN can be involved with Notch3 signalling. Therefore, PTEN inactivation in PCs could possibly impair Notch3 normal functions of PC arrest and maturation, leading to a more immature vasculature. Actually, there are

5. Discussion

several lines of evidence that point to a link between the Notch and PI3K pathways and their regulation by PTEN (Bailis and Pear, 2012).

Taken together, our data suggest that PTEN in PCs seems to counterbalance the effect of p110 β -PI3K promoting a more quiescent and more mature PC. It is reasonable to speculate that PI3K activation in PCs is essential for the early processes of angiogenesis, promoting a more immature PC and vasculature, whereas PTEN activity is increased later, leading to a more quiescent PC and vessel maturation and stability.

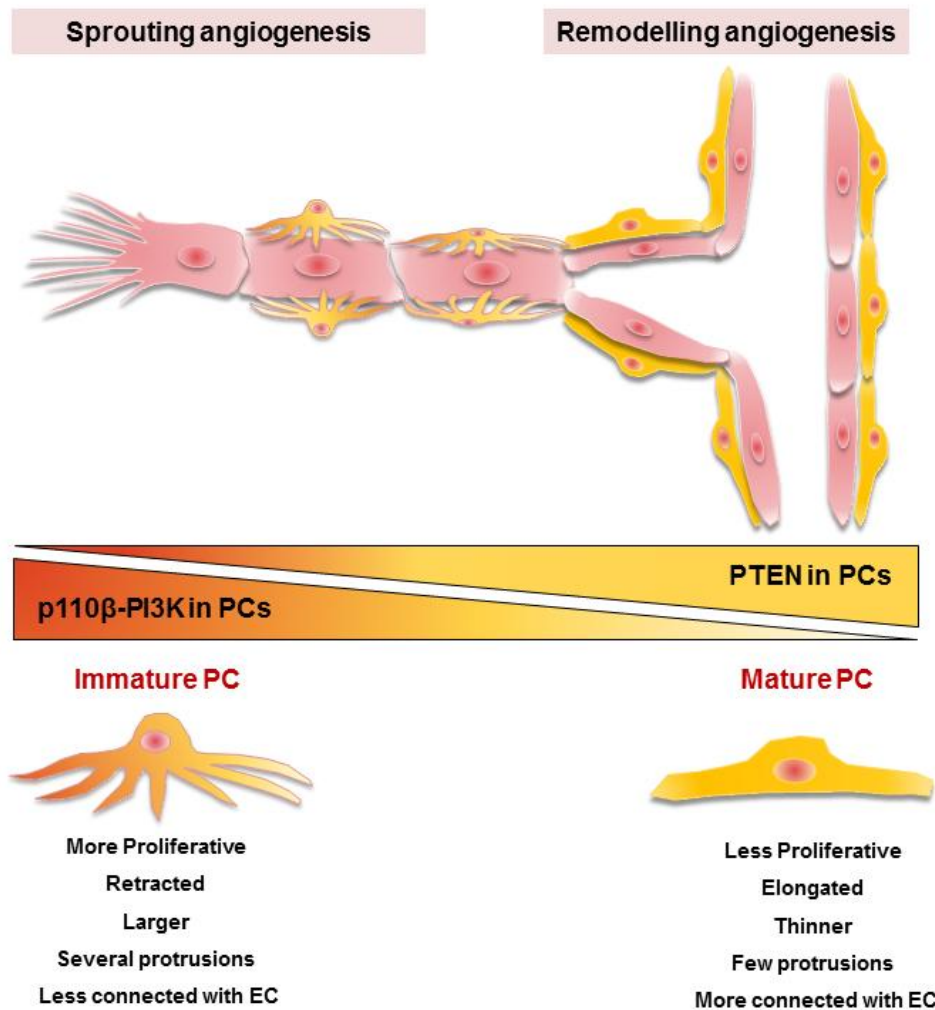


Figure 5.1. Schematic model of PI3K and PTEN regulation of PCs during sprouting angiogenesis. Our study suggests that PI3K activity is essential to regulate PC biology during sprouting angiogenesis. PI3K activation in PCs leads to a more immature PC state, which is more proliferative, retracted, larger, with several protrusions and less connected with the endothelium. This PC state also affects the vasculature, promoting ECs proliferation and vessel growth. In contrast, PTEN possibly is more essential during the

remodelling angiogenesis. PTEN activation leads to a more mature PC, which is less proliferative, thinner, elongated and more connected with the endothelium. This mature PC promotes ECs quiescence and vessel stabilization.

5.7. p110 β impacts on tumour PCs and impairs tumour progression

Highly metastatic tumours have reduced PC coverage and targeting these cells have shown to reduce tumour volume but enhanced metastasis. On the other hand, in tumours with high coverage, PC-targeting therapies has proved to be efficient since it facilitates the access of immune system cells and other therapeutic agents (Bergers and Hanahan, 2008). PI3K pathway is frequently overexpressed in human cancer as a consequence of multiple molecular alterations. Moreover, this pathway is not only important for tumoural cells but is also required for stromal cells functions such as, angiogenesis and recruitment of inflammatory cells (Fruman and Rommel, 2014; Hirsch et al., 2014b; Murillo et al., 2014; Soler et al., 2013, 2015). Several strategies aimed to interfere with the PI3K cascade are currently being tested in clinical trials including isoform-selective PI3K inhibitors (Fruman and Rommel, 2014; Soler et al., 2015). However, it is not clear how PI3K pathway inhibition affect the tumour stroma, including the vasculature (Soler et al., 2015).

Therefore, we sought to investigate the therapeutic benefit of inhibiting the p110 β isoform in the RIP1-Tag2 mouse model. The RIP1-Tag2 is a transgenic mouse model of pancreatic neuroendocrine tumours (PNETs) that is frequently used to study several aspects of tumour angiogenesis once it develops spontaneously and synchronously tumours progressing from incipient neoplasia to invasive carcinomas (Bill et al., 2015; Soler et al., 2015). Moreover, in RIP1-Tag2 model all class IA PI3K isoforms are expressed and the PI3K/AKT/mTOR signalling pathway was found to be gradually activated across the disease progressions. Treatment with a pan-PI3K inhibitor results in reduced tumour growth with no impact in tumour vessels. However, the selective inactivation of p110 α proved to be more efficient showing reduced tumour growth, reduced vascular area and also impacts on the tumour metastatic potential (Soler et al., 2016).

5. Discussion

Since p110 β -PI3K controls PC proliferation, it suggests that the use of p110 β inhibitors in cancer may promote metastasis. We sought to investigate where this pathway could also be involved in PCs biology during tumour angiogenesis, controlling tumour dissemination and metastasis. Using pharmacological inhibition of p110 β (KIN-193) in a PanNETs mouse model (RIP1-Tag2), we detected that inactivation of p110 β impacts on tumour progression comprising PCs growth and reduced vasculature. However, we have seen a slight reduction in the overall survival that could be associated with increased metastatic potential. Different studies have shown that targeting PCs results in decreased tumour volume but enhanced metastasis (Cooke et al., 2012; Meng et al., 2015). However, we did not find more metastasis in the treated animals with p110 β inhibitor. These effects could be explained by the fact that KIN-193 could not only affect p110 β isoform but also p110 δ (Ni et al., 2012), interfering with other cell types, such immune cells or even with PCs. We have seen that like vSMC (Vantler et al., 2015) PCs do express p110 δ . Despite the inconclusive results, p110 β inactivation appears to affect PCs in tumour cells and also impacts in the tumour volume. It would be interesting to analyse p110 β inactivation in a more metastatic tumour model, where the vessels are less covered with PCs, which is usually associated with cancer dissemination (Meng et al., 2015).

5.8. Concluding remarks

PCs are known to play a major role in angiogenesis, participating in vessel formation, remodelling and stabilization. Although, the role of ECs during sprouting angiogenesis is well characterised, the physiology and differentiation of PCs in this process is not fully understood. I have followed for the first time the PCs maturation during the retinal vascular development. I have found that transient phenotypes of PCs exist during vessel maturation. Immature and proliferative PCs are present in areas of active sprouting angiogenesis, promoting vessel growth. In contrast, mature and quiescent PCs are found in more mature vessels promoting their stabilization.

Several signalling pathways and factors have been reported to be important for the intercellular communication between ECs and PCs, providing suitable molecular targets for pharmacological interventions. One of the major pathways leading to cellular proliferation, migration, and survival is relayed by PI3K. The class IA is the best understood and appears to be the central class in the control of angiogenesis. The p110 α appears as the sole class I PI3K member that is absolutely required for vessel development and remodelling, being implicated in ECs and vSMCs functions. However, the role of class IA - PI3K isoforms in PCs during angiogenesis was never explored. I have accessed for the first time the impact that different PI3K isoforms, namely p110 α and p110 β , have in PCs biology and how they interfere with the endothelium during the vascular development. Overall, I have found that surprisingly it is p110 β , and not p110 α , the key regulator of PCs biology during the angiogenesis. The p110 β isoform is controlled by autocrine and paracrine mechanisms the PCs and the ECs functions, respectively. Thus, p110 β promotes cell proliferation and an immature cell phenotype that is essential for the active sprouting angiogenesis. The mechanisms behind these functions remain unknown but GPCRs could perhaps mediate p110 β functions in PCs. Moreover, PTEN appears to counterbalance the effect of p110 β in PCs, promoting cell maturation and maybe proliferation arrest contributing to the vascular stabilization of the new formed vessels.

The implications of p110 β in the regulation of PCs during pathological angiogenesis remain unclear. p110 β inactivation in PCs in the RIP1-Tag2 mice did not show benefits in the overall survival of the animals. However, impacts in PCs number and in the tumour progression. It would be interesting, to investigate the impact of p110 β inactivation in a more PC-directed therapy.

These findings shed light on new potential therapeutic targets for several diseases where PCs have a fundamental role. Therefore, targeting p110 β and promoting vessel quiescence would be more relevant in diseases, such as cancer, where anti-angiogenics are advantageous. In contrast, therapies against PTEN in PCs would be more beneficial in those pathologies, like Alzheimer disease, where the promotion of angiogenesis is essential.

6. Conclusions

1. **PCs are present at very early time points of vessel development** and PC coverage becomes more widespread during vessel maturation.
2. **PCs start to proliferate earlier than ECs**, possibly promoting their activation. PCs and ECs become quiescent during the vascular remodelling, promoting vessel stabilization.
3. **PCs pass through different states during maturation**, suggesting the existence of PCs subpopulations in the retina. A retracted and proliferative PC (immature PC) promotes an active sprouting angiogenesis while, quiescent PCs (mature PC) are well connected with the endothelium leading to vascular remodelling.
4. **PCs have a dual role in the regulation of ECs**. They promote ECs proliferation and migration by paracrine regulation and ECs proliferation arrest by direct cell-to-cell contacts.
5. **Class IA-PI3K selectively regulates PCs biology *in vitro***. The p110 α isoform regulates PC migration and viability in AKT dependent manner and p110 β controls cell proliferation by an unknown mechanism.
6. **The p110 β isoform is the key regulator of PCs biology during *in vivo* sprouting angiogenesis**. Inactivation of p110 β in PCs, and not p110 α , promotes cell proliferation arrest and morphological changes that resemble a more mature PC.
7. **The p110 β isoform mediates PC-ECs cross talk**. The inactivation of p110 β in PCs results in EC proliferation arrest, hypovascularization and BM components deposition, resembling a more quiescent vasculature.

8. **The p110 α isoform is not fundamental to PC functions during the sprouting angiogenesis.** Inactivation of p110 α in PCs does not interfere with PC coverage or proliferation, and only causes a delayed in the expansion of the vasculature, which probably is related to PC migration defects.

9. **PTEN regulates p110 β signalling in PCs.** Inactivation of PTEN specifically in PCs, opposes to the p110 β inactivation, which results in increased PC coverage, in an immature PC morphology and in hypervascularization.

10. **Inactivation of p110 β in RIP1-Tag2 model impacts on tumour progression comprising PCs growth.** However, it regulates negatively the overall survival of the animals without interfering with the metastatic potential. Therefore, more directed therapies to PC would be needed to further investigate the role of p110 β in PCs during pathological conditions.

7. References

Abramsson, A., Kurup, S., Busse, M., Yamada, S., Lindblom, P., Schallmeiner, E., Stenzel, D., Sauvaget, D., Ledin, J., Ringvall, M., et al. (2007). Defective N-sulfation of heparan sulfate proteoglycans limits PDGF-BB binding and pericyte recruitment in vascular development. *Genes Dev.* *21*, 316–331.

Adair, T.H., and Montani, J.-P. (2010). Overview of Angiogenesis (Morgan & Claypool Life Sciences).

Adams, R.H., and Alitalo, K. (2007). Molecular regulation of angiogenesis and lymphangiogenesis. *Nat. Rev. Mol. Cell Biol.* *8*, 464–478.

Albanese, C., Hult, J., Sakamaki, T., and Pestell, R.G. (2002). Recent advances in inducible expression in transgenic mice. *Semin. Cell Dev. Biol.* *13*, 129–141.

Alessi, D.R., Andjelkovic, M., Caudwell, B., Cron, P., Morrice, N., Cohen, P., and Hemmings, B.A. (1996). Mechanism of activation of protein kinase B by insulin and IGF-1. *EMBO J.* *15*, 6541–6551.

Ali, K., Bilancio, A., Thomas, M., Pearce, W., Gilfillan, A.M., Tkaczyk, C., Kuehn, N., Gray, A., Giddings, J., Peskett, E., et al. (2004). Essential role for the p110delta phosphoinositide 3-kinase in the allergic response. *Nature* *431*, 1007–1011.

Ali, K., Soond, D.R., Piñeiro, R., Hagemann, T., Pearce, W., Lim, E.L., Bouabe, H., Scudamore, C.L., Hancox, T., Maecker, H., et al. (2014). Inactivation of PI(3)K p110δ breaks regulatory T-cell-mediated immune tolerance to cancer. *Nature* *510*, 407–411.

Alimandi, M., Heidarani, M.A., Gutkind, J.S., Zhang, J., Ellmore, N., Valius, M., Kazlauskas, A., Pierce, J.H., and Li, W. (1997). PLC-gamma activation is required for PDGF-betaR-mediated mitogenesis and monocytic differentiation of myeloid progenitor cells. *Oncogene* *15*, 585–593.

Allende, M.L., and Proia, R.L. (2002). Sphingosine-1-phosphate receptors and the development of the vascular system. *Biochim. Biophys. Acta BBA - Mol. Cell Biol. Lipids* *1582*, 222–227.

Allende, M.L., Yamashita, T., and Proia, R.L. (2003). G-protein-coupled receptor S1P1 acts within endothelial cells to regulate vascular maturation. *Blood* *102*, 3665–3667.

Allt, G., and Lawrenson, J.G. (2001). Pericytes: Cell Biology and Pathology. *Cells Tissues Organs* *169*, 1–11.

Alon, T., Hemo, I., Itin, A., Pe'er, J., Stone, J., and Keshet, E. (1995). Vascular endothelial growth factor acts as a survival factor for newly formed retinal vessels and has implications for retinopathy of prematurity. *Nat. Med.* *1*, 1024–1028.

Arboleda, M.J., Lyons, J.F., Kabbinnavar, F.F., Bray, M.R., Snow, B.E., Ayala, R., Danino, M., Karlan, B.Y., and Slamon, D.J. (2003). Overexpression of AKT2/protein kinase Bbeta leads to up-regulation of beta1 integrins, increased invasion, and metastasis of human breast and ovarian cancer cells. *Cancer Res.* *63*, 196–206.

- Arboleda-Velasquez, J.F., Primo, V., Graham, M., James, A., Manent, J., and D'Amore, P.A. (2014). Notch Signaling Functions in Retinal Pericyte Survival. *Invest. Ophthalmol. Vis. Sci.* *55*, 5191–5199.
- Arimura, K., Ago, T., Kamouchi, M., Nakamura, K., Ishitsuka, K., Kuroda, J., Sugimori, H., Ooboshi, H., Sasaki, T., and Kitazono, T. (2012). PDGF receptor β signaling in pericytes following ischemic brain injury. *Curr. Neurovasc. Res.* *9*, 1–9.
- Armulik, A. (2005). Endothelial/Pericyte Interactions. *Circ. Res.* *97*, 512–523.
- Armulik, A., Genové, G., Mäe, M., Nisancioglu, M.H., Wallgard, E., Niaudet, C., He, L., Norlin, J., Lindblom, P., Strittmatter, K., et al. (2010). Pericytes regulate the blood–brain barrier. *Nature* *468*, 557–561.
- Armulik, A., Genové, G., and Betsholtz, C. (2011). Pericytes: Developmental, Physiological, and Pathological Perspectives, Problems, and Promises. *Dev. Cell* *21*, 193–215.
- Augustin, H.G., Koh, G.Y., Thurston, G., and Alitalo, K. (2009). Control of vascular morphogenesis and homeostasis through the angiopoietin-Tie system. *Nat. Rev. Mol. Cell Biol.* *10*, 165–177.
- Bai, Y., Zhu, X., Chao, J., Zhang, Y., Qian, C., Li, P., Liu, D., Han, B., Zhao, L., Zhang, J., et al. (2015). Pericytes Contribute to the Disruption of the Cerebral Endothelial Barrier via Increasing VEGF Expression: Implications for Stroke. *PLoS ONE* *10*.
- Bailis, W., and Pear, W.S. (2012). Notch and PI3K: how is the road traveled? *Blood* *120*, 1349–1350.
- Baluk, P., Lee, C.G., Link, H., Ator, E., Haskell, A., Elias, J.A., and McDonald, D.M. (2004). Regulated Angiogenesis and Vascular Regression in Mice Overexpressing Vascular Endothelial Growth Factor in Airways. *Am. J. Pathol.* *165*, 1071–1085.
- Bautch, V.L. (2011). Stem cells and the vasculature. *Nat. Med.* *17*, 1437–1443.
- Bazzoni, G., and Dejana, E. (2004). Endothelial cell-to-cell junctions: molecular organization and role in vascular homeostasis. *Physiol. Rev.* *84*, 869–901.
- Beenken, A., and Mohammadi, M. (2009). The FGF family: biology, pathophysiology and therapy. *Nat. Rev. Drug Discov.* *8*, 235–253.
- Benjamin, L.E., Golijanin, D., Itin, A., Podes, D., and Keshet, E. (1999). Selective ablation of immature blood vessels in established human tumors follows vascular endothelial growth factor withdrawal. *J. Clin. Invest.* *103*, 159–165.
- Berg, J.N., Gallione, C.J., Stenzel, T.T., Johnson, D.W., Allen, W.P., Schwartz, C.E., Jackson, C.E., Porteous, M.E., and Marchuk, D.A. (1997). The activin receptor-like kinase 1 gene: genomic structure and mutations in hereditary hemorrhagic telangiectasia type 2. *Am. J. Hum. Genet.* *61*, 60–67.
- Bergers, G., and Hanahan, D. (2008). Modes of resistance to anti-angiogenic therapy. *Nat. Rev. Cancer* *8*, 592–603.
- Bergers, G., and Song, S. (2005). The role of pericytes in blood-vessel formation and maintenance. *Neuro-Oncol.* *7*, 452–464.

7. References

- Bergers, G., Javaherian, K., Lo, K.M., Folkman, J., and Hanahan, D. (1999). Effects of angiogenesis inhibitors on multistage carcinogenesis in mice. *Science* *284*, 808–812.
- Betsholtz, C. (2004). Insight into the physiological functions of PDGF through genetic studies in mice. *Cytokine Growth Factor Rev.* *15*, 215–228.
- Betz, C., Lenard, A., Belting, H.-G., and Affolter, M. (2016). Cell behaviors and dynamics during angiogenesis. *Development* *143*, 2249–2260.
- Bhaskar, P.T., and Hay, N. (2007). The two TORCs and Akt. *Dev. Cell* *12*, 487–502.
- Bill, R., and Christofori, G. (2016). The Rip1Tag2 Transgenic Mouse Model. In *Tumor Angiogenesis Assays: Methods and Protocols*, D. Ribatti, ed. (New York, NY: Springer New York), pp. 151–161.
- Bill, R., Fagiani, E., Zumsteg, A., Antoniadis, H., Johansson, D., Haefliger, S., Albrecht, I., Hilberg, F., and Christofori, G. (2015). Nintedanib Is a Highly Effective Therapeutic for Neuroendocrine Carcinoma of the Pancreas (PNET) in the Rip1Tag2 Transgenic Mouse Model. *Clin. Cancer Res. Off. J. Am. Assoc. Cancer Res.* *21*, 4856–4867.
- Bjarnegård, M., Enge, M., Norlin, J., Gustafsdottir, S., Fredriksson, S., Abramsson, A., Takemoto, M., Gustafsson, E., Fässler, R., and Betsholtz, C. (2004). Endothelium-specific ablation of PDGFB leads to pericyte loss and glomerular, cardiac and placental abnormalities. *Development* *131*, 1847–1857.
- Blume-Jensen, P., and Hunter, T. (2001). Oncogenic kinase signalling. *Nature* *411*, 355–365.
- Boroujerdi, A., Tigges, U., Welser-Alves, J.V., and Milner, R. (2014). Isolation and culture of primary pericytes from mouse brain. *Methods Mol. Biol. Clifton NJ* *1135*, 383–392.
- Bouabe, H., and Okkenhaug, K. (2013). Gene Targeting in Mice: a Review. *Methods Mol. Biol. Clifton NJ* *1064*, 315–336.
- Brachmann, S.M., Yballe, C.M., Innocenti, M., Deane, J.A., Fruman, D.A., Thomas, S.M., and Cantley, L.C. (2005a). Role of Phosphoinositide 3-Kinase Regulatory Isoforms in Development and Actin Rearrangement. *Mol. Cell. Biol.* *25*, 2593–2606.
- Brachmann, S.M., Ueki, K., Engelman, J.A., Kahn, R.C., and Cantley, L.C. (2005b). Phosphoinositide 3-kinase catalytic subunit deletion and regulatory subunit deletion have opposite effects on insulin sensitivity in mice. *Mol. Cell. Biol.* *25*, 1596–1607.
- Brock, C., Schaefer, M., Reusch, H.P., Czupalla, C., Michalke, M., Spicher, K., Schultz, G., and Nürnberg, B. (2003). Roles of G beta gamma in membrane recruitment and activation of p110 gamma/p101 phosphoinositide 3-kinase gamma. *J. Cell Biol.* *160*, 89–99.
- Bryan, B.A., and D'Amore, P.A. (2008). Chapter 16 Pericyte Isolation and Use in Endothelial/Pericyte Coculture Models. B.-M. in *Enzymology*, ed. (Academic Press), pp. 315–331.
- Buschard, K., Horn, T., Aaen, K., Josefsen, K., Persson, H., and Fredman, P. (1996). Presence of sulphatide (3'-sulphogalactosylceramide) in pericytes in the choroid layer of the eye: sharing of this glycolipid autoantigen with islets of Langerhans. *Diabetologia* *39*, 658–666.

- Caglayan, E., Vantler, M., Leppänen, O., Gerhardt, F., Mustafov, L., Ten Freyhaus, H., Kappert, K., Odenthal, M., Zimmermann, W.H., Tallquist, M.D., et al. (2011). Disruption of platelet-derived growth factor-dependent phosphatidylinositol 3-kinase and phospholipase C γ 1 activity abolishes vascular smooth muscle cell proliferation and migration and attenuates neointima formation in vivo. *J. Am. Coll. Cardiol.* 57, 2527–2538.
- Cao, Y., Sonveaux, P., Liu, S., Zhao, Y., Mi, J., Clary, B.M., Li, C.-Y., Kontos, C.D., and Dewhirst, M.W. (2007). Systemic overexpression of angiotensin-2 promotes tumor microvessel regression and inhibits angiogenesis and tumor growth. *Cancer Res.* 67, 3835–3844.
- Caporali, A., Martello, A., Miscianinov, V., Maselli, D., Vono, R., and Spinetti, G. (2016). Contribution of pericyte paracrine regulation of the endothelium to angiogenesis. *Pharmacol. Ther.*
- Carmeliet, P. (2003). Angiogenesis in health and disease. *Nat. Med.* 9, 653–660.
- Carmeliet, P. (2005). Angiogenesis in life, disease and medicine. *Nature* 438, 932–936.
- Carroll, P.E., Okuda, M., Horn, H.F., Biddinger, P., Stambrook, P.J., Gleich, L.L., Li, Y.Q., Tarapore, P., and Fukasawa, K. (1999). Centrosome hyperamplification in human cancer: chromosome instability induced by p53 mutation and/or Mdm2 overexpression. *Oncogene* 18, 1935–1944.
- Casanovas, O., Hicklin, D.J., Bergers, G., and Hanahan, D. (2005). Drug resistance by evasion of antiangiogenic targeting of VEGF signaling in late-stage pancreatic islet tumors. *Cancer Cell* 8, 299–309.
- Cattaruzza, S., Ozerdem, U., Denzel, M., Ranscht, B., Bulian, P., Cavallaro, U., Zanocco, D., Colombatti, A., Stallcup, W.B., and Perris, R. (2013). MULTIVALENT PROTEOGLYCAN MODULATION OF FGF MITOGENIC RESPONSES IN PERIVASCULAR CELLS. *Angiogenesis* 16, 309–327.
- Chappell, J.C., and Bautch, V.L. (2010). Vascular development: genetic mechanisms and links to vascular disease. *Curr. Top. Dev. Biol.* 90, 43–72.
- Chaudhury, A., and Howe, P.H. (2009). The tale of transforming growth factor-beta (TGF β) signaling: A soigné enigma. *IUBMB Life* 61, 929–939.
- Chen, Q., Zhang, H., Liu, Y., Adams, S., Eilken, H., Stehling, M., Corada, M., Dejana, E., Zhou, B., and Adams, R.H. (2016a). Endothelial cells are progenitors of cardiac pericytes and vascular smooth muscle cells. *Nat. Commun.* 7, 12422.
- Chen, Q., Zhang, H., Liu, Y., Adams, S., Eilken, H., Stehling, M., Corada, M., Dejana, E., Zhou, B., and Adams, R.H. (2016b). Endothelial cells are progenitors of cardiac pericytes and vascular smooth muscle cells. *Nat. Commun.* 7.
- Chen, S., Kulik, M., and Lechleider, R.J. (2003). Smad proteins regulate transcriptional induction of the SM22 α gene by TGF- β . *Nucleic Acids Res.* 31, 1302–1310.
- Choorapoikayil, S., Weijts, B., Kers, R., Bruin, A. de, and Hertog, J. den (2013). Loss of Pten promotes angiogenesis and enhanced vegfaa expression in zebrafish. *Dis. Model. Mech.* 6, 1159–1166.

7. References

- Ciraolo, E., Iezzi, M., Marone, R., Marengo, S., Curcio, C., Costa, C., Azzolino, O., Gonella, C., Rubinetto, C., Wu, H., et al. (2008). Phosphoinositide 3-kinase p110 β activity: key role in metabolism and mammary gland cancer but not development. *Sci. Signal.* 1, ra3.
- Connor, K.M., Krah, N.M., Dennison, R.J., Aderman, C.M., Chen, J., Guerin, K.I., Sapieha, P., Stahl, A., Willett, K.L., and Smith, L.E.H. (2009). Quantification of oxygen-induced retinopathy in the mouse: a model of vessel loss, vessel regrowth and pathological angiogenesis. *Nat. Protoc.* 4, 1565–1573.
- Cooke, V.G., LeBleu, V.S., Keskin, D., Khan, Z., O'Connell, J.T., Teng, Y., Duncan, M.B., Xie, L., Maeda, G., Vong, S., et al. (2012). Pericyte Depletion Results in Hypoxia-Associated Epithelial-to-Mesenchymal Transition and Metastasis Mediated by Met Signaling Pathway. *Cancer Cell* 21, 66–81.
- Costa, C., Ebi, H., Martini, M., Beausoleil, S.A., Faber, A.C., Jakubik, C.T., Huang, A., Wang, Y., Nishtala, M., Hall, B., et al. (2015). Measurement of PIP3 Levels Reveals an Unexpected Role for p110 β in Early Adaptive Responses to p110 α -Specific Inhibitors in Luminal Breast Cancer. *Cancer Cell* 27, 97–108.
- Crisan, M., Corselli, M., Chen, W.C.W., and Péault, B. (2012). Perivascular cells for regenerative medicine. *J. Cell. Mol. Med.* 16, 2851–2860.
- Crosby, J.R., Seifert, R.A., Soriano, P., and Bowen-Pope, D.F. (1998). Chimaeric analysis reveals role of Pdgf receptors in all muscle lineages. *Nat. Genet.* 18, 385–388.
- Daly, C., Wong, V., Burova, E., Wei, Y., Zabski, S., Griffiths, J., Lai, K.-M., Lin, H.C., Ioffe, E., Yancopoulos, G.D., et al. (2004). Angiotensin-1 modulates endothelial cell function and gene expression via the transcription factor FKHR (FOXO1). *Genes Dev.* 18, 1060–1071.
- Daly, C., Pasnikowski, E., Burova, E., Wong, V., Aldrich, T.H., Griffiths, J., Ioffe, E., Daly, T.J., Fandl, J.P., Papadopoulos, N., et al. (2006). Angiotensin-2 functions as an autocrine protective factor in stressed endothelial cells. *Proc. Natl. Acad. Sci.* 103, 15491–15496.
- Daneman, R., Zhou, L., Kebede, A.A., and Barres, B.A. (2010). Pericytes are required for blood-brain barrier integrity during embryogenesis. *Nature* 468, 562–566.
- Davis, G.E., and Senger, D.R. (2005). Endothelial extracellular matrix: biosynthesis, remodeling, and functions during vascular morphogenesis and neovessel stabilization. *Circ. Res.* 97, 1093–1107.
- Davis, S., Aldrich, T.H., Jones, P.F., Acheson, A., Compton, D.L., Jain, V., Ryan, T.E., Bruno, J., Radziejewski, C., Maisonpierre, P.C., et al. (1996). Isolation of Angiotensin-1, a Ligand for the TIE2 Receptor, by Secretion-Trap Expression Cloning. *Cell* 87, 1161–1169.
- Dayanir, V., Meyer, R.D., Lashkari, K., and Rahimi, N. (2001). Identification of Tyrosine Residues in Vascular Endothelial Growth Factor Receptor-2/FLK-1 Involved in Activation of Phosphatidylinositol 3-Kinase and Cell Proliferation. *J. Biol. Chem.* 276, 17686–17692.
- Dbouk, H.A., and Backer, J.M. (2010). A beta version of life: p110 β takes center stage. *Oncotarget* 1, 729–733.

- De Spiegelaere, W., Casteleyn, C., Van den Broeck, W., Plendl, J., Bahramsoltani, M., Simoens, P., Djonov, V., and Cornillie, P. (2012). Intussusceptive Angiogenesis: A Biologically Relevant Form of Angiogenesis. *J. Vasc. Res.* *49*, 390–404.
- Dejana, E., Tournier-Lasserre, E., and Weinstein, B.M. (2009). The Control of Vascular Integrity by Endothelial Cell Junctions: Molecular Basis and Pathological Implications. *Dev. Cell* *16*, 209–221.
- Delgado, P., Cubelos, B., Calleja, E., Martínez-Martín, N., Ciprés, A., Mérida, I., Bellas, C., Bustelo, X.R., and Alarcón, B. (2009). Essential function for the GTPase TC21 in homeostatic antigen receptor signaling. *Nat. Immunol.* *10*, 880–888.
- Dell, S., Peters, S., Müther, P., Kociok, N., and Jousen, A.M. (2006). The role of PDGF receptor inhibitors and PI3-kinase signaling in the pathogenesis of corneal neovascularization. *Invest. Ophthalmol. Vis. Sci.* *47*, 1928–1937.
- DeRuiter, M.C., Poelmann, R.E., VanMunsteren, J.C., Mironov, V., Markwald, R.R., and Gittenberger-de Groot, A.C. (1997). Embryonic Endothelial Cells Transdifferentiate Into Mesenchymal Cells Expressing Smooth Muscle Actins In Vivo and In Vitro. *Circ. Res.* *80*, 444–451.
- Dey, N., Crosswell, H.E., De, P., Parsons, R., Peng, Q., Su, J.D., and Durden, D.L. (2008). The protein phosphatase activity of PTEN regulates SRC family kinases and controls glioma migration. *Cancer Res.* *68*, 1862–1871.
- Díaz-Flores, L., Gutiérrez, R., Varela, H., Rancel, N., and Valladares, F. (1991). Microvascular pericytes: a review of their morphological and functional characteristics. *Histol. Histopathol.* *6*, 269–286.
- Díaz-Flores, L., Gutiérrez, R., Madrid, J.F., Varela, H., Valladares, F., Acosta, E., Martín-Vasallo, P., and Díaz-Flores, L. (2009). Pericytes. Morphofunction, interactions and pathology in a quiescent and activated mesenchymal cell niche. *Histol. Histopathol.* *24*, 909–969.
- Dickson, M.C., Martin, J.S., Cousins, F.M., Kulkarni, A.B., Karlsson, S., and Akhurst, R.J. (1995). Defective haematopoiesis and vasculogenesis in transforming growth factor-beta 1 knock out mice. *Dev. Camb. Engl.* *121*, 1845–1854.
- van Dijk, C.G.M., Nieuweboer, F.E., Pei, J.Y., Xu, Y.J., Burgisser, P., van Mulligen, E., el Azzouzi, H., Duncker, D.J., Verhaar, M.C., and Cheng, C. (2015). The complex mural cell: pericyte function in health and disease. *Int. J. Cardiol.* *190*, 75–89.
- ten Dijke, P., and Arthur, H.M. (2007). Extracellular control of TGF β signalling in vascular development and disease. *Nat. Rev. Mol. Cell Biol.* *8*, 857–869.
- Domenga, V., Fardoux, P., Lacombe, P., Monet, M., Maciazek, J., Krebs, L.T., Klonjowski, B., Berrou, E., Mericskay, M., Li, Z., et al. (2004). Notch3 is required for arterial identity and maturation of vascular smooth muscle cells. *Genes Dev.* *18*, 2730–2735.
- Dore-Duffy, P., and Cleary, K. (2011). Morphology and properties of pericytes. *Methods Mol. Biol. Clifton NJ* *686*, 49–68.
- Dummler, B., Tschopp, O., Hynx, D., Yang, Z.-Z., Dirnhofer, S., and Hemmings, B.A. (2006). Life with a single isoform of Akt: mice lacking Akt2 and Akt3 are viable but

7. References

- display impaired glucose homeostasis and growth deficiencies. *Mol. Cell. Biol.* 26, 8042–8051.
- Dumont, D.J., Gradwohl, G., Fong, G.H., Puri, M.C., Gertsenstein, M., Auerbach, A., and Breitman, M.L. (1994). Dominant-negative and targeted null mutations in the endothelial receptor tyrosine kinase, tek, reveal a critical role in vasculogenesis of the embryo. *Genes Dev.* 8, 1897–1909.
- Durand, C.A., Hartvigsen, K., Fogelstrand, L., Kim, S., Iritani, S., Vanhaesebroeck, B., Witztum, J.L., Puri, K.D., and Gold, M.R. (2009). Phosphoinositide 3-kinase p110 delta regulates natural antibody production, marginal zone and B-1 B cell function, and autoantibody responses. *J. Immunol. Baltim. Md 1950* 183, 5673–5684.
- Dvorak, A.M., and Feng, D. (2001). The vesiculo-vacuolar organelle (VVO). A new endothelial cell permeability organelle. *J. Histochem. Cytochem. Off. J. Histochem. Soc.* 49, 419–432.
- Eberhard, A., Kahlert, S., Goede, V., Hemmerlein, B., Plate, K.H., and Augustin, H.G. (2000). Heterogeneity of angiogenesis and blood vessel maturation in human tumors: implications for antiangiogenic tumor therapies. *Cancer Res.* 60, 1388–1393.
- Eberth, C.J. (1871). *Handbuch der Lehre von der Gewegen des Menschen und der Tiere.* (Leipzig).
- Eble, J.A., and Niland, S. (2009). The extracellular matrix of blood vessels. *Curr. Pharm. Des.* 15, 1385–1400.
- Eickholt, B.J., Ahmed, A.I., Davies, M., Papakonstanti, E.A., Pearce, W., Starkey, M.L., Bilancio, A., Need, A.C., Smith, A.J.H., Hall, S.M., et al. (2007). Control of Axonal Growth and Regeneration of Sensory Neurons by the p110 δ PI 3-Kinase. *PLOS ONE* 2, e869.
- Eilken, H.M., and Adams, R.H. (2010). Dynamics of endothelial cell behavior in sprouting angiogenesis. *Curr. Opin. Cell Biol.* 22, 617–625.
- Fang, J., Ding, M., Yang, L., Liu, L.-Z., and Jiang, B.-H. (2007). PI3K/PTEN/AKT signaling regulates prostate tumor angiogenesis. *Cell. Signal.* 19, 2487–2497.
- Ferrara, N., and Kerbel, R.S. (2005). Angiogenesis as a therapeutic target. *Nature* 438, 967–974.
- Fokas, E., Im, J.H., Hill, S., Yameen, S., Stratford, M., Beech, J., Hackl, W., Maira, S.-M., Bernhard, E.J., McKenna, W.G., et al. (2012). Dual Inhibition of the PI3K/mTOR Pathway Increases Tumor Radiosensitivity by Normalizing Tumor Vasculature. *Cancer Res.* 72, 239–248.
- Foo, S.S., Turner, C.J., Adams, S., Compagni, A., Aubyn, D., Kogata, N., Lindblom, P., Shani, M., Zicha, D., and Adams, R.H. (2006). Ephrin-B2 Controls Cell Motility and Adhesion during Blood-Vessel-Wall Assembly. *Cell* 124, 161–173.
- Foukas, L.C., Claret, M., Pearce, W., Okkenhaug, K., Meek, S., Peskett, E., Sancho, S., Smith, A.J.H., Withers, D.J., and Vanhaesebroeck, B. (2006). Critical role for the p110 α phosphoinositide-3-OH kinase in growth and metabolic regulation. *Nature* 441, 366–370.

- Fritsch, C., Huang, A., Chatenay-Rivauday, C., Schnell, C., Reddy, A., Liu, M., Kauffmann, A., Guthy, D., Erdmann, D., Pover, A.D., et al. (2014). Characterization of the Novel and Specific PI3K α Inhibitor NVP-BYL719 and Development of the Patient Stratification Strategy for Clinical Trials. *Mol. Cancer Ther.* *13*, 1117–1129.
- Fritsch, R., de Krijger, I., Fritsch, K., George, R., Reason, B., Kumar, M.S., Diefenbacher, M., Stamp, G., and Downward, J. (2013). RAS and RHO families of GTPases directly regulate distinct phosphoinositide 3-kinase isoforms. *Cell* *153*, 1050–1063.
- Fruman, D.A., and Rommel, C. (2014). PI3K and Cancer: Lessons, Challenges and Opportunities. *Nat. Rev. Drug Discov.* *13*, 140–156.
- Fruttiger, M., Calver, A.R., Krüger, W.H., Mudhar, H.S., Michalovich, D., Takakura, N., Nishikawa, S., and Richardson, W.D. (1996). PDGF mediates a neuron-astrocyte interaction in the developing retina. *Neuron* *17*, 1117–1131.
- Fukuhara, S., Sako, K., Minami, T., Noda, K., Kim, H.Z., Kodama, T., Shibuya, M., Takakura, N., Koh, G.Y., and Mochizuki, N. (2008). Differential function of Tie2 at cell–cell contacts and cell–substratum contacts regulated by angiopoietin-1. *Nat. Cell Biol.* *10*, 513–526.
- Furuyama, T., Kitayama, K., Shimoda, Y., Ogawa, M., Sone, K., Yoshida-Araki, K., Hisatsune, H., Nishikawa, S., Nakayama, K., Nakayama, K., et al. (2004). Abnormal Angiogenesis in Foxo1 (Fkhr)-deficient Mice. *J. Biol. Chem.* *279*, 34741–34749.
- Gallione, C.J., Repetto, G.M., Legius, E., Rustgi, A.K., Schelley, S.L., Tejpar, S., Mitchell, G., Drouin, E., Westermann, C.J.J., and Marchuk, D.A. (2004). A combined syndrome of juvenile polyposis and hereditary haemorrhagic telangiectasia associated with mutations in MADH4 (SMAD4). *Lancet Lond. Engl.* *363*, 852–859.
- Gamble, J.R., Drew, J., Trezise, L., Underwood, A., Parsons, M., Kasminkas, L., Rudge, J., Yancopoulos, G., and Vadas, M.A. (2000). Angiopoietin-1 Is an Antipermeability and Anti-Inflammatory Agent In Vitro and Targets Cell Junctions. *Circ. Res.* *87*, 603–607.
- Garl, P.J., Wenzlau, J.M., Walker, H.A., Whitelock, J.M., Costell, M., and Weiser-Evans, M.C.M. (2004). Perlecan-Induced Suppression of Smooth Muscle Cell Proliferation Is Mediated Through Increased Activity of the Tumor Suppressor PTEN. *Circ. Res.* *94*, 175–183.
- Gebala, V., Collins, R., Geudens, I., Phng, L.-K., and Gerhardt, H. (2016). Blood flow drives lumen formation by inverse membrane blebbing during angiogenesis in vivo. *Nat. Cell Biol.* *18*, 443–450.
- Geering, B., Cutillas, P.R., Nock, G., Gharbi, S.I., and Vanhaesebroeck, B. (2007). Class IA phosphoinositide 3-kinases are obligate p85-p110 heterodimers. *Proc. Natl. Acad. Sci. U. S. A.* *104*, 7809–7814.
- Geng, L., Tan, J., Himmelfarb, E., Schueneman, A., Niemann, K., Brousal, J., Fu, A., Cuneo, K., Kesicki, E.A., Treiberg, J., et al. (2004). A specific antagonist of the p110delta catalytic component of phosphatidylinositol 3'-kinase, IC486068, enhances radiation-induced tumor vascular destruction. *Cancer Res.* *64*, 4893–4899.

7. References

- Gerber, H.-P., McMurtrey, A., Kowalski, J., Yan, M., Keyt, B.A., Dixit, V., and Ferrara, N. (1998). Vascular Endothelial Growth Factor Regulates Endothelial Cell Survival through the Phosphatidylinositol 3'-Kinase/Akt Signal Transduction Pathway REQUIREMENT FOR Flk-1/KDR ACTIVATION. *J. Biol. Chem.* 273, 30336–30343.
- Gerhardt, H., and Betsholtz, C. (2003). Endothelial-pericyte interactions in angiogenesis. *Cell Tissue Res.* 314, 15–23.
- Gerhardt, H., Wolburg, H., and Redies, C. (2000). N-cadherin mediates pericytic-endothelial interaction during brain angiogenesis in the chicken. *Dev. Dyn. Off. Publ. Am. Assoc. Anat.* 218, 472–479.
- Gerhardt, H., Golding, M., Fruttiger, M., Ruhrberg, C., Lundkvist, A., Abramsson, A., Jeltsch, M., Mitchell, C., Alitalo, K., Shima, D., et al. (2003). VEGF guides angiogenic sprouting utilizing endothelial tip cell filopodia. *J. Cell Biol.* 161, 1163–1177.
- Geudens, I., and Gerhardt, H. (2011). Coordinating cell behaviour during blood vessel formation. *Dev. Camb. Engl.* 138, 4569–4583.
- Glaser, S.S., Gaudio, E., and Alpini, G. (2010). Vascular factors, angiogenesis and biliary tract disease. *Curr. Opin. Gastroenterol.* 26, 246–250.
- Goettsch, W., Gryczka, C., Korff, T., Ernst, E., Goettsch, C., Seebach, J., Schnittler, H.-J., Augustin, H.G., and Morawietz, H. (2008). Flow-dependent regulation of angiopoietin-2. *J. Cell. Physiol.* 214, 491–503.
- Gordan, J.D., Bertout, J.A., Hu, C.-J., Diehl, J.A., and Simon, M.C. (2007). HIF-2alpha promotes hypoxic cell proliferation by enhancing c-myc transcriptional activity. *Cancer Cell* 11, 335–347.
- Goumans, M.-J., Valdimarsdottir, G., Itoh, S., Rosendahl, A., Sideras, P., and ten Dijke, P. (2002). Balancing the activation state of the endothelium via two distinct TGF- β type I receptors. *EMBO J.* 21, 1743–1753.
- Goumans, M.J., Valdimarsdottir, G., Itoh, S., Lebrin, F., Larsson, J., Mummery, C., Karlsson, S., and ten Dijke, P. (2003). Activin receptor-like kinase (ALK)1 is an antagonistic mediator of lateral TGFbeta/ALK5 signaling. *Mol. Cell* 12, 817–828.
- Graneß, A., Adomeit, A., Heinze, R., Wetzker, R., and Liebmann, C. (1998). A Novel Mitogenic Signaling Pathway of Bradykinin in the Human Colon Carcinoma Cell Line SW-480 Involves Sequential Activation of a Gq/11 Protein, Phosphatidylinositol 3-Kinase β , and Protein Kinase C ϵ . *J. Biol. Chem.* 273, 32016–32022.
- Graupera, M., and Potente, M. (2013). Regulation of angiogenesis by PI3K signaling networks. *Exp. Cell Res.* 319, 1348–1355.
- Graupera, M., Guillermet-Guibert, J., Foukas, L.C., Phng, L.-K., Cain, R.J., Salpekar, A., Pearce, W., Meek, S., Millan, J., Cutillas, P.R., et al. (2008). Angiogenesis selectively requires the p110 α isoform of PI3K to control endothelial cell migration. *Nature* 453, 662–666.
- Greenberg, J.I., Shields, D.J., Barillas, S.G., Acevedo, L.M., Murphy, E., Huang, J., Schepke, L., Stockmann, C., Johnson, R.S., Angle, N., et al. (2008). A role for VEGF as a negative regulator of pericyte function and vessel maturation. *Nature* 456, 809–813.

- Groppa, E., Brkic, S., Bovo, E., Reginato, S., Sacchi, V., Di Maggio, N., Muraro, M.G., Calabrese, D., Heberer, M., Gianni-Barrera, R., et al. (2015). VEGF dose regulates vascular stabilization through Semaphorin3A and the Neuropilin-1+ monocyte/TGF- β 1 paracrine axis. *EMBO Mol. Med.* 7, 1366–1384.
- Guillermet-Guibert, J., Bjorklof, K., Salpekar, A., Gonella, C., Ramadani, F., Bilancio, A., Meek, S., Smith, A.J.H., Okkenhaug, K., and Vanhaesebroeck, B. (2008a). The p110 β isoform of phosphoinositide 3-kinase signals downstream of G protein-coupled receptors and is functionally redundant with p110 γ . *Proc. Natl. Acad. Sci. U. S. A.* 105, 8292–8297.
- Guillermet-Guibert, J., Bjorklof, K., Salpekar, A., Gonella, C., Ramadani, F., Bilancio, A., Meek, S., Smith, A.J.H., Okkenhaug, K., and Vanhaesebroeck, B. (2008b). The p110 β isoform of phosphoinositide 3-kinase signals downstream of G protein-coupled receptors and is functionally redundant with p110 γ . *Proc. Natl. Acad. Sci.* 105, 8292–8297.
- Guillermet-Guibert, J., Smith, L.B., Halet, G., Whitehead, M.A., Pearce, W., Rebourcet, D., León, K., Crépieux, P., Nock, G., Strömstedt, M., et al. (2015). Novel Role for p110 β PI 3-Kinase in Male Fertility through Regulation of Androgen Receptor Activity in Sertoli Cells. *PLoS Genet.* 11.
- Gutiérrez R. and Varela H, D.-F.L. (1992a). Behavior and lineage of postcapillary venule pericytes during postnatal angiogenesis. *J Morphol* 213, 33–45.
- Hamada, K., Sasaki, T., Koni, P.A., Natsui, M., Kishimoto, H., Sasaki, J., Yajima, N., Horie, Y., Hasegawa, G., Naito, M., et al. (2005). The PTEN/PI3K pathway governs normal vascular development and tumor angiogenesis. *Genes Dev.* 19, 2054–2065.
- Hammes, H.-P., Lin, J., Wagner, P., Feng, Y., Hagen, F. vom, Krzizok, T., Renner, O., Breier, G., Brownlee, M., and Deutsch, U. (2004). Angiopoietin-2 Causes Pericyte Dropout in the Normal Retina. *Diabetes* 53, 1104–1110.
- Hanahan, D. (1985). Heritable formation of pancreatic beta-cell tumours in transgenic mice expressing recombinant insulin/simian virus 40 oncogenes. *Nature* 315, 115–122.
- Helker, C.S.M., Schuermann, A., Karpanen, T., Zeuschner, D., Belting, H.-G., Affolter, M., Schulte-Merker, S., and Herzog, W. (2013). The zebrafish common cardinal veins develop by a novel mechanism: lumen ensheathment. *Dev. Camb. Engl.* 140, 2776–2786.
- Hellstrom, M., Lindahl, P., Abramsson, A., Betsholtz, C., and others (1999). Role of PDGF-B and PDGFR-beta in recruitment of vascular smooth muscle cells and pericytes during embryonic blood vessel formation in the mouse. *Development* 126, 3047–3055.
- Hellström, M., Gerhardt, H., Kalén, M., Li, X., Eriksson, U., Wolburg, H., and Betsholtz, C. (2001a). Lack of pericytes leads to endothelial hyperplasia and abnormal vascular morphogenesis. *J. Cell Biol.* 153, 543–553.
- Hellström, M., Gerhardt, H., Kalén, M., Li, X., Eriksson, U., Wolburg, H., and Betsholtz, C. (2001b). Lack of pericytes leads to endothelial hyperplasia and abnormal vascular morphogenesis. *J. Cell Biol.* 153, 543–553.

7. References

- Hennessy, B.T., Smith, D.L., Ram, P.T., Lu, Y., and Mills, G.B. (2005). Exploiting the PI3K/AKT Pathway for Cancer Drug Discovery. *Nat. Rev. Drug Discov.* *4*, 988–1004.
- Henshall, T.L., Keller, A., He, L., Johansson, B.R., Wallgard, E., Raschperger, E., Mäe, M.A., Jin, S., Betsholtz, C., and Lendahl, U. (2015). Notch3 is necessary for blood vessel integrity in the central nervous system. *Arterioscler. Thromb. Vasc. Biol.* *35*, 409–420.
- Herbert, S.P., Huisken, J., Kim, T.N., Feldman, M.E., Houseman, B.T., Wang, R.A., Shokat, K.M., and Stainier, D.Y.R. (2009). Arterial-Venous Segregation by Selective Cell Sprouting: An Alternative Mode of Blood Vessel Formation. *Science* *326*, 294–298.
- Herwig, L., Blum, Y., Krudewig, A., Ellertsdottir, E., Lenard, A., Belting, H.-G., and Affolter, M. (2011). Distinct cellular mechanisms of blood vessel fusion in the zebrafish embryo. *Curr. Biol. CB* *21*, 1942–1948.
- Higaki, M., Sakaue, H., Ogawa, W., Kasuga, M., and Shimokado, K. (1996). Phosphatidylinositol 3-kinase-independent signal transduction pathway for platelet-derived growth factor-induced chemotaxis. *J. Biol. Chem.* *271*, 29342–29346.
- Hirsch, E., Ciraolo, E., Franco, I., Ghigo, A., and Martini, M. (2014a). PI3K in cancer-stroma interactions: bad in seed and ugly in soil. *Oncogene* *33*, 3083–3090.
- Hirsch, E., Ciraolo, E., Franco, I., Ghigo, A., and Martini, M. (2014b). PI3K in cancer-stroma interactions: bad in seed and ugly in soil. *Oncogene* *33*, 3083–3090.
- Hirschi, K.K., Burt, J.M., Hirschi, K.D., and Dai, C. (2003). Gap junction communication mediates transforming growth factor-beta activation and endothelial-induced mural cell differentiation. *Circ. Res.* *93*, 429–437.
- Hoch, R.V., and Soriano, P. (2003). Roles of PDGF in animal development. *Dev. Camb. Engl.* *130*, 4769–4784.
- Hooshmand-Rad, R., Hajkova, L., Klint, P., Karlsson, R., Vanhaesebroeck, B., Claesson-Welsh, L., and Heldin, C.H. (2000). The PI 3-kinase isoforms p110(alpha) and p110(beta) have differential roles in PDGF- and insulin-mediated signaling. *J Cell Sci* *113*, 207–214.
- Hopkins, B.D., Hodakoski, C., Barrows, D., Mense, S., and Parsons, R.E. (2014). PTEN function, the long and the short of it. *Trends Biochem. Sci.* *39*, 183–190.
- Hosaka, T., Biggs, W.H., Tieu, D., Boyer, A.D., Varki, N.M., Cavenee, W.K., and Arden, K.C. (2004). Disruption of forkhead transcription factor (FOXO) family members in mice reveals their functional diversification. *Proc. Natl. Acad. Sci. U. S. A.* *101*, 2975–2980.
- Hu, L., Hofmann, J., and Jaffe, R.B. (2005). Phosphatidylinositol 3-Kinase Mediates Angiogenesis and Vascular Permeability Associated with Ovarian Carcinoma. *Clin. Cancer Res.* *11*, 8208–8212.
- Huang, J., and Manning, B.D. (2008). The TSC1-TSC2 complex: a molecular switchboard controlling cell growth. *Biochem. J.* *412*, 179–190.
- Huang, F.-J., You, W.-K., Bonaldo, P., Seyfried, T.N., Pasquale, E.B., and Stallcup, W.B. (2010). Pericyte deficiencies lead to aberrant tumor vascularization in the brain of the NG2 null mouse. *Dev. Biol.* *344*, 1035–1046.

- Hughes, S., and Chan-Ling, T. (2004). Characterization of Smooth Muscle Cell and Pericyte Differentiation in the Rat Retina In Vivo. *Invest. Ophthalmol. Vis. Sci.* *45*, 2795–2806.
- Hutchinson, J.A., Shanware, N.P., Chang, H., and Tibbetts, R.S. (2011). Regulation of Ribosomal Protein S6 Phosphorylation by Casein Kinase 1 and Protein Phosphatase 1. *J. Biol. Chem.* *286*, 8688–8696.
- Hutchinson, J.N., Jin, J., Cardiff, R.D., Woodgett, J.R., and Muller, W.J. (2004). Activation of Akt-1 (PKB-alpha) can accelerate ErbB-2-mediated mammary tumorigenesis but suppresses tumor invasion. *Cancer Res.* *64*, 3171–3178.
- Iivanainen, E., Nelimarkka, L., Elenius, V., Heikkinen, S.-M., Junttila, T.T., Sihombing, L., Sundvall, M., Maatta, J.A., Laine, V.J.O., Yla-Herttuala, S., et al. (2003). Angiopoietin-regulated recruitment of vascular smooth muscle cells by endothelial-derived heparin binding EGF-like growth factor. *FASEB J. Off. Publ. Fed. Am. Soc. Exp. Biol.* *17*, 1609–1621.
- Im, E., and Kazlauskas, A. (2007). Src Family Kinases Promote Vessel Stability by Antagonizing the Rho/ROCK Pathway. *J. Biol. Chem.* *282*, 29122–29129.
- Irie, H.Y., Pearline, R.V., Grueneberg, D., Hsia, M., Ravichandran, P., Kothari, N., Natesan, S., and Brugge, J.S. (2005). Distinct roles of Akt1 and Akt2 in regulating cell migration and epithelial-mesenchymal transition. *J. Cell Biol.* *171*, 1023–1034.
- Jain, R.K. (2009). A new target for tumor therapy. *N. Engl. J. Med.* *360*, 2669–2671.
- Jain, R.K. (2013). Normalizing tumor microenvironment to treat cancer: bench to bedside to biomarkers. *J. Clin. Oncol. Off. J. Am. Soc. Clin. Oncol.* *31*, 2205–2218.
- Jean, S., and Kiger, A.A. (2014). Classes of phosphoinositide 3-kinases at a glance. *J. Cell Sci.* *127*, 923–928.
- Ji, W., Chen, X., Lv, J., Wang, M., Ren, S., Yuan, B., Wang, B., and Chen, L. (2014). Liraglutide Exerts Antidiabetic Effect via PTP1B and PI3K/Akt2 Signaling Pathway in Skeletal Muscle of KKAY Mice. *Int. J. Endocrinol.* *2014*, 312452.
- Jia, S., Liu, Z., Zhang, S., Liu, P., Zhang, L., Lee, S.H., Zhang, J., Signoretti, S., Loda, M., Roberts, T.M., et al. (2008a). Essential roles of PI(3)K-p110beta in cell growth, metabolism and tumorigenesis. *Nature* *454*, 776–779.
- Jia, S., Liu, Z., Zhang, S., Liu, P., Zhang, L., Lee, S.H., Zhang, J., Signoretti, S., Loda, M., Roberts, T.M., et al. (2008b). Direct positive regulation of PTEN by the p85 subunit of phosphatidylinositol 3-kinase. *Nature* *454*, 776–779.
- Jia, S., Roberts, T.M., and Zhao, J.J. (2009). Should individual PI3 kinase isoforms be targeted in cancer? *Curr. Opin. Cell Biol.* *21*, 199–208.
- Jiang, B.-H., and Liu, L.-Z. (2009). PI3K/PTEN Signaling in Angiogenesis and Tumorigenesis. *Adv. Cancer Res.* *102*, 19–65.
- Jiang, Q., Arnold, S., Heanue, T., Kilambi, K.P., Doan, B., Kapoor, A., Ling, A.Y., Sosa, M.X., Guy, M., Jiang, Q., et al. (2015). Functional loss of semaphorin 3C and/or semaphorin 3D and their epistatic interaction with ret are critical to hirschsprung disease liability. *Am. J. Hum. Genet.* *96*, 581–596.

7. References

- Jimenez, C., Hernandez, C., Pimentel, B., and Carrera, A.C. (2002). The p85 regulatory subunit controls sequential activation of phosphoinositide 3-kinase by Tyr kinases and Ras. *J. Biol. Chem.* 277, 41556–41562.
- Jin, S., Hansson, E.M., Tikka, S., Lanner, F., Sahlgren, C., Farnebo, F., Baumann, M., Kalimo, H., and Lendahl, U. (2008). Notch signaling regulates platelet-derived growth factor receptor-beta expression in vascular smooth muscle cells. *Circ. Res.* 102, 1483–1491.
- Josephs, D.H., and Sarker, D. (2015). Pharmacodynamic Biomarker Development for PI3K Pathway Therapeutics. *Transl. Oncogenomics* 7, 33–49.
- Juric, D., Castel, P., Griffith, M., Griffith, O.L., Won, H.H., Ellis, H., Ebbesen, S.H., Ainscough, B.J., Ramu, A., Iyer, G., et al. (2015). Convergent loss of PTEN leads to clinical resistance to a PI(3)K α inhibitor. *Nature* 518, 240–244.
- Kelly-Goss, M.R., Sweat, R.S., Stapor, P.C., Peirce, S.M., and Murfee, W.L. (2014). Targeting pericytes for angiogenic therapies. *Microcirc. N. Y. N* 1994 21, 345–357.
- Kim, J.A., Tran, N.D., Li, Z., Yang, F., Zhou, W., and Fisher, M.J. (2006). Brain endothelial hemostasis regulation by pericytes. *J. Cereb. Blood Flow Metab. Off. J. Int. Soc. Cereb. Blood Flow Metab.* 26, 209–217.
- Klarlund, J.K., Guilherme, A., Holik, J.J., Virbasius, J.V., Chawla, A., and Czech, M.P. (1997). Signaling by phosphoinositide-3,4,5-trisphosphate through proteins containing pleckstrin and Sec7 homology domains. *Science* 275, 1927–1930.
- Klippel, A., Escobedo, J.A., Hirano, M., and Williams, L.T. (1994). The interaction of small domains between the subunits of phosphatidylinositol 3-kinase determines enzyme activity. *Mol. Cell. Biol.* 14, 2675–2685.
- Kłosowska-Wardęga, A., Hasumi, Y., Burmakin, M., Åhgren, A., Stuhr, L., Moen, I., Reed, R.K., Rubin, K., Hellberg, C., and Heldin, C.-H. (2009). Combined Anti-Angiogenic Therapy Targeting PDGF and VEGF Receptors Lowers the Interstitial Fluid Pressure in a Murine Experimental Carcinoma. *PLOS ONE* 4, e8149.
- Knight, Z.A., Gonzalez, B., Feldman, M.E., Zunder, E.R., Goldenberg, D.D., Williams, O., Loewith, R., Stokoe, D., Balla, A., Toth, B., et al. (2006). A pharmacological map of the PI3-K family defines a role for p110 α in insulin signaling. *Cell* 125, 733–747.
- Kofler, N.M., Cuervo, H., Uh, M.K., Murtomäki, A., and Kitajewski, J. (2015). Combined deficiency of Notch1 and Notch3 causes pericyte dysfunction, models CADASIL, and results in arteriovenous malformations. *Sci. Rep.* 5, 16449.
- Kok, K., Geering, B., and Vanhaesebroeck, B. (2009). Regulation of phosphoinositide 3-kinase expression in health and disease. *Trends Biochem. Sci.* 34, 115–127.
- Kong, D., Okamura, M., Yoshimi, H., and Yamori, T. (2009). Antiangiogenic effect of ZSTK474, a novel phosphatidylinositol 3-kinase inhibitor. *Eur. J. Cancer Oxf. Engl.* 1990 45, 857–865.
- Kontos, C.D., Cha, E.H., York, J.D., and Peters, K.G. (2002). The Endothelial Receptor Tyrosine Kinase Tie1 Activates Phosphatidylinositol 3-Kinase and Akt To Inhibit Apoptosis. *Mol. Cell. Biol.* 22, 1704–1713.

- Korpisalo, P., Karvinen, H., Rissanen, T.T., Kilpijoki, J., Marjomäki, V., Baluk, P., McDonald, D.M., Cao, Y., Eriksson, U., Alitalo, K., et al. (2008). Vascular endothelial growth factor-A and platelet-derived growth factor-B combination gene therapy prolongs angiogenic effects via recruitment of interstitial mononuclear cells and paracrine effects rather than improved pericyte coverage of angiogenic vessels. *Circ. Res.* *103*, 1092–1099.
- Krugmann, S., Anderson, K.E., Ridley, S.H., Risso, N., McGregor, A., Coadwell, J., Davidson, K., Eguinoa, A., Ellson, C.D., Lipp, P., et al. (2002). Identification of ARAP3, a novel PI3K effector regulating both Arf and Rho GTPases, by selective capture on phosphoinositide affinity matrices. *Mol. Cell* *9*, 95–108.
- Kubo, H., Hazeki, K., Takasuga, S., and Hazeki, O. (2005). Specific role for p85/p110 β in GTP-binding-protein-mediated activation of Akt. *Biochem. J.* *392*, 607–614.
- Kundra, V., Escobedo, J.A., Kazlauskas, A., Kim, H.K., Rhee, S.G., Williams, L.T., and Zetter, B.R. (1994). Regulation of chemotaxis by the platelet-derived growth factor receptor- β . *Nature* *367*, 474–476.
- Kurig, B., Shymanets, A., Bohnacker, T., Prajwal, Brock, C., Ahmadian, M.R., Schaefer, M., Gohla, A., Harteneck, C., Wymann, M.P., et al. (2009). Ras is an indispensable coregulator of the class IB phosphoinositide 3-kinase p87/p110 γ . *Proc. Natl. Acad. Sci. U. S. A.* *106*, 20312–20317.
- Kurosu, H., Maehama, T., Okada, T., Yamamoto, T., Hoshino, S., Fukui, Y., Ui, M., Hazeki, O., and Katada, T. (1997). Heterodimeric Phosphoinositide 3-Kinase Consisting of p85 and p110 β Is Synergistically Activated by the $\beta\gamma$ Subunits of G Proteins and Phosphotyrosyl Peptide. *J. Biol. Chem.* *272*, 24252–24256.
- Kurup, S., Abramsson, A., Li, J.P., Lindahl, U., Kjellen, L., Betsholtz, C., Gerhardt, H., and Spillmann, D. (2006). Heparan sulphate requirement in platelet-derived growth factor B-mediated pericyte recruitment. *Biochem. Soc. Trans.* *34*, 454–455.
- Kurz, H., Fehr, J., Nitschke, R., and Burkhardt, H. (2008). Pericytes in the mature chorioallantoic membrane capillary plexus contain desmin and alpha-smooth muscle actin: relevance for non-sprouting angiogenesis. *Histochem. Cell Biol.* *130*, 1027–1040.
- LaBarbera, K.E., Hyldahl, R.D., O'Fallon, K.S., Clarkson, P.M., and Witkowski, S. (2015). Pericyte NF- κ B activation enhances endothelial cell proliferation and proangiogenic cytokine secretion in vitro. *Physiol. Rep.* *3*.
- Lan, Y., Liu, B., Yao, H., Li, F., Weng, T., Yang, G., Li, W., Cheng, X., Mao, N., and Yang, X. (2007). Essential Role of Endothelial Smad4 in Vascular Remodeling and Integrity. *Mol. Cell. Biol.* *27*, 7683–7692.
- Larsson, J., Goumans, M.-J., Sjöstrand, L.J., van Rooijen, M.A., Ward, D., Levéen, P., Xu, X., ten Dijke, P., Mummery, C.L., and Karlsson, S. (2001). Abnormal angiogenesis but intact hematopoietic potential in TGF- β type I receptor-deficient mice. *EMBO J.* *20*, 1663–1673.
- Lelievre, E., Bourbon, P.-M., Duan, L.-J., Nussbaum, R.L., and Fong, G.-H. (2005). Deficiency in the p110 α subunit of PI3K results in diminished Tie2 expression and Tie2(-/-)-like vascular defects in mice. *Blood* *105*, 3935–3938.

7. References

- Lemmon, M.A. (2008). Membrane recognition by phospholipid-binding domains. *Nat. Rev. Mol. Cell Biol.* 9, 99–111.
- Lenard, A., Ellertsdottir, E., Herwig, L., Krudewig, A., Sauteur, L., Belting, H.-G., and Affolter, M. (2013). In vivo analysis reveals a highly stereotypic morphogenetic pathway of vascular anastomosis. *Dev. Cell* 25, 492–506.
- Leslie, N.R., Yang, X., Downes, C.P., and Weijer, C.J. (2007). PtdIns(3,4,5)P(3)-dependent and -independent roles for PTEN in the control of cell migration. *Curr. Biol. CB* 17, 115–125.
- Leslie, N.R., Maccario, H., Spinelli, L., and Davidson, L. (2009). The significance of PTEN's protein phosphatase activity. *Adv. Enzyme Regul.* 49, 190–196.
- Levéen, P., Pekny, M., Gebre-Medhin, S., Swolin, B., Larsson, E., and Betsholtz, C. (1994). Mice deficient for PDGF B show renal, cardiovascular, and hematological abnormalities. *Genes Dev.* 8, 1875–1887.
- Li, D.M., and Sun, H. (1997). TEP1, encoded by a candidate tumor suppressor locus, is a novel protein tyrosine phosphatase regulated by transforming growth factor beta. *Cancer Res.* 57, 2124–2129.
- Li, D.Y., Sorensen, L.K., Brooke, B.S., Urness, L.D., Davis, E.C., Taylor, D.G., Boak, B.B., and Wendel, D.P. (1999). Defective angiogenesis in mice lacking endoglin. *Science* 284, 1534–1537.
- Li, J., Yen, C., Liaw, D., Podsypanina, K., Bose, S., Wang, S.I., Puc, J., Miliaresis, C., Rodgers, L., McCombie, R., et al. (1997). PTEN, a putative protein tyrosine phosphatase gene mutated in human brain, breast, and prostate cancer. *Science* 275, 1943–1947.
- Lindahl, P., Johansson, B.R., Levéen, P., and Betsholtz, C. (1997). Pericyte Loss and Microaneurysm Formation in PDGF-B-Deficient Mice. *Science* 277, 242–245.
- Lindblom, P., Gerhardt, H., Liebner, S., Abramsson, A., Enge, M., Hellström, M., Bäckström, G., Fredriksson, S., Landegren, U., Nyström, H.C., et al. (2003). Endothelial PDGF-B retention is required for proper investment of pericytes in the microvessel wall. *Genes Dev.* 17, 1835–1840.
- Lindsay, Y., McCoull, D., Davidson, L., Leslie, N.R., Fairservice, A., Gray, A., Lucocq, J., and Downes, C.P. (2006). Localization of agonist-sensitive PtdIns(3,4,5)P3 reveals a nuclear pool that is insensitive to PTEN expression. *J. Cell Sci.* 119, 5160–5168.
- Liu, H., Kennard, S., and Lilly, B. (2009). NOTCH3 expression is induced in mural cells through an autoregulatory loop that requires endothelial-expressed JAGGED1. *Circ. Res.* 104, 466–475.
- Liu, H., Zhang, W., Kennard, S., Caldwell, R.B., and Lilly, B. (2010). Notch3 Is Critical for Proper Angiogenesis and Mural Cell Investment Novelty and Significance. *Circ. Res.* 107, 860–870.
- Liu, Y., Wada, R., Yamashita, T., Mi, Y., Deng, C.-X., Hobson, J.P., Rosenfeldt, H.M., Nava, V.E., Chae, S.-S., Lee, M.-J., et al. (2000). Edg-1, the G protein-coupled receptor for sphingosine-1-phosphate, is essential for vascular maturation. *J. Clin. Invest.* 106, 951–961.

- Liu, Y., Wilkinson, F., Kirton, J., Jeziorska, M., Iizasa, H., Sai, Y., Nakashima, E., Heagerty, A., Canfield, A., and Alexander, M. (2007). Hepatocyte growth factor and c-Met expression in pericytes: implications for atherosclerotic plaque development. *J. Pathol.* 212, 12–19.
- Lobov, I.B., Rao, S., Carroll, T.J., Vallance, J.E., Ito, M., Ondr, J.K., Kurup, S., Glass, D.A., Patel, M.S., Shu, W., et al. (2005). WNT7b mediates macrophage-induced programmed cell death in patterning of the vasculature. *Nature* 437, 417–421.
- London, A., Benhar, I., and Schwartz, M. (2013). The retina as a window to the brain—from eye research to CNS disorders. *Nat. Rev. Neurol.* 9, 44–53.
- Maier, U., Babich, A., and Nürnberg, B. (1999). Roles of Non-catalytic Subunits in Gβγ-induced Activation of Class I Phosphoinositide 3-Kinase Isoforms β and γ. *J. Biol. Chem.* 274, 29311–29317.
- Majesky, M.W. (2007). Developmental Basis of Vascular Smooth Muscle Diversity. *Arterioscler. Thromb. Vasc. Biol.* 27, 1248–1258.
- Majesky, M.W., Dong, X.R., Regan, J.N., and Hoglund, V.J. (2011). Vascular smooth muscle progenitor cells: building and repairing blood vessels. *Circ. Res.* 108, 365–377.
- Mäkinen, T., Veikkola, T., Mustjoki, S., Karpanen, T., Catimel, B., Nice, E.C., Wise, L., Mercer, A., Kowalski, H., Kerjaschki, D., et al. (2001). Isolated lymphatic endothelial cells transduce growth, survival and migratory signals via the VEGF-C/D receptor VEGFR-3. *EMBO J.* 20, 4762–4773.
- Manchado, E., Eguren, M., and Malumbres, M. (2010). The anaphase-promoting complex/cyclosome (APC/C): cell-cycle-dependent and -independent functions. *Biochem. Soc. Trans.* 38, 65–71.
- Manning, B.D., and Cantley, L.C. (2007). AKT/PKB signaling: navigating downstream. *Cell* 129, 1261–1274.
- Mavria, G., Vercoulen, Y., Yeo, M., Paterson, H., Karasarides, M., Marais, R., Bird, D., and Marshall, C.J. (2006). ERK-MAPK signaling opposes Rho-kinase to promote endothelial cell survival and sprouting during angiogenesis. *Cancer Cell* 9, 33–44.
- Mayer, I.A., Abramson, V., Formisano, L., Balko, J.M., Estrada, M.V., Sanders, M., Juric, D., Solit, D., Berger, M.F., Won, H., et al. (2016). A Phase Ib Study of Alpelisib (BYL719), a PI3Kα-specific Inhibitor, with Letrozole in ER+/HER2-Negative Metastatic Breast Cancer. *Clin. Cancer Res.* clincanres.0134.2016.
- Mayo, L.D., and Donner, D.B. (2002). The PTEN, Mdm2, p53 tumor suppressor-oncoprotein network. *Trends Biochem. Sci.* 27, 462–467.
- McCann, A.H., Kirley, A., Carney, D.N., Corbally, N., Magee, H.M., Keating, G., and Dervan, P.A. (1995). Amplification of the MDM2 gene in human breast cancer and its association with MDM2 and p53 protein status. *Br. J. Cancer* 71, 981–985.
- Mellor, P., Furber, L.A., Nyarko, J.N.K., and Anderson, D.H. (2012). Multiple roles for the p85α isoform in the regulation and function of PI3K signalling and receptor trafficking. *Biochem. J.* 441, 23–37.

7. References

- Meng, M.-B., Zaorsky, N.G., Deng, L., Wang, H.-H., Chao, J., Zhao, L.-J., Yuan, Z.-Y., and Ping, W. (2015). Pericytes: a double-edged sword in cancer therapy. *Future Oncol. Lond. Engl.* *11*, 169–179.
- Morikawa, S., Baluk, P., Kaidoh, T., Haskell, A., Jain, R.K., and McDonald, D.M. (2002). Abnormalities in pericytes on blood vessels and endothelial sprouts in tumors. *Am. J. Pathol.* *160*, 985–1000.
- Mourani, P.M., Garl, P.J., Wenzlau, J.M., Carpenter, T.C., Stenmark, K.R., and Weiser-Evans, M.C.M. (2004). Unique, Highly Proliferative Growth Phenotype Expressed by Embryonic and Neointimal Smooth Muscle Cells Is Driven by Constitutive Akt, mTOR, and p70S6K Signaling and Is Actively Repressed by PTEN. *Circulation* *109*, 1299–1306.
- Mundi, P.S., Sachdev, J., McCourt, C., and Kalinsky, K. (2016). AKT in cancer: new molecular insights and advances in drug development. *Br. J. Clin. Pharmacol.* *82*, 943–956.
- Murillo, M.M., Zelenay, S., Nye, E., Castellano, E., Lassailly, F., Stamp, G., and Downward, J. (2014). RAS interaction with PI3K p110 α is required for tumor-induced angiogenesis. *J. Clin. Invest.* *124*, 3601–3611.
- Muzumdar, M.D., Tasic, B., Miyamichi, K., Li, L., and Luo, L. (2007). A global double-fluorescent Cre reporter mouse. *Genes. N. Y. N 2000* *45*, 593–605.
- Nehls, V., Denzer, K., and Drenckhahn, D. (1992). Pericyte involvement in capillary sprouting during angiogenesis in situ. *Cell Tissue Res.* *270*, 469–474.
- Nemenoff, R.A., Simpson, P.A., Furgeson, S.B., Kaplan-Albuquerque, N., Crossno, J., Garl, P.J., Cooper, J., and Weiser-Evans, M.C.M. (2008). Targeted Deletion of PTEN in Smooth Muscle Cells Results in Vascular Remodeling and Recruitment of Progenitor Cells Through Induction of Stromal Cell-Derived Factor-1 α . *Circ. Res.* *102*, 1036–1045.
- Ni, J., Liu, Q., Xie, S., Carlson, C.B., Von, T., Vogel, K.W., Riddle, S.M., Benes, C.H., Eck, M.J., Roberts, T.M., et al. (2012). Functional characterization of an isoform-selective inhibitor of PI3K-p110 β as a potential anti-cancer agent. *Cancer Discov.* *2*, 425–433.
- Nicoli, S., Knyphausen, C.-P., Zhu, L.J., Lakshmanan, A., and Lawson, N.D. (2012). miR-221 is required for endothelial tip cell behaviors during vascular development. *Dev. Cell* *22*, 418–429.
- Nishishita, T., and Lin, P.C. (2004). Angiopoietin 1, PDGF-B, and TGF-beta gene regulation in endothelial cell and smooth muscle cell interaction. *J. Cell. Biochem.* *91*, 584–593.
- le Noble, F., Moyon, D., Pardanaud, L., Yuan, L., Djonov, V., Matthijsen, R., Bréant, C., Fleury, V., and Eichmann, A. (2004). Flow regulates arterial-venous differentiation in the chick embryo yolk sac. *Dev. Camb. Engl.* *131*, 361–375.
- Oellerich, M.F., and Potente, M. (2012). FOXOs and sirtuins in vascular growth, maintenance, and aging. *Circ. Res.* *110*, 1238–1251.

- Ogura, S., Kurata, K., Hattori, Y., Takase, H., Ishiguro-Oonuma, T., Hwang, Y., Ahn, S., Park, I., Ikeda, W., Kusahara, S., et al. (2017). Sustained inflammation after pericyte depletion induces irreversible blood-retina barrier breakdown. *JCI Insight* 2.
- Oh, S.P., Seki, T., Goss, K.A., Imamura, T., Yi, Y., Donahoe, P.K., Li, L., Miyazono, K., ten Dijke, P., Kim, S., et al. (2000). Activin receptor-like kinase 1 modulates transforming growth factor-beta 1 signaling in the regulation of angiogenesis. *Proc. Natl. Acad. Sci. U. S. A.* 97, 2626–2631.
- Okkenhaug, K., Bilancio, A., Farjot, G., Priddle, H., Sancho, S., Peskett, E., Pearce, W., Meek, S.E., Salpekar, A., Waterfield, M.D., et al. (2002). Impaired B and T cell antigen receptor signaling in p110delta PI 3-kinase mutant mice. *Science* 297, 1031–1034.
- Okkenhaug, K., Graupera, M., and Vanhaesebroeck, B. (2016). Targeting PI3K in Cancer: Impact on Tumor Cells, Their Protective Stroma, Angiogenesis, and Immunotherapy. *Cancer Discov.* 6, 1090–1105.
- Orlidge, A., and D'Amore, P.A. (1987). Inhibition of capillary endothelial cell growth by pericytes and smooth muscle cells. *J. Cell Biol.* 105, 1455–1462.
- Oshima, M., Oshima, H., and Taketo, M.M. (1996). TGF-beta receptor type II deficiency results in defects of yolk sac hematopoiesis and vasculogenesis. *Dev. Biol.* 179, 297–302.
- Ostman, A., Andersson, M., Betsholtz, C., Westermark, B., and Heldin, C.H. (1991). Identification of a cell retention signal in the B-chain of platelet-derived growth factor and in the long splice version of the A-chain. *Cell Regul.* 2, 503–512.
- Ota, T., Fujii, M., Sugizaki, T., Ishii, M., Miyazawa, K., Aburatani, H., and Miyazono, K. (2002). Targets of transcriptional regulation by two distinct type I receptors for transforming growth factor-beta in human umbilical vein endothelial cells. *J. Cell. Physiol.* 193, 299–318.
- Ozerdem, U., and Stallcup, W.B. (2004). Pathological angiogenesis is reduced by targeting pericytes via the NG2 proteoglycan. *Angiogenesis* 7, 269–276.
- Ozerdem, U., Alitalo, K., Salven, P., and Li, A. (2005). Contribution of bone marrow-derived pericyte precursor cells to corneal vasculogenesis. *Invest. Ophthalmol. Vis. Sci.* 46, 3502–3506.
- Pacold, M.E., Suire, S., Perisic, O., Lara-Gonzalez, S., Davis, C.T., Walker, E.H., Hawkins, P.T., Stephens, L., Eccleston, J.F., and Williams, R.L. (2000). Crystal structure and functional analysis of Ras binding to its effector phosphoinositide 3-kinase gamma. *Cell* 103, 931–943.
- Pàez-Ribes, M., Allen, E., Hudock, J., Takeda, T., Okuyama, H., Viñals, F., Inoue, M., Bergers, G., Hanahan, D., and Casanovas, O. (2009). Antiangiogenic therapy elicits malignant progression of tumors to increased local invasion and distant metastasis. *Cancer Cell* 15, 220–231.
- Paik, J.-H., Skoura, A., Chae, S.-S., Cowan, A.E., Han, D.K., Proia, R.L., and Hla, T. (2004). Sphingosine 1-phosphate receptor regulation of N-cadherin mediates vascular stabilization. *Genes Dev.* 18, 2392–2403.

7. References

- Papakonstanti, E.A., Zwaenepoel, O., Bilancio, A., Burns, E., Nock, G.E., Houseman, B., Shokat, K., Ridley, A.J., and Vanhaesebroeck, B. (2008). Distinct roles of class IA PI3K isoforms in primary and immortalised macrophages. *J. Cell Sci.* 121, 4124–4133.
- Papapetropoulos, A., Fulton, D., Mahboubi, K., Kalb, R.G., O'Connor, D.S., Li, F., Altieri, D.C., and Sessa, W.C. (2000). Angiopoietin-1 Inhibits Endothelial Cell Apoptosis via the Akt/Survivin Pathway. *J. Biol. Chem.* 275, 9102–9105.
- Park, C.S., Schneider, I.C., and Haugh, J.M. (2003). Kinetic Analysis of Platelet-derived Growth Factor Receptor/Phosphoinositide 3-Kinase/Akt Signaling in Fibroblasts. *J. Biol. Chem.* 278, 37064–37072.
- Parsons, R. (2004). Human cancer, PTEN and the PI-3 kinase pathway. *Semin. Cell Dev. Biol.* 15, 171–176.
- Patan, S. (1998). TIE1 and TIE2 receptor tyrosine kinases inversely regulate embryonic angiogenesis by the mechanism of intussusceptive microvascular growth. *Microvasc. Res.* 56, 1–21.
- Patel-Hett, S., and D'Amore, P.A. (2011). Signal transduction in vasculogenesis and developmental angiogenesis. *Int. J. Dev. Biol.* 55, 353–363.
- Paz-Ares, L., Blanco-Aparicio, C., García-Carbonero, R., and Carnero, A. (2009). Inhibiting PI3K as a therapeutic strategy against cancer. *Clin. Transl. Oncol. Off. Publ. Fed. Span. Oncol. Soc. Natl. Cancer Inst. Mex.* 11, 572–579.
- Petrova, T.V., Karpanen, T., Norrmén, C., Mellor, R., Tamakoshi, T., Finegold, D., Ferrell, R., Kerjaschki, D., Mortimer, P., Ylä-Herttua, S., et al. (2004). Defective valves and abnormal mural cell recruitment underlie lymphatic vascular failure in lymphedema distichiasis. *Nat. Med.* 10, 974–981.
- Phng, L.-K., and Gerhardt, H. (2009). Angiogenesis: a team effort coordinated by notch. *Dev. Cell* 16, 196–208.
- Phng, L.-K., Stanchi, F., and Gerhardt, H. (2013). Filopodia are dispensable for endothelial tip cell guidance. *Development* 140, 4031–4040.
- Pitulescu, M.E., Schmidt, I., Benedito, R., and Adams, R.H. (2010). Inducible gene targeting in the neonatal vasculature and analysis of retinal angiogenesis in mice. *Nat. Protoc.* 5, 1518–1534.
- Pöschl, E., Schlötzer-Schrehardt, U., Brachvogel, B., Saito, K., Ninomiya, Y., and Mayer, U. (2004). Collagen IV is essential for basement membrane stability but dispensable for initiation of its assembly during early development. *Development* 131, 1619–1628.
- Potente, M., and Carmeliet, P. (2016). The Link Between Angiogenesis and Endothelial Metabolism. *Annu. Rev. Physiol.*
- Potente, M., Urbich, C., Sasaki, K., Hofmann, W.K., Heeschen, C., Aicher, A., Kollipara, R., DePinho, R.A., Zeiher, A.M., and Dimmeler, S. (2005). Involvement of Foxo transcription factors in angiogenesis and postnatal neovascularization. *J. Clin. Invest.* 115, 2382–2392.
- Potente, M., Gerhardt, H., and Carmeliet, P. (2011). Basic and therapeutic aspects of angiogenesis. *Cell* 146, 873–887.

- Puri, K.D., Doggett, T.A., Douangpanya, J., Hou, Y., Tino, W.T., Wilson, T., Graf, T., Clayton, E., Turner, M., Hayflick, J.S., et al. (2004). Mechanisms and implications of phosphoinositide 3-kinase δ in promoting neutrophil trafficking into inflamed tissue. *Blood* 103, 3448–3456.
- Qayum, N., Muschel, R.J., Im, J.H., Balathasan, L., Koch, C.J., Patel, S., McKenna, W.G., and Bernhard, E.J. (2009). Tumor Vascular Changes Mediated by Inhibition of Oncogenic Signaling. *Cancer Res.* 69, 6347–6354.
- Qayum, N., Im, J., Stratford, M.R., Bernhard, E.J., McKenna, W.G., and Muschel, R.J. (2012). Modulation of the Tumor Microvasculature by Phosphoinositide-3 Kinase Inhibition Increases Doxorubicin Delivery In Vivo. *Clin. Cancer Res.* 18, 161–169.
- Raftopoulou, M., Etienne-Manneville, S., Self, A., Nicholls, S., and Hall, A. (2004). Regulation of cell migration by the C2 domain of the tumor suppressor PTEN. *Science* 303, 1179–1181.
- Rameh, L.E., Chen, C.S., and Cantley, L.C. (1995). Phosphatidylinositol (3,4,5)P3 interacts with SH2 domains and modulates PI 3-kinase association with tyrosine-phosphorylated proteins. *Cell* 83, 821–830.
- Reif, K., Okkenhaug, K., Sasaki, T., Penninger, J.M., Vanhaesebroeck, B., and Cyster, J.G. (2004). Cutting Edge: Differential Roles for Phosphoinositide 3-Kinases, p110 γ and p110 δ , in Lymphocyte Chemotaxis and Homing. *J. Immunol.* 173, 2236–2240.
- Ribatti, D., Nico, B., and Crivellato, E. (2011). The role of pericytes in angiogenesis. *Int. J. Dev. Biol.* 55, 261–268.
- Rocha, S.F., and Adams, R.H. (2009). Molecular differentiation and specialization of vascular beds. *Angiogenesis* 12, 139–147.
- Roche, S., Downward, J., Raynal, P., and Courtneidge, S.A. (1998). A Function for Phosphatidylinositol 3-Kinase β (p85 α -p110 β) in Fibroblasts during Mitogenesis: Requirement for Insulin- and Lysophosphatidic Acid-Mediated Signal Transduction. *Mol. Cell. Biol.* 18, 7119–7129.
- Rodon, J., Dienstmann, R., Serra, V., and Tabernero, J. (2013). Development of PI3K inhibitors: lessons learned from early clinical trials. *Nat. Rev. Clin. Oncol.* 10, 143–153.
- Rodriguez-Viciana, P., Sabatier, C., and McCormick, F. (2004). Signaling specificity by Ras family GTPases is determined by the full spectrum of effectors they regulate. *Mol. Cell. Biol.* 24, 4943–4954.
- Rouget, C. (1873). Memoire sur le developpement, la structures et les proprietes des capillaires sanguins et lymphatiques. *Archs Physiol Norm Pathol* 5, 603–633.
- Roux, P.P., Shahbazian, D., Vu, H., Holz, M.K., Cohen, M.S., Taunton, J., Sonenberg, N., and Blenis, J. (2007). RAS/ERK Signaling Promotes Site-specific Ribosomal Protein S6 Phosphorylation via RSK and Stimulates Cap-dependent Translation. *J. Biol. Chem.* 282, 14056–14064.
- Ruan, G.-X., and Kazlauskas, A. (2012). Axl is essential for VEGF-A-dependent activation of PI3K/Akt. *EMBO J.* 31, 1692–1703.

7. References

S, S., J, C., Gj, F., K, D., P, H., and L, S. (2005). p84, a new Gbetagamma-activated regulatory subunit of the type IB phosphoinositide 3-kinase p110gamma. *Curr. Biol. CB* 15, 566–570.

Saharinen, P., Eklund, L., Miettinen, J., Wirkkala, R., Anisimov, A., Winderlich, M., Nottebaum, A., Vestweber, D., Deutsch, U., Koh, G.Y., et al. (2008). Angiopoietins assemble distinct Tie2 signalling complexes in endothelial cell–cell and cell–matrix contacts. *Nat. Cell Biol.* 10, 527–537.

Sainson, R.C.A., and Harris, A.L. (2008). Regulation of angiogenesis by homotypic and heterotypic notch signalling in endothelial cells and pericytes: from basic research to potential therapies. *Angiogenesis* 11, 41–51.

Sanchez, T., Thangada, S., Wu, M.-T., Kontos, C.D., Wu, D., Wu, H., and Hla, T. (2005). PTEN as an effector in the signaling of antimigratory G protein-coupled receptor. *Proc. Natl. Acad. Sci. U. S. A.* 102, 4312–4317.

Sarbassov, D.D., Guertin, D.A., Ali, S.M., and Sabatini, D.M. (2005). Phosphorylation and regulation of Akt/PKB by the rictor-mTOR complex. *Science* 307, 1098–1101.

Sato, Y., and Rifkin, D.B. (1989). Inhibition of endothelial cell movement by pericytes and smooth muscle cells: activation of a latent transforming growth factor-beta 1-like molecule by plasmin during co-culture. *J. Cell Biol.* 109, 309–315.

Saudemont, A., Garçon, F., Yadi, H., Roche-Molina, M., Kim, N., Segonds-Pichon, A., Martín-Fontecha, A., Okkenhaug, K., Colucci, F., and Fearon, D.T. (2009). p110 γ and p110 δ Isoforms of Phosphoinositide 3-kinase Differentially Regulate Natural Killer Cell Migration in Health and Disease. *Proc. Natl. Acad. Sci. U. S. A.* 106, 5795–5800.

Saunders, W.B., Bayless, K.J., and Davis, G.E. (2005). MMP-1 activation by serine proteases and MMP-10 induces human capillary tubular network collapse and regression in 3D collagen matrices. *J. Cell Sci.* 118, 2325–2340.

Sawyer, C., Sturge, J., Bennett, D.C., O'Hare, M.J., Allen, W.E., Bain, J., Jones, G.E., and Vanhaesebroeck, B. (2003). Regulation of breast cancer cell chemotaxis by the phosphoinositide 3-kinase p110delta. *Cancer Res.* 63, 1667–1675.

Schlingemann, R.O., Oosterwijk, E., Wesseling, P., Rietveld, F.J., and Ruiter, D.J. (1996). Aminopeptidase a is a constituent of activated pericytes in angiogenesis. *J. Pathol.* 179, 436–442.

Schmid, M.C., Avraamides, C.J., Dippold, H.C., Franco, I., Foubert, P., Ellies, L.G., Acevedo, L.M., Manglicmot, J.R.E., Song, X., Wrasidlo, W., et al. (2011). Receptor tyrosine kinases and TLR/IL1Rs unexpectedly activate myeloid cell PI3k γ , a single convergent point promoting tumor inflammation and progression. *Cancer Cell* 19, 715–727.

Schmid, M.C., Franco, I., Kang, S.W., Hirsch, E., Quilliam, L.A., and Varner, J.A. (2013). PI3-kinase γ promotes Rap1a-mediated activation of myeloid cell integrin $\alpha\beta$ 1, leading to tumor inflammation and growth. *PLoS One* 8, e60226.

Schnell, C.R., Stauffer, F., Allegrini, P.R., O'Reilly, T., McSheehy, P.M.J., Dartois, C., Stumm, M., Cozens, R., Littlewood-Evans, A., García-Echeverría, C., et al. (2008). Effects of the Dual Phosphatidylinositol 3-Kinase/Mammalian Target of Rapamycin

- Inhibitor NVP-BEZ235 on the Tumor Vasculature: Implications for Clinical Imaging. *Cancer Res.* 68, 6598–6607.
- Schulz, B., Pruessmeyer, J., Maretzky, T., Ludwig, A., Blobel, C.P., Saftig, P., and Reiss, K. (2008). ADAM10 regulates endothelial permeability and T-Cell transmigration by proteolysis of vascular endothelial cadherin. *Circ. Res.* 102, 1192–1201.
- Schulz, G.B., Wieland, E., Wüsthube-Lausch, J., Boulday, G., Moll, I., Tournier-Lasserre, E., and Fischer, A. (2015). Cerebral Cavernous Malformation-1 Protein Controls DLL4-Notch3 Signaling Between the Endothelium and Pericytes. *Stroke* 46, 1337–1343.
- Schwartz, S., Wongvipat, J., Trigwell, C.B., Hancox, U., Carver, B.S., Rodrik-Outmezguine, V., Will, M., Yellen, P., de Stanchina, E., Baselga, J., et al. (2015). Feedback Suppression of PI3K α Signaling in PTEN-Mutated Tumors Is Relieved by Selective Inhibition of PI3K β . *Cancer Cell* 27, 109–122.
- Seasholtz, T.M., Zhang, T., Morissette, M.R., Howes, A.L., Yang, A.H., and Brown, J.H. (2001). Increased Expression and Activity of RhoA Are Associated With Increased DNA Synthesis and Reduced p27Kip1 Expression in the Vasculature of Hypertensive Rats. *Circ. Res.* 89, 488–495.
- Sekimoto, T., Fukumoto, M., and Yoneda, Y. (2004). 14-3-3 suppresses the nuclear localization of threonine 157-phosphorylated p27Kip1. *EMBO J.* 23, 1934–1942.
- Semenza, G.L. (2003). Targeting HIF-1 for cancer therapy. *Nat. Rev. Cancer* 3, 721–732.
- Serra, H., Chivite, I., Angulo-Urarte, A., Soler, A., Sutherland, J.D., Arruabarrena-Aristorena, A., Ragab, A., Lim, R., Malumbres, M., Fruttiger, M., et al. (2015). PTEN mediates Notch-dependent stalk cell arrest in angiogenesis. *Nat. Commun.* 6, 7935.
- Sherr, C.J., and Weber, J.D. (2000). The ARF/p53 pathway. *Curr. Opin. Genet. Dev.* 10, 94–99.
- Shimura, T., Noma, N., Oikawa, T., Ochiai, Y., Kakuda, S., Kuwahara, Y., Takai, Y., Takahashi, A., and Fukumoto, M. (2012). Activation of the AKT/cyclin D1/Cdk4 survival signaling pathway in radioresistant cancer stem cells. *Oncogenesis* 1, e12.
- Siekman, A.F., Affolter, M., and Belting, H.-G. (2013). The tip cell concept 10 years after: new players tune in for a common theme. *Exp. Cell Res.* 319, 1255–1263.
- Simonavicius, N., Ashenden, M., Weverwijk, A. van, Lax, S., Huso, D.L., Buckley, C.D., Huijbers, I.J., Yarwood, H., and Isacke, C.M. (2012). Pericytes promote selective vessel regression to regulate vascular patterning. *Blood* 120, 1516–1527.
- Sims, D.E. (1986). The pericyte—A review. *Tissue Cell* 18, 153–174.
- Sims, D.E. (2000). Diversity within pericytes. *Clin. Exp. Pharmacol. Physiol.* 27, 842–846.
- Soler, A., Serra, H., Pearce, W., Angulo, A., Guillermet-Guibert, J., Friedman, L.S., Viñals, F., Gerhardt, H., Casanovas, O., Graupera, M., et al. (2013). Inhibition of the p110 α isoform of PI 3-kinase stimulates nonfunctional tumor angiogenesis. *J. Exp. Med.* 210, 1937–1945.

7. References

- Soler, A., Angulo-Urarte, A., and Graupera, M. (2015). PI3K at the crossroads of tumor angiogenesis signaling pathways. *Mol. Cell. Oncol.* 2, e975624.
- Soler, A., Figueiredo, A.M., Castel, P., Martin, L., Monelli, E., Angulo-Urarte, A., Mila-Guasch, M., Viñals, F., Baselga, J., Casanovas, O., et al. (2016). Therapeutic benefit of selective inhibition of p110 α PI3-kinase in pancreatic neuroendocrine tumors. *Clin. Cancer Res. clincanres.3051.2015*.
- Song, M.S., Carracedo, A., Salmena, L., Song, S.J., Egia, A., Malumbres, M., and Pandolfi, P.P. (2011). Nuclear PTEN regulates the APC-CDH1 tumor-suppressive complex in a phosphatase-independent manner. *Cell* 144, 187–199.
- Song, M.S., Salmena, L., and Pandolfi, P.P. (2012). The functions and regulation of the PTEN tumour suppressor. *Nat. Rev. Mol. Cell Biol.* 13, 283–296.
- Song, N., Huang, Y., Shi, H., Yuan, S., Ding, Y., Song, X., Fu, Y., and Luo, Y. (2009). Overexpression of Platelet-Derived Growth Factor-BB Increases Tumor Pericyte Content via Stromal-Derived Factor-1 α /CXCR4 Axis. *Cancer Res.* 69, 6057–6064.
- Sopasakis, V.R., Liu, P., Suzuki, R., Kondo, T., Winnay, J., Tran, T.T., Asano, T., Smyth, G., Sajan, M.P., Farese, R.V., et al. (2010). Specific roles of the p110 α isoform of phosphatidylinositol 3-kinase in hepatic insulin signaling and metabolic regulation. *Cell Metab.* 11, 220–230.
- Soriano, P. (1994). Abnormal kidney development and hematological disorders in PDGF beta-receptor mutant mice. *Genes Dev.* 8, 1888–1896.
- Srinivas, S., Watanabe, T., Lin, C.-S., Williams, C.M., Tanabe, Y., Jessell, T.M., and Costantini, F. (2001). Cre reporter strains produced by targeted insertion of EYFP and ECFP into the ROSA26 locus. *BMC Dev. Biol.* 1, 4.
- Stambolic, V., Suzuki, A., de la Pompa, J.L., Brothers, G.M., Mirtsos, C., Sasaki, T., Ruland, J., Penninger, J.M., Siderovski, D.P., and Mak, T.W. (1998). Negative regulation of PKB/Akt-dependent cell survival by the tumor suppressor PTEN. *Cell* 95, 29–39.
- Stapor, P.C., Sweat, R.S., Dashti, D.C., Betancourt, A.M., and Murfee, W.L. (2014). Pericyte Dynamics during Angiogenesis: New Insights from New Identities. *J. Vasc. Res.* 51, 163–174.
- Steck, P.A., Pershouse, M.A., Jasser, S.A., Yung, W.K., Lin, H., Ligon, A.H., Langford, L.A., Baumgard, M.L., Hattier, T., Davis, T., et al. (1997). Identification of a candidate tumour suppressor gene, MMAC1, at chromosome 10q23.3 that is mutated in multiple advanced cancers. *Nat. Genet.* 15, 356–362.
- Stephens, L.R., Eguinoa, A., Erdjument-Bromage, H., Lui, M., Cooke, F., Coadwell, J., Smrcka, A.S., Thelen, M., Cadwallader, K., Tempst, P., et al. (1997). The G beta gamma sensitivity of a PI3K is dependent upon a tightly associated adaptor, p101. *Cell* 89, 105–114.
- Stratman, A.N., and Davis, G.E. (2012). Endothelial cell-pericyte interactions stimulate basement membrane matrix assembly: influence on vascular tube remodeling, maturation, and stabilization. *Microsc. Microanal. Off. J. Microsc. Soc. Am. Microbeam Anal. Soc. Microsc. Soc. Can.* 18, 68–80.

- Stratman, A.N., Schwindt, A.E., Malotte, K.M., and Davis, G.E. (2010). Endothelial-derived PDGF-BB and HB-EGF coordinately regulate pericyte recruitment during vasculogenic tube assembly and stabilization. *Blood* 116, 4720–4730.
- Suire, S., Condliffe, A.M., Ferguson, G.J., Ellson, C.D., Guillou, H., Davidson, K., Welch, H., Coadwell, J., Turner, M., Chilvers, E.R., et al. (2006). Gβγs and the Ras binding domain of p110γ are both important regulators of PI3Kγ signalling in neutrophils. *Nat. Cell Biol.* 8, 1303–1309.
- Sundberg, C., Ljungström, M., Lindmark, G., Gerdin, B., and Rubin, K. (1993). Microvascular pericytes express platelet-derived growth factor-beta receptors in human healing wounds and colorectal adenocarcinoma. *Am. J. Pathol.* 143, 1377–1388.
- Suri, C., Jones, P.F., Patan, S., Bartunkova, S., Maisonpierre, P.C., Davis, S., Sato, T.N., and Yancopoulos, G.D. (1996). Requisite Role of Angiopoietin-1, a Ligand for the TIE2 Receptor, during Embryonic Angiogenesis. *Cell* 87, 1171–1180.
- Suzuki, A., Yamaguchi, M.T., Ohteki, T., Sasaki, T., Kaisho, T., Kimura, Y., Yoshida, R., Wakeham, A., Higuchi, T., Fukumoto, M., et al. (2001). T Cell-Specific Loss of Pten Leads to Defects in Central and Peripheral Tolerance. *Immunity* 14, 523–534.
- Suzuki, A., Nakano, T., Mak, T.W., and Sasaki, T. (2008). Portrait of PTEN: Messages from mutant mice. *Cancer Sci.* 99, 209–213.
- Sweeney, M.D., Ayyadurai, S., and Zlokovic, B.V. (2016). Pericytes of the neurovascular unit: key functions and signaling pathways. *Nat. Neurosci.* 19, 771–783.
- Taddei, A., Giampietro, C., Conti, A., Orsenigo, F., Breviario, F., Pirazzoli, V., Potente, M., Daly, C., Dimmeler, S., and Dejana, E. (2008). Endothelial adherens junctions control tight junctions by VE-cadherin-mediated upregulation of claudin-5. *Nat. Cell Biol.* 10, 923–934.
- Taeger, J., Moser, C., Hellerbrand, C., Mycielska, M.E., Glockzin, G., Schlitt, H.J., Geissler, E.K., Stoeltzing, O., and Lang, S.A. (2011). Targeting FGFR/PDGFR/VEGFR impairs tumor growth, angiogenesis, and metastasis by effects on tumor cells, endothelial cells, and pericytes in pancreatic cancer. *Mol. Cancer Ther.* 10, 2157–2167.
- Takata, F., Dohgu, S., Matsumoto, J., Takahashi, H., Machida, T., Wakigawa, T., Harada, E., Miyaji, H., Koga, M., Nishioku, T., et al. (2011). Brain pericytes among cells constituting the blood-brain barrier are highly sensitive to tumor necrosis factor-α, releasing matrix metalloproteinase-9 and migrating in vitro. *J. Neuroinflammation* 8, 106.
- Tallquist, M.D., Klinghoffer, R.A., Heuchel, R., Mueting-Nelsen, P.F., Corrin, P.D., Heldin, C.-H., Johnson, R.J., and Soriano, P. (2000). Retention of PDGFR-β function in mice in the absence of phosphatidylinositol 3'-kinase and phospholipase Cγ signaling pathways. *Genes Dev.* 14, 3179–3190.
- Thakker, G.D., Hajjar, D.P., Muller, W.A., and Rosengart, T.K. (1999). The Role of Phosphatidylinositol 3-Kinase in Vascular Endothelial Growth Factor Signaling. *J. Biol. Chem.* 274, 10002–10007.
- Theis, M., de Wit, C., Schlaeger, T.M., Eckardt, D., Krüger, O., Döring, B., Risau, W., Deutsch, U., Pohl, U., and Willecke, K. (2001). Endothelium-specific replacement of the connexin43 coding region by a lacZ reporter gene. *Genes. N. Y. N* 2000 29, 1–13.

7. References

- Thomas, W.E. (1999). Brain macrophages: on the role of pericytes and perivascular cells. *Brain Res. Brain Res. Rev.* 31, 42–57.
- Thorpe, L.M., Yuzugullu, H., and Zhao, J.J. (2015). PI3K in cancer: divergent roles of isoforms, modes of activation and therapeutic targeting. *Nat. Rev. Cancer* 15, 7–24.
- Tigges, U., Welser-Alves, J.V., Boroujerdi, A., and Milner, R. (2012). A novel and simple method for culturing pericytes from mouse brain. *Microvasc. Res.* 84, 74–80.
- Toska, E., and Baselga, J. (2016). Pharmacology in the Era of Targeted Therapies: The Case of PI3K Inhibitors. *Clin. Cancer Res.* 22, 2099–2101.
- Trost, A., Lange, S., Schroedl, F., Bruckner, D., Motloch, K.A., Bogner, B., Kaser-Eichberger, A., Strohmaier, C., Runge, C., Aigner, L., et al. (2016). Brain and Retinal Pericytes: Origin, Function and Role. *Front. Cell. Neurosci.* 20.
- Uemura, A., Ogawa, M., Hirashima, M., Fujiwara, T., Koyama, S., Takagi, H., Honda, Y., Wiegand, S.J., Yancopoulos, G.D., and Nishikawa, S.-I. (2002). Recombinant angiopoietin-1 restores higher-order architecture of growing blood vessels in mice in the absence of mural cells. *J. Clin. Invest.* 110, 1619–1628.
- Urness, L.D., Sorensen, L.K., and Li, D.Y. (2000). Arteriovenous malformations in mice lacking activin receptor-like kinase-1. *Nat. Genet.* 26, 328–331.
- Utermark, T., Rao, T., Cheng, H., Wang, Q., Lee, S.H., Wang, Z.C., Iglehart, J.D., Roberts, T.M., Muller, W.J., and Zhao, J.J. (2012). The p110 α and p110 β isoforms of PI3K play divergent roles in mammary gland development and tumorigenesis. *Genes Dev.* 26, 1573–1586.
- Vadas, O., Dbouk, H.A., Shymanets, A., Perisic, O., Burke, J.E., Abi Saab, W.F., Khalil, B.D., Harteneck, C., Bresnick, A.R., Nürnberg, B., et al. (2013). Molecular determinants of PI3K γ -mediated activation downstream of G-protein-coupled receptors (GPCRs). *Proc. Natl. Acad. Sci. U. S. A.* 110, 18862–18867.
- Valladares F., D.-F.L., Gutiérrez R., Varela H, and Rancel N (1991a). Microvascular pericytes: a review of their morphological and functional characteristics. *Histol Histopathol* 6, 269–286.
- Vander Haar, E., Lee, S.-I., Bandhakavi, S., Griffin, T.J., and Kim, D.-H. (2007). Insulin signalling to mTOR mediated by the Akt/PKB substrate PRAS40. *Nat. Cell Biol.* 9, 316–323.
- Vanhaesebroeck, B., Welham, M.J., Kotani, K., Stein, R., Warne, P.H., Zvelebil, M.J., Higashi, K., Volinia, S., Downward, J., and Waterfield, M.D. (1997). P110delta, a novel phosphoinositide 3-kinase in leukocytes. *Proc. Natl. Acad. Sci. U. S. A.* 94, 4330–4335.
- Vanhaesebroeck, B., Leever, S.J., Ahmadi, K., Timms, J., Katso, R., Driscoll, P.C., Woscholski, R., Parker, P.J., and Waterfield, M.D. (2001). Synthesis and function of 3-phosphorylated inositol lipids. *Annu. Rev. Biochem.* 70, 535–602.
- Vanhaesebroeck, B., Ali, K., Bilancio, A., Geering, B., and Foukas, L.C. (2005). Signalling by PI3K isoforms: insights from gene-targeted mice. *Trends Biochem. Sci.* 30, 194–204.

- Vanhaesebroeck, B., Guillermet-Guibert, J., Graupera, M., and Bilanges, B. (2010). The emerging mechanisms of isoform-specific PI3K signalling. *Nat. Rev. Mol. Cell Biol.* *11*, 329–341.
- Vanhaesebroeck, B., Stephens, L., and Hawkins, P. (2012). PI3K signalling: the path to discovery and understanding. *Nat. Rev. Mol. Cell Biol.* *13*, 195–203.
- Vanhaesebroeck, B., Whitehead, M.A., and Piñeiro, R. (2016). Molecules in medicine mini-review: isoforms of PI3K in biology and disease. *J. Mol. Med.* *94*, 5–11.
- Vantler, M., Jesus, J., Leppänen, O., Scherner, M., Berghausen, E.M., Mustafov, L., Chen, X., Kramer, T., Zierden, M., Gerhardt, M., et al. (2015). Class IA Phosphatidylinositol 3-Kinase Isoform p110 α Mediates Vascular Remodeling Significance. *Arterioscler. Thromb. Vasc. Biol.* *35*, 1434–1444.
- Vasudevan, K.M., Barbie, D.A., Davies, M.A., Rabinovsky, R., McNear, C.J., Kim, J.J., Hennessy, B.T., Tseng, H., Pochanard, P., Kim, S.Y., et al. (2009). AKT-independent signaling downstream of oncogenic PIK3CA mutations in human cancer. *Cancer Cell* *16*, 21–32.
- Vestweber, D. (2007). Adhesion and signaling molecules controlling the transmigration of leukocytes through endothelium. *Immunol. Rev.* *218*, 178–196.
- Vikkula, M., Boon, L.M., Carraway, K.L., Calvert, J.T., Diamonti, A.J., Goumnerov, B., Pasyk, K.A., Marchuk, D.A., Warman, M.L., Cantley, L.C., et al. (1996). Vascular dysmorphogenesis caused by an activating mutation in the receptor tyrosine kinase TIE2. *Cell* *87*, 1181–1190.
- Voigt, P., Dorner, M.B., and Schaefer, M. (2006). Characterization of p87PIKAP, a Novel Regulatory Subunit of Phosphoinositide 3-Kinase γ That Is Highly Expressed in Heart and Interacts with PDE3B. *J. Biol. Chem.* *281*, 9977–9986.
- Vontell, D., Armulik, A., and Betsholtz, C. (2006). Pericytes and vascular stability. *Exp. Cell Res.* *312*, 623–629.
- Wang, G.L., Jiang, B.H., Rue, E.A., and Semenza, G.L. (1995). Hypoxia-inducible factor 1 is a basic-helix-loop-helix-PAS heterodimer regulated by cellular O₂ tension. *Proc. Natl. Acad. Sci. U. S. A.* *92*, 5510–5514.
- Wang, J.F., Zhang, X., and Groopman, J.E. (2004). Activation of Vascular Endothelial Growth Factor Receptor-3 and Its Downstream Signaling Promote Cell Survival under Oxidative Stress. *J. Biol. Chem.* *279*, 27088–27097.
- Wang, X., Trotman, L.C., Koppie, T., Alimonti, A., Chen, Z., Gao, Z., Wang, J., Erdjument-Bromage, H., Tempst, P., Cordon-Cardo, C., et al. (2007). NEDD4-1 is a proto-oncogenic ubiquitin ligase for PTEN. *Cell* *128*, 129–139.
- Wang, Y., Pan, L., Moens, C.B., and Appel, B. (2014). Notch3 establishes brain vascular integrity by regulating pericyte number. *Dev. Camb. Engl.* *141*, 307–317.
- Warren, C.M., and Iruela-Arispe, M.L. (2010). Signaling circuitry in vascular morphogenesis. *Curr. Opin. Hematol.* *17*, 213–218.
- Watanabe, S., Morisaki, N., Tezuka, M., Fukuda, K., Ueda, S., Koyama, N., Yokote, K., Kanzaki, T., Yoshida, S., and Saito, Y. (1997). Cultured retinal pericytes stimulate in

7. References

- vitro angiogenesis of endothelial cells through secretion of a fibroblast growth factor-like molecule. *Atherosclerosis* 130, 101–107.
- Wee, S., Wiederschain, D., Maira, S.-M., Loo, A., Miller, C., deBeaumont, R., Stegmeier, F., Yao, Y.-M., and Lengauer, C. (2008). PTEN-deficient cancers depend on PIK3CB. *Proc. Natl. Acad. Sci. U. S. A.* 105, 13057–13062.
- Wei, W., Shin, Y.S., Xue, M., Matsutani, T., Masui, K., Yang, H., Ikegami, S., Gu, Y., Herrmann, K., Johnson, D., et al. (2016). Single-Cell Phosphoproteomics Resolves Adaptive Signaling Dynamics and Informs Targeted Combination Therapy in Glioblastoma. *Cancer Cell* 29, 563–573.
- Weigelt, B., and Downward, J. (2012). Genomic Determinants of PI3K Pathway Inhibitor Response in Cancer. *Front. Oncol.* 2, 109.
- Welch, H.C.E., Coadwell, W.J., Ellson, C.D., Ferguson, G.J., Andrews, S.R., Erdjument-Bromage, H., Tempst, P., Hawkins, P.T., and Stephens, L.R. (2002). P-Rex1, a PtdIns(3,4,5)P3- and Gbetagamma-regulated guanine-nucleotide exchange factor for Rac. *Cell* 108, 809–821.
- Welti, J., Loges, S., Dimmeler, S., and Carmeliet, P. (2013). Recent molecular discoveries in angiogenesis and antiangiogenic therapies in cancer. *J. Clin. Invest.* 123, 3190–3200.
- Wennström, S., Siegbahn, A., Yokote, K., Arvidsson, A.K., Heldin, C.H., Mori, S., and Claesson-Welsh, L. (1994). Membrane ruffling and chemotaxis transduced by the PDGF beta-receptor require the binding site for phosphatidylinositol 3' kinase. *Oncogene* 9, 651–660.
- Winkler, E.A., Bell, R.D., and Zlokovic, B.V. (2011). Central nervous system pericytes in health and disease. *Nat. Neurosci.* 14, 1398–1405.
- Xian, X., Håkansson, J., Ståhlberg, A., Lindblom, P., Betsholtz, C., Gerhardt, H., and Semb, H. (2006). Pericytes limit tumor cell metastasis. *J. Clin. Invest.* 116, 642–651.
- Xu, K., and Cleaver, O. (2011). Tubulogenesis during blood vessel formation. *Semin. Cell Dev. Biol.* 22, 993–1004.
- Yang, W., Hosford, S.R., Dillon, L.M., Shee, K., Liu, S.C., Bean, J.R., Salphati, L., Pang, J., Zhang, X., Nannini, M.A., et al. (2016). Strategically Timing Inhibition of Phosphatidylinositol 3-Kinase to Maximize Therapeutic Index in Estrogen Receptor Alpha-Positive, PIK3CA-Mutant Breast Cancer. *Clin. Cancer Res.* 22, 2250–2260.
- Yang, X., Castilla, L.H., Xu, X., Li, C., Gotay, J., Weinstein, M., Liu, P.P., and Deng, C.X. (1999). Angiogenesis defects and mesenchymal apoptosis in mice lacking SMAD5. *Development* 126, 1571–1580.
- Yoeli-Lerner, M., Yiu, G.K., Rabinovitz, I., Erhardt, P., Jauliac, S., and Toker, A. (2005). Akt blocks breast cancer cell motility and invasion through the transcription factor NFAT. *Mol. Cell* 20, 539–550.
- Yu, J., Zhang, Y., McIlroy, J., Rordorf-Nikolic, T., Orr, G.A., and Backer, J.M. (1998a). Regulation of the p85/p110 Phosphatidylinositol 3'-Kinase: Stabilization and Inhibition of the p110 α Catalytic Subunit by the p85 Regulatory Subunit. *Mol. Cell. Biol.* 18, 1379–1387.

- Yu, J., Wjasow, C., and Backer, J.M. (1998b). Regulation of the p85/p110alpha phosphatidylinositol 3'-kinase. Distinct roles for the n-terminal and c-terminal SH2 domains. *J. Biol. Chem.* *273*, 30199–30203.
- Yu, X., Radulescu, A., Chen, C.-L., James, I.O., and Besner, G.E. (2012). Heparin-binding EGF-like Growth Factor Protects Pericytes from Injury. *J. Surg. Res.* *172*, 165–176.
- Yuan, T.L., and Cantley, L.C. (2010). Introduction. In *Phosphoinositide 3-Kinase in Health and Disease*, C. Rommel, B. Vanhaesebroeck, and P.K. Vogt, eds. (Springer Berlin Heidelberg), pp. 1–7.
- Yuan, T.L., Choi, H.S., Matsui, A., Benes, C., Lifshits, E., Luo, J., Frangioni, J.V., and Cantley, L.C. (2008). Class 1A PI3K regulates vessel integrity during development and tumorigenesis. *Proc. Natl. Acad. Sci.* *105*, 9739–9744.
- Zhao, J.J., Gjoerup, O.V., Subramanian, R.R., Cheng, Y., Chen, W., Roberts, T.M., and Hahn, W.C. (2003). Human mammary epithelial cell transformation through the activation of phosphatidylinositol 3-kinase. *Cancer Cell* *3*, 483–495.
- Zhao, J.J., Cheng, H., Jia, S., Wang, L., Gjoerup, O.V., Mikami, A., and Roberts, T.M. (2006). The p110 α isoform of PI3K is essential for proper growth factor signaling and oncogenic transformation. *Proc. Natl. Acad. Sci.* *103*, 16296–16300.
- Zhou, G.-L., Tucker, D.F., Bae, S.S., Bhatheja, K., Birnbaum, M.J., and Field, J. (2006). Opposing roles for Akt1 and Akt2 in Rac/Pak signaling and cell migration. *J. Biol. Chem.* *281*, 36443–36453.
- Zimmermann, K.W (1923). Der feinere bau der blutcapillares. *Z Anat Entwicklungsgesch* *68*, 3–109.

Appendix

A first author manuscript based on my thesis work is under preparation to be submitted to an international journal relevant to the field. In addition, during this period I have participated in several enriching collaborations that have given rise to the following publications:

- Soler A, **Figueiredo AM**, Castel P, Martin L, Monelli E, Angulo-Urarte A, et al. Therapeutic benefit of selective inhibition of p110alpha PI3-kinase in pancreatic neuroendocrine tumors. Clin Cancer Res 2016. DOI:10.1158/1078-0432.CCR-15-3051.
- Castillo SD, Tzouanacou E, ZawThin M, Berenjeno IM, Parker VE, Chivite I, **Figueiredo AM**, et al. Somatic activating mutations in Pik3ca cause sporadic venous malformations in mice and humans. Sci Transl Med 2016;8:332ra43.
- Esteban J. Rozen, Julia Roewenstrunk, Carole Jung, Chiara Di Vona, María José Barallobre, **Ana Martins Figueiredo**, Jeroni Luna, Cristina Fillat, Maria L. Arbonés, Mariona Graupera, Miguel A. Valverde and Susana de la Luna. The DYRK1A kinase positively regulates angiogenic responses in endothelial cells. EMBO Mol Med (Submitted).
- Elisenda Alsina-Sanchís, Yaiza García-Ibáñez, **Ana M. Figueiredo**, Carla RieraDomingo, Agnès Figueras, Xavier Matias-Guiu , Oriol Casanovas, Luisa María Botella , Miquel Angel Pujana, Antoni Riera-Mestre, Mariona Graupera & Francesc Viñals. BMP9/ALK1 regulates vascular quiescence by repressing the PI3 kinase signaling pathway. Blood (Submitted).